



Pacific Northwest
NATIONAL LABORATORY

Proudly Operated by Battelle Since 1965

Gas Retention, Gas Release, and Fluidization of Spherical Resorcinol-Formaldehyde (sRF) Ion Exchange Resin

April 2018

PA Gauglitz
SD Rassat
DT Linn
CLH Bottenus
GK Boeringa
CM Stewart
BJ Riley
PP Schonewill

DISCLAIMER

This report was prepared as an account of work sponsored by an agency of the United States Government. Neither the United States Government nor any agency thereof, nor Battelle Memorial Institute, nor any of their employees, makes **any warranty, express or implied, or assumes any legal liability or responsibility for the accuracy, completeness, or usefulness of any information, apparatus, product, or process disclosed, or represents that its use would not infringe privately owned rights.** Reference herein to any specific commercial product, process, or service by trade name, trademark, manufacturer, or otherwise does not necessarily constitute or imply its endorsement, recommendation, or favoring by the United States Government or any agency thereof, or Battelle Memorial Institute. The views and opinions of authors expressed herein do not necessarily state or reflect those of the United States Government or any agency thereof.

PACIFIC NORTHWEST NATIONAL LABORATORY
operated by
BATTELLE
for the
UNITED STATES DEPARTMENT OF ENERGY
under Contract DE-AC05-76RL01830

Printed in the United States of America

Available to DOE and DOE contractors from the
Office of Scientific and Technical Information,
P.O. Box 62, Oak Ridge, TN 37831-0062;
ph: (865) 576-8401
fax: (865) 576-5728
email: reports@adonis.osti.gov

Available to the public from the National Technical Information Service
5301 Shawnee Rd., Alexandria, VA 22312
ph: (800) 553-NTIS (6847)
email: orders@ntis.gov <<http://www.ntis.gov/about/form.aspx>>
Online ordering: <http://www.ntis.gov>



This document was printed on recycled paper.

(8/2010)

Gas Retention, Gas Release, and Fluidization of Spherical Resorcinol-Formaldehyde (sRF) Ion Exchange Resin

PA Gauglitz
SD Rassat
DT Linn
CLH Bottenus
G Boeringa
CM Stewart
BJ Riley
PP Schonewill

April 2018

Prepared for
the U.S. Department of Energy
under Contract DE-AC05-76RL01830

Pacific Northwest National Laboratory
Richland, Washington 99352

Executive Summary

The Low-Activity Waste Pretreatment System (LAWPS) is being developed to provide treated supernatant liquid from the Hanford tank farms directly to the Low-Activity Waste (LAW) Vitrification Facility at the Hanford Tank Waste Treatment and Immobilization Plant. The design and development of the LAWPS is being conducted by Washington River Protection Solutions, LLC. A key process in LAWPS is the removal of radioactive Cs from LAW liquids using ion exchange (IX) columns filled with spherical resorcinol-formaldehyde (sRF) resin. When loaded with radioactive Cs, radiolysis of water in the LAW liquid will generate hydrogen gas. In normal operations, the generated hydrogen is expected to remain dissolved in the liquid and be continuously removed by liquid flow. One accident scenario being evaluated is the loss of liquid flow through the sRF resin bed after it has been loaded with radioactive Cs and hydrogen gas is being generated by radiolysis. For an accident scenario with a loss of flow, hydrogen gas can be retained within the IX column both in the sRF resin bed and below the bottom screen that supports the resin within the column, which creates a hydrogen flammability hazard. Because there is a potential for a large fraction of the retained hydrogen to be released over a short duration as a gas release event, there is a need to quantify the size and rate of potential gas release events. Due to the potential for a large, rapid gas release event, an evaluation of mitigation methods to eliminate the hydrogen hazard is also needed. One method being considered for mitigating the hydrogen hazard during a loss of flow accident is to have a secondary flow system, with two redundant pumps operating in series, that re-circulates liquid upwards through the bed and into a vented break tank where hydrogen gas is released from the liquid and removed by venting the headspace of the break tank. The mechanism for inducing release of gas from the sRF bed is to fluidize the bed, which should allow retained bubbles to rise and be carried to the break tank.

Currently, neither the ability of fluidizing a settled sRF bed to release gas nor the quantity of hydrogen gas that can be retained and the corresponding potential for large, rapid gas release events has been tested and evaluated. Accordingly, the purpose of this study was to conduct experiments and develop models that evaluate the ability of a re-circulating flow system to fluidize an sRF resin bed as a method to release retained hydrogen gas and maintain hydrogen gas retention at low levels, thereby avoiding conditions where hydrogen gas poses a flammability hazard. The purpose of the study was also to determine if effective hydrogen gas release would occur using a single constant fluidization velocity, because this is the most simple safety system to implement, for the range of fluid and sRF resin conditions anticipated in the column (because a velocity that is effective for one fluid/resin pair can be ineffective for different resin/fluid pairs). Finally, the study also included quantifying the volume of gas that can be retained in an sRF bed and the behavior of spontaneous, rather than fluidization-induced, gas release events.

Gas retention and release and fluidization experiments were conducted using simulants with physical properties that spanned the expected range of fluids that may be processed through the ion exchange columns, from a low viscosity and low density condition of 55 °C water to a high-limit LAW simulant solution with a viscosity of 15 mPa·s (cP) and density of 1.35 g/mL. The sRF resin particles exchange cations (H^+ , Na^+), depending on the solution composition that has been in contact with the resin, and this causes the sRF particles to change diameter and density, which then affects fluidization behavior. In the experiments conducted, the sRF resin was in the Na^+ form in LAW simulants and alkaline water and in the H^+ form when equilibrated in acidic water. Densities and viscosities of fluids in contact with the sRF resin and particle diameter and density were measured for sRF resin equilibrated with alkaline water,

acidic water, nominal LAW simulant (targets of 1.25 g/mL density and 2-7 mPa·s (cP) viscosity), and the high-limit LAW simulant test liquids. Both tests with bench-scale columns and a full-height column with an internal diameter of 10 in. (full-scale column is 42 in.), were used to investigate gas retention, gas release, and fluidization behavior of beds of sRF resin. Fluidization tests without gas generation were conducted at both ambient temperature (20-27 °C) with a range of fluids and at 55 °C with water. Gas retention and release (GR&R) experiments, with and without fluidization, were conducted at ambient temperature (15-23 °C). Two bench-scale GR&R tests at 55 °C were also completed. Previously developed methods of generating in situ gas bubbles did not work with the sRF resin and alkaline LAW simulants. Accordingly, a new method of gas generation was developed using hydrolysis of sodium borohydride to create hydrogen gas.

The key findings of the study are the following:

- The sRF resin bed fluidized readily and expansion of the bed with increasing fluidization velocity followed expected behavior. A literature model for predicting bed expansion was compared with the experimental data for all of the fluids and sRF resin conditions studied, and the model had good agreement with the data and is suitable for estimating bed expansion with different fluid and resin pairs that were not specifically tested.
- A fluidization velocity giving 3% bed expansion was adequate to release both gas retained in an initially settled sRF resin bed and gas continuously generated in a fluidized sRF resin bed. Typically, initially-retained gas was released at velocities less than the velocity needed to achieve 3% bed expansion; however, a velocity giving 3% bed expansion is recommended as a robust fluidization velocity for effective gas release.
- Retained gas fractions (holdup) in multiple continuous gas release tests at steady-state fluidization velocity conditions ranging from 3% to 40% bed expansion was at most 0.7 vol% (average) and was near zero in some cases. If the presence of a large bubble below the bottom screen (a pancake bubble) were eliminated by an appropriate column re-design, gas holdup would likely be reduced closer to zero.
- In addition to the gas volume retained in the gas below the screen, it was demonstrated that the pancake bubble caused flow maldistribution resulting in lower than expected bed expansion. The gas retention below the bottom screen increases the total retained hydrogen, thus increasing the hydrogen flammability hazard, and flow maldistribution interferes with the ability of bed fluidization to release gas.
- Fluidization of Na⁺ form sRF resin in alkaline water was more difficult (required a higher velocity) than H⁺ form sRF resin in acidic water. Accordingly, Na⁺ form sRF resin in 55 °C water was considered to be the most challenging liquid/resin pair, and test data show 5.2 cm/min. fluidization velocity is needed to reach 3% bed expansion under these conditions.
- A two-pump safety system, with both pumps operating in series, and with each pump individually capable of providing 5.2 cm/min. fluidization velocity, would flow with 7.4 cm/min. This is defined as the LAWPS single-fluidization velocity.

- With a constant fluidization velocity of 7.4 cm/min., an upper packed bed of sRF resin will form in most LAW fluids. Testing results show upper bed formation would occur at this velocity for a nominal LAW simulant (nominally 1.25 g/mL density and about 4 mPa·s viscosity) and a high-limit LAW simulant (nominally 1.35 g/mL density and 15 mPa·s viscosity). An upper packed bed is expected to retain hydrogen gas and pose a flammability hazard and in one test a stable upper packed bed with retained gas was observed.
- Cyclical fluidization/settling, with cycles of 5 min on followed by 55 min. off, did not form an upper packed bed at a fluidization velocity of 10.0 cm/min (this was the predicted two-pump flow prior to conducting fluidization tests at 55 °C) even for the high-limit LAW and was effective at releasing gas from sRF resin in a GR&R LAW simulant with nominal properties. This suggests that on:off fluidization could be developed as an approach for using a single fluidization velocity to release hydrogen gas for all fluid and sRF resin pairs. There are three known limitations for this approach that have not been fully quantified: 1) the “on” period of fluidization needs to be sufficiently short to avoid forming an upper bed, 2) the initial retained gas when the first cycle begins must be relatively low, and 3) although not specifically studied, it is expected that the duration of the settling period needs to be sufficiently long to allow a reasonable degree of settling. For example, in a 15:45 cycle test with a considerably-higher retained gas fraction than would be expected in the sRF column, a stable upper packed bed formed on the first cycle before all gas was released, and the upper bed did not collapse when flow was stopped. This led to the use of shorter on-cycles and/or the use of more realistic and bounding retained gas fractions in other noted cyclic GR&R tests.
- Five different types of bubbles were observed during testing. These were 1) particle-displacing bubbles in the settled sRF resin bed; 2) interstitial-liquid displacing bubbles in the settled sRF resin bed; 3) a pancake-shaped bubble that could span the column cross section below the screen supporting the sRF resin; 4) a vessel-spanning bubble that formed within the settled sRF bed during fluidization for gas release; and 5) hitchhiker bubbles where sRF particles attached to individual bubbles and moved as aggregates. These bubble types affect gas retention and release in different ways.
- The overall conclusion of the testing is that fluidization is an effective method to remove hydrogen gas from a bed of sRF resin, but that a single fluidization velocity that is adequate to release gas in 55 °C water will over-fluidize sRF resin in most LAW liquids, including both nominal and high-limit LAW simulants used in testing. An upper packed bed can retain hydrogen gas and pose a flammability hazard. Using periodic on:off fluidization, such as 5:55 min. on:off cycles, is effective at releasing gas while not creating an upper packed bed. Note that lengthening the fluidization duration in a one-hour cycle did result in a stable upper packed bed in one case with the nominal LAW simulant, so testing focused on shorter “on” periods which are needed for effective hydrogen release with periodic on:off fluidization.

Acknowledgements

The authors would like to thank Lenna Mahoney for her review of some of the calculations and Richard Daniel for his overall review of the report and the resulting improvement in technical clarity. We would also like to thank Bill Dey for his guidance on quality assurance matters, Tom Loftus for his assistance in fabricating the fluidization test system, and John Linehan and Mark Bowden for input on hydrogen generation methods and initial co-investigation of the safe use of sodium borohydride with SRF resin.

Acronyms and Abbreviations

COC	Chain of Custody (form)
DI	deionized (water)
FIO	For Information Only
G-F	gas free
GLS	gas-liquid separator
GR&R	gas retention and release
GRE	gas release event
ILDB	interstitial-liquid-displacing bubbles
IX	ion exchange
LAW	low activity waste
LAWPS	Low-Activity Waste Pretreatment System
LPIST	LAWPS Integrated Support Testing
LRB	Laboratory Record Book
M&TE	measuring and test equipment
QA	quality assurance
PDB	particle-displacing bubbles
PNNL	Pacific Northwest National Laboratory
RV	Resin Vessel
SBH	sodium borohydride
SOW	Statement of Work
R&D	research and development
sRF	spherical resorcinol-formaldehyde (resin for ion exchange)
TI	Test Instruction
TP	Test Plan
VSF	vessel-spanning bubble
WRPS	Washington River Protection Solutions, LLC
WWFTP	WRPS Waste Form Testing Program

Nomenclature

Nomenclature – Latin Alphabet

A_c	cross-sectional area
Ar	Archimedes number
D_c	cylindrical column diameter
D_p	diameter of particles (resin beads)
E	fluidization bed expansion ratio
f_v	fraction of a reference velocity
f_α	fraction of the peak gas retention
g	gravitational acceleration, 9.8 m/s ²
h	height of pancake bubble
H_b	resin bed height
$H_{b,E}$	expanded bed height
$H_{b,0}$	initial gas-free resin bed height
$H_{b,0s}$	gas-free resin bed height at the onset of settling
H_c	column height or maximum liquid height within an open column
H_L	supernatant liquid (surface) level (height)
$H_{L,0}$	initial supernatant liquid level (with a “gas-free” resin bed)
$H_{L,max}$	maximum liquid level due to peak gas retention
$H_{L,ss}$	liquid level during steady-state fluidization
$\Delta H_{L,max}$	maximum liquid level change due to peak gas retention
m_t	total mass of liquid and resin in the test vessel
n	exponent in fluidization and settling models
Q	volumetric flow rate of liquid
Re_p	Reynolds number of a particle
$Re_{p,t}$	Reynolds number of a particle at terminal particle settling velocity
V_b	volume of settled resin bed
$V_{b,E}$	volume of expanded (fluidized) resin bed
$V_{b,gf}$	gas-free resin bed volume
$V_{b,0}$	initial gas-free resin bed volume
V_g	volume of gas retained; target volume of retained gas to initiate fluidization
$V_{g,ss}$	volume of gas retained under steady-state flow (fluidization) conditions
V_L	volume of supernatant liquid
$V_{L,0}$	initial volume of supernatant liquid (with a gas-free resin bed)
V_t	total volume of liquid and resin in the test vessel

v	superficial velocity of liquid
v_{hs}	hindered settling velocity of suspended sRF resin particles
v_E	velocity needed to achieve target bed expansion
v_f	incipient (minimum) superficial velocity for fluidization
v_{min}	minimum superficial velocity (target) to effectively release gas
v_p	velocity of a particle
$v_{p,t}$	terminal settling velocity of a particle
v_{40}	velocity for 40% bed expansion, $E = 1.4$ or 140%

Nomenclature – Greek Alphabet

α	retained gas volume fraction
α_{NB}	retained gas fraction at neutral buoyancy
α_{max}	gas fraction at peak retention ($\Delta\alpha_{max}$)
α_{ss}	retained gas fraction under steady-state flow (fluidization) conditions
$\Delta\alpha$	change in retained gas volume fraction
$\Delta\alpha_L$	apparent minimum “liquid void fraction” in the bed
$\Delta\alpha_{PDB}$	change in the fraction of gas retained as particle-displacing bubbles
$\Delta\alpha_{ILDB}$	change in the fraction of gas retained as interstitial-liquid-displacing bubbles
ϵ_b	resin bed interstitial (inter-particle) porosity
ϵ_p	particle (resin bead) internal porosity
ϵ_t	total porosity of resin bed
μ_L	viscosity of contacting liquid
ρ_b	density of settled resin bed
$\rho_{b,drain}$	density resin bed after draining liquid
$\rho_{b,gf}$	gas-free resin bed density
ρ_{db}	dry resin bed density
ρ_p	density of particles (resin beads)
ρ_s	density of solid resin in the bead (skeletal density)
ρ_L	density of contacting liquid
$\Delta\rho$	difference in particle and liquid density ($\rho_p - \rho_L$)

Subscripts

b	resin bed
db	dry resin bed
g	gas
gf	gas-free

<i>ILDB</i>	interstitial-liquid-displacing bubbles
<i>L</i>	liquid
<i>L1</i>	first liquid
<i>L2</i>	second liquid
<i>max</i>	maximum (peak) retained gas
<i>NB</i>	neutral buoyancy
<i>p</i>	particle (bead)
<i>PDB</i>	particle-displacing bubbles
<i>s</i>	solid (skeletal)
<i>ss</i>	steady-state (constant) flow condition (fluidization)
<i>t</i>	total or terminal

Contents

Executive Summary	iii
Acknowledgements.....	vii
Acronyms and Abbreviations	viii
Nomenclature.....	ix
1.0 Introduction.....	1.1
1.1 Previous Studies of Gas Retention and Release.....	1.5
1.2 Gas Generation Methods and Rates for Experimental Studies.....	1.8
2.0 Objectives.....	2.1
3.0 Quality Assurance	3.1
4.0 Background and Technical Approach for measuring sRF Particle Properties and Fluidization Modeling.....	4.1
4.1 sRF Resin Particle and Bed Properties.....	4.1
4.1.1 Primary Particle Properties – Density and Diameter.....	4.1
4.1.2 Initial Resin Bed Properties – Bulk Density and Porosity	4.4
4.2 Fluidization, Upper Packed Bed Formation, and Settling.....	4.5
4.2.1 Fluidization Bed Height	4.5
4.2.2 Upper Packed Bed Height	4.7
4.2.3 Hindered Settling Velocity.....	4.9
5.0 Simulant and Resin Properties	5.1
5.1 Simulant Targets, Selection, and Nominal Properties.....	5.1
5.2 sRF Resin Preparation.....	5.2
5.3 sRF Resin and Liquid Properties.....	5.4
5.3.1 Fluidization-Column Tests.....	5.4
5.3.2 Bench-Scale Tests	5.7
5.4 Effect of Temperature on sRF Resin.....	5.10
6.0 Experimental and Analysis Methods and Approach.....	6.1
6.1 Bench-Top Gas Retention and Release Tests.....	6.1
6.1.1 Benchtop Test Operation.....	6.3
6.2 Fluidization Column with Gas Retention and Release.....	6.4
6.2.1 Fluidization Column Test Operation.....	6.9
6.2.2 Hydrogen Management in Fluidization Column.....	6.12
6.3 Measuring and Test Equipment Summary	6.12
6.4 Hydrogen Gas Generation Method and Measurements.....	6.14
6.5 Gas Retention and Release and In-Test Resin Bed Properties	6.21
6.6 Test Matrix	6.27
7.0 Results: Fluidization, Upper Bed Formation, and Settling	7.1
7.1 Bed Expansion.....	7.1

7.2	Upper Packed Bed Formation	7.4
7.3	Settling	7.7
7.4	Fluidization and Upper Bed Formation Summary	7.8
8.0	Results: Gas Generation, Retention, and Spontaneous Release	8.1
8.1	Gas Generation (Ambient Temperature)	8.1
8.1.1	Bench-Scale Experiments	8.1
8.1.2	Fluidization-Column GR&R Tests.....	8.8
8.2	Gas Retention and Spontaneous Release.....	8.16
8.2.1	Bench-Scale Experiments	8.16
8.2.2	Fluidization-Column GR&R Tests.....	8.24
8.3	Observed Mechanisms of Gas Retention and Bubble Types	8.32
8.4	Elevated-Temperature Gas Retention.....	8.39
8.5	Gas Retention and Spontaneous Release Summary	8.47
9.0	Results: Fluidization-Induced Gas Release.....	9.1
9.1	Determining Minimum Effective Fluidization Velocity	9.6
9.2	Gas Release with Varying Initial Gas Fraction and Fluidization Velocity	9.11
9.2.1	Characteristics of a Typical Test.....	9.11
9.2.2	Initial Fluidization-Induced Gas Release	9.13
9.2.3	Continuous Fluidization and Gas Release.....	9.20
9.3	Gas Release with Cyclic Fluidization.....	9.30
9.4	Fluidization Gas Release Summary.....	9.36
10.0	Conclusions.....	10.1
11.0	References.....	11.1
	Appendix A Additional Test Data	A.1

Figures

Figure 1.1. Planned full-scale sRF resin IX bed and conceptual configuration of a break tank for removal of flammable gases with resin bed fluidization (Aguilar 2016). Note that the break tank depicted in this conceptual configuration is not considered in the current laboratory study..... 1.4

Figure 1.2. Interstitial-liquid-displacing, particle-displacing, and hitchhiker bubbles 1.5

Figure 1.3. Top-view of a Vee-Wire[®] Johnson screen and side-view of gas necking through the slots in the screen..... 1.7

Figure 1.4. Simplified configuration of an IX column without (left) and with retained gas (right). 1.7

Figure 4.1. Configuration and heights of an initial settled bed and fluidized bed of sRF resin..... 4.6

Figure 4.2. Configuration and heights of an initial bed and an over-fluidized bed with a packed upper bed of sRF resin..... 4.9

Figure 5.1. Measured average shear strength as a function of test temperature for various settled beds of sRF resin in different fluids (water, GR&R LAW, and Nominal LAW), and with different quiescent periods (12 hours and 48 hours)..... 5.13

Figure 6.1. Schematic Drawing of a Bench-Top Test Setup for Gas Generation, Retention, and Release Measurements using sRF Resin. The drawing is not to scale, and the relative and absolute sRF resin bed and supernatant liquid layer depths may vary. 6.2

Figure 6.2. Schematic of the Fluidization Test Column, Flow Equipment, and Instruments for Gas Retention and Release Experiments with Fluidization (gray shading on the 3-way valves indicates the common port, figure not to scale)..... 6.6

Figure 6.3. Photograph of Fluidization Column Test System, As-Built, with Key Equipment Labeled. (The gas-collection system is not shown.) 6.8

Figure 6.4. Diagram of an Expected Resin Bed/Liquid Configuration in an Ion Exchange Column with Reference Dimensions (not to scale). Interstitial-liquid-displacing bubbles (lower) and particle-displacing (rounded) bubbles (upper) are depicted schematically in the resin bed. 6.22

Figure 7.1. Bed expansion as a function of fluidization velocity for Na⁺ form sRF resin in ambient temperature alkaline water 7.1

Figure 7.2. Comparison of fluidization model as given by Eq. (4.13) with test data for Na⁺ form sRF resin in ambient temperature alkaline water 7.3

Figure 7.3. Comparison of fluidization model (solid lines) with test data (discrete points) for a range of test fluids and sRF resin properties at ambient and elevated temperature..... 7.3

Figure 7.4. Comparison of fluidization model with three different estimates of particle density (based on different assumed bed porosities) with test data for bed expansion as a function of fluidization velocity for Na⁺ form sRF resin in the high-limit LAW simulant. 7.4

Figure 7.5. Resin height and height at the bottom of the upper bed as a function of time at fixed fluidization velocity for Na⁺ form sRF resin in high-limit LAW simulant. 7.5

Figure 7.6. Resin height and height at the bottom of the upper bed as a function of time at two fluidization velocities for Na⁺ form sRF resin in high-limit LAW simulant. 7.5

Figure 7.7. Upper bed height $h_u/H_{b,o}$ [depth from top of liquid, see Figure 4.2 and Eq. (4.18)] as a function of fluidization velocity for Na⁺ form sRF resin in various simulants. Model predictions are shown by the solid lines. The vertical line shows the the LAWPS single-fluidization velocity sufficient to release gas, which is discussed in Section 9.1. 7.6

Figure 7.8.	Resin height measured as a function of time during 5 min on:55 min off fluidization for Na ⁺ form sRF resin in high-limit LAW simulant.....	7.7
Figure 7.9.	Resin height and upper bed depth measured as a function of time during 5 min on:35 min off fluidization for Na ⁺ form sRF resin in high-limit LAW simulant.....	7.7
Figure 7.10.	Resin height as a function of settling time for Na ⁺ form sRF resin in various simulants. Model predictions are shown by the solid lines.....	7.8
Figure 8.1.	Generated Gas Volumes Represented as Molar Equivalents of Hydrogen as a Function of Elapsed Time (ET) from the Start of Tests GC-01 (sRF Resin in Alkaline Water, pH 12.2 to 12.5) and MD-01 (sRF Resin in 6.1-M Na LAW Simulant) at Constant SBH Concentration (0.7 g SBH/L sRF Resin). Equivalents from gas collection cylinder and retained gas volumes are compared, and ETs of VSB formation and remixing to release gas are shown.	8.2
Figure 8.2.	Normalized Gas Generation Rates in Graduated Cylinder Tests – Generated Gas Volumes Represented as Molar Equivalents of Hydrogen from Gas Retained in Resin as a Function of Elapsed Time (ET) from the Start of Tests GC-01, GC-01A, and GC-16 (sRF Resin in Alkaline Water, pH 12.0 to 12.5) and MD-01 and MD-03 (sRF Resin in 6.1-M Na LAW Simulant) with Varying SBH Concentration and Sources of sRF Resin (see legend). ETs of select VSB formation and remixing to release gas events are shown.	8.4
Figure 8.3.	Normalized Gas Generation Rates in Bench-Scale Tests – Generated Gas Volumes Represented as Molar Equivalents of Hydrogen from Gas Retained in Resin as a Function of ET from the Start of Graduated Cylinder Tests GC-01, MD-07, MD-05, MD-04, MD-03, and MD-08, in Order of Increasing Alkalinity. For 6.1 M Na simulant, results are also shown for 5-in. (MD-02) and 10-in. (MD-06) diameter vessels. The SBH concentration is constant (0.5 g SBH/L sRF Resin) except for Test GC-01 (0.7 g SBH/L sRF Resin).	8.6
Figure 8.4.	Absolute Gas Generation Rates in Graduated Cylinder Tests – Generated Gas Volumes from Gas Retention per Unit Volume of Gas-Free Resin Bed (Specific Gas Volume) as a Function of Elapsed Time from the Start of Tests GC-01, GC-01A, and GC-16 (sRF Resin in Alkaline Water) and MD-01 and MD-03 (sRF Resin in GR&R LAW Simulant) with Varying SBH Concentration and Sources of sRF Resin (see legend). A target growth period for fluidization-GR&R tests is compared to a range of possible retained gas fractions (α_{ILD}).....	8.8
Figure 8.5.	Upper: Comparison of Generated Gas (from collection cylinder) and Retained Gas (in resin bed) Volumes in sRF Resin / Water as a Function of Elapsed Time from the Start of Growth for a Representative Peak Retention / Spontaneous Gas Release Test (Test 10-04 Phase 2); Lower: Incremental Gas Generation Rates in the Same Test Compared to First Day and Overall Average Rates and the Hourly Equivalent of 1 L/day.....	8.11
Figure 8.6.	Gas Generation Determined from Gas Collection Cylinder Volume Measurements as a Function of Elapsed Time from the Start of Quiescent Growth Periods of Spontaneous and Fluidization-Induced Gas Release Tests for sRF Resin in Alkaline Water: Upper, Molar Equivalents of Hydrogen; and Lower, Measured Gas Volume. A generation rate of 1 L/day, equivalent to ~18 L/day in a full-scale IX column, is shown for reference. Legend entries include the “SBHx.y” sequence identifier. A coGR&R test phase is shown in the lower plot.	8.13
Figure 8.7.	Gas Generation Determined from Gas Collection Cylinder Volume Measurements as a Function of Elapsed Time from the Start of Quiescent Growth Periods of Spontaneous and Fluidization-Induced Gas Release Tests for sRF Resin in 6.1-M Na LAW Simulant: Upper, Molar Equivalents of Hydrogen; and Lower, Measured Gas Volume. A generation rate of 1 L/day, equivalent to ~18 L/day in a full-scale IX column, is shown for reference. Legend entries include the “SBHx.y” sequence identifier.....	8.15

Figure 8.8. Gas Retention and Release for sRF Resin/Alkaline Water in Graduated-Cylinder Test GC-01 Depicted in Terms of: (Left y-axis) Changes in Volume of the Resin Bed, Retained Gas, and Liquid in the Resin Bed; and (Right y-axis) Estimated Gas-Free Resin Bed Porosity (0.36 initial assumed). The time of formation of an unstable VSB and an ensuing large spontaneous gas release is shown. 8.17

Figure 8.9. Retained Gas Volume Fraction for sRF Resin/Alkaline Water in Graduated-Cylinder Test GC-01 as a Function of Elapsed Time from the Start of Growth. The estimated time-varying PDB and ILDB neutral-buoyancy gas fractions are shown for reference, as is the time of formation of an unstable VSB and an ensuing large spontaneous gas release. 8.18

Figure 8.10. Retained Gas Volume Fractions for sRF Resin /Alkaline Water in Graduated-Cylinder Tests as a Function of Time from the Start of Level Measurements after SBH Addition. The times of formation of unstable VSBs and ensuing large spontaneous gas releases and representative neutral buoyancy gas fractions (initial as ILDBs and PDBs and measured throughout as PDBs) in Test GC-16 are shown..... 8.19

Figure 8.11. Retained Gas Volume Fractions for sRF Resin/6.1-M Na LAW Simulant as Function of Time from the Start of Level Measurements in Graduated-Cylinder Tests MD-01 and MD-03. The times of formation of stable VSBs, remixing to release gas, and large spontaneous gas releases are shown, as are representative neutral buoyancy gas fractions (initial as ILDBs and PDBs and measured throughout as PDBs) in Test MD-01. 8.20

Figure 8.12. Gas Retention and Release for sRF Resin/6.1-M Na LAW Simulant Tests in Vessels of Varying Diameter (Graduated Cylinder, 5 in., and 10-in.) Presented as Retained Gas Fraction as Function of Time from the Start of Level Measurements after SBH Addition. The initial neutral buoyancy gas fractions as particle-displacing bubbles for each test are shown for reference. 8.22

Figure 8.13. Gas Retention and Release in Graduated Cylinder Tests using sRF Resin in Varying Concentration of NaOH Presented as Retained Gas Fraction versus Elapsed Time from the Start of Level Measurements after SBH Addition. The initial neutral buoyancy gas fractions as particle-displacing bubbles for each test are shown for reference..... 8.23

Figure 8.14. Peak Gas Retention and Spontaneous Gas Release for sRF Resin in Alkaline Water in Test 10-04 Phase 4 shown as Measured (α), Calculated Particle-Displacing (α_{PD}), and Calculated Interstitial-Liquid-Displacing (α_{ILD}) Retained Gas Fraction vs. Elapsed Time from the Start of Growth. The estimated neutral buoyancy gas fractions for ILDBs and PDBs based on initial gas-free conditions are shown for reference..... 8.25

Figure 8.15. Reproducible Peak Gas Retention in Spontaneous Gas Release Tests for sRF Resin in Alkaline Water shown as Retained Gas Fraction as a Function of Elapsed Time from the Start of Growth (Tests 10-04 Phase 2, 10-04 Phase 4, and 10-07 Phase 1)..... 8.26

Figure 8.16. Peak Gas Retention and Spontaneous Gas Release for sRF Resin in 6.1-M Na LAW Simulant in Test 10-08 Phase 2 shown as Measured (α), Calculated Particle-Displacing (α_{PD}), and Calculated Interstitial-Liquid-Displacing (α_{ILD}) Retained Gas Fraction vs. Elapsed Time from the Start of Growth. α measured at 470 hours in opportunistic Test 10-09 Phase 7 is shown at 15-hr ET for comparison. The estimated neutral buoyancy gas fractions for ILDBs and PDBs based on initial gas-free conditions are shown for reference. 8.27

Figure 8.17. Gas Retention in Quiescent Growth Periods of Spontaneous and Fluidization-Induced Gas Release Tests for sRF Resin in Alkaline Water (upper) and in 6.1-M Na Simulant (lower), shown as the Fraction of Peak Gas Retention versus Elapsed Time from the Start of Growth. Legend entries include the “SBHx.y” sequence identifier..... 8.30

Figure 8.18. Retained Gas in Fluidization-Column Tests, Represented by Supernatant Liquid Level Change, as a Function of Gas Volume Generated (Collected) in sRF Resin in Alkaline

Water (upper plot) and in 6.1-M Na Simulant (lower plot). 100% gas retention reference lines are shown, indicating liquid level change if all generated gas is retained.....	8.31
Figure 8.19. Images of particle-displacing bubbles in the upper portion of the column (left two images), interstitial-liquid displacing bubbles (bottom right-hand image), and bubbles in the transition between these two bubble types (upper right hand image). Ruler shows height in cm above the bottom screen. Image taken about 15 hrs after start of bubble growth with about 6.2% retained gas fraction (see Figure 8.15 Test 10-04 Phase 2).	8.33
Figure 8.20. Close-up image of interstitial-liquid-displacing bubbles at a height of ~ 50 cm above the bottom screen. Image taken about 22 hrs after start of bubble growth with about 6.6% retained gas fraction (see Figure 8.15 Test 10-04 Phase 2).....	8.34
Figure 8.21. Vessel-spanning bubble observed after an initial short period of fluidization where the fluidization pump did not run continuously. Approximately 10 minutes after formation, the VSB released spontaneously (fluidization pump was not running).	8.35
Figure 8.22. Small bubbles, bubbles in channels, and a partial pancake bubble beneath the lower Johnson screen. Image taken about 22 hrs after start of bubble growth with about 6.6% retained gas fraction (see Figure 8.15 Test 10-04 Phase 2).....	8.36
Figure 8.23. Pancake bubble spanning nearly the entire cross section of the column beneath lower Johnson screen. Image taken during fluidization and the openings in the pancake bubble were created by the up flow through the screen.....	8.37
Figure 8.24. Hitchhiker bubbles at the top of the fluidized resin bed (right hand image is expanded view of left hand image). sRF resin particles attached to a bubble would typically rise (upward arrow is an example), reach the upper gas/liquid surface where the gas bubble would coalesce and release the gas to the headspace, then the individual sRF resin particles would fall (downward arrows highlight examples).	8.38
Figure 8.25. Hitchhiker bubbles collecting on the upper Johnson screens during fluidization with withdrawal of liquid through the upper screens.....	8.38
Figure 8.26. Water Bath and <i>In Situ</i> Resin Bed Heating Profiles in Jacketed Graduated Cylinder Tests from a Baseline Pre-GR&R Evaluation Compared to the Consistent Measured Water Bath Temperatures in GR&R Tests MD-09 (0.3-M NaOH) and MD-10 (0.1-M NaOH) Using the Same Amounts of Resin and Liquid and Following the Same Heating Protocol.....	8.40
Figure 8.27. Comparison of (Left y-axis) Water Bath and <i>In Situ</i> Resin Bed Heating Profiles to (Right y-axis) Change in Total Volume (Supernatant Liquid Level) in a Nominally “Gas-Free” Baseline Pre-GR&R Jacketed Cylinder Test with sRF Resin in Alkaline Water (Initial Volumes: 110 mL Resin Bed and 160 mL Total). The estimated minimum and maximum volume expansion due to decrease in water density at 55 °C are shown for reference.	8.42
Figure 8.28. Apparent “Retained Gas”, Apparent “Generated Gas”, and Change in Resin Bed Volumes as a Function of Elapsed Time from the Start of Heating to 55 °C for sRF Resin in 0.3-M NaOH (Test MD-09). Cooling was started at 46-hours ET. Volumes are shown adjacent to select key or representative data points. Downward vertical arrows and negative values at ~50-hours and 66-hours ET indicate changes in volume upon cooling.....	8.45
Figure 8.29. Apparent “Retained Gas”, Apparent “Generated Gas”, and Change in Resin Bed Volumes as a Function of Elapsed Time from the Start of Heating to 55 °C for sRF Resin in 0.1-M NaOH (Test MD-10). Water bath heating was stopped at 20-hours ET and the system was allowed to cool naturally to room temperature. Measurements made at ambient temperature at an ET of 117 hours are shown on the plot at 25 hours (for convenience). Volumes are shown adjacent to select key or representative data points. Downward vertical arrows and negative values at 25-hours ET indicate changes in volume upon cooling.....	8.46

Figure 8.30. Comparison of “Gas Generation Rates” in Tests at Room Temperature and 55 °C Presented in Terms of (Apparent) Retained Gas Fractions as a Function of Elapsed Time from the Start of Level Measurements..... 8.47

Figure 9.1. Effective Fluidization-Induced Gas Release from sRF Resin in Water with ~50% of Peak (Initial) Retained Gas at Flow Rates Starting Below that for Incipient Fluidization determined in fluidization only tests (2.2 cm/min. at 0.3 gpm, see Table 7.1) shown by: Upper – Retained Gas Fraction as a Function of Time and Fluid Velocity (flow rate); and Lower – Retained Gas as a Fraction of Peak and Resin Bed Expansion vs. Time and Fluid Velocity in Test 10-05 Phase 1A. The defined minimum effective fluidization velocity for gas release (3.0 cm/min. at 0.4 gpm for 3% bed expansion, see Table 7.1 and footnote 4 in Section 9.1 above) and target 3% bed expansion at that flow rate are identified in the lower plot. 9.8

Figure 9.2. Effective Fluidization-Induced Gas Release from sRF Resin in 6.1-M Na Simulant with ~50% of Peak (Initial) Retained Gas at Velocities (0.15 cm/min. and 0.3 cm/min.) Below that for Incipient Fluidization, shown by: Upper – Retained Gas Fraction as a Function of Time and Fluid Velocity (flow rate); and Lower – Retained Gas as a Fraction of Peak and Resin Bed Expansion vs. Time and Fluid Velocity in Test 10-09 Phase 1A. 9.10

Figure 9.3. Quiescent Growth to ~50% of Peak Retained Gas in sRF Resin / Water and Fluidization-Induced Gas Release at the Established Minimum Effective Flow Rate for Gas Release (3.0 cm/min. [0.4 gpm], 3% Bed Expansion Target): Upper – Retained Gas Fraction in the Growth and the Initial and Continuous Fluidization-Induced Gas Release Phases; and Lower – Early Stages of the fiGR&R Period Shown in Terms of Fraction of Peak Retention and Resin Bed Expansion (Test 10-05 Phases 1B and 2). 9.12

Figure 9.4. Retained Gas Fractions During Fluidization-Induced Gas Releases from sRF Resin in Alkaline Water at Flow Rates for 3%, 10%, and 40% Resin Bed Expansion Targets ($v_3 = v_{min} = 3.0$ cm/min., $v_{10} = 4.0$ cm/min., and $v_{40} = 10.0$ cm/min., respectively) with an Initial Gas Fraction of ~50% of Peak Retention (Test 10-05 Phases 1B, 3A, and 3B and Test 10-07 Phase 3). Repeatability is demonstrated at the lowest (minimum effective) flow rate. 9.15

Figure 9.5. Retained Gas Fractions During Fluidization-Induced Gas Releases from sRF Resin in GR&R LAW Simulant at Flow Rates for <3%, 3%, 10%, 40%, and >40% Resin Bed Expansion Targets ($v \leq 0.3$ cm/min., $v_3 = v_{min} = 0.5$ cm/min., $v_{10} = 0.7$ cm/min., $v_{40} = 1.8$ cm/min., and $v = 10.0$ cm/min. [1.34 gpm], respectively) with an Initial Gas Fraction of ~50% of Peak Retention (Test 10-09 Phases 1A, 1B, 3A, 3B, and 6). Times of flow stoppage in on:off cycle Test 10-09 Phase 6 and a step-change in flow rate for Test 10-09 Phase 1A are shown. 9.16

Figure 9.6. Retained Gas Fractions During Fluidization-Induced Gas Releases from sRF Resin in Alkaline Water at Flow Rates for 3% and 40% Resin Bed Expansion Targets ($v_3 = v_{min} = 3.0$ cm/min. and $v_{40} = 10.0$ cm/min.) with an Initial Gas Fraction of ~90% of Peak Retention (Tests 10-06 Phase 3A and 10-07 Phase 2). 9.17

Figure 9.7. Retained Gas Fractions During Fluidization-Induced Gas Releases from sRF Resin in Alkaline Water (upper plot) in GR&R LAW Simulant (lower plot) with Initial Gas Fractions of ~50% and ~90% of Peak Retention at the Flow Rate for 40% Resin Bed Expansion ($v_{40} = 10.0$ cm/min. in water [Tests 10-05 Phase 3B and 10-07 Phase 2] and 1.8 cm/min. in simulant [Tests 10-08 Phase 3 and 10-09 Phase 3B])..... 9.19

Figure 9.8. Retained Gas Fractions During Fluidization-Induced Gas Releases from sRF Resin in Alkaline Water with Varying Initial Gas Fractions (f_a of ~25%, ~50%, and ~90%) at the Identified Minimum Effective Flow Rate for Gas Release and 3% Resin Bed Expansion ($v_3 = v_{min} = 3.0$ cm/min. [Tests 10-05 Phase 1B and 10-06 Phases 1A and 3A])..... 9.20

Figure 9.9. Continuous Gas Release Following an Initial Fluidization-Induced Release Phase at v_{min} (3.0 cm/min.) for sRF Resin in Alkaline Water: Upper – Measured Retained Gas Fraction and Theoretical Gas Fraction if All Generated Gas was Retained, Shown as Liquid Level Increase from Gas-Free; Lower – Fraction of Peak Retention and Resin Bed Expansion Throughout the fiGR&R and coGR&R Phases (y-axis compressed to show detail). Plots show the effects of removing the pancake bubble at the end of the experiment (Test 10-05 Phases 1B and 2). 9.22

Figure 9.10. Continuous Gas Release Following an Initial Fluidization-Induced Release Phase at v_{40} (10.0 cm/min.) for sRF Resin in Alkaline Water: Upper – Measured Retained Gas Fraction and Theoretical Gas Fraction if All Generated Gas was Retained, Shown as Liquid Level Increase from Gas-Free; Lower – Fraction of Peak Retention and Resin Bed Expansion Throughout the fiGR&R and coGR&R Phases. Plots show the effects of clearing the gas/liquid separator and gas release events (Test 10-05 Phases 3B and 4)..... 9.24

Figure 9.11. Continuous Gas Release Following an Initial Fluidization-Induced Release Phase at v_{min} (0.5 cm/min.) for sRF Resin in 6.1-M Na Simulant: Upper – Measured Retained Gas Fraction and Theoretical Gas Fraction if All Generated Gas was Retained, Shown as Liquid Level Increase from Gas-Free; Lower – Fraction of Peak Retention and Resin Bed Expansion Throughout the fiGR&R and coGR&R Phases (y-axis compressed to show detail). Plot shows the times of clearing the gas/liquid separator (Test 10-09 Phases 1B and 2). 9.26

Figure 9.12. Retained Gas Fractions During Continuous Fluidization-Induced Gas Releases from sRF Resin in Alkaline Water at the Established Minimum Effective Flow Rate for Gas Release ($v_{min} = 3.0$ cm/min.) with Initial Gas Fractions of ~25%, ~50%, and ~90% of Peak Retention and at v_{40} (10.0 cm/min.) with Initial $f_a \sim 50\%$ (Tests 10-06 Phases 1A and 2, 10-05 Phases 1B and 2, 10-06 Phases 3A and 4, and 10-05 Phases 3B and 4, respectively)..... 9.27

Figure 9.13. Gas Volumes Generated During Continuous Fluidization-Induced Gas Release Tests with sRF Resin in Alkaline Water (Upper) and in 6.1-M Na Simulant (Lower) Compared to a 1 L/day Gas Generation Rate (equivalent to ~18 L/day in a full-scale IX column) and to the Gas Volume Equivalent of 3.0-cm Gas Retention. Initial retained gas fractions (f_a), fluidization velocities, and Test IDs are shown in the plot legends..... 9.29

Figure 9.14. Gas Release and Resin Bed Expansion During 15 min./45 min. On/Off Fluidization Cycles with sRF Resin in 6.1-M Na Simulant at an Initial Gas Fraction of ~80% of Peak Retention and at the Predicted Off-Normal Event Flow Rate, $v = 10.0$ cm/min. (Test 10-09 Phase 4)..... 9.31

Figure 9.15. Gas Release and Resin Bed Expansion During 15 min./45 min. On/Off Fluidization Cycles with sRF Resin in 6.1-M Na Simulant at an Initial Gas Fraction of ~10% of Peak Retention and at the Predicted Off-Normal Event Flow Rate, $v = 10.0$ cm/min. (Test 10-09 Phase 5)..... 9.32

Figure 9.16. Gas Release and Resin Bed Expansion During 5 min./55 min. On/Off Fluidization Cycles with sRF Resin in 6.1-M Na Simulant at an Initial Gas Fraction of ~50% of Peak Retention and at the Predicted Off-Normal Event Flow Rate, $v = 10.0$ cm/min. (Test 10-09 Phase 6)..... 9.33

Figure 9.17. Gas Release and Resin Bed Expansion During 5 min./10 min. On/Off Fluidization Cycles with sRF Resin in 6.1-M Na Simulant at an Initial Gas Fraction of ~100% of Peak Retention and at the Predicted Off-Normal Event Flow Rate, $v = 10.0$ cm/min. (Test 10-09 Phase 7)..... 9.34

Figure 9.18. Resin Bed Expansion and Upper Packed Bed Formation During 8 min./10 min. On/Off Fluidization Cycles with sRF Resin in 6.1-M Na Simulant at the Predicted Off-

Normal Event Flow Rate, $v = 10.0$ cm/min. (Test 10-09 Phase 7; immediately following six 5 min./10 min. on/off cycles in which gas was released). 9.35

Figure 9.19. Retained Gas Fractions During First Cycles of Cyclic Fluidization-Induced Gas Releases from sRF Resin in 6.1-M Na Simulant with Varying Initial Gas Fractions and On/Off Cycle Durations, All at the Predicted Off-Normal Event Flow Rate, $v = 10.0$ cm/min. (Test 10-09 Phases 4, 5, 6, and 7; see plot legend for on/off cycle periods in minutes and initial gas content as a fraction of peak retention). 9.36

Tables

Table 5.1. Liquid and sRF Resin Particle and Bed Properties in Fluidization-Column Tests	5.6
Table 5.2. Liquid and sRF Resin Bed Properties and Test Parameters in Bench-Scale Tests in Order of Increasing Alkalinity and Density	5.9
Table 5.3. Sample Conditions and Measurement Data for Shear Vane Tests.	5.12
Table 6.1. Components and Instruments for Fluidization Column System Shown in Figure 6.2.....	6.7
Table 6.2. Testing M&TE Specifications and Requirements	6.13
Table 6.3. Test Matrix of Fluidization Column Tests for Gas Retention and Release	6.30
Table 7.1. Fluidization Velocity to Achieve Different Bed Expansion and Upper Bed Height Conditions	7.9
Table 9.1. Sequence and Conditions for Fluidization-Column GR&R Tests Using sRF Resin / Alkaline Water (in Order of Completion).....	9.3
Table 9.2. Sequence and Conditions for Fluidization-Column GR&R Tests Using sRF Resin / 6.1-M Na LAW Simulant (in Order of Completion)	9.5

1.0 Introduction

The Low-Activity Waste Pretreatment System (LAWPS) is being developed to provide treated supernatant liquid from the Hanford tank farms directly to the Low-Activity Waste (LAW) Vitrification Facility at the Hanford Tank Waste Treatment and Immobilization Plant (Ansolabehere 2016). The design and development of the LAWPS is being conducted by Washington River Protection Solutions, LLC. A key process in LAWPS is the removal of radioactive Cs through ion exchange (IX) using spherical resorcinol-formaldehyde (sRF) resin-filled columns.

When loaded with radioactive Cs, radiolysis of water in the LAW liquid will generate hydrogen gas. In normal operations, the generated hydrogen is expected to remain dissolved in the liquid and be continuously removed by liquid flow¹. One accident scenario being evaluated is the loss of liquid flow through the sRF resin bed after it has been loaded with radioactive Cs and hydrogen gas is being generated by radiolysis (Aguilar 2016). For an accident scenario with a loss of flow, hydrogen gas can be retained within the IX column both in the sRF resin bed and below the bottom screen that supports the resin within the column, which creates a hydrogen flammability hazard. Because there is a potential for a large fraction of the retained hydrogen to be released over a short duration as a gas release event, there is a need to quantify the size and rate of potential gas release events. Due to the potential for a large, rapid gas release event, an evaluation of mitigation methods to eliminate the hydrogen hazard is also needed. One method being considered for mitigating the hydrogen hazard during a loss of flow accident is to have a secondary flow system, with two redundant pumps operating in series, that re-circulates liquid upwards through the bed and into a vented break tank where hydrogen gas is released from the liquid and removed by venting the headspace of the break tank. The mechanism for inducing release of gas from the sRF bed is to fluidize the bed, which should allow retained bubbles to rise and be carried to the break tank.

A number of previous studies have evaluated sRF physical and chemical properties, including hydraulic and fluidization behavior, and Brown (2014) provides a literature review of these studies. More recently, Duignan et al. (2016) have also studied the flow behavior of sRF resin slurries and Wilson and Landon (2017) summarize testing, conducted in parallel with the work reported here, of a full-scale LAWPS IX column that included fluidization and limited gas injection studies. Currently, neither the ability of fluidizing a settled sRF bed to release gas nor the quantity of hydrogen gas that can be retained and the corresponding potential for large, rapid gas release events has been tested and evaluated. Accordingly, the purpose of this study was to conduct experiments and develop models that evaluate the ability of a re-circulating flow system to fluidize an sRF resin bed as a method to release retained hydrogen gas and maintain hydrogen gas retention at low levels, thereby avoiding conditions where hydrogen gas poses a flammability hazard. The sRF resin particles exchange cations (H^+ , Na^+), depending on the solution composition that has been in contact with the resin, and this causes the sRF particles to change diameter and density, which then affects fluidization behavior. According, sRF resin needs to be equilibrated with the potential range of fluids as part of the testing. The purpose of the testing was also to determine if effective hydrogen gas release would occur using a single constant fluidization velocity, because this is the most simple safety system to implement, for all fluid and sRF resin conditions

¹ In Calculation No. 31269-21-CALC-0034, entitled *LAWPS IX Sizing Calculation*, by R Adams dated 1/23/17 that was provided to WRPS, the approach for removing generated hydrogen as dissolved gas by flow through the column is discussed and quantified.

in the column (because a velocity that is effective for one fluid/resin pair can be ineffective for different resin/fluid pairs). Finally, the study also included quantifying the volume of gas that can be retained in an sRF bed and the behavior of spontaneous, rather than fluidization-induced, gas release events.

Figure 1.1 shows a general schematic of the planned full-scale sRF resin IX bed and the conceptual configuration of a break tank for removal of hydrogen gas that might be released from the IX column (Aguilar 2016). The dimensions and components shown in Figure 1.1 were used to design the laboratory column for conducting gas retention, gas release, and fluidization studies with sRF resin. Note that recirculation through a break tank, as depicted in Figure 1.1, was not implemented in the current study, although a headspace was used in the laboratory column to allow gas release. Ansolabehere (2016) defines the range of LAW feed physical properties that need to be considered when evaluating gas retention and release and fluidization and also gives a temperature range for the LAW feed of 20-45 °C. For testing, WRPS requested that 55 °C be used as a bounding upper temperature limit that accounts for an increase in temperature during a loss of flow accident condition and further assumed a 12 hr duration for the loss of flow before the fluidization system for hydrogen gas release would be started¹. Accordingly, testing at 55 °C will include holding the sRF resin at this temperature for this duration prior to conducting fluidization testing for gas release behavior. In addition to LAW feed solutions, conditioning and re-generation of the sRF resin will use nitric acid and sodium hydroxide solutions and rinse water (Aguilar 2016). These fluids also need to be evaluated as part of the testing.

Figure 1.1 shows two pumps being used in series for the planned system for fluidizing the sRF bed to release hydrogen gas (Wilson and Landon 2017). The two pump system gives redundancy for this safety system and the two pumps are intended to be run simultaneously. In the event one of the pumps failed the second pump would still operate but would provide less flow for fluidization. Wilson and Landon (2017) measured the flow from a full-scale prototype of this system and found that two-pump operation provides ~ 30 gpm flow and when a single pump was operating the flow was reduced to ~21 gpm. Should the two-pump gas release system be used, the fluidization velocity provided by a single pump needs to be sufficient to fluidize the sRF bed and release hydrogen gas. As discussed below in Section 7.1, the most difficult to fluidize sRF resin/ liquid pair is sRF resin in alkaline water that rises in temperature to 55 °C, primarily because the viscosity of the hot alkaline water is low compared with other more viscous LAW solutions. The intention of the system is to operate continuously at a single fluidization velocity, though periodic on:off operation where the fluidization pumps are run followed by a settling period was considered in this study. When operating continuously at the flow sufficient to fluidize the sRF bed with the most difficult to fluidize fluid, consideration must also be made for what happens when sRF resin is fluidized in the more viscous LAW solutions. For the more viscous solutions, the potential exists for the sRF resin particles to be pushed upward and form an upper packed bed at the top of the IX column. This behavior was also quantified in the current study.

In Section 1.1 below, a summary is given of previous studies of gas retention and release with an emphasis on bubble retention and gas release mechanisms. Section 1.2 gives a summary of previous gas generation methods used for laboratory studies and Section 2.0 gives the objectives of the current study. Quality assurance requirements are given in Section 3.0. Section 4.0 gives background information and the technical approach for measuring sRF particle properties and fluidization modeling, Section 5.0

¹ In an e-mail from Matthew Landon of WRPS to Philip Schonewill on May 9, 2016, PNNL was directed to use 55 °C as the upper temperature limit for testing and this assumed a 12 hr duration for loss of flow.

summarizes the selection basis of simulants and the properties of the sRF resin and liquid simulants used in the testing, and Section 6.0 summarizes the experimental and analysis methods and the test matrix. Sections 7.0, 8.0, and 9.0 give the results of the study and Section 10.0 summarizes the key conclusions.

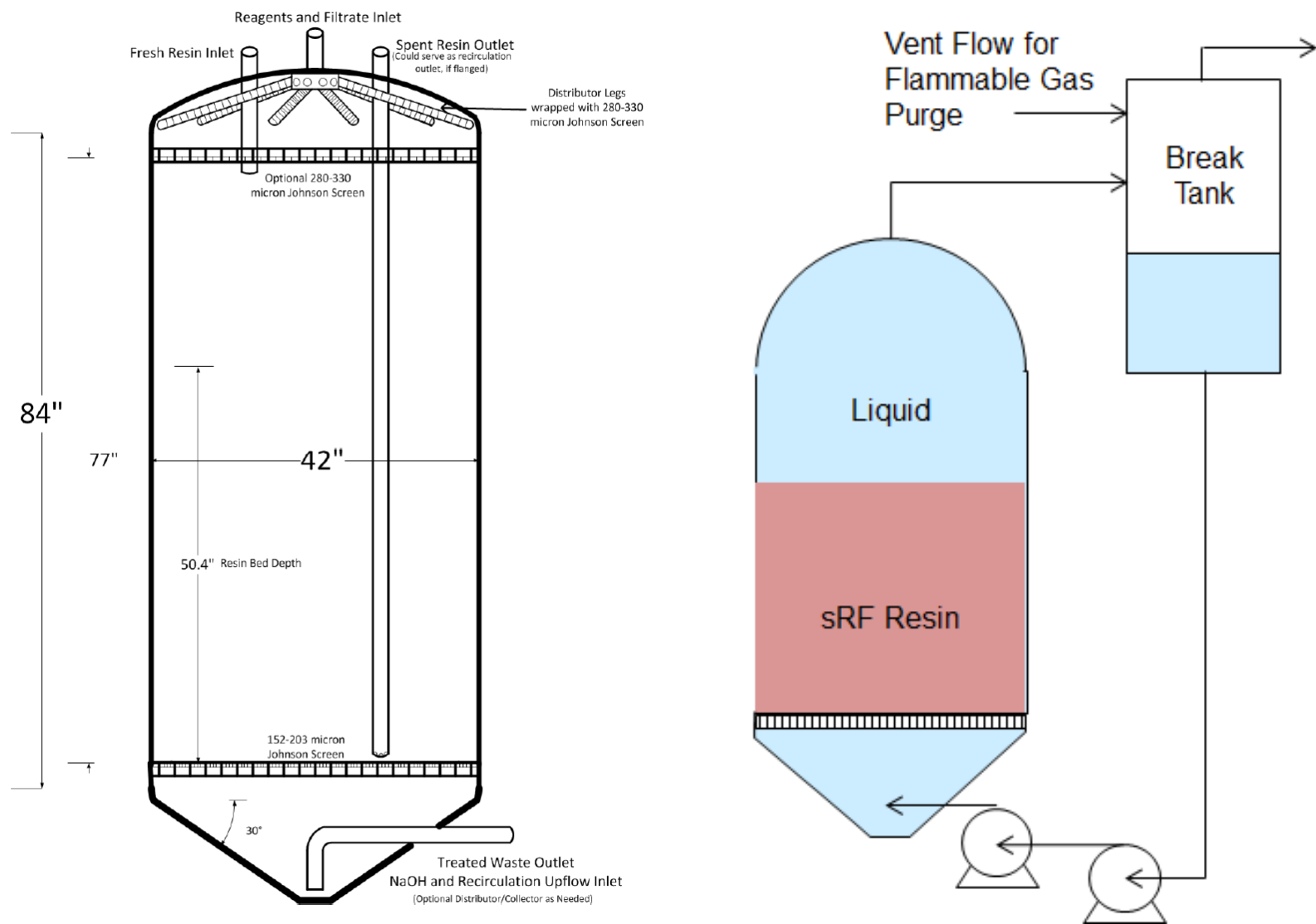


Figure 1.1. Planned full-scale sRF resin IX bed and conceptual configuration of a break tank for removal of flammable gases with resin bed fluidization (Aguilar 2016). Note that the break tank depicted in this conceptual configuration is not considered in the current laboratory study.

1.1 Previous Studies of Gas Retention and Release

Gauglitz et al. (2009) and Schonewill et al. (2014) summarize previous studies of gas retention and release, including discussions of different bubble retention mechanisms that were originally described by Gauglitz et al. (1994). The principal mechanisms of bubble retention can be grouped into three categories:

- particle-displacing bubbles retained by the surrounding bed of particles
- interstitial-liquid-displacing bubbles retained between particles by capillary forces
- bubbles retained by direct attachment to particles, which have previously been called hitchhiker bubbles (Peurrung et al. 1998) and/or armored bubbles (Gauglitz et al. 1994)

Figure 1.2 shows representative configurations of bubbles retained by these three mechanisms. For settled beds of relatively large particles, such as sRF resin beads, particle-displacing and interstitial-liquid-displacing bubbles are the primary two retained bubble types. Typically, there is a transition between particle-displacing bubbles in the upper region and interstitial-liquid-displacing bubbles in the lower region of a settled bed with retained gas. Gauglitz et al. (2009) summarizes previous work on estimating the depth for the transition between the two types of bubbles. In the current study, we will not evaluate the transition depth, but we will seek to observe the retention mechanisms and whether this transition can be identified. Recognizing the presence of these two types of bubbles is helpful for interpreting gas retention results. Specifically, for interstitial-liquid-displacing bubbles, liquid is expelled from the bed, causing a rise in liquid level, but the sRF resin bed itself does not expand. In contrast, particle-displacing bubbles displace both particles and liquid, and this causes expansion of the sRF resin bed together with a rise in liquid level. Hitchhiker bubbles were not anticipated with settled and fluidized sRF resin particles, but they were observed in a few experiments as described below in Section 8.3.

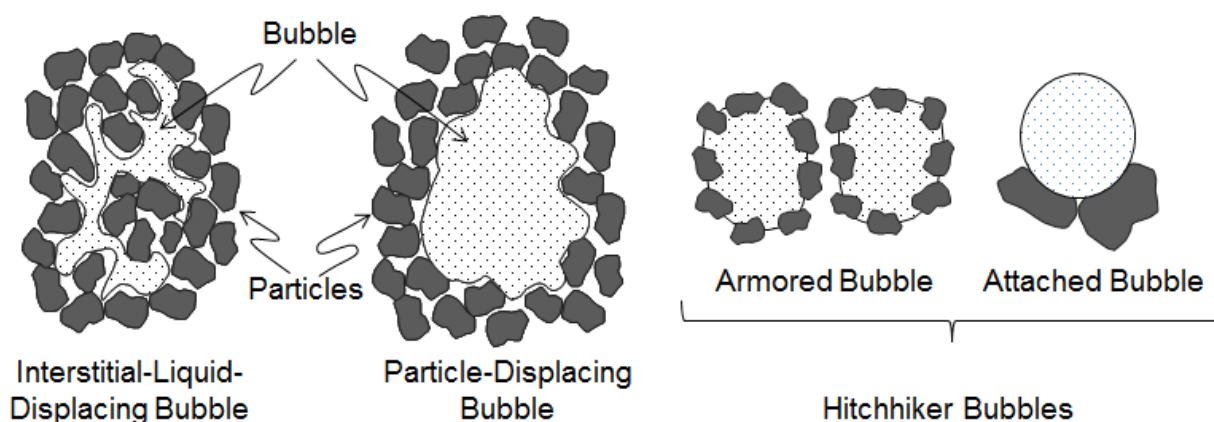


Figure 1.2. Interstitial-liquid-displacing, particle-displacing, and hitchhiker bubbles

With regards to gas retention by interstitial-liquid-displacing and particle-displacing bubbles in sRF resin beds, previous studies of gas retention in glass bead packs are insightful. In approximately 15-cm deep beds of spherical glass beads saturated in water, Gauglitz et al. (1995) observed that gas was

retained predominantly as dendritic interstitial-liquid-displacing bubbles for 1-mm (1000- μm) nominal diameter beads, primarily as particle-displacing-bubbles for 0.2-mm and smaller spheres, and as a combination of the bubble types with 0.5-mm glass beads. Similarly, a mixture of particle-displacing and interstitial-liquid displacing bubble types would be expected for the $>400\text{-}\mu\text{m}$ (0.4-mm) diameter (Section 5.3.1) spherical sRF resin beads, depending on resin bed depth, as noted above, and other factors including liquid and resin bed densities (Gauglitz et al. 1995, Rassat et al. 1997).

The bottom screen, as indicated in Figure 1.1, is intended to be a Johnson screen (Johnson Screens, Aqseptence Group, Inc., New Brighton, MN), which is composed of vee-shaped wires (Vee-Wire[®]) supported by rods with uniform slots between the wires. Figure 1.3 shows a typical configuration of a Johnson screen. Figure 1.3 also shows the configuration of gas as it necks into the slots between the wires from below the screen, forming multiple individual bubble fronts. The surface tension between the gas and liquid creates a capillary force that resists the movement of a gas bubble front through these narrow openings. Because of the capillary force, a large bubble can easily be held below the bottom screen. The potential for trapping gas below the bottom Johnson screen had previously been identified in studies supporting the IX columns in the WTP¹, and the potential quantity of gas that might be retained below the bottom screen was studied in a companion effort (Gauglitz et al. 2018) to the work described in this report. When bubbles beneath a slotted screen expand and connect they can form a large and flat bubble that spans most or all of the cross section of the column. This type of bubble can be described as a pancake bubble. In their analysis, Gauglitz et al. determined that 9- to 10-cm-thick pancake bubbles could form below the Johnson screen for fluids of composition representative of those used in this GR&R testing. Bubbles of this height and smaller should be restrained by and “retained” beneath the screen, such that the gas does not impart an upward buoyant force on the resin bed above it in the way that bubbles retained in the resin bed would.

Figure 1.4 shows a simplified configuration of an IX column and the location of retained gas as bubbles in the sRF resin bed and as a pancake bubble below the bottom screen. A different amount of level increase in the sRF resin and the liquid are shown as an example of having both particle-displacing bubbles and interstitial-liquid-displacing bubbles.

The final bubble type that can be retained in beds of particles is a vessel-spanning bubble (VSB), which for the current study is considered an experimental artifact that occurs when conducting gas retention tests in columns with sufficiently small diameters. Previous studies by Epstein and Gauglitz (2010) and Gauglitz et al. (2010) have shown that smaller diameter columns are more able to retain VSBs. Small-diameter columns are more susceptible to stable VSBs, in part, because the wall surface area in the column (per unit volume) is inversely proportional to column diameter for beds of fixed depth, resulting in relatively greater wall-friction resistance to gas release. For sufficiently large column diameters, a gas pocket that seeks to span the cross section of the column will be released. When conducting experiments, the presence of VSBs needs to be noted and the volume of retained gas will be affected by them.

¹ M Thorson discussed this topic with PA Gauglitz in 2007 and a few experimental and modeling results were conducted at that time demonstrating the retention of bubbles below slotted screens. A WTP memorandum (CCN 238984) entitled “WTP Ion Exchange Column Design Document” and dated October 27, 2011 consolidated information on this topic.

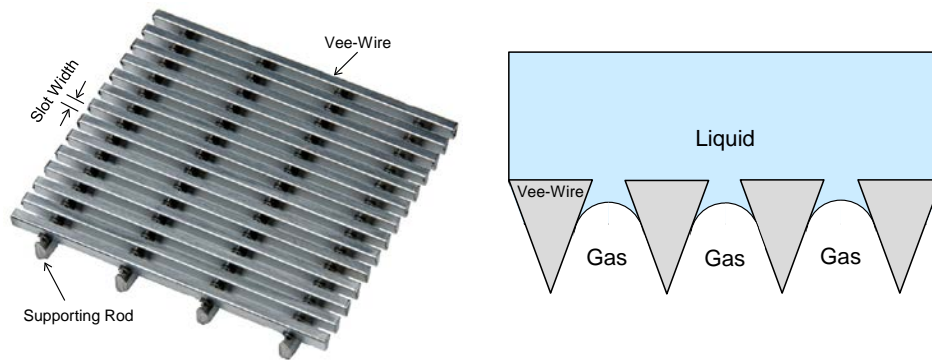


Figure 1.3. Top-view of a Vee-Wire[®] Johnson screen and side-view of gas necking through the slots in the screen.

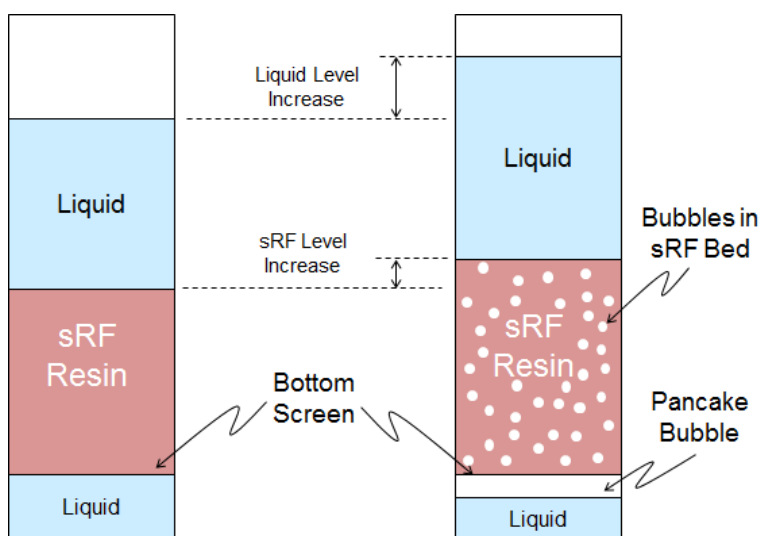


Figure 1.4. Simplified configuration of an IX column without (left) and with retained gas (right).

As the volume of retained gas increases in a bed of resin, a point will eventually be reached at which a spontaneous gas release occurs. The retained gas volume is typically at a maximum just prior to the spontaneous release. The releases can be small and steady, essentially matching the rate of gas generation, or they can be fast and release a large fraction of the retained gas. One example of a slow and steady release is individual bubbles becoming sufficiently large such that their buoyant force causes them to rise and be released (Stewart et al. 1996). A second example of a slow and steady release is bubbles that interconnect and form continuous channels for gas to percolate through the bed (Gauglitz et al. 1996; Stewart et al. 1996; Schonewill et al. 2014). For example, in a follow-up evaluation of the gas retention test data with spherical glass beads noted above, Gauglitz et al. (1996) reported a maximum retained gas fraction of 8.3 vol% for the 1.0-mm beads. Considering that the bubbles were primarily dendritic, the maximum gas fraction is an indicator of the percolation threshold above which connected gas channels allowed gas to be transported through the packed bed. This more generally suggests a possible limitation on retained gas fraction at the point of spontaneous release for gas retained by interstitial-liquid-displacing bubbles. There are two primary types of large spontaneous releases. One mechanism is a buoyant displacement that occurs when a settled bed with retained gas is neutrally buoyant in the

supernatant liquid (Stewart et al. 1996; Meyer et al. 1997) and the settled bed rises and releases its gas. A second primary type of large spontaneous release is a bubble cascade (Gauglitz et al. 2015). This mechanism typically occurs in weaker settled beds where the small motion of one bubble disturbs the bed sufficiently to cause other bubbles to move that further disturb the bed causing yet more bubbles to move and be released. When conducting gas retention and release tests with beds of sRF resin, it is useful to make observations to determine if the mechanism(s) of gas release is (are) similar to any of these previously observed gas release mechanisms.

1.2 Gas Generation Methods and Rates for Experimental Studies

For evaluating gas retention and release mechanisms in sRF resin beds, the preferred method of generating retained gas bubbles is to generate gas in situ because this mimics the radiolytic generation of hydrogen gas. A number of different methods of in situ gas generation have been developed in previous studies. These existing methods were evaluated with sRF resin during preliminary studies¹, but they were found to be unsuitable for the planned gas retention and release studies. The methods investigated include:

- 1) Hydrogen peroxide decomposition to generate oxygen gas (see for example Gauglitz et al. 1996, 2015) – This method did not work, because, it is suspected, the sRF resin consumed the generated oxygen.
- 2) Addition of reactive metal powder that corrodes to form hydrogen gas (see, for example, Gauglitz et al. 2012, Schonewill et al. 2014 for iron powder) – Iron powder does not react to generate hydrogen gas until the pH is acidic, so this metal not suitable for alkaline water or LAW simulant solutions. Aluminum powder was also evaluated, because it is reactive in alkaline solutions; however, it was determined that the reaction rate was too fast if the pH was greater than about 10, which is too low for Na⁺ form sRF resin conditions. Further, the aluminum powder was expected to become non-uniformly distributed in the sRF resin bed during both settling and fluidization test steps, and it might lead to plugging of the bottom Johnson screen. The maldistribution would also make test results difficult to interpret and not representative of uniform radiolytic hydrogen generation.
- 3) Applying a vacuum to the top of the column to nucleate and grow bubbles with or without the addition of a soluble gas (see for example Rassat et al. 1998, Gauglitz et al. 1996) – This method had previously been used successfully with small (short) samples. For the planned fluidization column, the difference in hydrostatic head from top to bottom in the resin bed was expected to result in non-uniform generation of gas bubbles (volumetrically) when a vacuum was applied. Further, because of the reduction in gas solubility in LAW simulant solutions due to the high concentration of dissolved salts, it was difficult to generate enough in situ gas by this method. Nitrous oxide (considered previously by Rassat et al. 1998) and trifluoromethane were both evaluated with preliminary sparging to increase the concentration of the relatively-soluble gases. Carbon dioxide was not tested, because it was expected to react with the alkaline LAW simulant solutions to form an insoluble carbonate.

¹ The preliminary studies did not follow the full requirements of the QA program outlined in Section 3.0 and should be considered For Information Only.

Because these previous methods were not suitable for testing gas retention and release with sRF resin in a full-height test column and with LAW simulants, a new method was developed. The method is based on the hydrolysis of sodium borohydride (SBH), which is a water soluble salt, to form hydrogen gas. The rate of hydrogen generation can be controlled by SBH concentration and to some extent by pH adjustments in the alkaline conditions needed for the tests, the reaction rate was suitable for laboratory testing (tests spanning a few hours to a day), and the SBH was completely dissolved and thus uniformly distributed within the sRF bed. Details of this method are described further in Section 6.4, and gas generation test results are discussed in Section 8.1.

In addition to the need to be experimentally practicable, gas generation rates are of interest for comparison to those expected in a full-scale ion exchange column. The main goal of continuous gas retention and release tests reported here is to evaluate steady-state gas holdup (retained gas fraction, α_{ss}) during “long-term” constant-velocity fluidization with continuous gas generation. In previous studies, the steady-state gas holdup in continuously mixed non-Newtonian fluids, such as Hanford tank waste simulants with pulse jet mixers, has been shown to be a linear function of the gas generation rate for rates greatly exceeding those of actual waste (e.g., Russell et al. 2005). Therefore, scaled gas generation rates in continuous-GR&R tests greater than or equal to the maximum generation rate expected from sRF resin in a full-scale plant should conservatively (over)estimate α_{ss} . Using experimental hydrogen gas generation rate (HGR) data collected at 25 °C for sRF resin in water, Colburn et al. (2018) provide a model-based estimate of the maximum HGR at 45 °C in the case of the expected upper-bounding dose rate in a full-scale ion exchange column. From these data, a maximum HGR of 14 L/day (at 25 °C and 1 atm) for a full-scale column is estimated, and the volumetrically-scaled gas generation rate in the 10-in. diameter fluidization-column test configuration used in this work is 0.8 L/day.¹

¹ Colburn et al. (2018) measured hydrogen generation rates in water (alkaline), 5.6 M sodium LAW simulant, and 0.45 M nitric acid without and with sRF resin at temperatures of 25, 45, and 70 °C. The highest HGR was for sRF resin/water at 25 °C. At an expected bounding dose rate of 43 krad/hr in a full-scale ion exchange column, the 25 °C data resulted in a model-based estimate of the maximum HGR at 45 °C of 4.52×10^{-4} mol H₂/kg liq.·day (Table 5.4 in Section 5.4 of Colburn et al.). The water experiments were conducted with a liquid-saturated sRF resin bed of 30 mL containing (a maximum) 32.7 g of water (in replicate #1 at 25 °C; Table 4.4 in Section 4.6.1 of Colburn et al.), which gives a resin-volume-specific HGR of 4.93×10^{-4} mol H₂/L resin·day (= 4.52×10^{-4} mol H₂/kg liq.·day \times 32.7-g liq. \times 1 kg/1000 g \div 30-mL resin \times 1 L/1000 mL). Scaling based on resin volume, the generation rate in a nominal 10-in. (25.4 cm) diameter test vessel with 50.4-in. (128 cm) resin depth (resin volume = 64.9 L = $\pi[25.4 \text{ cm}]^2/4 \times 128 \text{ cm} \times 1 \text{ L}/1000 \text{ cm}^3$) is 0.0320 mol H₂/day (= 4.93×10^{-4} mol H₂/L resin·day \times 64.9 L), which corresponds to 0.78 L/day at 25 °C and 1-atm pressure from the ideal gas law (= 0.0320 mol H₂/day \times 0.08206 L·atm/mol·K \times 298.15 K/1 atm). Again scaling volumetrically, the equivalent HGR in a 42-in. diameter full-scale column with a 50.4-in. deep resin bed is 13.8 L/day (= 0.78 L/day \times [42 in./10 in.]²).

2.0 Objectives

The overall objective of this study is to quantify the gas retention and release (GR&R) characteristics of prototypic beds of sRF resin for both spontaneous gas releases and releases induced by bed fluidization. Fluids with a range of densities and viscosities are expected during waste processing and regeneration of the sRF resin, and the sRF may be in either Na^+ or H^+ form, so the testing needs to quantify the role of fluid properties and sRF resin properties in gas retention and release behavior and gas release by fluidization. The information on gas retention and release behavior will be used by WRPS to support design activities for the fluid recirculation/bed fluidization system and the break tank for managing the potential hazard of hydrogen gas accumulation in the LAWPS equipment. The specific objectives for gas retention and release task are:

- Quantify the fluidization behavior of sRF resin, specifically bed expansion and upper bed formation as a function of fluidization velocity, for fluid and sRF properties that span the expected ranges for LAW feed and regeneration fluids.
- Quantify gas retention behavior, including peak gas retention at the onset of spontaneous gas release, of beds of Na^+ form sRF resin in alkaline water and in a LAW simulant with a target density of 1.25 g/mL.
- Quantify how fluidization of an sRF bed with retained gas releases the gas, the minimum velocity for effective gas release, and whether continuous fluidization releases gas as it is being generated.
- Determine the most difficult to fluidize (highest fluidization velocity) combination of sRF resin form (H^+ or Na^+) and fluid and sRF resin properties. Determine the fluidization velocity needed to release gas from the worst case condition and then estimate the fluidization velocity that would be used if two pumps were operated in series as part of having redundant pumps in a safety system for releasing hydrogen gas.
- Additional studies will be conducted to develop recipes for using SBH to generate gas in beds of sRF resin and evaluate whether vessel-spanning bubbles will be an issue in planned column testing.
- Evaluate sRF resin for changes in settled bed behavior when held at temperatures up to 70 °C.

3.0 Quality Assurance

This work was conducted with funding from WRPS under contract 36437-187, “*LAWPS Integrated Support Testing*,” *Low-Activity Waste Pretreatment System (LAWPS) Integrated Testing Project*. The work was conducted as part of Pacific Northwest National Laboratory (PNNL) project 67535.

All research and development (R&D) work at PNNL is performed in accordance with PNNL’s Laboratory-Level Quality Management Program, which is based on a graded application of NQA-1-2000, *Quality Assurance Requirements for Nuclear Facility Applications*, to R&D activities. To ensure that all client QA expectations were addressed, the QA controls of the WRPS Waste Form Testing Program (WWFTP) QA program were also implemented for this work. The WWFTP QA program implements the requirements of NQA-1-2008, *Quality Assurance Requirements for Nuclear Facility Applications*, and NQA-1a-2009, *Addenda to ASME NQA-1–2008*, and consists of the *WWFTP Quality Assurance Plan* (QA-WWFTP-001) and associated QA-NSLW-numbered procedures that provide detailed instructions for implementing NQA-1 requirements for R&D work.

Specific details of this project’s approach to assuring quality are contained in the *LAWPS Testing Program Quality Assurance Plan* (67535-QA-001, Rev. 0) and associated implementing procedures. The QA plan describes how the procedures of the WWFTP QA program were used in conducting the work. The work described in this report was assigned the technology level “Applied Research,” and was planned, performed, documented, and reported in accordance with procedure QA-NSLW-1102, *Scientific Investigation for Applied Research*. All staff members contributing to the work received proper technical and QA training prior to performing quality-affecting work.

4.0 Background and Technical Approach for measuring sRF Particle Properties and Fluidization Modeling

The gas retention and release and fluidization testing were designed to quantify the gas retention and release (GR&R) characteristics of prototypic beds of sRF resin for both spontaneous gas releases and releases induced by bed fluidization. An important element of developing an understanding of gas release during fluidization is the fluidization behavior of the sRF resin in different fluids. To support developing an understanding of fluidization and to estimate fluidization behavior of fluids not tested, models of fluidization behavior were developed to compare with test data and measurement were made to determine the model inputs, such sRF particle diameter and density. Gas retention and release also depends on sRF particle density and diameter, and the measurement of sRF particle properties is important for addressing this testing objective. Section 4.1 summarizes how the sRF resin particle density and diameter were measured on samples and also how estimates of the sRF particle density were obtained from mass and volume measurements on settled beds in the test columns. Section 4.2 presents models for bed expansion and upper packed bed formation during fluidization, and resin hindered settling.

4.1 sRF Resin Particle and Bed Properties

As will be discussed in Section 4.2, fluidization, upper bed formation, and settling models depend on a number of liquid, sRF particle (resin bead), and resin bed physical properties. For comparison to results obtained in this work and as a general overview of historic measurements, the sRF resin literature was surveyed and reported properties are summarized in this section. Key model parameters include the density and diameter of particles (resin beads). Measurement methods for these two primary resin particle properties are presented in the first subsection along with the literature review. The fluidization models also depend on the bulk resin bed void fraction (porosity). Void fractions of the sRF resin beds used in testing were not measured directly, but they can be, and were, estimated from other measured values – the interrelationship of bed porosity, particle and liquid densities, and measured resin bed density are discussed in the second subsection. The resin bed density measurement method is also described. Properties measured in this work are presented in Section 5.3.

4.1.1 Primary Particle Properties – Density and Diameter

Individual resin beads are porous and their density varies with the chemistry and density of the liquid, ρ_L , in which they are contacted, equilibrated, and internally saturated. Fundamentally, the bead (particle) density, ρ_p , is a function of the internal (intrastitial) particle porosity, ε_p , the skeletal density of the solid RF resin in the bead, ρ_s , and the liquid density, as follows

$$\rho_p = \rho_s(1 - \varepsilon_p) + \rho_L\varepsilon_p \quad (4.1)$$

sRF particle porosity data for all operating conditions of interest are not readily available, but values can be estimated from skeletal density and other measured and reported resin properties:

$$\varepsilon_p = 1 - \frac{(1 - \varepsilon_t)}{(1 - \varepsilon_b)} = 1 - \frac{\rho_{db}/\rho_s}{(1 - \varepsilon_b)} \quad (4.2)$$

Equation (4.2) shows that ε_p can be written in terms of the resin bed interstitial void fraction (bed porosity), ε_b , and the total porosity of the resin bed, ε_t , both inter- and intra-particle. In the right-hand form of the equation, the solids volume fraction in the bulk resin bed, $1 - \varepsilon_t$, is written as the ratio of the dry resin bed density, ρ_{db} , to the skeletal density.

Following is a summary of information and literature data sources for relevant sRF resin particle (Microbeads AS, Skedsmokorset, Norway) and bed properties in Na^+ - and H^+ -forms from prior studies:

D_p – Typical H^+ -form bead diameters are 421-427 μm , and Na^+ -form bead diameters are 452-461 μm ; see, for example, Fiskum et al. (2006a), Nash et al. (2006), and Adamson (2009). The ratio of bead volumes derived from these diameters is consistent with resin bed volume changes when cycling between H^+ - and Na^+ -forms. Measured particle diameters for Na^+ - and H^+ -form sRF resin used in this work are summarized in Table 5.1 in Section 5.3.1, and the reported measurement standard deviations indicate that the beads are monodisperse.

ρ_s – Representative skeletal resin densities are in the range of 1.47-1.54 g/mL for H^+ -form and 1.59-1.64 g/mL for Na^+ -form (Fiskum et al. 2006b, and Adamson et al. 2006). Higher Na^+ -form density is attributed to affiliation of higher-mass sodium ions with the RF, which dominates over density reduction associated with resin swelling upon conversion from H^+ - to Na^+ -form.

ρ_{db} – Dry resin bed densities from vacuum-oven drying tests are variously reported in three combinations of hydrogen- and sodium-form for the ratios of mass of dried resin (numerator) and volume of resin bed before drying (denominator):¹ H/H, H/Na, and Na/Na, with the first two appearing more commonly in reports. Typical H/H ρ_{db} values are 0.34-0.369 g/mL (e.g., Fiskum et al. 2006a, 2006b; and Nash et al. 2006), but Brown et al. (2011) achieved a higher H/H density (0.456 g/mL) by repeatedly tap-vibrating the graduated cylinder containing the sample. All else equal, the difference in these two H/H ρ_{db} ranges (subscript 1, low and subscript 2, high) is related to a difference in void fraction in the settled resin beds: from Eq. (4.2), $\varepsilon_{b,2} = 1 - \rho_{db,2}/\rho_{db,1} \times (1 - \varepsilon_{b,1})$. Using 0.369 g/mL as the lower density, 0.456 g/mL as the higher density, and assuming $\varepsilon_{b,1} = 0.42$, then $\varepsilon_{b,2}$ is a very low 0.28 (see the ε_b bullet below). Representative H/Na ρ_{db} values are 0.25-0.26 g/mL (e.g., Fiskum et al. 2006c; Nash et al. 2006). The volume change associated with swelling of resin during cycling from H^+ - to Na^+ -form (after initial processing) is given by the ratio of H/H ρ_{db} and H/Na ρ_{db} . Fiskum et al. (2006b) report Na/Na ρ_{db} values of 0.367-0.376 g/mL (for the newest “Wave 4” resin samples they reported on). Nash et al. (2006) specify an I-factor of 1.25 to relate the ratio of masses of resin in Na^+ - and H^+ -forms. Aleman et al. (2007) and Smith et al. (2009) applied (multiplied) this I-factor to H/Na ρ_{db} values to convert them to Na/Na ρ_{db} equivalents and subsequently estimated Na^+ -form particle porosity from Eq. (4.2).

ε_b – In modeling studies, Aleman et al. (2007) (and similarly Smith et al. (2009)) used a “drainable” RF resin bed void fraction of 0.42 (citing a personal communication). Because some liquid would likely be retained between resin particles by capillary forces in gravity draining, 0.42 may underestimate ε_b for sRF. Fiskum et al. (2004) reported duplicate bed void measurements of 0.36 and 0.39 for an sRF resin variant (#3). Current sRF resin batches are relatively monodisperse (uniformly sized). The highest packing density for monodisperse spheres is a void fraction of 0.26 (0.2595) in a

¹ For example H/H is the mass of hydrogen-form resin divided by the volume of hydrogen-form resin.

rhombohedral- (hexagonal-) close-packed arrangement, and common, less-dense configurations of beds of monodisperse spheres are defined for close random packing (0.359 to 0.375 void), poured random packing (0.375 to 0.391 void), loose random packing (0.40 to 0.41 void), and very loose random packing (~0.44 void) (Dullien 1992). Dullien also notes that the latter occurs, for example, “when the fluid velocity is slowly reduced in a fluidized bed”. Without a means to enhance packing efficiency (e.g., vigorously tapping/vibrating a column, see previous bullet), a naturally settled bed of fluidized sRF resin might be expected to have $\epsilon_b \geq 0.36$, although compressive forces, including the self-weight of the resin bed or down-flow of liquid, and any non-uniformity in bead size could lead to higher packing efficiency and lower void.

As an example, and for the purpose of estimating Na⁺-form bead densities from Eq. (4.1) for comparison to measured values (Section 5.3.1), assume the following nominal resin properties from the tabulation above: $\rho_s = 1.62$ g/mL; Na/Na $\rho_{db} = 0.37$ g/mL; and $\epsilon_b = 0.40$. These values result in a bead porosity of 0.619 from Eq. (4.2), and Na⁺-form particle densities of 1.23 and 1.39 g/mL for beads saturated in alkaline water (0.997 g/mL) and a 6.1-M Na LAW simulant of 1.254-g/mL, respectively.

Several of the combinations of sRF resin and equilibrated liquid used in fluidization testing were unique compared to the systems from which the literature data above were derived. Because of this, and for the purposes of modeling fluidization, upper packed bed, and settling behavior, it was preferred to have measured resin particle properties for each sRF resin/liquid pair rather than assume generalized literature values. Resin particle densities and particle diameters were measured using the following experimental methods, and the results are presented in Section 5.3.1.

The density of sRF resin particles from equilibrated resin/liquid batches were measured with a displacement method (Flint and Flint 2002). For the displacement method: a) the density of the equilibrated liquid (ρ_L), which also serves here as the suspending fluid in later steps, is independently determined using a pycnometer; b) separately, “conditioned” (see below) sRF resin particles are added to a dry pycnometer having a calibrated total volume (V_t) and weighed to give the mass of particles, m_p ; c) the pycnometer is then filled with the suspending liquid and re-weighed to give the total mass of particles and bulk liquid, m_t . From these data, the particle density is determined from the relationship

$$\rho_p = \frac{m_p}{V_p} = \frac{m_p}{V_t - V_L} = \frac{m_p}{V_t - (m_t - m_p)/\rho_L} \quad (4.3)$$

where V_p and V_L are the volumes of particles and suspending liquid, respectively. As shown in the right-hand form of the equation, these volumes do not need to be determined separately or known explicitly. In this experimental approach, the porous sRF resin particles contain the suspending liquid within the particles (i.e., internally saturated) and, initially, on the external surfaces of the particles from prior equilibration in the liquid during preparation of a larger resin batch. Before weighing, the equilibrated and saturated particles were conditioned by removing them from the batch liquid and hand-drying by blotting with absorbent paper until the surface moisture was removed but the particles still contained the internal liquid.

The diameters of sRF resin particles were determined using optical microscopy photographs having a calibrated micro-ruler in the field of view. Twenty particles were randomly selected from the macroscopic images, and the dimensions were measured manually with calibrated calipers. The 20

caliper results were numerically scaled to the micro-ruler length, after which the average particle diameter and standard deviation were calculated.

4.1.2 Initial Resin Bed Properties – Bulk Density and Porosity

For analysis and modeling of test results, sufficient settled resin bed mass, volume, and density data were obtained in most experiments to allow the liquid-saturated resin bed bulk density to be measured and particle density and/or bed porosity to be estimated. The concept is the same for any volume-characterized cylindrical test vessel (e.g., graduated cylinder or test column with an established level-volume correlation) that can be weighed. First, to the extent possible, a gas-free settled bed was established in the test vessel by thoroughly mixing to remove any entrained or previously generated gas bubbles. Preferably, this measurement was made before gas-generating SBH was added or as soon after the bed was settled as possible, if it had been added. The total mass and volume of liquid plus settled resin slurry in the test vessel,¹ m_t and V_t , respectively, and the volume of the settled gas-free resin bed, $V_{b,0}$, were measured. The difference in volumes is the volume of supernatant liquid, $V_L (= V_t - V_{b,0})$. From these data, and the independently measured density of the supernatant liquid that was in equilibrium with the saturated resin slurry (e.g., using a pycnometer or a volumetric flask), the initial density of the settled gas-free resin bed, $\rho_{b,0}$, is calculated by

$$\rho_{b,0} = \frac{m_t - (V_t - V_{b,0})\rho_L}{V_{b,0}} \quad (4.4)$$

In turn, the particle density can be calculated from the bed density and a known or assumed settled gas-free bed void fraction, $\varepsilon_{b,0}$,

$$\rho_p = \frac{\rho_{b,0} - \rho_L \varepsilon_{b,0}}{(1 - \varepsilon_{b,0})} \quad (4.5)$$

or, by rearranging, the bed void fraction can be calculated from measured bed and particle densities,

$$\varepsilon_{b,0} = \frac{\rho_{b,0} - \rho_p}{\rho_L - \rho_p} \quad (4.6)$$

Equation (4.6) shows that bed porosity is related to resin bed, particle, and liquid densities through the ratio of density differences. These differences tend to be small, especially with increasing liquid density, and as such, results are highly sensitive to uncertainty in any of the parameter values.

¹ During initial filling of the fluidization-column with each unique batch of resin/liquid slurry, the floor scale was zeroed when liquid only (no resin) was at the level of the bottom Johnson screen. Mass and volumes of resin/liquid added above the screen were subsequently measured and used to calculate bed density in the manner described. In some tests, the floor scale was zeroed with liquid level readings a few millimeters above the bottom screen. In these cases, the measured total mass was corrected upward for use in Eq. (4.4) by the mass of the liquid initially above the screen (i.e., corrected total mass = measured total mass + volume of liquid initially above zero level \times liquid density).

4.2 Fluidization, Upper Packed Bed Formation, and Settling

This section discusses the approach and resulting equations for models for fluidization bed height as a function of fluidization velocity, the height of an upper packed as a function of fluidization velocity, and the hindered settling velocity of a suspended bed of sRF resin particles. The model for bed height as a function of velocity was developed to compare with experimental data and determined if the experimental system was behaving as expected for a simple system of spherical particles. If the model agrees with the data, it suggests that the model could be used to predict bed expansion behavior for liquids and sRF resin particles with different viscosities and densities. The model for the height of an upper bed was developed for similar reasons; to compare with test data and evaluate if the sRF resin was behaving in a predictable way. This model could also be used for predicting behavior with sRF resin and different fluids, with a likely emphasis on predicting conditions that avoid an upper packed bed. The model for hindered settling was developed to compare with settling data of a fluidized bed of sRF particles when the fluidization velocity is stopped. Hindered settling and fluidization are very similar and the same model (Eq. (4.8) through Eq. (4.12) below) can be used for both. The hindered settling model was developed primarily to evaluate what appeared to be poor agreement between bed expansion test results and the model for the high-limit LAW simulant (15 cP, see Section 5.1). The origin of the poor agreement appears to be that the bed expansion model is very sensitive to the density different between the sRF particles and suspending liquid and the sRF particle density measurement is uncertain (see Section 7.1 and discussion of Figure 7.2).

4.2.1 Fluidization Bed Height

Figure 4.1 shows the configurations of an initial settled bed and a fluidized bed of sRF resin. The porosity of the resin bed, ε_b , is the volume fraction of interstitial liquid (excluding liquid within the internal pores of the sRF resin bead) within a settled or fluidized bed. For a fluidized bed with an initial porosity of $\varepsilon_{b,o}$, the porosity can be expressed as a function of the bed height as follows:

$$\varepsilon_b = \frac{H_b - H_{b,o}(1 - \varepsilon_{b,o})}{H_b} \quad (4.7)$$

where

- H_b = height of fluidized resin bed
- $H_{b,o}$ = resin bed height no fluidization
- ε_b = resin bed interstitial porosity (liquid fraction)
- $\varepsilon_{b,o}$ = resin bed porosity no fluidization

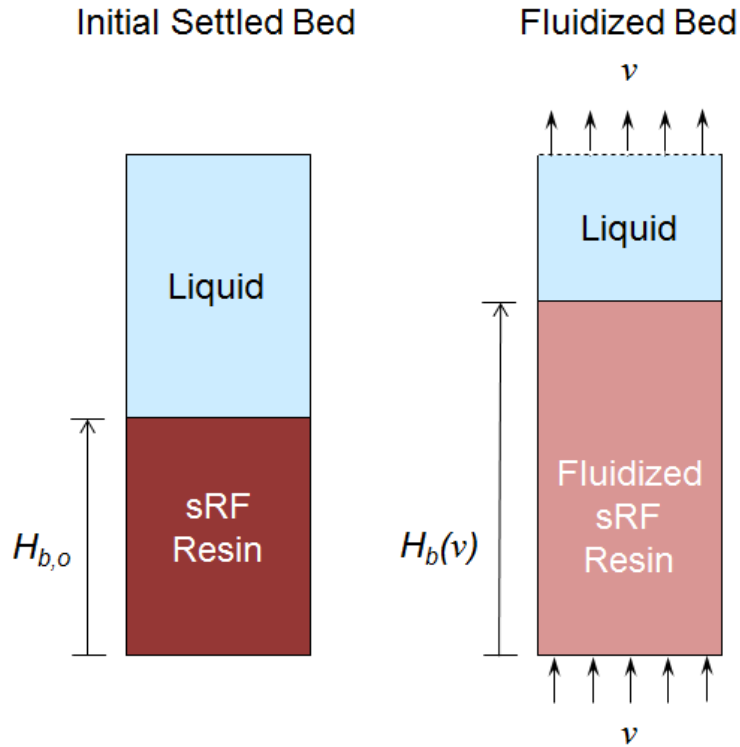


Figure 4.1. Configuration and heights of an initial settled bed and fluidized bed of sRF resin

The height of the resin bed as a function of the fluidization velocity, v , can be estimated from models of fluidization behavior that give bed porosity during fluidization when combined with Eq. (4.7) that relates bed height and porosity. For the bed porosity as a function of the fluidization velocity, Richardson (1971) recommends the following equation:

$$\frac{v}{v_{p,t}} = (\varepsilon_b)^n \quad (4.8)$$

where

- v = superficial velocity of liquid (fluidization velocity)
- $v_{p,t}$ = terminal settling velocity of sRF resin particle
- n = exponent that depends on Reynolds number

This empirical relationship is one of the most simple for predicting bed expansion. Chhabra (1993) and Richardson (1971) discuss the basis and limitations of the model above and alternate models. Both the terminal particle settling velocity $v_{p,t}$ and exponent n depend on the particle Reynolds number at the terminal settling velocity $Re_{p,t}$ (Richardson 1971) which is given by:

$$Re_{p,t} = \frac{\rho_L v_{p,t} D_p}{\mu_L} \quad (4.9)$$

where

- μ_L = liquid viscosity
- ρ_L = liquid density
- D_p = particle diameter

For uniform spherical particles that do not stick to each other and when the particle diameter is much less than the column diameter ($D_p \ll D_c$), Richardson (1971) gives the following expressions for n , after simplification to neglect terms where D_p/D_c is small:

$$\begin{aligned}
 n &= 4.65 & Re_{p,t} < 0.2 \\
 n &= 4.4 Re_{p,t}^{-0.03} & 0.2 < Re_{p,t} < 1 \\
 n &= 4.4 Re_{p,t}^{-0.1} & 1 < Re_{p,t} < 200
 \end{aligned}
 \tag{4.10}$$

For spherical particles, Camenen (2007) provides a convenient expression for the terminal settling velocity as a function of the liquid and particle densities and liquid viscosity that spans from low to high settling velocities (and thus low to high $Re_{p,t}$) (see also Wells et al. 2012):

$$v_{p,t} = \frac{\mu_L}{\rho_L D_p} \left(\sqrt{15 + \sqrt{Ar/0.3}} - \sqrt{15} \right)^2
 \tag{4.11}$$

$$Ar = \frac{\left(\frac{\rho_p}{\rho_L} - 1 \right) g D_p^3}{(\mu_L/\rho_L)^2}
 \tag{4.12}$$

where

- Ar = Archimedes number
- ρ_p = particle density
- g = gravitational acceleration

Rearranging Eq. (4.7) and combining with Eq. (4.8), together with Eqs. (4.9) through (4.12), gives the following result for predicting bed height (expansion) as a function of fluidization velocity:

$$\frac{H_b}{H_{b,o}} = \frac{(1 - \varepsilon_{b,o})}{1 - \left(\frac{v}{v_{p,t}} \right)^{1/n}}
 \tag{4.13}$$

4.2.2 Upper Packed Bed Height

When the fluidization velocity is sufficiently high, the fluidized particles can pack at the top of the column (or top of the liquid when liquid is removed through screens below the surface of the liquid). Figure 4.2 shows the configuration of an initial settled bed of sRF resin and an over-fluidized bed with an upper packed bed of sRF resin. The height of the upper packed bed can be determined by using the fluidization model given by Eqs. (4.8) through (4.12) for the bed porosity in the fluidized region together with a material balance for the sRF resin in the packed bed and the fluidized region. For a column with a cross sectional area of A_c , and the configuration shown in Figure 4.2, a material balance on the volume of sRF resin particles is the following:

$$\left(\begin{array}{c} \text{Initial Volume of} \\ \text{sRF Resin in} \\ \text{Settled Bed} \end{array} \right) = \left(\begin{array}{c} \text{Volume of} \\ \text{sRF Resin in} \\ \text{Fluidized Region} \end{array} \right) + \left(\begin{array}{c} \text{Volume of} \\ \text{sRF Resin in} \\ \text{Upper Packed Bed} \end{array} \right) \quad (4.14)$$

Representing the volume of sRF resin particles with bed heights and porosities gives:

$$\left(\begin{array}{c} \text{Initial Volume of} \\ \text{sRF Resin in} \\ \text{Settled Bed} \end{array} \right) = H_{b,o} A_c (1 - \varepsilon_{b,o}) \quad (4.15)$$

$$\left(\begin{array}{c} \text{Volume of} \\ \text{sRF Resin in} \\ \text{Fluidized Region} \end{array} \right) = (H_c - h_u) A_c (1 - \varepsilon_b) \quad (4.16)$$

$$\left(\begin{array}{c} \text{Volume of} \\ \text{sRF Resin in} \\ \text{Upper Packed Bed} \end{array} \right) = h_u A_c (1 - \varepsilon_{b,o}) \quad (4.17)$$

where

h_u = height of upper packed bed (see Figure 4.2)

Note that Eq. (4.17) assumes the porosity of the upper packed is equal to the initial porosity of the settled bed prior to fluidization ($\varepsilon_{b,o}$). Combining Eqs. (4.14) through (4.17) gives the following result for the height of the upper packed bed as a function of bed porosity:

$$\frac{h_u}{H_{b,o}} = \frac{(1 - \varepsilon_{b,o}) - \frac{H_c}{H_{b,o}} (1 - \varepsilon_b)}{\varepsilon_b - \varepsilon_{b,o}} \quad (4.18)$$

This result, together with Eqs. (4.8) through (4.12) for the porosity of the bed during fluidization, gives the model for predicting the upper bed height as a function of fluidization velocity, fluid and sRF particle properties, and the initial bed porosity and column height. Results from this model are obtained by selecting a fluidization velocity (sufficiently high to give a positive value for h_u) and using Eq. (4.8) to determine ε_b . The other parameters in Eq. (4.18) are known initial conditions and the column height H_c .

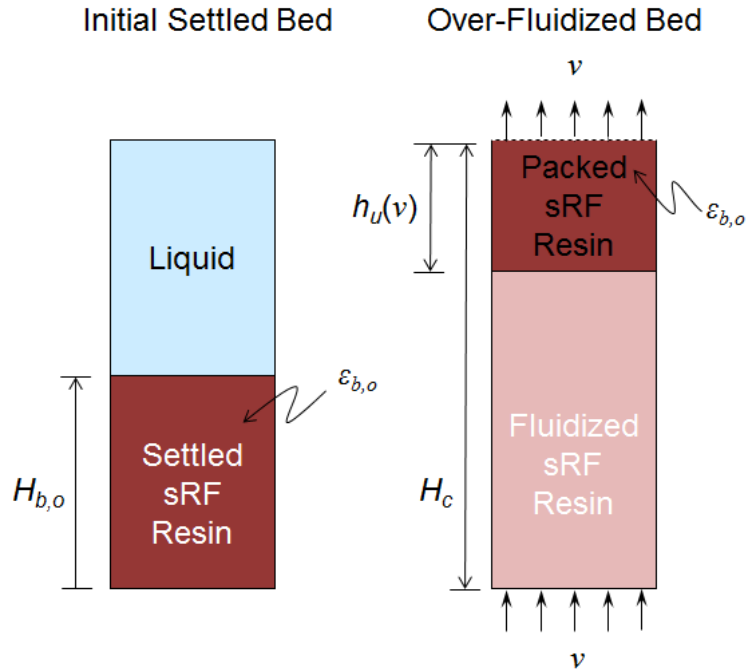


Figure 4.2. Configuration and heights of an initial bed and an over-fluidized bed with a packed upper bed of sRF resin

4.2.3 Hindered Settling Velocity

The settling behavior of a suspended bed of sRF particles, after fluidization is stopped, can provide additional information on the behavior of the sRF particles. For hindered settling, Eq. (4.8) gives the hindered settling velocity of suspended sRF particles as a function of the bed porosity and the constant n [see Eq. (4.10)] (Richardson 1971) and Eq. (4.7) gives the bed porosity at the beginning of settling in terms of height of the suspended bed. Combining these equations gives the following results for the hindered settling velocity:

$$v_{hs} = v_{p,t} \left[1 - \frac{H_{b,o}(1 - \epsilon_{b,o})}{H_{b,os}} \right]^n \quad (4.19)$$

where

- v_{hs} = hindered settling velocity
- $H_{b,os}$ = height of suspended resin bed when settling begins

The following relationship, which assumes a constant settling velocity, gives the height of the settling bed as a function of time and can be used for comparison with experimental observations of bed height as a function of time during settling.

$$H_{b,s} = H_{b,os} - v_{hs} * t \quad (4.20)$$

where

$H_{b,s}$ = height of resin bed during settling
 t = time since settling began

Eqs. (4.19) and (4.20), together with Eqs. (4.8) through (4.12) for $v_{p,t}$, can be used to predict the settling velocity of an initially suspended bed and compare with measured settling behavior.

5.0 Simulant and Resin Properties

A primary element of the planned testing is to use liquid simulants that span the expected ranges for LAW feed solutions and regeneration fluids. In the sections below, the targets for liquid simulant properties are given, the specific solution mixtures selected to meet these targets are described, and the measured properties of the liquid simulants and sRF resin equilibrated with these liquid simulants are summarized.

5.1 Simulant Targets, Selection, and Nominal Properties

Ansolabehere (2016) defines the range of LAW feed physical properties that need to be considered and Aguilar (2016) discusses the sRF resin elution and regeneration processes for LAWPS, which are planned to use 0.45 M HNO₃, 0.1 M and 1.0 M NaOH, and demineralized water. For fluidization and gas retention and releases, the liquid viscosity and density are the most important liquid simulant physical properties. The sRF resin, when equilibrated with a solution, is further affected by the composition of the liquid and will change particle diameter and density, which also affects fluidization behavior (see Section 4.2.1). Based on this information, the full ranges of liquid stimulant properties are:

- Density – 1.0 to 1.35 g/mL
- Viscosity – 1 to 15 mPa·s (cP)
- Viscosity of water at 55 °C (for elevated-temperature tests) – 0.5 mPa·s (cP)¹
- Chemical composition – acidic to caustic

To span this range of physical properties and chemical composition, the following simulant targets, and specific liquid simulants, were selected for testing:

- 1 g/mL density and 1 mPa·s (cP) viscosity targets
 - alkaline water equilibrated with Na⁺ form sRF resin
 - acidic water equilibrated with H⁺ form sRF resin
- 1 g/mL density and 0.5 mPa·s (cP) viscosity targets
 - alkaline water at 55 °C equilibrated with Na⁺ form sRF resin
- Nominal GR&R LAW - 1.25 g/mL density and 2-7 mPa·s (cP) viscosity targets²
 - 6.1 M Na (4.12 M NaOH + 2.0 M NaNO₃) equilibrated with Na⁺ form sRF resin
- High-Limit LAW – 1.35 g/mL density and 15 mPa·s (cP) viscosity targets
 - 10.8 M (32.11 wt.%) NaOH equilibrated with Na⁺ form sRF resin

¹ Aguilar (2016) does not specify water at an elevated temperature but does identify water as a regeneration fluid and an e-mail from MR Landon of WRPS dated May 19, 2016 defined an upper temperature of 55 °C for testing to represent an accident scenario. It is anticipated that water at 55 °C will give the most difficult to fluidize liquid simulant/sRF resin pair, so it is included as part of the full range of liquid simulant properties.

² Ansolabehere (2016) and Aguilar (2016) both give nominal density (1.28 g/mL) and viscosity (6 or 11 mPa·s [cP], respectively) values. Russell et al. (2017) developed a nominal LAW simulant for the LAWPS effort, which had a measured density of 1.26 g/mL and viscosity of 3.82 mPa·s (cP); these values were used as targets for nominal GR&R LAW.

The composition of the nominal GR&R LAW was selected to meet density and viscosity targets and also provide an appropriate hydrolysis rate of SBH for generation hydrogen gas. A mixture of NaOH and NaNO₃ was selected because these chemicals are common in LAW solutions. The 10.8 M NaOH solution was selected for the high-limit LAW because this composition matches the target density and has a viscosity near the target, depending on the test temperature. These liquid simulants were obtained in Reagent Grade from NOAH Chemical. Chemicals used for conditioning the sRF resin were 0.5 M HNO₃ and 1.0 M NaOH that were also Reagent Grade and obtained from NOAH Chemical¹. Distilled water was used for sRF resin washing during resin conditioning and when preparing the sRF resin for being equilibrated with different liquid simulants.

Sodium borohydride, for generating hydrogen gas, is an additional important component of the liquid simulants. The choice of sodium borohydride concentration for use in fluidization-GR&R tests was driven by the general hydrogen gas quantity and generation rate targets outlined in Section 6.4, guided to some extent by FIO scoping studies, and confirmed / finalized through experimental results that are discussed in Section 8.1. In all ambient-temperature bench-scale and fluidization-GR&R tests, the SBH concentration ranged from 0.5 to 1.4 g SBH/L sRF resin. This SBH concentration is equivalent to 0.013 – 0.037 M SBH (NaBH₄, $M_{SBH} = 37.833$ g/mol) and has a small contribution to the sodium concentration in the test solutions. On a test-by-test basis, the SBH concentrations are summarized in Table 5.2 (Section 5.3.2) for bench-scale tests and in Table 9.1 and Table 9.2 (Section 9.0) for fluidization-column tests. A lower concentration (0.2 g SBH/L resin) was selected for bench-scale elevated-temperature tests (Section 8.4). The sodium borohydride powder used in all tests was Aldrich® brand with an indicated purity of ≥98.0% (Product No. 452882-500G; Lot No. SHBG0259V).

5.2 sRF Resin Preparation

The gas retention, gas release, and fluidization testing used sRF resin identified as batch 6C-370/745. The resin was provided by WRPS in a large, pressurized storage container. The Chain of Custody (COC) form identified the container for this material as resin vessel RV-02². The container for this material had previously been identified as FINNCONT-2 as given in the report by RG Lee Group³. Resin was needed for both full depth column and smaller studies, with a total estimated resin volume of about 100 L (Na⁺ form), and was pre-treated following the out-of-column guidelines described in Nash (2004) as general guidance. The out-of-column guidelines in Nash (2004) are more appropriate for smaller bench-scale quantities of sRF resin, rather than the approximately 100 L resin batch. To accommodate the large volume of resin and pre-treatment fluids need for the fluidization column testing, some adjustments to the steps proposed by Nash (2004) were enacted. Notable differences from the guidelines are described in the remainder of this section.

To minimize resin damage, the resin was removed from the FINNCONT-2 storage vessel by pulling a vacuum on a receiver vessel and withdrawing the resin as a slurry into the receiver vessel. Multiple

¹ Nash (2004) recommends 0.5 M HNO₃ for resin conditioning, so this composition was used rather than 0.45 M as identified in Aguilar (2016)

² Chain of Custody form COC-LPIST-002, dated 9/8/15, documents the receipt of 100 gallons (nominal) of sRF Batch 6C-370/745.

³ The report by the RJ Lee Group, Inc./CLS is entitled “*Sampling and Shipment of Spherical Resorcinol Formaldehyde Resin*” and is dated October 6, 2014.

smaller batches were withdrawn from the storage vessel to make-up the 100 L (Na^+ form) volume of resin. The contents in the receiver vessel were then transferred by hand to a 65 gal plastic mixing vessel for contacting with conditioning fluids. Once the resin conditioning was complete and the pH of the water contacting the resin was below 12.5, the resin was transferred by hand or peristaltic pump to the fluidization column and/or sealed storage buckets.

The as-received sRF resin was in H^+ form and contacted with water. The steps for resin pre-treatment (conditioning) implemented the following general approach (note that the fluids used were sparged with nitrogen prior to use to minimize the potential for resin damage from dissolved oxygen):

- Rinse the resin with five bed volumes of distilled water periodically stirring gently (with an overhead mixer) then remove the water by decanting
- Contact the resin with five bed volumes 1.0 M NaOH
- Rinse the resin with three bed volumes of DI (or distilled) water three times
- Contact the resin with ten bed volumes of 0.5 M HNO_3
- Rinse the resin with three bed volumes of DI (or distilled) water three times
- Contact the resin with five bed volumes 1.0 M NaOH
- Rinse the resin with three bed volumes of DI (or distilled) water three times

Because of the large volume of resin needed for testing, the pre-treatment (conditioning) cycle was not conducted a second time as suggested in Nash (2004). After these steps were completed, the sRF resin was in Na^+ form and ready for testing. Resin used in H^+ form testing was prepared by converting Na^+ form resin that had been used back to H^+ via contact with 0.5 M HNO_3 .

A resin volume of about 20 gallons was needed for the initial full-height column testing together with supporting tests. Accordingly, about 200 gallons (100 gallons, twice) of NaOH and 200 gallons of HNO_3 were needed for the conditioning steps. The equipment for handling the required volume of fluids and providing good contacting with the resin included:

- A hydraulically-operated overhead agitator to mix the resin slurry
- 2-inch plastic air-driven diaphragm pumps with appropriate lengths of hose to feed and remove pre-treating fluids from the resin
- 25-gallon poly vessels for intermediate storage of slurried resin or preparation of chemicals
- 55-gallon drums of pre-treatment chemicals
- 275-gallon totes to manage distilled water
- Nitrogen gas cylinders and associated equipment for deoxygenating chemicals

Even with equipment listed above, contacting the resin with multiple bed volumes of fluids was challenging. The original intent was to recirculate the required chemicals between a 275-gallon tote and the mixing vessel, with the resin gently suspended using the overhead mechanical mixer. Upon further consideration, an alternate approach for conducting the contacting was used: a batch method where the resin was contacted with one bed volume (nominally) of a fluid in the mixing vessel. The single bed volume of fluid was gently mixed with the resin and then, after a short period, the liquid was decanted from the sRF resin. The process was repeated again with another bed volume equivalent until the requisite number of bed volumes were contacted with the resin. This approach was followed for contact steps using either acid or base and the rinsing steps (with distilled water).

For conditioning smaller volumes of resin needed for the bench-scale testing, the pretreatment steps were conducted in a manner following the guidance of Nash (2004). For these smaller resin volumes, conditioning was conducted by contacting the resin with the entire required volume all at once, with the aid of hand-mixing. Resin conditioning fluids (0.5 HNO₃ and 1.0 M NaOH) were blended or purchased at the desired concentrations. All solutions prepared in the laboratory were made with DI (or distilled) water.

The fluidization column testing also periodically required exchanging various fluids that were in contact with the sRF resin, i.e., the liquid simulants. The equilibration of the resin with these simulants, despite not being a “conditioning” step per se, was conducted in a similar manner to the conditioning process as described above. Resin and liquid was removed from the column and placed in the 65-gallon mixing vessel. The equilibrations were then conducted in the mixing vessel by batch contacting the resin with the new liquid simulant, which slowly exchange the new simulant with the old simulant the resin had been in contact with. Batch contacts were continued until the resin and liquid simulant was determined to have reached a target parameter (for example: bulk density, pH, or viscosity). When deemed ready, the resin and liquid simulant were returned to the column by pumping or manual addition. With the exception of brief periods, the resin remained fully submerged in a fluid and was not permitted to contact air during these processes.

5.3 sRF Resin and Liquid Properties

This section summarizes resin particle, resin bed, and liquid properties for the sRF resin/liquid systems used in all the testing. In Section 5.3.1, the physical properties are presented for the fluidization-column tests, including the fluidization-only and GR&R tests. These properties were also used as inputs in fluidization models (see Sections 4.2 and 6.4). Relevant properties for the sRF resin/liquid pairs used in bench-scale GR&R tests are covered in Section 5.3.2. The physical properties for the bench-scale tests are also associated with individual tests conducted at that scale.

5.3.1 Fluidization-Column Tests

Measured and estimated resin particle, resin bed, and liquid properties for all sRF resin/liquid pairs used in fluidization-column tests are shown in Table 5.1. These include parameters measured from samples that were removed from the resin batch or the column itself, as well as parameters calculated from in-column data measured during testing. Samples were collected for sRF particle density, sRF particle diameter, liquid density, and liquid viscosity. These quantities were measured for each sRF resin/liquid pair that was tested. In-column data includes initial gas-free settled bed density, sRF particle density calculated assuming a bed porosity of 0.40, and the viscosity estimated at various test temperatures (using a measurement of temperature in the column). The in-column data was assembled for a select set of tests where information was needed to construct fluidization models for bed expansion, upper bed formation, and settling behavior.

For the sample data, sRF particle density and diameter was determined as discussed in Section 4.1.1. Liquid density was determined by using calibrated glassware (pycnometer), and liquid viscosity (as a function of temperature, if required) was measured with an Anton Paar Physica MCR 301 following the PNNL technical procedure RPL-COLLOID-02, Rev. 2. In-column data was estimated using the approaches described in Section 4.1.2. The assumed value for bed porosity ($\epsilon_{b,0} = 0.40$) is a typical value

for randomly packed bed of spheres (see Section 4.1.1, Dullien 1992) and, when used as a model input, provided good agreement with test data (see Section 7.1). The initial gas-free resin bed density was measured, and in conjunction with the liquid density, used to calculate the resin particle density using Eq. (4.5). Viscosity estimates at various in-column temperatures were performed by interpolation between measured or reference data.

Table 5.1. Liquid and sRF Resin Particle and Bed Properties in Fluidization-Column Tests

Sample sRF Resin / Liquid (description)	Measurements on Samples Removed from Column or Batch					In-Column Data and Estimated Viscosity at Column Test Temperature		
	Liquid Density (g/mL)	sRF Particle Density (g/mL)	Measurement Temperature (Liquid & Particle Densities) (°C)	sRF Particle Diameter ± Std. Dev. (µm)	Viscosity ^(h) (Temp °C) (mPa·s or cP)	sRF Resin Bed Density (g/mL)	sRF Particle Density Assuming Void Fraction of 0.4 (g/mL)	Test Temperature (T2 ^(e)), Estimated Viscosity ^(f) for F: Fluidization U: Upper Bed Formation S: Settling (°C, mPa·s or cP)
H ⁺ form / acidic water (sample collected after 1 st conversion to H ⁺ form during initial conditioning)	0.997	1.190	21	414 ± 7	-	-	-	-
Na ⁺ form / alkaline water (sample collected after final conversion to Na ⁺ form during initial conditioning)	0.998	1.224	21	439 ± 7	-	-	-	-
Na ⁺ form / alkaline water (sample collected at beginning of testing)	0.998 0.997 ^(b) 0.998	1.218 1.214 1.218	23 22 22	438 ± 24	1.04 (20 °C)	1.131	1.220	F: 20 °C, 1.04 mPa·s U: 15 °C, 1.19 mPa·s ^(g)
Na ⁺ form / alkaline water (sample collected after completing water testing ^(a))	1.000	1.218	22	440 ± 8	1.05 (20 °C)	-	-	-
Na ⁺ form / GR&R 6.12 M LAW (sample collected prior to characterization of sRF resin beds with shear vane)	1.240	1.376	22	459 ± 4	3.7 (20 °C) ^(d)	-	-	-
Na ⁺ form / Nominal 5.6 M LAW (sample collected during characterization of sRF resin beds with shear vane)	1.231	1.367	23	455 ± 8	3.1 (20 °C) ^(d)	-	-	-
Na ⁺ form / GR&R 6.12 M LAW (sample collected at beginning of testing)	1.254	1.385	22	462 ± 26	3.9 (20 °C) 3.4 (25 °C)	1.337	1.393	F: 21-23 °C, 3.7 mPa·s U: 23-24 °C, 3.5 mPa·s S: 23 °C, 3.6 mPa·s
Na ⁺ form / GR&R 6.12 M LAW (sample collected after completing GR&R LAW testing)	1.256	1.373	23	462 ± 14	3.95 (20 °C) 3.4 (25 °C)	-	-	-
H ⁺ form / acidic water (sample collected at beginning of testing)	1.001	1.158	22	419 ± 23	1.09 (20 °C) 0.91 (25 °C)	1.108	1.179	F: 25 °C, 0.91 mPa·s
Na ⁺ form / 10.8 M NaOH (sample collected at beginning of testing)	1.345 (1.344 ^(c))	1.417	23	459 ± 17	16.6 (20 °C) 13.0 (25 °C) 10.5 (30 °C)	1.412	1.457	F: 26-28 °C, 12.0 mPa·s U: 28-30 °C, 11.0 mPa·s S: 30 °C, 10.5 mPa·s
Na ⁺ form / 10.8 M NaOH (additional samples collected from batch)	1.345 1.345 1.344 1.345	1.449 - 1.446 1.405	22 23 23 22	- - - -	- - -	- - -	- -	- -
Na ⁺ form / alkaline water (sample collected prior to elevated temp fluidization tests)	0.998	1.197	23	456 ± 12	1.06 (20 °C) 0.93 (25 °C) 0.85 (30 °C) 0.57 (55 °C)	1.127	1.213	F, S: 26 °C, 0.91 mPa·s F: 27 °C, 0.90 mPa·s F, S: 53 °C, 0.59 mPa·s

“-“ – Not measured.
(a) – One final water test was conducted after the conclusion of the planned water testing and the collection of this sample.
(b) – this is the average value of the three data when measure values are averaged and rounded and truncated to 0.001 g/mL.
(c) – Average of the liquid in this row and the four measurements on the additional samples (next row in this table). This value will be used as a model input in fluidization and settling calculations.
(d) – Viscosity measured on stock solution prior to contacting with sRF resin.
(e) – T2 is located 33 cm above the bottom screen (see Table 6.1 and Figure 6.2).
(f) – If a temperature range is shown for a specific test, the midpoint of the range was selected for estimating viscosity. Viscosity estimates from linear interpolation or extrapolation.
(g) – Viscosity data from last row in this table for “Na⁺ form / alkaline water (sample collected prior to elevated temp fluidization tests)” used for this estimate.
(h) – Viscosity data were measured twice on two aliquots from the same sample and the first measurement is reported here.

5.3.2 Bench-Scale Tests

Table 5.2 summarizes liquid and resin batch properties for completed bench-scale gas retention and spontaneous gas release tests. The indicated Test IDs are the abbreviated forms from the three Test Instructions that governed the work. Tests are listed in order of increasing alkalinity (sodium hydroxide concentration) and density of the stock liquid simulant that was contacted with sRF resin in batch preparation: alkaline water, in two slightly different / overlapping pH ranges (minimally pH 12.0 or ~ 0.01 M NaOH¹), 0.1 M, 0.3 M, and 1.0 M NaOH, 6.1 M Na LAW simulant (4.1 M NaOH), and 10.8 M NaOH. In all bench-scale tests, the source sRF resin used in batch preparation was always Na⁺ form in alkaline water (pH \leq 12.5). As shown in the Resin History column of Table 5.2, the source resin was typically “fresh”, indicating that it had not previously been contacted with SBH, versus previously “used” in other GR&R tests. For example, the resin for Test MD-03 had been used in fluidization-GR&R Tests 10-04 to 10-07 with alkaline water before being water-washed and equilibrated with 6.1 M Na LAW simulant. This bench-scale test was completed to pre-evaluate expected GR&R performance in the planned fluidization-column experiments using the same simulant (i.e., completed Tests 10-08 and 10-09).

Where available, the measured density of the contacted (source) liquid, $\rho_{L,0}$, is shown in Table 5.2 in addition to the final equilibrated liquid density, ρ_L . The latter was typically measurably lower owing to dilution by alkaline water initially present in the stock resin, despite multiple contacting steps with aliquots of fresh stock liquid in the batch preparation process. Therefore, the composition of the liquid in the prepared resin batch is nominally the same as, but is slightly lower concentration than, the stock liquid. The experimentally measured initial gas-free resin bed densities ($\rho_{b,0}$) for the bench-scale tests using the method described in Section 4.1.2 are tabulated in Table 5.2. The bed densities were measured prior to SBH addition, except in Test GC-01A, which was a second SBH addition to the as-is contents from Test GC-01 following mixing to release gas and re-measure the bed density. The theoretical neutral buoyancy gas fractions for gas retained as PDBs and ILDBs that are calculated using the measured ρ_L and $\rho_{b,0}$ values and Eq. (6.15) and Eq. (6.16) (in Section 6.5), respectively, are shown in Table 5.2. These estimates are discussed further in Section 8.2.1 in the context of spontaneous gas releases. Note that resin particle sizes and densities and liquid viscosities were not measured for bench-scale test resin batches in the way they were for fluidization-column experiments (discussed above). However, resin particle densities at assumed resin bed porosity (ϵ_b) values of 0.36 and 0.40 that are estimated from measured ρ_L and $\rho_{b,0}$ values using Eq. (4.5) (Section 4.1.2) are summarized in Table 5.2. These two porosity values were selected from the typical values of porosity discussed in Dullien (1992) and represent an estimate for the likely range of porosity (see Section 4.1.1 for additional discussion). The ρ_p estimates and measured resin bed densities for the bench-scale tests with alkaline water, 6.1 M Na simulant, and 10.8 M NaOH from Table 5.2 can be compared to the measured and estimated properties shown in Table 5.1 for resin batches of similar composition (but prepared separately and, therefore, unique).

¹ For the pH ranges shown in Table 5.2, the lower pH was measured in the equilibrated resin slurry by direct insertion of the pH probe, whereas the pH of the supernatant liquid was 0.3 to 0.4 units higher. A bounding low sodium hydroxide concentration of ~ 0.01 M is estimated from the minimum measured pH (12.0) using the idealized relationship found in chemistry textbooks: $\text{pH} = -\log [\text{H}^+] = 14 + \log [\text{OH}^-]$, where $[\text{H}^+]$ and $[\text{OH}^-]$ are the molar concentrations of hydrogen and hydroxyl ions, respectively.

Table 5.2 also identifies other test parameters and conditions including the test vessel type and the SBH concentration in each bench-scale GR&R test. The SBH concentration is relevant to gas generation rate and is discussed further in Section 8.1.1.

Table 5.2. Liquid and sRF Resin Bed Properties and Test Parameters in Bench-Scale Tests in Order of Increasing Alkalinity and Density

Test ID ^(a)	Test Vessel ^(b)	Resin History ^(c)	Contacted (Stock) Liquid Composition ^(d)	Measured Densities (g/mL)			Est. Particle Densities at Given Porosities ^(e) (g/mL)		Theoretical Neutral Buoyancy Gas Fractions ^(f) (vol%)		SBH Conc. (g/L Resin)	Comments	
				Stock Liquid, $\rho_{L,0}$	Equil. Liquid, ρ_L	Gas-Free Resin Bed, $\rho_{b,0}$	ρ_p w/ 0.36 ϵ_b	ρ_p w/ 0.40 ϵ_b	w/ PDBs $\alpha_{NB0,PB}$	w/ ILDBs $\alpha_{NB0,ILD}$			
GC-16	250 mL GC	Fresh	Alkaline Water (pH 12.0-12.4) ^(g)	0.998 ^(h)	0.998	1.133	1.210	1.224	12.0	13.6	0.71		
GC-01	250 mL GC	Fresh	Alkaline Water (pH 12.2-12.5) ^(g)	0.998 ^(h)	0.998	1.138	1.217	1.231	12.3	14.0	0.70	Second SBH addition after mixing to release GC-01 gas	
GC-01A		Re-used (GC-01)				1.136	1.213	1.228	12.1	13.8	1.40		
MD-07	250 mL GC	Fresh	0.1 M NaOH	1.001	1.000	1.141	1.220	1.235	12.4	14.1	0.52	Elevated temperature test w/ same resin batch as MD-07	
MD-10	200 mL Jacketed GC					1.147	1.230	1.246	12.9	14.8	0.21		
MD-05	250 mL GC	Fresh	0.3 M NaOH	1.010	1.007	1.155	1.238	1.254	12.8	14.7	0.51	Elevated temperature test w/ same resin batch as MD-05	
MD-09	200 mL Jacketed GC					1.155	1.238	1.253	12.8	14.7	0.21		
MD-04	250 mL GC	Fresh	1.0 M NaOH	1.039	1.036	1.175	1.254	1.269	11.9	13.5	0.52		
MD-01	250 mL GC	Fresh	6.1 M Na Simulant (4.1 M NaOH + 2.0 M NaNO ₃)	1.256		1.248	1.384	1.393	6.5	7.0	0.73	Using same resin batch as MD-01 Extra contact steps required ⁽ⁱ⁾	
MD-03	250 mL GC	Used				1.247	1.327	1.373	1.381	6.1	6.5		0.50
MD-02	5-in. I.D.	Fresh				1.248	1.332	1.379	1.388	6.3	6.8		0.50
MD-06	10-in. I.D.	Fresh				1.256	1.349	1.402	1.412	6.9	7.5		0.50
MD-08	250 mL GC	Fresh	10.8 M NaOH	–	1.349	1.414	1.450	1.457	4.6	4.8	0.52		

“–” – Not measured

(a) – The unique, abbreviated Test IDs from three governing Test Instructions are shown. GC denotes “graduated cylinder” and was used in alkaline water Test IDs; MD indicates “method development” tests conducted with other liquid simulants. Note that a number of MD tests were also conducted in graduated cylinders with similar test objectives.

(b) – The majority of tests were conducted in graduated cylinders (GCs) with the indicated marked total volume; two elevated-temperature tests used a water-jacketed GC. One test was conducted in a 5-in. I.D. vessel and another in a 10-in. I.D. vessel. The latter is the same diameter as the fluidization-column, but it is shorter.

(c) – “Fresh” indicates that the source Na⁺ form sRF resin (in alkaline water) utilized in batch preparation had not previously been contacted with SBH, versus previously “used” in other GR&R tests. The resin in Test GC-01A was re-used as-is after Test GC-01. The resin for Test MD-03 had previously been used in fluidization-GR&R tests with alkaline water before being water-washed and equilibrated with 6.1 M Na LAW simulant.

(d) – The composition of the source liquid that was contacted and equilibrated with sRF resin in batch preparation is shown. Although multiple aliquots of fresh contact liquid were used in the preparation process, the composition of the equilibrated liquid was typically more dilute (e.g., lower density) owing to the alkaline water in the source resin slurry.

(e) – Estimated particle densities (ρ_p) at assumed resin bed ϵ_b values of 0.36 and 0.40 are calculated using measured ρ_L and $\rho_{b,0}$ values in Eq. (4.5).

(f) – Theoretical neutral buoyancy gas fractions for gas retained as PDBs and ILDBs are calculated using measured ρ_L and $\rho_{b,0}$ values in Eq. (6.15) and Eq. (6.16), respectively.

(g) – The “Contacted Liquid” is the composition of the “Equilibrated Liquid”. The lower and upper ends of the pH range are for resin slurry and supernatant liquid, respectively.

(h) – The assumed density is a handbook value for water at a nominal room temperature of 22 °C (Weast 1985).

(i) – “Dirty” simulant (bottom of drum suspected) required additional contacts with clean simulant in batch preparation and resulted in higher equilibrated ρ_L than comparable tests.

5.4 Effect of Temperature on sRF Resin

The impact of testing at elevated temperature, i.e. up to 55°C, with sRF resin on gas retention and release was not well-understood. Resin property measurements applicable to the relevant physical phenomena are not available as a function of temperature. A major concern was that the resin would be degraded or altered at elevated temperature and become more cohesive, forming stronger resin beds that would potentially hold on to retained gas more effectively. More cohesive beds could also be more difficult to fluidize, and as a consequence, require higher flow rates to release gas. In order to ascertain that planned testing at 55°C would not create a significantly more cohesive resin bed, a parametric study of sRF resin bed shear strength was performed. This method was chosen since it was an in-situ measurement that allowed a quantitative assessment of the bed's strength at temperatures of interest.

The shear strength testing was conducted to evaluate the effects of fluid type (water, simplified GR&R LAW (6.12 M Na) simulant, and Nominal LAW simulant), temperature (ambient, 55°C, and 70°C), and contact duration (12 hours and 48 hours) on the stability and strength of Na⁺-form sRF resin beds. The selected simulants represent a sub-set of the range of simulants that were used in gas retention and release testing discussed in this document, as well as an opportunistic measurement using the Nominal LAW simulant. The Nominal LAW simulant was a 5.6 M Na simulant obtained from a batch that had been prepared and tested in the PNNL crossflow filtration system (Daniel et al. 2018). The preparation and composition of the Nominal LAW simulant are described in Russell et al. 2017. The Nominal LAW simulant is of wider interest because it is chemically representative of an average expected LAWPS feed and it has been used in other, related testing programs (see, for example, Colburn et al. 2018). Note that if the sRF resin was observed to become “sticky”, “clumpy”, or cohesive at elevated temperature in these measurements, the mechanism causing the change in characterization may also be affected by the history of resin use, resin cycling, and chemical exposure, and radiation dose. The impacts of these other potential factors were not evaluated in this study. In order to compare measurement values to each other, all shear strength tests used fresh, Na⁺-form sRF resin samples that had not been used previously in other experiments.

Shear strength characterization was performed on a Haake VT550 (Thermo Fischer HAAKE Viscotester 550, serial number: TYP002-7026-110003745003) that employed a 1.6-cm × 3.2-cm (Diameter × Height) shear vane, which can measure shear strengths from ~20 Pa up to ~2000 Pa. Control and data acquisition for the Haake VT550 rheometer was accomplished through a remote computer connection using the RheoWin Pro Job Manager Software, Version 4.30. Shear strength measurements followed the PNNL technical procedure RPL-COLLOID-02, *Measurement of Physical and Rheological Properties of Solutions, Slurries and Sludges*, Rev. 2, Section 7.7, “Process for Determination of Shear Strength (Vane Method)”. Rheometer performance checks were conducted before initial use and at least once every 30 days of use thereafter with certified Newtonian viscosity standards traceable to the manufacturer's lot number (a viscosity standard is used because no shear strength standards are available to calibrate the shear vane). The rheometer has demonstrated an accuracy of ±15% at apparent viscosity measurements less than 10 cP or ±10% at apparent viscosity measurements greater than 10 cP, as specified in RPL-COLLOID-02, Rev. 2. By analog, the expected accuracy of the shear vane method is approximately ±10%, though the measurement also depends on geometry and sample history. Each settled resin bed sample was measured in duplicate.

The sRF resin samples in LAW simulants for shear strength evaluations were prepared by contacting approximately 2 liters of fresh, Na⁺-form sRF resin with equal-volume aliquots of the respective simulant at least 5 times or until the measured density of the liquid above the resin was within 3% of the measured density of the uncontacted simulant. After the simulant contact, individual resin bed samples were prepared by placing approximately 450 mL of simulant-contacted, Na⁺-form sRF resin and supernatant fluid in a 600-mL Pyrex beaker. The supernatant liquid layer over the resin bed was approximately 100 mL. The sRF resin samples were allowed to settle and held undisturbed (quiescent) at room temperature, 55°C, or 70°C for 12 or 48 hours (70°C only). The ambient temperature resin bed samples were placed on a sturdy benchtop. The elevated resin bed samples were placed inside a mechanical Lindberg/BlueM oven (model: MO1490GPAA, serial number: P24J-428020-TJ) that was held at 55°C or 70°C. For each set of resin samples at a specified temperature, a surrogate sRF resin sample containing liquid and approximately 450 mL of used sRF resin that was used in previous testing was placed adjacent to the shear vane samples on the bench top or in the oven at 55°C or 70°C. This permitted monitoring of the sample temperature without inserting a thermocouple into the sample itself, i.e. to minimize sample disturbance. The hold duration of the test began once the temperature of the surrogate sRF resin sample was within 5°C of the target test temperature. To minimize evaporation of the liquid layer while the resin samples were allowed to rest undisturbed at test temperature, each sample was covered with a Pyrex watch glass.

The specified conditions for individual resin bed samples are provided in Table 5.3. At the completion of the specified quiescent period, the temperature of the surrogate resin sample was measured. The surrogate sample temperature was used to represent the initial temperature of the settled resin bed samples prior to performing the shear strength measurements. Shear strength for each sample was measured in duplicate at two radially opposite locations. Shear strength measurements for the heated resin samples were performed within 5 – 10 minutes after the samples were removed from the oven to minimize cooling. The temperature of each shear strength sample was also measured after the shear strength measurements. All temperature measurements were collected using a calibrated thermocouple. Table 5.3 also summarizes the actual measurement temperature (initial settled bed temperature), duration of the hold, and the average shear strength measured.

Table 5.3. Sample Conditions and Measurement Data for Shear Vane Tests.

Description of Sample Conditions (all samples with Na⁺-form sRF resin)	Target Duration (hr)	Initial Temperature of the Settled Bed (°C)	Actual Duration (hr)	Average Shear Strength (Pa)
Water + resin, held at ambient temperature	12	21.9	11	133
GR&R LAW simulant + resin, held at ambient temperature	12	21.9	11.5	111
Nominal LAW simulant + resin, held at ambient temperature	12	21.9	12	116
Water + resin, held at 55°C	12	54.3	11.5	89.3
GR&R LAW simulant + resin, held at 55°C	12	54.3	12	97.9
Nominal LAW simulant + resin, held at 55°C	12	54.3	12	85.9
Water + resin, held at 70°C	12	68.5	12	107
GR&R LAW simulant + resin, held at 70°C	12	68.5	12	85.9
Nominal LAW simulant + resin, held at 70°C	12	68.5	12.5	94.6
Water + resin, held at 70°C	48	69.2	48	102
GR&R LAW simulant + resin, held at 70°C	48	69.2	48	71.9
Nominal LAW simulant + resin, held at 70°C	48	69.0	48	74.6

Figure 5.1 summarizes the average shear strength results for all samples as a function of the hold temperature. The results show a slight decrease in shear strength of the settled sRF resin bed with an increase in temperature from ambient to 55°C. The corresponding measurements conducted at 70°C do not continue the decreasing trend and cannot be distinguished from the measurements at 55°C (shear strength measurement uncertainty in the range of interest is about $\pm 10\%$). If anything, holding the temperature at 70°C for a longer time period indicates a further decrease of shear strength for all fluids tested. Thus, the shear strength data collected by this method suggest that extended periods (up to 48 hours) of elevated temperature (up to 70 °C) do not increase the cohesiveness or strength of Na⁺-form sRF resin beds. Ambient temperature resin beds appear to be stronger than heated beds and thus are conservative with respect to gas retention and release.

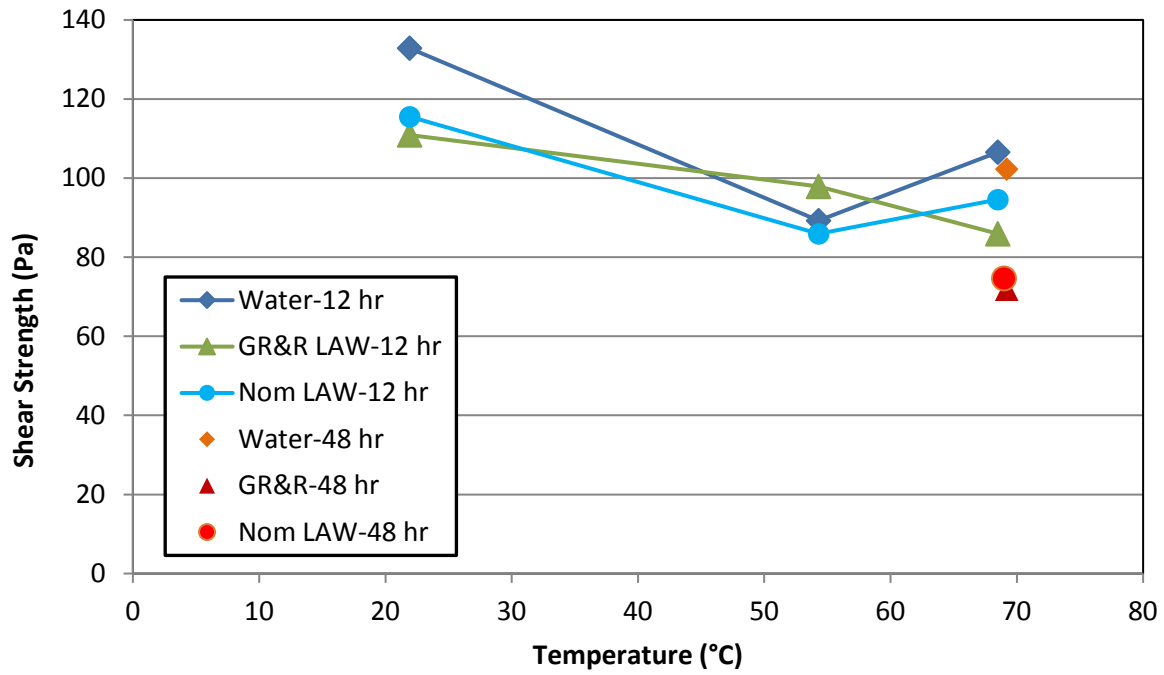


Figure 5.1. Measured average shear strength as a function of test temperature for various settled beds of sRF resin in different fluids (water, GR&R LAW, and Nominal LAW), and with different quiescent periods (12 hours and 48 hours).

6.0 Experimental and Analysis Methods and Approach

This section covers the methods and approach for conducting gas retention and release and fluidization tests and for analysis of the collected GR&R test data. A test matrix further summarizes the approach.

The test equipment and experimental methods used to address the objectives as found in Section 2.0 are described first. The test program contained two elements:

- Gas retention and release tests conducted at bench-scale. Bench-scale (or bench-top) tests were conducted for kinetic studies of hydrogen generation, understanding scale-up behavior, and validating planned conditions (SBH loading) for the fluidization column experiments. The test equipment and test methods for experiments at the bench-scale (which includes vessels of varying size) are discussed in Section 6.1.
- Gas retention, release and fluidization tests conducted at engineering-scale. These tests included experiments focused on (1) gas retention and release in the absence of flow, (2) fluidization without gas generation, and (3) gas retention followed by release via fluidization. The test system used for this study is referred to throughout this document as the fluidization column. The column was able to be operated in a number of modes and contained a resin bed height equivalent to the planned full-scale LAWPS IX columns. The test equipment and methods for experiments in the fluidization column are discussed in Section 6.2.

The description of the test methods used for the bench-top and fluidization-column tests discuss the typical elements of the testing, but do not elucidate some of the permutations. Section 6.3 summarizes the test equipment and instruments used to conduct the testing at both scales. The test equipment is summarized together because the physical characterizations and experimental data obtained from the experiments were similar across test scales.

Section 6.4 summarizes the methods and approach for generating hydrogen gas from the hydrolysis of SBH, measuring gas generation during experiments, and analyzing the data to assess cumulative gas volume generated and generation rates. Section 6.5 discusses how gas retention and release volumes are quantified from test data and analysis methods used to assess gas bubble retention mechanisms and characteristics of the sRF resin bed. Finally, Section 6.6 summarizes the test matrix.

6.1 Bench-Top Gas Retention and Release Tests

The bench-top tests to assess gas generation and gas retention and release in sRF resin slurries were conducted using the equipment depicted schematically in Figure 6.1. The actual test systems differed in some details, depending on the test column that was being used and the objective of the test. Not shown in the schematic is the recirculating water bath used to heat the test column contents for the tests conducted at elevated temperature.

Bench-top GR&R testing included testing in the following vessels:

- 250-mL graduated cylinder with a nominal inside diameter of 1.4 inches and 10 millimeters per centimeter height (ambient temperature)
- 200-mL jacketed graduated cylinder (elevated temperature)
- Acrylic, flat-bottomed vessel with a nominal inside diameter of 5 inches (ambient temperature)
- Acrylic, flat-bottomed vessel with a nominal inside diameter of 10 inches (ambient temperature)

The acrylic vessels had multiple uniquely-identified rulers attached to the exterior surface to measure the fill-levels of the sRF resin bed and the supernatant liquid. These rulers and level readings from them were correlated to the volume contained in the vessel. Level readings taken to the nearest 1 mm (or less)¹ during GR&R tests were subsequently converted to volumes using these correlations. Volumes were read directly from the graduated cylinders used as the GR&R test column and gas collection cylinder. The gas collection cylinder volumes varied with the size of the GR&R test column and the corresponding amount of gas that was generated.

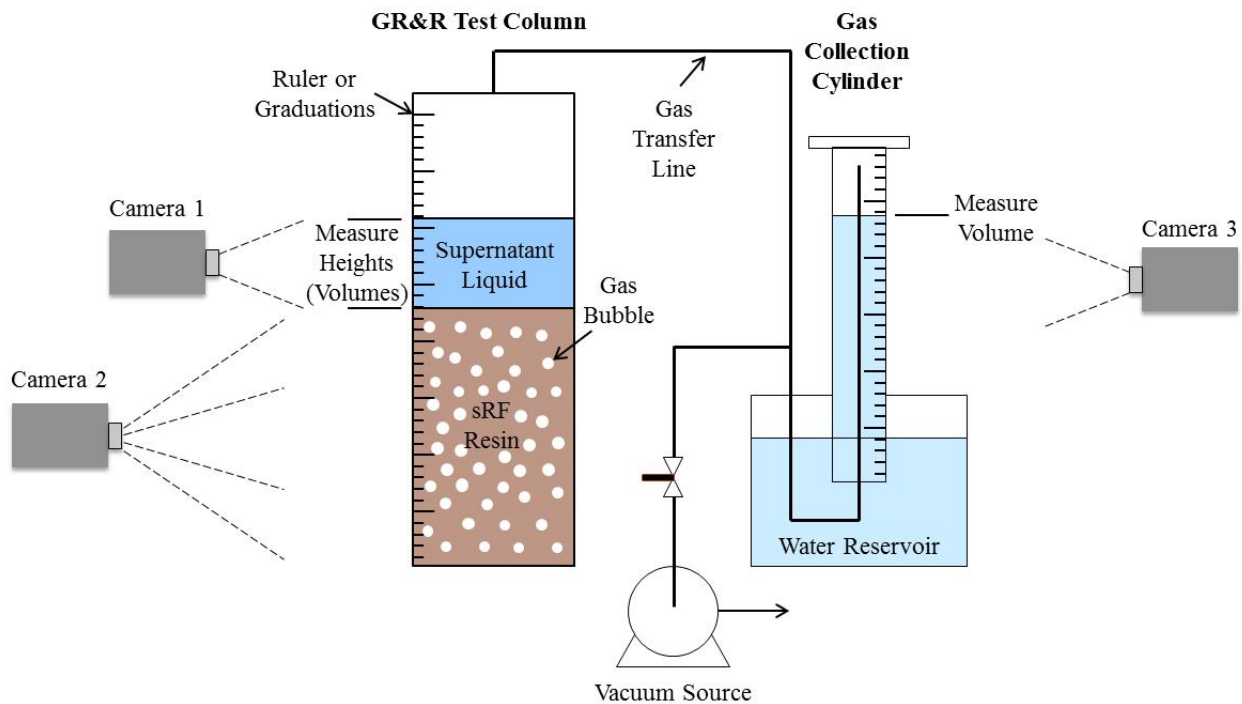


Figure 6.1. Schematic Drawing of a Bench-Top Test Setup for Gas Generation, Retention, and Release Measurements using sRF Resin. The drawing is not to scale, and the relative and absolute sRF resin bed and supernatant liquid layer depths may vary.

¹ Level (volume) measurement resolution and accuracy was reduced for uneven resin surfaces or if supernatant liquid was not present.

Other auxiliary equipment used in bench-top testing included:

- Standard bench-scale mixing and handling equipment
- Thermocouple and reader to monitor temperatures
- Vacuum pump to generate vacuum in the gas collection system
- Heating source for elevated temperature testing (recirculating water bath)
- Balances to measure resin, liquid, and SBH components to target masses
- pH/conductivity meter to monitor liquid pH
- Video cameras to record level and volume data over test durations, or capture specific gas retention events or configurations

Table 6.2 contains some additional details on the measuring and testing equipment used, such as the types used, methods of collection, and expected accuracy of the collected data. Selected samples were collected during testing to assess the liquid and resin density, sRF particle diameter, and rheology for the unique fluid/resin combinations. For more information on resin and fluid property characterization, refer to Sections 4.1 (methodology) and 5.0 (results).

6.1.1 Benchtop Test Operation

As shown in Figure 6.1, each bench-top test was conducted using two cylindrical, graduated or ruled, clear-plastic or glass vessels: the primary GR&R test column was a closed vessel with the exception of a port in the top lid to which tubing was attached to transfer generated gas to the gas collection cylinder (i.e., the second vessel). Just prior to the start of a test, SBH was added to and thoroughly mixed with separately-prepared slurry containing sRF resin and the fluid being tested (refer to Table 5.2 for a complete list of the test configurations). The sRF resin-liquid mixture was added to the GR&R test column (if not already in place) and the more-dense resin beads allowed to settle into a bed; a supernatant liquid layer formed as the resin settles. The primary test vessel was capped, and the gas transfer line connected to the gas collection cylinder, which was typically an inverted graduated cylinder with the opening submerged in a larger liquid (e.g., water) reservoir.

For elevated temperature testing, the operating temperature was not confirmed during the experiments themselves. Rather, a heating protocol was developed (prior to performing the tests where SBH was added) to establish the required set-point on the water bath needed to maintain a stable temperature of $55 \pm 2^\circ\text{C}$. This approach was used to avoid inserting a thermocouple in the resin bed itself during a GR&R test and influencing the retention and release of generated gas. The SBH was typically added to the resin/liquid slurry first and then the heating was applied as rapidly as practical (typically ramping up to target temperature in 60 minutes).

A liquid-column was established in the inverted graduated gas collection cylinder (under vacuum equivalent to the column height), and gas bubbles that were generated and retained in the resin bed caused the overall supernatant liquid level, indicated on rulers (graduations) affixed to the vessel, to increase.

The increase represents the amount of gas retained in the bed. Both retained gas and gas that is generated but not retained displace the liquid-column in the gas collection cylinder over time and give a volume change indication of the total gas volume generated.

One gas retention mechanism of particular interest was the formation of vessel-spanning bubbles. A key objective of the bench-top tests was to determine if VSBs were formed and whether they were stable (or release spontaneously) as the column diameter was increased from a graduated cylinder up to a 10-in. diameter column (the fluidization column diameter). A sufficiently large (say more than a few small, individual bubbles) release of gas from the resin bed by any mechanism was indicated by a decrease in the observed supernatant liquid level.

Note that SBH can react in the liquid phase alone in the absence of sRF resin. Therefore, the change in the volume of gas in the collection cylinder was representative of the total amount of gas generated in the resin bed and in the supernatant liquid, where it is not retained. By tracking the volume of gas collected over time, gas generation rates were determined, and by further comparison to changes in liquid level in the GR&R test column, including level decreases due to gas release, it was possible to estimate the fractions of gas generated within the resin bed and in the supernatant liquid. Therefore, in all bench-top GR&R tests, the key measurements were supernatant liquid level and gas collection cylinder volume vs. time data. Other data collected during testing included resin bed level vs. time, and qualitative real-time observations of bubble retention and release behavior, or post-test observation of photographs and video recordings. Some tests were concerned only with the kinetics of gas generation; in these cases only the gas volume collected over time was of interest.

6.2 Fluidization Column with Gas Retention and Release

The system used to conduct sRF resin fluidization and gas generation, retention, and release tests is depicted schematically in Figure 6.2 with supporting information in Table 6.1. The 10-in. diameter and ~8-ft tall “fluidization column” is shown on the right side of the schematic. The height of the column permitted a resin bed to be tested that was full-height with respect to the expected LAWPS IX column beds, which is nominally 50.4-in as shown in Figure 1.1. Figure 6.2 is an overview schematic that depicts all of the system components, not all of which were used in every test. In general, the system has many similarities to the bench-top systems, only larger in scale. Resin and fluid were located in the fluidization column and interfaced with a gas collection system during periods of active gas generation. For an annotated photograph of the as-built system when it was filled with sRF resin and fluid, refer to Figure 6.3.

One major element not present in the bench-top systems was a recirculation system for fluidization. The fluidization column recirculation system could motivate and meter fluid using a centrifugal pump at known flow rates either from the bottom (up flow) or the top (down flow) of the column. Since the column was outfitted with a recirculation system, the resin bed was supported by a Johnson screen on the bottom (nominally 6-in from the column bottom) with a flow distributor beneath it. The flow distributor at the top of the column was also installed with Johnson screen filters to prevent the migration of the sRF resin out of the column while flow was present. The recirculating fluid could be directed in a series of configurations to allow draining and rinsing of various sub-systems, or mixing of the column itself (for instance, when SBH was initially added). The recirculated liquid was stripped of any residual gas in a separator, and could be heated via a liquid pre-heater. For tests conducted at elevated temperature, the

liquid was pre-heated, followed by the chamber housing the fluidization column was air heated to the temperature of interest to maintain it.

The primary data collected were the supernatant level and resin bed level vs. time using the rulers installed on the sides of the fluidization column. The entire column was placed on a scale so that changes in mass could be tracked with time. Other data of interest were gas collection volume vs. time, qualitative real-time and photographic observations, temperatures, and flow rates. Table 6.2 contains some additional details on the measuring and testing equipment used, such as the types used, methods of collection, and expected accuracy of the collected data. Selected samples were collected in order to assess the liquid and resin density, sRF particle diameter, and rheology for the unique fluid/resin combinations. For more information on resin and fluid property characterization, refer to Sections 4.1 (methodology) and 5.0 (results).

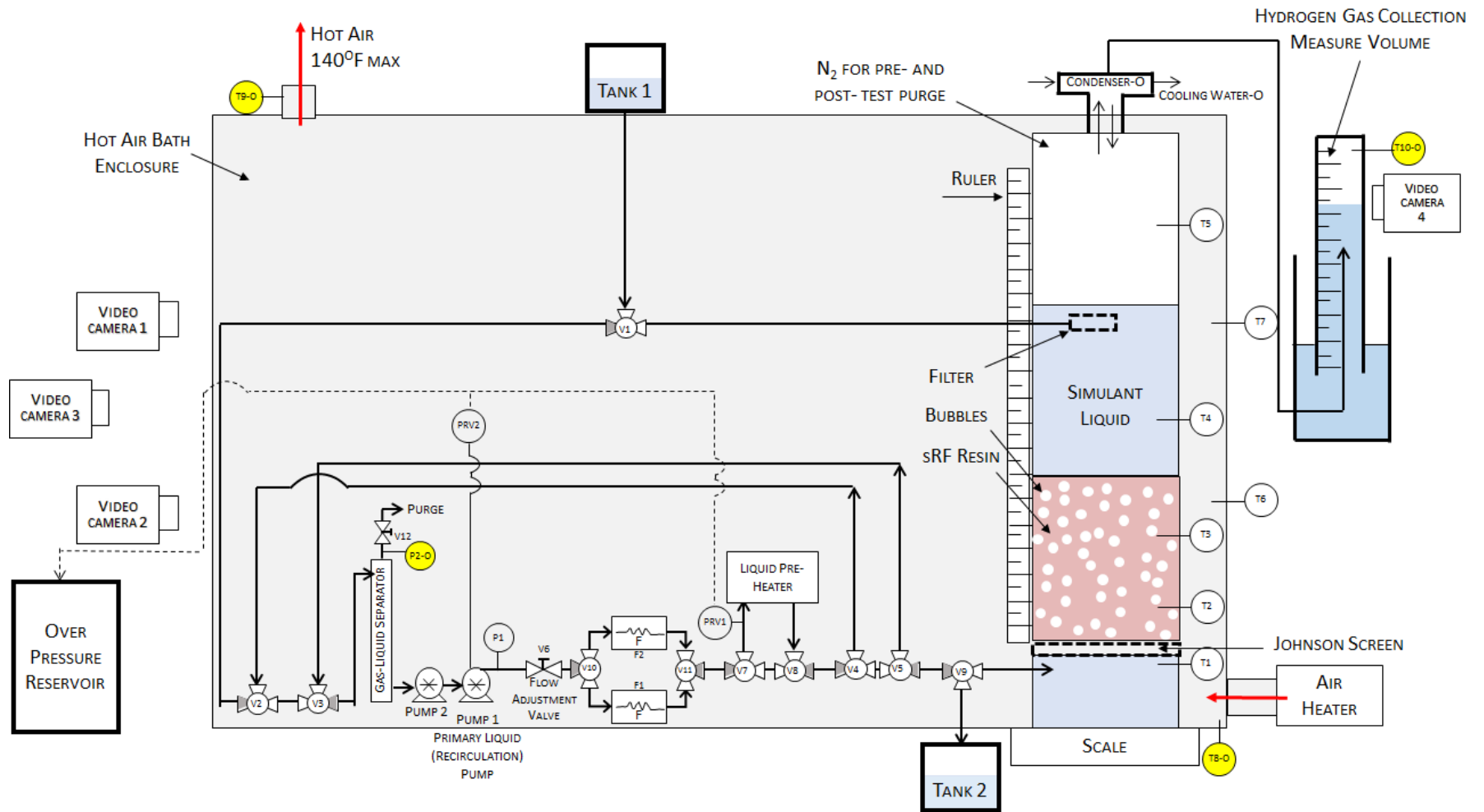


Figure 6.2. Schematic of the Fluidization Test Column, Flow Equipment, and Instruments for Gas Retention and Release Experiments with Fluidization (gray shading on the 3-way valves indicates the common port, figure not to scale).

Table 6.1. Components and Instruments for Fluidization Column System Shown in Figure 6.2.

Instrument/Component	Label	Description / Location
Thermocouple	T1	Recirculation liquid inlet temperature (below bottom screen)
Thermocouple	T2	sRF resin temperature (~33 cm above bottom screen)
Thermocouple	T3	sRF resin temperature (~86 cm above bottom screen)
Thermocouple	T4	Column liquid temperature (~170 cm above bottom screen)
Thermocouple	T5	Column gas space temperature (~239 cm above bottom screen)
Thermocouple	T6	Hot air enclosure temperature (back of heated box ~90 cm above bottom screen)
Thermocouple	T7	Hot air enclosure temperature (back of heated box ~170 cm above bottom screen)
Thermocouple	T8-O	Optional: Hot air enclosure inlet temperature (~5 cm in front of air inlet)
Thermocouple	T9-O	Optional: Hot air enclosure outlet temperature (centered below air outlet)
Thermocouple	T10-O	Optional: collected gas column temperature
Pressure Relief Valves	PRV1, PRV2	Recirculation line over-pressure and liquid heater over-pressure
3-way valve	V1	Reverse flow valve
3-way valve	V2	Reverse flow valve coupled with V4 around recirculation pump (pump outlet)
3-way valve	V3	Reverse flow valve coupled with V5 around recirculation pump (pump inlet)
3-way valve	V4	Reverse flow valve coupled with V2 around recirculation pump (pump outlet)
3-way valve	V5	Reverse flow valve coupled with V3 around recirculation pump (pump inlet)
Flow Adjustment Valve	V6	Flow adjustment valve (needle valve or similar) for flow adjustment
Flow meters	F1, F2	Flow Meters
3-way valve	V7	liquid heater recirculation outlet
3-way valve	V8	liquid heater recirculation inlet
3-way valve	V9	Drain valve
3-way valve	V10	Flow meter selection valve
3-way valve	V11	Flow meter selection valve
Recirculation Pump	Recirculation Pump	Recirculation Pump (centrifugal that allows flow adjustment with a valve)
Video Camera 1	Video Camera 1	Liquid level camera
Video Camera 2	Video Camera 2	sRF resin level camera
Video Camera 3	Video Camera 3	Full view camera
Video Camera 4	Video Camera 4	Hydrogen gas collection level
Condenser	Condenser-O	Optional: Cooling loop for potential moisture removal in H ₂ gas collection line
Pressure Gauges	P1, P2	Optional pressure gauges (used For Information Only)

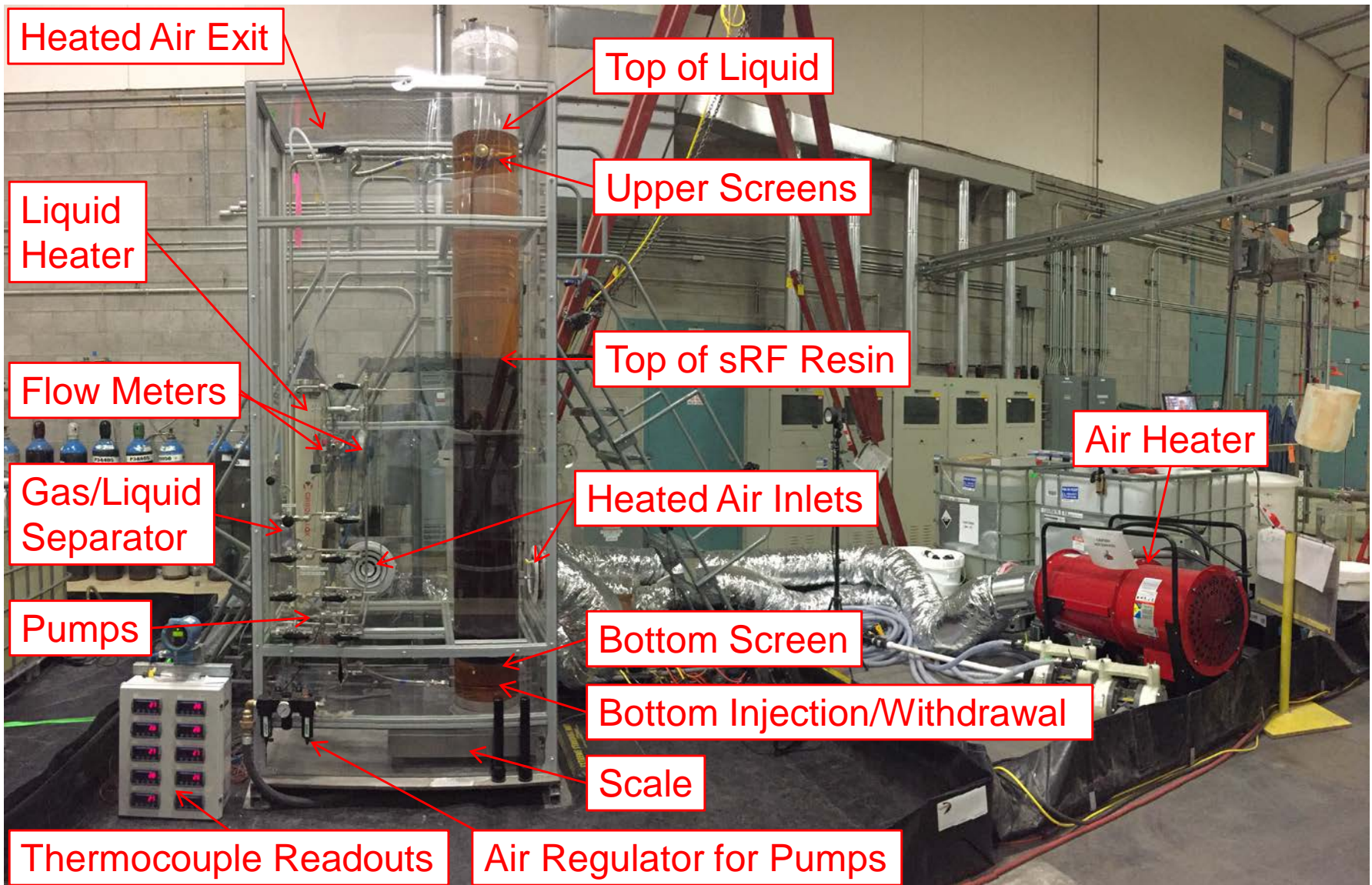


Figure 6.3. Photograph of Fluidization Column Test System, As-Built, with Key Equipment Labeled. (The gas-collection system is not shown.)

6.2.1 Fluidization Column Test Operation

This section summarizes the general steps used for conducting the fluidization column testing. Tests in the fluidization column included fluidization tests without gas generation and tests with gas generation, retention, and release both with and without fluidization. Observations were also made for settling of suspended beds of sRF resin in the absence of flow. The set of steps outlined below describe the process by which experiments were typically performed; in some cases deviation from these steps were taken to collect data opportunistically, observe gas retention or fluidization phenomena, repeat a test condition, or immediately transition to another test type, e.g., fluidization with no gas generation to fluidization with gas generation.

Fluidization testing in the absence of gas generation was performed as follows:

- A simulant solution was prepared and equilibrated with sRF resin in vessels ancillary to the column.
- The empty column was weighed.
- The column and recirculation flow system were loaded with resin and simulant solution (the gas collection system was not needed for tests of this type).
- The resin bed was fluidized to release any retained gas that was present, then allowed to settle until no noticeable settling behavior was observed.
- A liquid sample for density and viscosity measurements and an sRF particle sample for diameter and density measurement were collected.
- The initial column mass (now loaded), the initial resin level, and the initial liquid levels were measured and recorded.
- Video recording cameras to be used during the test were prepared and activated.
- The column was fluidized in up flow and bed expansion was measured for a range of velocities. These velocities were typically selected to span from below the onset of fluidization to 50% bed expansion. In some test cases alternate velocity targets were tested.
- In selected tests, fluidization of the bed continued to progressively higher velocities; if an upper packed bed formed, its thickness was measured and recorded. Observations concerning potential blockage of fluid withdrawal screen and upper sRF bed formation were collected as applicable.
- In selected tests, fluidization was stopped and the height of the settling sRF resin bed as a function of time was measured and recorded.

Fluidization testing at elevated temperature (55°C) in the absence of gas generation required a few extra processes compared to ambient fluidization, and was performed as follows:

- A simulant solution was prepared and equilibrated with sRF resin in vessels ancillary to the column.
- The empty column was weighed (or resin previously loaded into column was used).
- The column and recirculation flow system were loaded with resin and simulant solution (the gas collection system was not needed for this test).
- The resin bed was fluidized to release any retained gas that was present, then allowed to settle until no noticeable settling behavior was observed.
- A liquid sample for density and viscosity measurements and a second sample of sRF particles for diameter and density measurement were collected.
- The initial column mass (now loaded), the initial resin level, and the initial liquid levels were measured and recorded.
- Video recording cameras to be used during the test were prepared and activated.
- While recirculation was conducted in down flow, the liquid and air heaters were used to achieve a column temperature of 55 °C. The target temperature was reached in approximately 1 hour.
- When temperature target was achieved, the liquid heater was turned off and recirculation stopped. This began a 12 hour period of holding the resin at 55 °C.
- After 12 hours at the target temperature of 55 °C, fluidization was started at selected velocities, and resin levels during fluidization were observed and recorded.
- After a series of fluidization velocities, the bed was allowed to settle and the height of the resin bed was measured and recorded.

Tests where gas retention and release were actively occurring (both with and without fluidization) were performed following the steps outlined below:

- A simulant solution was prepared and equilibrated with sRF resin in vessels ancillary to the column.
- The empty column was weighed.
- The column and recirculation flow system were loaded with resin and simulant solution, and the gas collection system was connected with the column headspace.
- The resin bed was fluidized to release any retained gas that was present, then allowed to settle until no noticeable settling behavior was observed.
- A liquid sample was taken for pH (for alkaline water only), density and viscosity

measurements.

- The initial column mass (now loaded), the initial resin level, and the initial liquid levels were measured and recorded.
- Fluidization tests were conducted as required to collect bed expansion data. Typically, the bed height was measured as a function of fluidization velocity and any potential blockage of the fluid withdrawal screen was observed.
- The pump and flow adjustment valve was adjusted to give the desired fluidization velocity for the gas release test.
- Video recording cameras to be used during the test were prepared and activated.
- A known volume of SBH solution (per recipe) was added to column and the bed was fluidized with recirculating flow to distribute SBH. After the distribution was completed, fluidization was stopped. This would also release any retained gas prior to growth of retained gas.
- The column was isolated from the flow system. Flow systems lines containing simulant with SBH were purged.
- The initial column mass (now loaded with SBH), the initial resin level, and the initial liquid levels were measured and recorded.
- Liquid level, resin level, and gas volume data were collected until a spontaneous gas release occurred in the column.
- Retained gas was allowed to accumulate to the desired or target volume.
- Fluidization at the desired velocity was begun; liquid and resin levels were measured and recorded frequently during fluidization release.
- Following the initial release, fluidization was continued for a sufficient period to demonstrate gas is continually released and does not accumulate.
- Fluidization was stopped, and the column was again isolated from flow system. Flow systems lines containing simulant with SBH were purged.
- Retained gas was again allowed to accumulate to the desired or target volume.
- Fluidization at the desired velocity was begun; liquid and resin levels were measured and recorded frequently during fluidization release.
- Fluidization was stopped; the gas retention/fluidization process was repeated as needed.

Additional tests in this group also occasionally used the following steps if the gas generation rate was not sufficient for more gas retention tests with the current simulant/resin slurry:

- A known volume of SBH solution (per recipe) was added to column and the bed was fluidized with recirculating flow to distribute SBH. After the distribution was completed, fluidization was stopped.
- The steps describing the retention/fluidization process that follow SBH addition in the list above were repeated (not necessarily all steps) after the SBH addition step at desired retained gas volume and fluidization velocity.

Note that in all cases, the use of a different simulant for a new test required removal of the existing resin/simulant slurry from the fluidization column. The sRF resin was then washed to remove the prior simulant and then contacted with the new simulant fluid once certain criteria were met. In a couple cases, conversion of the resin between Na⁺ and H⁺ form was required to transition between simulants.

6.2.2 Hydrogen Management in Fluidization Column

SBH hydrolysis to create hydrogen gas in the gas retention tests created a flammability hazard that was actively managed. The approach for managing this hazard was to inert the column with nitrogen gas prior to hydrogen being generated in the column. Before adding SBH, the column lid was attached and the column head space was purged with approximately 5 volumes of nitrogen. SBH was then added through a fitting on the top of the column lid so the headspace would remain inerted. During testing, despite the generation of hydrogen and release into the column headspace, no oxygen was present and the hydrogen had no fuel with which to burn. The gas collection cylinder was periodically evacuated in such a manner that it was drawn into a vessel that was also nitrogen purged. At the end of a testing sequence when the column needed to be opened, the column was purged again with 5 volumes of nitrogen prior to removing the column lid.

6.3 Measuring and Test Equipment Summary

Table 6.2 summarizes the measuring and test equipment, target accuracy, and data collection methods for measurement equipment used in the fluidization and bench-scale test columns. This includes equipment used to perform physical characterization measurements of the resin and simulants used in testing.

Table 6.2. Testing M&TE Specifications and Requirements

Required Measurement	Instrument (General and/or Specific Examples)	M&TE Category¹	Target Accuracy (meets or exceeds min. accuracy requirements)	Data Collection Method
Simulant Component Masses for Preparation	Scale	1	± 1% of mass	Recorded manually by test operator
Simulant Mass in Test Vessel	10-inch (Tall) Vessel Scale: Sartorius Combics (600 lb) 10-inch (Short) Vessel Scale: Sartorius CP 34001 S 5-inch Vessel Scale: Sartorius CP 34001 S 250 mL Grad Cylinder (and similar vessels): Mettler PM2500	1	10-in./Tall vessel: ± 20 g 10-in./Short vessel: ± 1 g 5-in. vessel: ± 1 g 250 mL grad cyl: ± 0.1 g	Recorded manually by test operator
Simulant Mass for Density	Scale or Balance	1	± 0.1% of mass	Recorded manually by test operator
Time	Commercial clocks, watches, and video camera time stamps	3	Accuracy of ± 5 s Synchronize before start of test	Recorded manually by test operator or recorded on video image
Level (Height or Depth)	Ruler	3	± 1 mm	Recorded manually by test operator or recorded on video image
Video Images	Video Camera	NA	NA	Video recorded on memory card
Temperature of Water, Simulant, Heated Air, and Laboratory	Thermocouple and Readout	1	± 2.2 °C	Recorded manually by test operator or recorded on video image
Shear Strength (Vane Method)	HAAKE VT550 with Shear Vane	2	Torque within ±10% or ±15% depending on selected certified viscosity standard	Recorded by instrument software
Rheogram	Anton-Paar Physica CR301	2	Torque within ±10% or ±15% depending on selected certified viscosity standard	Recorded by instrument software
pH	pH meter	2	±0.1 pH unit using certified pH buffer solutions	Recorded manually by test operator
Volumetric Glassware for Density	Pycnometer or volumetric flask	3	± 1.0% of measurement volume	Recorded manually by test operator
Graduated Cylinders for Gas Collection	Commercial Graduated Cylinders	3	± 2.0% of measurement volume	Recorded manually by test operator
Flow Rate for Fluidization	Flow meter	1	± 5% of flow	Recorded manually by test operator
Particle Size Distribution	Optical Microscope Images with Microruler and Caliper	2	± 10% of average diameter	Recorded manually by test operator from image

¹ **M&TE Categories:**

Category 1 – M&TE that is calibrated with traceability to a nationally recognized standard or physical constant, performed under controlled conditions and by an evaluated and accepted calibration laboratory, agency, or metrology facility.

Category 2 – M&TE that can be calibrated prior to and verified prior to and after use, by the User, with certified standards traceable to a nationally recognized standard or physical constant. The calibration frequency shall be called out in the associated instrument operating procedure.

Category 3 - Commercial devices procured as normal commercial equipment that provide adequate accuracy, such as rulers, tape measures, graduated glassware.

6.4 Hydrogen Gas Generation Method and Measurements

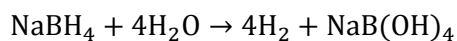
Primary goals of GR&R testing are to investigate gas retention and release behavior from sRF resin, in general, and to evaluate the efficacy of fluidization to induce gas release, in particular. Gas generation within the resin bed is obviously necessary to accomplish this. However, quantifying the amounts of gas generated and the generation rates, and the accuracy of such measurements, are to a certain extent secondary. Nonetheless, understanding approximate gas generation rates is of interest for the following reasons:

- The generation rate needs to be experimentally practicable. For fluidization-column experiments in particular, this means that the reaction rate is not so fast that the gas generating reagent is consumed while it is being mixed with the resin slurry, that significant generation and retention occur while the resin bed settles initially (to a preferably gas-free state), that other test preparations and operations cannot be completed, and/or that the retained gas fraction changes significantly over the time frame of a fluidization-induced release test. On the other hand, experimental delays and inefficiency were a consideration for very slow gas generation rates. An ideal target window of 6 to 12 hours for the gas retention period preceding fluidization-induced gas release tests was identified and is discussed further in Section 8.1.1. Additionally, sustained generation was preferred so that multiple fluidization-GR&R tests could be completed on a single charge of gas-generating reagent (see below).
- As noted in Section 1.2, scaled gas generation rates in continuous gas retention and release (coGR&R) tests greater than those expected in a full-scale sRF resin ion exchange column should conservatively (over)estimate the retained gas holdup during steady-state fluidization. The estimated upper-bounding volumetrically-scaled gas generation rate in the 10-in. fluidization-column test configuration is 0.8 L/day (Section 1.2). An even-more-conservative 1-L/day (17.6 L/day at full-scale = $[42\text{-in.}/10\text{-in.}]^2 \times 1 \text{ L/day}$) generation rate line is shown for reference on a number of test result plots in Sections 8.1.2 and 9.2.3.

This section further describes the methods of gas generation and quantification. See Sections 8.0 and 9.0 for additional discussion of the application and observed characteristics of gas generation.

Sodium borohydride (NaBH_4 , SBH; $M_{SBH} = 37.833 \text{ g/mol}$) is a well-known reducing agent and source of hydrogen gas (H_2). It is soluble in water, water reactive, and the rate of reaction in water can be controlled through pH adjustments (lower rate under alkaline, high-pH conditions)¹ and concentration, having pseudo first-order kinetics (Yamamoto 2003). These characteristics make it useful for homogeneous distribution and gas generation in aqueous slurries of sRF resin and led to its selection for use in these studies. The hydrolysis reaction of SBH to generate H_2 is given by

¹ In agreement with literature (Yamamoto 2003), early scoping experiments using an existing automated gas burette system (Zheng et al. 2008) showed that the rate of hydrogen gas generation increased demonstrably as the sRF resin slurry/alkaline water pH decreased in steps from pH 12.0/12.3 to pH 11.5/11.9 and to pH 10.4/10.5. Results were compared on a hydrogen molar equivalents basis (see Eq. (6.3) in this section and the results of later tests in Section 8.1). The sRF resin in all these tests had been contacted with water/trifluoromethane and used in soluble gas evacuation scoping studies (Section 1.2) before being washed multiple times with deionized water. Additional water washes were used to lower the pH to 11.5/11.9, and 0.5 M hydrochloric acid was added to get to the lowest pH. These preliminary studies did not follow the full requirements of the QA program outlined in Section 3.0 and should be considered For Information Only.



The hydrated sodium borate (NaB(OH)_4) reaction product can also be represented as an equimolar mixture of sodium hydroxide (NaOH) + boric acid (H_3BO_3). Ideally, based on reaction stoichiometry, 4 molar equivalents of H_2 are generated in the complete oxidation of SBH (i.e., 4 moles H_2 per mole SBH). However, in FIO scoping studies and in this report, only 1 to 2 equivalents of H_2 were typically generated in the presence of sRF resin at $\text{pH} \geq \sim 12$. The measured (simulant-dependent) generation stoichiometry and the requirements (targets) for the volume and rate of H_2 generation in GR&R experiments dictate the controlled amount of SBH to be used in an sRF resin bed of known volume. It is demonstrated in Section 8.1 that multiple successive SBH additions may be made to an sRF resin/liquid simulant batch to further generate H_2 without washing or otherwise reconditioning the sRF resin in between, although with different kinetics and total gas yield.

In these tests, SBH concentration, C_{SBH} , was defined in terms of mass SBH (m_{SBH}) added in grams per unit volume (liter) of settled gas-free sRF resin bed (g SBH/L resin). Alternatively, the concentration could be based on the total volume of resin and supernatant liquid or the total volume of free liquid (supernatant and resin bed pore space), for example. The choice of a resin-volume basis is convenient and more directly relevant, because the majority of gas is generated within the resin bed (at least in the early stages of retention periods), as will be shown in Section 8.2. However, there were variations in the proportions of resin and supernatant liquid in the various test vessels, and, therefore, the concentrations are not absolutely comparable or transferable between the test scales: a) Graduated cylinder tests – 110-mL resin and 160-mL total, or 69% resin; b) Bench-scale tests in 5-in. and 10-in. diameter vessel – 15-cm resin and 22-cm total, or 68% resin; and c) fluidization-column tests – 50.4-in. resin and 84-in. total, or 60% resin. Additionally, the effective concentration in the fluidization-column is reduced because of dilution by the liquid below the bottom Johnson screen and in the recirculation system lines and components, and this reduces the resin fraction. The differences in concentration bases from the bench-scale tests (68 to 69% resin) and the fluidization column are not critical, because: the absolute SBH concentrations and resulting gas generation rates are not used in downstream analyses; all bench-scale test vessels had nominally the same resin fraction and the generation rates for these vessels can be, and are, compared directly; and the bench-scale experiments provided guidance for the SBH concentration to use in the fluidization GR&R tests, but the generation rates at the two scales are not compared to each other, and they did not need to be the same.

Gas generation was assessed in two ways in these experiments. First, in periods of active gas retention, increases in the supernatant liquid level provide evidence of generation within the resin bed and give quantitative information on the volumetric “rate of retention”, i.e., the measured volume of generated gas determined from gas retention (ΔV_g , the change in retained gas volume) as a function of elapsed time. (See additional discussion of gas retention metrics in Section 6.5.) To assess gas generation in periods of no or minimal apparent changes in retained gas volume, e.g., in continuous gas release tests, the volume of generated gas was measured independently by capturing the gas leaving the otherwise sealed test vessel. The collection and quantification method was similar to that used in previous GR&R experimental projects (e.g., Gauglitz et al. 1996 and Powell et al. 2014). As depicted schematically in Figure 6.1 in Section 6.1, a tube connected to the top of the vessel (headspace) is routed to an inverted graduated cylinder that is partially submerged in and prefilled with water from a larger reservoir by applying a vacuum to the headspace of the cylinder. Generated gas displaces water from the cylinder in roughly an equal volume.

In this report, gas collection cylinder volume readings, V_c , are used as-is to give the apparent volume of hydrogen gas generated. The cumulative volume of gas generated over a reaction period (or increment), ΔV_c , is simply the difference in V_c at the elapsed time (ET) of a second measurement (t_2) from an earlier volume reading at ET t_1 :

$$\Delta V_c = V_c(t_2) - V_c(t_1) \quad (6.1)$$

The overall cumulative volume of gas generated at t_2 is obtained by setting $V_c(t_1)$ equal to the initial (non-zero) volume reading at ET zero. As discussed more below, the apparent volume of gas generated determined by this direct method [Eq. (6.1)] is considered sufficiently accurate for the purposes of analysis and interpretation of results in this work.

From this point forward, the collected gas volume is used interchangeably with the total “generated” gas. Additionally, this gas is assumed to be and treated as 100% hydrogen. Doing so, the number of moles of H_2 generated, n_{H_2} , can be determined from the ideal gas molar volume (V_{ideal}/n_g) by

$$n_{H_2} = \frac{n_g}{V_{ideal}} \Delta V_c = \frac{P_g}{RT_g} \Delta V_c \quad (6.2)$$

where R is the ideal gas constant and P_g and T_g are the absolute pressure and temperature of the gas. For a typical 22-°C experiment temperature and 1-atm pressure, the molar volume is 24.2 L/mol. In this analysis, the average of measured room temperatures (bench-scale tests) or of measured collection cylinder headspace temperatures (fluidization-column tests), over the gas collection period of interest, is used for T_g . This temperature and an assumed standard 1.0 atm for P_g are used to calculate n_{H_2} from Eq. (6.2).

The ratio of moles of generated hydrogen to moles of added SBH ($n_{SBH} = m_{SBH}/M_{SBH}$) is used for the purpose of comparing rates in different liquid simulants with varying concentrations of added SBH. This mole ratio, which is also referred to here as molar equivalents of H_2 ($N_{H_2_eq}$; unit equiv.), is defined in terms of measured and calculated quantities as

$$N_{H_2_eq} = \frac{n_{H_2}}{n_{SBH}} \quad (6.3)$$

where n_{SBH} is that for the most recently added SBH, if multiple aliquots have been used. This neglects possible residual unreacted SBH in the sRF resin/liquid simulant batch, which cannot be quantified. The normalized generation unit given by Eq. (6.3), in conjunction with C_{SBH} , is also useful for scaling the quantity of SBH for use in different test vessels when trying to achieve target generation rates.

The ratio of absolute volume of gas per unit volume of settled gas-free resin bed ($V_{b,0}$) is more directly applicable to identifying the SBH concentration necessary for obtaining a target retained gas fraction in sRF resin in a desired time frame. This specific gas volume is generically defined as

$$\hat{V}_{gas} = \frac{V_{gas}}{V_{b,0}} \quad (6.4)$$

In application of this equation, the generalized gas volume V_{gas} can be either the generated gas volume ΔV_c or the (change in) retained gas volume ΔV_g (discussed in Section 6.5).

In this report, gas generation rates under various operating conditions, such as liquid simulant type and/or SBH concentration, are typically compared by plotting any of the gas generation metrics given in

Eqs. (6.1) to (6.4) against the elapsed time from an event marker (e.g., the time of initial level and volume measurements after SBH addition). Quantitative volumetric gas generation rates, \dot{V}_c , were also calculated for select periods of most fluidization GR&R tests using collection cylinder measurements in the relationship

$$\dot{V}_c = \frac{V_c(t_2) - V_c(t_1)}{t_2 - t_1} = \frac{\Delta V_c}{\Delta t} \quad (6.5)$$

The generation rate given by Eq. (6.5) is considered an incremental rate if t_1 and t_2 are the times of consecutive readings. Such rates are subject to increasing uncertainty (inaccuracy) with decreasing length of the time interval between readings (Δt). For example, no change in the collected gas volume may be observed over a 1 to 2 minute period, but 100 mL or more might be collected in the hour including those data. More commonly, average generation rates over extended periods are reported. Specifically, the “Overall” average generation rates in L/day for the duration of continuous gas release tests were determined for comparison to a 1-L/day benchmark (see above); and for general comparison amongst tests, the “1st-day” generation rate in quiescent gas retention periods (e.g., preceding fluidization-induced gas releases) were calculated and are reported. For the latter, t_1 in Eq. (6.5) is elapsed time 0 and t_2 is for the measurement closest to an ET of 24 hours from the start of gas retention, but using the actual t_2 in the calculation. In cases where the retention period was less than a day, t_2 of the latest measurement was used to determine the “1st-day” = “Overall” generation rate. An example of incremental generation rates is shown in Figure 8.5 in Section 8.1.2 for the purpose of demonstration and comparison to average generation rates over longer periods of time. In a couple of tests, gas generation rate data include interpolated estimates (based on before and after generation rates over “increments” of a few hours) for overnight periods in which the 4-L capacity of the collection cylinder was exceeded. Otherwise, incremental generation rates are not presented or used in other reported analyses.

To get the most accurate measure of the absolute amount of H₂ generated (e.g., n_{H_2}), a gas and vapor mole balance is needed over the entire system, including retained gas in the resin bed, the headspace of the GR&R test vessel, the headspace of the gas collection cylinder, and to a lesser extent, liquid throughout the system, to account for dissolved gas. A number of corrections could be, but are not, applied to ΔV_c to obtain a more accurate generated gas volume. For the level of accuracy in generated gas volumes and gas generation rates needed for this work, say $\pm 20\%$,¹ it is not necessary to make corrections, although it is worthwhile to understand the nature of them. Considerations for how the gas collection system was used and possible refinements, with assessment of the magnitude of impact to measurement accuracy, include:

- The pressure in the collection cylinder varied with the quantity of gas collected. The minimum pressure followed re-initialization (reset) steps in which vacuum was applied to the headspace of the inverted (closed) collection cylinder to draw water from a reservoir into the graduated collection cylinder. The maximum water column height in a completely filled (0-mL reading) 4000-mL graduated cylinder used in fluidization GR&R testing was ~20 in. (~0.5 m) corresponding to an absolute pressure of ~0.95 atm (~95 kPa)². If this pressure was

¹ For example, the low end of this range of accuracy would cover the over-conservatism of using a 1-L/day benchmark for continuous gas release tests in this work instead of the already-bounding 0.8-L/day maximum scaled HGR value. See the discussion earlier in this section.

² Standard atmospheric pressure (1 atm or 1.01325 kPa) corresponds to a water column height of 408 in. (10.4 m) at 20 °C with a water density of 0.998 g/mL. A ~20-in. (~0.5-m) water column in an inverted (closed) graduated

- maintained throughout the collection period, gas volumes would be overestimated by 5% compared to a 1-atm standard reference state owing to expansion into the vacuum headspace of the collection cylinder. However, increasing pressure in the collection cylinder (decreased water column height) with increasing collected gas volume means that all the collected gas is compressed resulting in lower apparent volumetric generation rates. In practice, the collection cylinder was typically operated between initial ~500 mL and final ~2500 to 3000 mL (~0.98 atm absolute) levels, and depending on the actual range, an overall correction to the cumulative volume collected to standard atmospheric pressure¹ would be at most a few percent increase, and possibly a fraction of a percent decrease, in the measured ΔV_c .
- In most fluidization-column and some bench-scale GR&R tests, the collection cylinder was reset multiple times over the course of the experiment. The volume of gas generated over the typical 3- to 5-minute re-initialization period cannot be accounted for directly, but could be estimated from incremental gas generation rates before and after the reset. With typical generation rates, the correction to the volume collected would be negligible. In practice, therefore, cumulative volumes generated before re-initialization were carried forward as-is and added to those measured after refilling the collection cylinder with water.
 - For similar reasons and in much the same way described in the first bullet above, complete corrections to apparent generated gas volumes would account for the fact that the GR&R test vessel headspace pressure was not at 1.0 atm.
 - In all bench-scale tests and a few initial fluidization-column tests, the headspaces of the GR&R vessel and the collection cylinder were directly connected by tubing and both experienced varying vacuum pressure equivalent to that of the water column height in the collection cylinder. Absolute volume correction to a standard reference state (e.g., 1 atm and 25 °C) requires knowledge of each headspace volume, the common pressure of the headspaces (from collection cylinder heights, if not measured directly), and the temperatures of each headspace in order to first determine the moles of gas present. For the majority of test vessels used in bench-scale tests, the total volumes of the GR&R vessels were not measured (and are not readily available), and, therefore, the headspace volume (= total volume - resin/retained gas/supernatant liquid volume) cannot be determined.
 - In all fluidization-column GR&R tests, except the few aforementioned initial experiments, gas from the column headspace was admitted to the collection cylinder at ~1 in. (~2.5 cm) below the water reservoir surface level and gas bubbled up through the water column in the collection cylinder into its headspace. While the vacuum pressure in the collection cylinder varied with collected gas volume, as above, the pressure at the gas inlet and in the GR&R vessel headspace remained

collection cylinder corresponds to a maximum vacuum of ~0.05 atm (= 20 in./408 in. \times 1 atm) or ~0.95 atm (~95 kPa) absolute pressure.

¹ Correction would entail determining the initial and final moles of gas in the collection cylinder using the ideal gas law, measured volumes, and absolute pressures determined from the equivalent water column heights. The ideal gas law molar volume at selected standard conditions (e.g., 1 atm and 25 °C) would then be applied to the moles of gas collected (final - initial). Note that applying the mean collection cylinder pressure to the collected volume, rather than determination from initial and final states, does not give the same number of moles. Also, counterintuitively, the measured cumulative ΔV_c may be larger than a corrected volume determined on an initial/final mole basis, if the collection cylinder is nearly drained before resetting and the associated net compression of the entire gas volume is sufficient, even though the cylinder headspace is always under vacuum.

relatively constant at ~+1-in. water column (1.0025 atm). This is so because the reservoir surface area was about 25-times larger than the cross-section of the collection cylinder, and, therefore, the reservoir surface level fluctuated relatively little compared to the height of water column in the cylinder. Assuming a constant GR&R vessel headspace pressure of 1.0025 atm and neglecting small temperature effects, a change (correction) in headspace volume at 1 atm standard pressure can be determined by applying the pressure ratio to the measured volume of gas in the vessel headspace (V_{hs})¹: correction volume = $1.0025 \text{ atm}/1.0 \text{ atm} \times V_{hs} - V_{hs} = 0.0025V_{hs}$, or in words, 0.25% of the headspace volume. At each time of measurement, this GR&R vessel headspace correction volume would be summed with the measured collection cylinder volume to correct it (for the vessel headspace contributions only), neglecting the secondary effects that a change in gas volume in the collection cylinder would have on the vacuum pressure in it. This relatively small volume adjustment was not made to the fluidization GR&R test data that was collected at the near-constant ~+1in. water-column pressure, but an analogous correction was applied to the few tests that were run under vacuum headspace conditions to make gas generation characteristics in them directly comparable to the others².

- Generated “gas” includes non-condensable H₂ and water vapor, which is expected to be present in bubbles at the equilibrium water vapor pressure for the given operating temperature and liquid composition. Gas in the GR&R test vessels and gas collection cylinders are also assumed to be saturated with water vapor. Using water as the liquid equilibrated with resin, for example, the vapor pressure of water is 20 mm Hg at 1-atm (760-mm Hg) total pressure and 22 °C. This corresponds to a mole fraction of water in bubbles and in other generated/released gas of 0.027 (= 20 mm Hg/760 mm Hg). Therefore, a correction of up to ~3% would need to be applied to the collected “wet” gas volume to determine the amount of “dry” H₂ generated. The correction is further dependent on the depth in the resin bed at which it is generated and retained, in which case the water vapor pressure is constant, but the mole fraction of H₂ increases with increasing hydrostatic pressure.

¹ The headspace volume was determinable from the difference in height at the top of the column (H_{top} = 254.1 cm from a ruler reading) and the measured supernatant liquid level (H_L) multiplied by the vessel cross-sectional area, A_c . (i.e., $V_{hs} = [H_{top} - H_L]A_c$).

² Pressure corrections were applied to the fluidization-column headspace volumes for Test 10-04 Phases 2, 3, and 4 (up through ~44-hr elapsed time, when the collection system configuration was changed) to make the collected gas volume data directly comparable to all later GR&R tests conducted in the fluidization column. The headspace volume at each measurement time was determined from the difference in height at the top of the column (H_{top} = 254.1 cm) and the measured supernatant liquid level (H_L) multiplied by the vessel cross-sectional area, A_c . (i.e., $V_{hs} = [H_{top} - H_L]A_c$). The absolute (vacuum) pressure in the column headspace, P_{hs} , was the same as in the collection cylinder headspace and was determined from the time-varying collected gas volume reading (V_c) in milliliters and the corresponding water column height, H_{wc} . Using 20 in. water-column vacuum pressure at 0 mL collected (uppermost reading) and a specific height of 20 in./4000 mL, $H_{wc} = 20 \text{ in.} - 20 \text{ in.}/4000 \text{ mL} \times V_c$, and with applicable unit conversions, $P_{hs} = P_{atm} - \rho_w g H_{wc}$, where P_{atm} is atmospheric pressure (1.0 atm assumed), ρ_w is the density of water (e.g., 0.99823 g/mL at 20 °C), and g is gravitational acceleration. The headspace volume at the reference pressure P_{ref} (e.g., 1.0025 atm) is $V_{hs,ref} = (P_{hs}/P_{ref})V_{hs}$; the change in headspace volume (correction volume) is $\Delta V_{hs} = V_{hs,ref} - V_{hs}$; and the corrected gas collection cylinder volume is the sum of the volume correction and the collection cylinder reading, $V_{c,corr} = V_c + \Delta V_{hs}$. This correction is applied at each measurement time (t), and the corrected cumulative volume of generated (collected) gas is the difference of $V_{c,corr}(t)$ and $V_{c,corr}(0)$, the corrected initial reading at, e.g., elapsed time zero.

- Correction to the volume of gas collected (“generated”) would also be needed to account for the varying hydrostatic load with depth in the resin bed and the corresponding variation in the expansion of retained non-condensable (H₂) gas as it is released. Release into the column headspace doesn’t change the total number of moles of gas in the system, but a change in volume due to expansion is registered in the gas collection cylinder¹. Similarly, the moles of as-retained gas are underrepresented by collection cylinder volume measurements when a reference pressure of 1 atm is applied to ΔV_c . To accurately determine the number of moles of retained gas (including water vapor), the vertical distribution of gas bubbles by volume is needed and a hydrostatic pressure correction, including the supernatant liquid, would be applied at each level in the resin bed (i.e., integration). Because experimental data do not provide quantitative information on the distribution of retained gas, a simplification would be to assume uniformly distributed retained gas and use the hydrostatic pressure at the vertical center of the bed to calculate compression during retention and expected expansion upon release. Doing this with measured liquid and resin bed densities given in Section 5.3.1 for sRF resin in alkaline water and in 6.1 M Na simulant, and using typical gas-free resin bed and supernatant liquid surface heights of 1.30 m (51.2 in.) and 2.17 m (85.4 in.), respectively, the calculated pressures at half resin bed depth are 1.155 atm in alkaline water and 1.190 atm in the simulant.² Therefore, upon release to an environment at 1 atm or, equivalently, correction to a standard reference pressure of 1 atm, the volume of retained gas would expand (increase) 16% (= [1.155 atm/1 atm – 1]100) and 19% from resin/water and resin/simulant, respectively. From a corrected volumetric gas generation perspective, the volume of gas generated that is retained is underrepresented by these amounts.
- In elevated temperature tests, contributions of water vapor become more significant, and gas thermal expansion (ideal gas law) and temperature differences between the GR&R test vessel and the collection cylinder are also factors to be considered. These are addressed separately in Section 8.4 with the discussion of the elevated-temperature test results.

Noting that the primary purpose of gas generation is to enable investigation of gas retention in and release from sRF resin, and not to investigate hydrogen generation from SBH in and of itself, we accept the uncertainty in the (hydrogen) gas generation rates and use the measured ΔV_c values without correction.

It should also be emphasized that the potential corrections noted above pertaining to retained gas volumes are only applicable to determination of generated gas volumes more accurately. From the

¹ Gas expansion effects were observed in fluidization-column tests during large spontaneous releases and in initial fluidization-induced gas releases. These periods were avoided in determination of apparent gas generation rates from collection cylinder volume measurements that are reported here. An example of observable expansion during a spontaneous gas release is shown in Figure 8.7 in Section 8.1.2.

² With a gas-free settled resin bed depth ($H_{b,0}$) of 1.30 m and a total height to the upper surface of the supernatant liquid (H_L) of 2.17 m, the depth of the supernatant liquid layer is 0.87 m (= $H_L - H_b$). The absolute pressure at half depth in the resin bed is: $P_{1/2b} = P_{atm} + [0.5\rho_{b,0}H_b + \rho_L(H_L - H_b)]g$, where P_{atm} is atmospheric pressure (1.0 atm [101325 Pa] assumed), $\rho_{b,0}$ and ρ_L are the gas-free resin bed and liquid densities, respectively, and g is gravitational acceleration. From Table 5.1 in Section 5.3.1, $\rho_{b,0}$ and ρ_L are 1,131 kg/m³ and 998 kg/m³, respectively, for sRF resin in alkaline water and are 1,337 kg/m³ and 1,254 kg/m³, respectively, for sRF resin in 6.1 M Na LAW simulant (“GR&R 6.12 M LAW”). Using the alkaline water system as an example, substituting these and other noted values and constants into the equation gives

$P_{1/2b} = 1.155 \text{ atm} = 1.0 \text{ atm} + [1,131 \text{ kg/m}^3 \times (0.5 \times 1.30 \text{ m}) + 998 \text{ kg/m}^3 \times 0.87 \text{ m}] \times 9.807 \text{ m/s}^2 \times 1 \text{ atm}/101325 \text{ Pa}$
 Similarly, $P_{1/2b}$ is 1.190 atm for the noted sRF resin/LAW simulant system.

perspective of determining retained gas fractions and evaluating gas releases, the directly measured in situ retained gas volumes are proper. In this, note also that no correction for water vapor in retained gas bubbles is necessary; it is realistic and representative of the retained gas composition in an actual waste processing environment.

6.5 Gas Retention and Release and In-Test Resin Bed Properties

Gas retention and release concepts, definitions, and calculations described in Section 1.1 and further in this section are generally applicable to all GR&R tests described in this report. Many fluidization-induced gas release experiments were conducted when the resin bed reached a defined target fraction of the maximum measured retained gas volume. Therefore, initial bench-scale and fluidization-column experiments were completed to assess the peak retention at the point of spontaneous gas release under stagnant (quiescent, no flow) conditions. Peak retention is also of interest in its own right for comparison to the theoretical retained gas fraction for the resin bed to become neutrally buoyant in the supernatant liquid. As noted in Section 1.1, the resin bed, or a portion of it, becoming neutrally buoyant and rising in the supernatant liquid was one of the anticipated mechanisms of gas release from sRF resin. As outlined below, the gas fraction at neutral buoyancy is a function of the resin bed density, which may vary during a test independent of the presence of retained gas, because of changes in the packing structure of the resin bed.

Similar to Figure 1.4 in Section 1.1, Figure 6.4 is a schematic diagram of the fluidization-column/ ion exchange resin bed/ retained gas/supernatant liquid configuration in stagnant and fluidization GR&R tests. The schematic is also conceptually applicable to bench-scale tests except that there is no resin support screen or liquid pool at the bottom of the smaller vessels, such as is depicted in the experimental setup shown in Figure 6.1 of Section 6.1. Figure 6.4 shows the primary gas retention and release metrics that are tracked during an experiment. These are the time-varying resin bed level, H_b (or volume, V_b), and the supernatant liquid level (topmost surface in Figure 6.4), H_L , or equivalently, the total volume of resin, liquid, and retained gas (V_t). As discussed further below, these data are used to: a) primarily, quantify changes in the volume of retained gas in periods of gas retention and resulting from spontaneous or fluidization-induced gas-release events; and b) secondarily, (semi-)quantitatively elucidate whether gas is retained in the resin bed by particle-displacing bubbles (PDBs) and/or interstitial-liquid-displacing bubbles (ILDDBs), as well as assess whether there are changes in the packing structure of the resin bed.

For the relatively-large sRF resin beads (particles) and porous resin bed structure used in these experiments, gas generated in the lower portion of deep resin beds (e.g., 50.4 in. [128 cm] in the fluidization-column) was expected to be retained as ILDBs. Such bubbles finger between and push liquid through the pore space between particles causing the supernatant liquid level to increase without (necessarily) moving particles or causing the resin bed level to increase. Therefore, gas retained in the resin bed only as ILDBs would be quantitatively expressed by no change in resin bed level from an initial gas-free reference state ($\Delta H_b = 0$) and have a positive change in supernatant liquid level compared to the same initial state ($\Delta H_L > 0$). In contrast, gas generated in shallow resin beds, or near the resin bed surface down to some transition depth in deep beds, was anticipated to be retained as relatively-round PDBs that cause the resin bed to expand and the supernatant liquid level to increase equally (i.e., $\Delta H_b = \Delta H_L$). However, the relatively-large pore bodies between spherical sRF resin beads can potentially accommodate a significant volume of round bubbles before particles are (necessarily) displaced. In this case, smaller would-be PDBs would have quantitative characteristics similar to ILDBs (i.e., $\Delta H_b = 0$,

$\Delta H_L > 0$). Both PDBs and ILDBs result in changes in the supernatant liquid level (total volume, V_t), equivalent to the volume of gas retained ($\Delta V_t = V_g$).

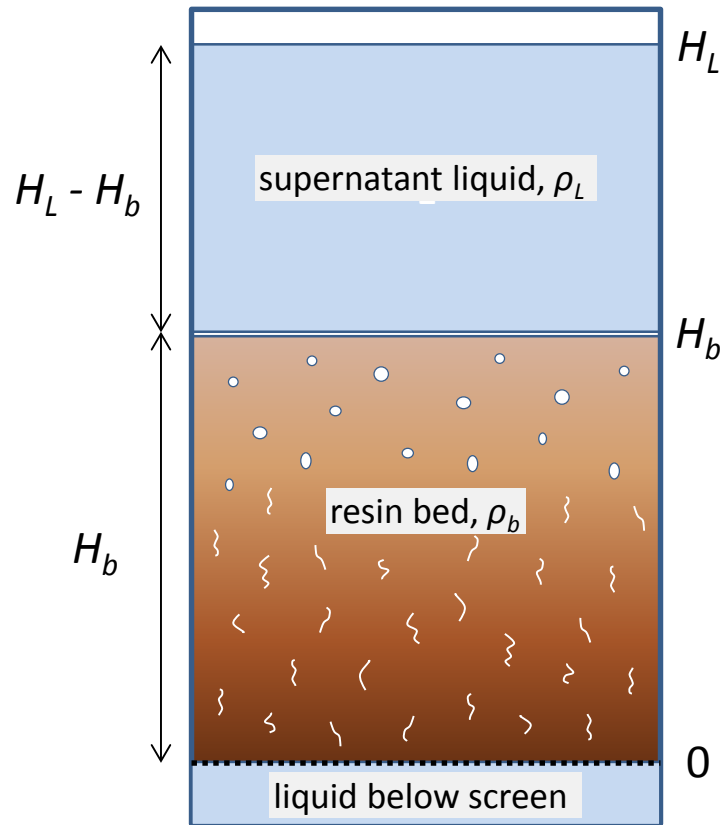


Figure 6.4. Diagram of an Expected Resin Bed/Liquid Configuration in an Ion Exchange Column with Reference Dimensions (not to scale). Interstitial-liquid-displacing bubbles (lower) and particle-displacing (rounded) bubbles (upper) are depicted schematically in the resin bed.

As noted in the discussion of gas bubble retention mechanisms in Section 1.1, vessel-spanning bubbles and pancake bubbles are also factors in GR&R tests in sRF resin beds. Experimentally, the presence of these bubble types is determined qualitatively through visual observations, and typically, the volume of gas in these bubbles cannot be quantified explicitly. However, VSBs and pancake bubbles affect quantitative analysis of the primary mechanisms of gas retention in the form of PDBs and ILDBs and demonstrate the following characteristics.

As noted previously, VSBs are a potential artifact of test vessel size: they are more likely to be observed and be stable (indefinitely) in tests conducted in small-diameter vessels (e.g., 250-mL graduated cylinders), whereas they are less likely to form in larger-diameter test vessels (e.g., 5-in. and 10-in. ID), and, if they do, they are more likely to be unstable (short-lived). In sRF resin beds, VSBs can be formed secondarily through the release of gas that is initially retained by other mechanisms below the VSB. Quantitatively, however, VSBs always behave like PDBs, because both the resin bed and supernatant liquid above them are displaced. The total volume of gas retained in the resin bed can increase after the formation of a stable VSB as a result of continued gas generation and retention in the resin below and/or above the VSB. Because a VSB is an artifact of a test conducted in a relatively small-diameter vessel,

retention beyond VSB formation leads to false-peak retained gas fractions. Reporting of such data below makes this clear.

As is also discussed in Section 1.1, gas bubbles were also often retained below and by the bottom Johnson screen in fluidization-column experiments. These bubbles, generally referred to as “pancake” bubbles, were sometimes individual round bubbles, contiguous lengths of bubble running down channels defined by support rods, sheet-like (pancake) bubbles covering multiple channels and visibly significant area (up to the entire screen), and/or a combination of these.¹ Conservation of volume dictates that a volume of liquid equal to the volume of the retained pancake bubble be displaced above the screen when the vessel bottom is closed, like it was when the fluidization column was isolated from the fluid recirculation system for periods of quiescent gas retention. Therefore, it is most likely that gas retained below the bottom screen in GR&R tests pushed liquid through the connected channels of the resin bed, and in this way would have presented quantitatively like ILDBs (i.e., increase in the supernatant liquid level without a change in the resin level). In most tests covered by this calculation, the quantity of gas below the screen varied over time and was not readily quantifiable volumetrically; and, there is no attempt for any of the GR&R tests to computationally correct the apparent total volume of retained gas by the volume of bottom screen cover gas to determine the “true” volume of gas retained in the resin bed.²

The measured retained gas volume fraction, α , is defined as the total volume of gas retained by all mechanisms noted above (e.g., PDBs, ILDBs, VSBs, and pancake bubbles) divided by the total volume of the resin bed including the retained gas, resin beads, and interstitial liquid contained therein. Per the discussion above, the retained gas volume, V_g , is determined from changes in the supernatant liquid level and is equal to the change in total volume of contents in the test vessel (retained gas, resin beads, interstitial liquid, and supernatant liquid) relative to an initial “gas-free” state (ΔV_t). In tests in graduated cylinders, the retained gas volume is obtained directly from changes in the measured total volume at the supernatant liquid surface, and in other cylindrical test vessels with affixed rulers and constant cross-sectional area, A_c , the gas volume is a function of the change in supernatant liquid surface height (ΔH_L). In terms of experimentally measured quantities, the retained gas fraction is

$$\alpha = \frac{V_g}{V_b} = \frac{\Delta V_t}{V_b} = \frac{\Delta H_L A_c}{V_b} \quad (6.6)$$

The total resin bed volume is measured directly in graduated cylinders, whereas it is determined by application of pre-established level-volume correlations and the measured resin bed height in other cylindrical test vessels.

¹ In most fluidization-column tests, visual observations of characteristics of bubbles below the bottom screen were made and documented. Typically, estimates were made of the “open” (O) screen area fraction that was nominally free of bubbles that might impede flow (subjective assessment) or, alternatively, of the total area fraction blocked or “covered” (C) by bubbles. The fraction of the screen area that was covered by contiguous “pancake” (P) bubble(s), if any, was also often estimated. The fraction, f , of the area covered by other bubbles (e.g., individual or channel slugs) can be determined from open screen and pancake bubble estimates: $1 = f_O + f_C = f_O + f_P + f_{C,other}$. In cases where the gas covered the entire screen, which is the basis of the term “pancake”, the height of the bubble was also occasionally measured with a ruler or otherwise visually estimated.

² The volume of gas below the screen was sometimes “measured” experimentally at the end of a GR&R test phase by extracting bubbles with an 1/8-in. OD tube connected to a vacuum chamber and returning any accompanying liquid to the fluidization column. Neglecting gas generation and retention in the period of bubble removal, the difference in supernatant liquid level is indicative of the gas volume removed from under the screen.

A change in total resin bed volume relative to the initially gas-free settled bed, ΔV_b , ($= \Delta H_b A_c$), can result from retained gas (e.g., as PDBs or VSBs) and/or changes in the resin bed packing structure. Assuming a constant mass and volume of resin beads (i.e., no particle shrinkage or swelling), a reduction in resin bed volume is indicative of a more compact resin packing structure and lower bed porosity. On the other hand, the resin bed could expand due to a net infiltration of supernatant liquid into the resin bed, in addition to possible contributions from retained gas, and result in apparent increases in gas-free bed porosity. In this sense, the change in total volume of the resin bed is a measure of the (change in) “total void” relative to the initially gas-free settled bed volume:

$$\Delta V_b = V_g + \Delta V_{L,\varepsilon} = \Delta V_t + \Delta V_{L,\varepsilon} \quad (6.7)$$

As shown, it is the sum of the retained gas volume (gas void) and the change in volume of interstitial liquid in the bed, $\Delta V_{L,\varepsilon}$, which is referred to as (the change in) “liquid void”. Rearranging Eq. (6.7) shows that $\Delta V_{L,\varepsilon}$ is determined directly from measured resin bed and total volumes. Below, this change in interstitial liquid content in the resin bed is further defined in terms of its two components, one associated with displacement by ILDBs and the other due to changes in resin bed packing structure.

Unambiguous identification and quantification of retained gas as PDBs and ILDBs is not possible from resin bed and supernatant liquid level (volume) measurements alone, for the following reasons. First, it is assumed in this analysis that the sizes of individual resin particles remain constant during an experiment, and therefore, changes in resin bed volume are due to other factors discussed below. For gas retained as interstitial-liquid-displacing bubbles and for round bubbles filling pore bodies between resin particles without disturbing the resin (i.e., total apparent ILDB content, neglecting contributions of bubbles beneath the bottom screen), the resin bed level does not change and the volume of liquid within the porous bed decreases equal to the volume of gas retained within the pores as ILDBs ($V_{g,ILD}$), thereby giving a change in total void of zero by Eq. (6.7) ($V_{g,ILD} = -\Delta V_{L,\varepsilon}$). For gas retained as particle-displacing bubbles, the change in resin bed and retained gas volumes are equal and there is no change in the volume of liquid within the porous bed. In this case, the volume of gas retained as PDBs ($V_{g,PD}$) is equal to the change in total void ($V_{g,PD} = \Delta V_b$). With either ILDBs or PDBs, the volume of liquid within the bed should decrease or remain constant. If not, a net infiltration to or exfiltration of liquid from the bed associated with a change in packing structure and gas-free bed porosity is indicated, also resulting in a change in the gas-free bed density. It is also possible, however, that resin bed expansion occurs due to liquid infiltration while a portion or all of the gas is retained as ILDBs, which gives the appearance of gas retained as PDBs. Nonetheless, the apparent volume fractions of gas retained as PDBs (f_{PD}) and ILDBs (f_{ILD}) are given by

$$f_{PD} = \frac{V_{g,PD}}{V_g} = \frac{\Delta V_b}{\Delta V_t} = 1 + \frac{\Delta V_{L,\varepsilon}}{\Delta V_t} \quad (6.8)$$

and

$$f_{ILD} = \frac{V_{g,ILD}}{V_g} = 1 - f_{PD} = \frac{-\Delta V_{L,\varepsilon}}{\Delta V_t} = 1 - \frac{\Delta V_b}{\Delta V_t} \quad (6.9)$$

Equations (6.8) and (6.9) show that a net infiltration of liquid into the bed and associated bed expansion (i.e., positive $\Delta V_{L,\varepsilon}$) will result in f_{PD} exceeding one and f_{ILD} being negative. These are nonsensical results, but they are a clear indication of decreased gas-free bed density and increased gas-free bed porosity per Eq. (6.14) and Eq. (6.17) below. More specifically, for $\Delta V_{L,\varepsilon} > 0$, gas retention is apparently 100% in PDBs ($V_g = V_{g,PD}$), and there is additionally an apparent increase in the liquid volume

(void) in the (hypothetically) gas-free resin bed, $\Delta V_{L,\varepsilon,gf}$, that is equal to the measured change in liquid void (i.e., positive $\Delta V_{L,\varepsilon,gf} = \Delta V_{L,\varepsilon}$). On the flip side, f_{ILD} greater than one and negative f_{PD} result from a decrease in the resin bed volume (i.e., negative ΔV_b) or, equivalently, a decrease in liquid volume in the resin bed exceeding the volume of liquid displaced by retained gas. This is indicative of reduced gas-free bed porosity and increased bed density. In other words, for $\Delta V_{L,\varepsilon} < 0$ and the magnitude (absolute value) of the change in liquid volume exceeding the volume of gas retained ($|\Delta V_{L,\varepsilon}| > V_g$), gas retention is apparently 100% in ILDBs ($V_g = V_{g,ILD}$), and there is additionally an apparent decrease in the liquid volume in the gas-free resin bed associated with formation of a more compact bed pore structure (i.e., negative $\Delta V_{L,\varepsilon,gf} = V_{g,ILD} - |\Delta V_{L,\varepsilon}| = V_{g,ILD} + \Delta V_{L,\varepsilon}$). Further, for f_{PD} and f_{ILD} both between 0 and 1 according to Eqs. (6.8) and (6.9) (i.e., $\Delta V_{L,\varepsilon} \leq 0$ and $V_g \geq |\Delta V_{L,\varepsilon}|$), there is insufficient experimental information to determine if any net decreases in liquid volume in the resin bed are due to pore structure changes in combination with retained gas, in which case it is appropriate to assume that $\Delta V_{L,\varepsilon,gf} = 0$, and the gas-free resin bed density and porosity are (apparently) unchanged.

During periods of quiescent gas retention and spontaneous gas release in GR&R tests, the retained gas fraction is defined and expressed by Eq. (6.6) using the time-varying measured bed volume in the denominator. In fluidization-induced gas release tests, however, it is necessary to define the retained gas fraction with reference to the initial gas-free settled resin bed volume, $V_{b,0}$. This is so when the resin bed is expanded due to fluidization, in addition to gas retention, because the bed expansion resulting from fluidization gives the appearance of a reduction in the retained gas fraction by definition even without gas release (i.e., α = retained gas volume/total [expanded] resin bed volume). From the discussion above, retained gas fractions for (theoretically) 100% PDBs, α_{PD} , and for 100% ILDBs, α_{ILD} , differ for the same volume of retained gas, because the bed volume either expands with gas retention or remains constant, respectively:

$$\alpha_{PD} = \frac{V_g}{V_{b,gf} + V_g} = \frac{\Delta V_t}{V_{b,gf} + \Delta V_t} \quad (6.10)$$

and

$$\alpha_{ILD} = \frac{V_g}{V_{b,gf}} = \frac{\Delta V_t}{V_{b,gf}} \quad (6.11)$$

These definitions are applicable to any gas-free resin bed volume ($V_{b,gf}$), and $V_{b,0}$ is the specific gas-free reference value used in the fluidization-induced gas release analyses mentioned above. Note in Eq. (6.10) and Eq. (6.11) that the total retained gas volume determined experimentally is used rather than the volume of gas retained in bubbles of the specific type, which can only be determined semi-quantitatively, as discussed in the previous paragraph. Here, the choice of using either α_{PD} or α_{ILD} from Eq. (6.10) or Eq. (6.11) is typically based on the higher of the fractions of retained bubble type, f_{PD} or f_{ILD} , demonstrated in quiescent gas retention (growth) periods. In continuous-fluidization GR&R tests, the steady-state gas holdup (α_{ss}) is given by Eq. (6.10) or Eq. (6.11).

The fraction of peak gas retention, f_α , is an alternative metric for retained gas content that is applicable throughout a gas retention and release experiment. It is defined as

$$f_\alpha = \frac{\Delta H_L}{\Delta H_{L,max}} = \frac{V_g}{V_{g,max}} \quad (6.12)$$

where $\Delta H_{L,max}$ and $V_{g,max}$ are the maximum level change (relative to the gas-free state) and equivalent volume of retained gas measured in peak retention and spontaneous gas release testing ($f_a = 1$) with the same sRF resin / liquid system. As opposed to retained gas fractions α , α_{PD} , and α_{ILD} , f_a is directly related to absolute measures of retained gas that are independent of the bubble type/location and the volume of the resin bed. In fluidization-induced gas release tests, fluidization was typically initiated at a target f_a (e.g., 0.5 or 50%), and in practice, the target was determined in terms of the supernatant liquid level when f_a was reached: H_L (at target) = $H_{L,0} + f_a \Delta H_{L,max}$, where $H_{L,0}$ is the initial gas-free liquid level.

The theoretical retained gas fraction for the resin bed to be neutrally buoyant in the supernatant liquid also differs for gas retained as PDBs or ILDBs, and again, this is true despite the same volume of retained gas being necessary for neutral buoyancy with the two bubble forms. In both cases, the density of the resin bed including the quantity of gas necessary for neutral buoyancy is equal to the supernatant liquid density (ρ_L), by definition. A general expression for the density of the bed, ρ_b , containing an arbitrary quantity of retained gas and possible liquid infiltration or exfiltration, is

$$\rho_b = \frac{V_{b,0}\rho_{b,0} + \Delta V_{L,\varepsilon}\rho_L}{V_b} = \frac{V_{b,0}\rho_{b,0} + \Delta V_{L,\varepsilon}\rho_L}{V_{b,0} + \Delta V_b} = \frac{V_{b,0}\rho_{b,0} + \Delta V_{L,\varepsilon}\rho_L}{V_{b,0} + V_g + \Delta V_{L,\varepsilon}} \quad (6.13)$$

where subscript “0” denotes a property of the initial gas-free settled resin bed.¹ The total mass of the resin bed shown in the numerator of Eq. (6.13) is that for the initial resin bed plus a correction for the mass of infiltrated or exfiltrated liquid; the mass of any retained gas is assumed to be negligible. The total resin bed volume is shown in three forms in the denominator of the equation. In the right-most version, the change in bed volume from the initial gas-free value is expressed in terms of Eq. (6.7).

Equation (6.13) gives the gas-free resin bed density, $\rho_{b,gf}$, by setting V_g to zero and, for ILDBs, by also assuming that a volume of liquid equal to V_g “reenters” the bed when the gas is hypothetically “removed” to achieve the gas-free state. In this case, the balance of the liquid void term ($\Delta V_{L,\varepsilon,gf}$) only accounts for changes in resin packing structure (porosity) that are independent of retained gas, although they may be initially caused by it; see the definition and discussion of $\Delta V_{L,\varepsilon,gf}$ following Eqs. (6.8) and (6.9) above. The gas-free bed density is

$$\rho_{b,gf} = \frac{V_{b,0}\rho_{b,0} + \Delta V_{L,\varepsilon,gf}\rho_L}{V_{b,gf}} = \frac{V_{b,0}\rho_{b,0} + \Delta V_{L,\varepsilon,gf}\rho_L}{V_{b,0} + \Delta V_{L,\varepsilon,gf}} \quad (6.14)$$

where subscript “gf” identifies properties of the gas-free resin bed. The gas-free bed density collapses to the initial settled bed value $\rho_{b,0}$ when $\Delta V_{L,\varepsilon,gf}$ is zero, meaning also that the bed porosity is unchanged from its initial gas-free value ($\varepsilon_{b,0}$).

The resin bed volume ($V_{b,gf} = V_{b,0} + \Delta V_{L,\varepsilon,gf}$) and resin bed density defined in Eq. (6.14) are used in part to calculate the theoretical retained gas fractions at neutral buoyancy for gas retained in PDBs ($\alpha_{NB,PD}$) or in ILDBs ($\alpha_{NB,ILD}$). This is done starting with the general definitions of α_{PD} and α_{ILD} given in Eq. (6.10) and Eq. (6.11), respectively, and setting ρ_b (from Eq. (6.13)) equal to ρ_L at neutral buoyancy. For gas retained strictly as PDBs, liquid is not displaced from the bed by the bubbles, and the generalized

¹ In fluidization-column experiments, the bed density given by Eq. (6.13) is considered the “apparent minimum” value, because it is assumed that all retained gas is in the resin bed. The actual volume of gas retained in the bed is less by the amount of any gas retained below the bottom Johnson screen (e.g., pancake bubble). Correcting for the bottom gas (if possible), would result in a higher liquid (to gas) fraction in the bed and a higher resin bed density.

liquid void terms in both the numerator and denominator of Eq. (6.13) are set to the gas-free value ($\Delta V_{L,\varepsilon,gf}$). Then, combining Eq. (6.10), Eq. (6.13), and Eq. (6.14) subject to $\rho_b = \rho_L$ gives

$$\alpha_{NB,PD} = 1 - \frac{\rho_L}{\rho_{b,gf}} \quad (6.15)$$

For gas retained as ILDBs, a volume of liquid equal to the volume of retained bubbles is displaced from the bed. Therefore, any change in bed volume is due only to liquid void from pore structure changes; in this case, the denominator of Eq. (6.13) is $\Delta V_b = V_g + \Delta V_{L,\varepsilon}$ (total) = $\Delta V_{L,\varepsilon,gf}$. In a related manner, the liquid void term in the numerator of Eq. (6.13) can be rewritten as a function of the retained gas volume: $\Delta V_{L,\varepsilon} = \Delta V_{L,\varepsilon,gf} - V_g$. Then, combining Eq. (6.11), Eq. (6.13), and Eq. (6.14) subject to $\rho_b = \rho_L$ gives

$$\alpha_{NB,ILD} = \frac{\rho_{b,gf}}{\rho_L} - 1 \quad (6.16)$$

These neutral buoyancy gas fraction equations can be applied to data collected throughout the course of an experiment. Of more general interest for comparison of different sRF resin/equilibrated liquid systems are the theoretical neutral buoyancy gas fractions based on initial gas-free settled bed conditions, $\alpha_{NB0,PD}$ and $\alpha_{NB0,ILD}$, which are determined by setting $\rho_{b,gf}$ to $\rho_{b,0}$ in Eq. (6.15) and Eq. (6.16), respectively.

As developed above, the resin bed density and neutral buoyancy gas fractions during a GR&R experiment can be determined from a (previously) measured initial gas-free bed density ($\rho_{b,0}$), without knowing either the initial bed porosity ($\varepsilon_{b,0}$) or the resin particle density (ρ_p). As discussed in Section 5.3, these are related by $\rho_{b,0} = (1 - \varepsilon_{b,0})\rho_p + \varepsilon_{b,0}\rho_L$, where the two terms account for resin particle and liquid contributions to the overall initial bed density. Similar to the requirement for a $\rho_{b,0}$ value for use in other bed density calculations, a known or estimated initial gas-free settled bed porosity ($\varepsilon_{b,0}$) is needed in order to assess the potentially varying resin bed porosity during a GR&R experiment, ε_b . This generalized bed porosity includes retained gas void from PDBs as well as changes in liquid volume resulting from shifts in the bed packing structure, but not displacement of liquid from the bed by ILDBs, which doesn't affect the porosity. Assuming that the resin particle density and the total volume and mass of resin particles are constant, the apparent (experimentally observed) resin bed porosity is

$$\varepsilon_b = 1 - \frac{V_{b,0}(1 - \varepsilon_{b,0})}{V_b} \quad (6.17)$$

The term in the numerator, $V_{b,0}(1 - \varepsilon_{b,0})$, is the total volume of particles. In this most-general form of the bed porosity equation, the (potentially) with-gas bed volume V_b is the total measured in an experiment and is the same as that used in the denominator of Eq. (6.13) for ρ_b . A gas-free bed porosity, $\varepsilon_{b,gf}$, is obtained by replacing V_b in the denominator of Eq. (6.17) with the gas-free bed volume from the denominator of Eq. (6.14) for $\rho_{b,gf}$. Note that Equation (6.17) is equivalent to Eq. (4.7) in Section 4.2.1, which is given in terms resin bed heights for analysis of gas-free fluidization behavior.

6.6 Test Matrix

The testing described in this report was performed at multiple scales. However, the smaller scale (bench-scale) testing was conducted to establish parameters used in the larger, fluidization column tests. The focus in this section is to discuss the test matrix for the tests conducted in the fluidization column;

consequently the bench-scale tests are not described in this section. Conditions investigated in smaller scale testing are discussed in more detail in Section 5.3.2 (see also Table 5.2).

There are multiple test phases (or types of tests) that were performed in the fluidization column testing. Not all phases were conducted for each set of conditions, and in some instances, phases were repeated or adjusted based on results from previous tests. At a summary level, the four categories of the test phases, their purposes, and test approaches are:

- **Fluidization-Only (fo)** – The purpose of the fluidization-only experiments was to characterize the degree of expansion of the initially settled resin bed (with no generated or retained gas) as a function of volumetric flow rate of the column liquid, Q , in a column up-flow configuration. The resin bed expansion ratio (factor), E , resulting from fluidization is defined as the resin level (height) in the (possibly) expanded state, H_b (also $H_{b,E}$) divided by the initial gas-free resin bed level with no liquid flowing, $H_{b,0}$ ($E = H_b/H_{b,0}$). The ratio E can also be defined in terms of its equivalent percent bed expansion; for example, $E = 1.4$ is often referred to as 40% bed expansion (the bed has expanded to 140% of its settled level). Bed expansions were measured for a range of volumetric flow rate (or velocity), and typically a Q_{min} was defined (the lowest flow rate that still caused measurable bed expansion, i.e. 3%). If bed expansion was such that the fluidized bed packed against the top of the fluidization column and formed an upper packed bed, the depth of this bed was measured as a function of applied fluidization velocity. In some instances, data on the settling behavior of the resin bed after fluidization was discontinued was also collected.
- **Gas Retention and Spontaneous Gas Release (spGR&R)** – The purposes of this type of test were to investigate the mechanisms of gas retention (e.g., interstitial-liquid-displacing bubbles and particle-displacing bubbles) and gas release; to quantify the amount of gas retained at the point of spontaneous (sp) gas release (i.e., not induced by mechanical disturbance such as mixing or fluidization); and to quantify the amount of released gas and the release rate. The fraction of the resin bed volume (height) retained as gas (retained gas fraction) at peak retention was determined. It was characterized by a change in total volume (height, level) contained in the column from the initial (nominally) gas-free state ($H_{L,0}$) and was reflected in the maximum change in the supernatant liquid level, $\Delta H_{L,max}$. This metric was used to establish test conditions for the fluidization-induced gas release tests that followed.
- **Gas Retention and Fluidization-Induced Gas Release (fiGR&R)** – The purpose of fluidization-induced (fi) gas release tests was to assess the efficacy of fluidization to release gas as a function of fluidization velocity (flow rate) and the amount of gas retained in the resin bed. A number of fluidization-induced gas release tests were conducted with a retained gas volume that is a specified fraction of the peak retained gas fraction, f_a . Experimentally, fluidization flow was initiated at a specified low rate when the supernatant liquid level (target level) was approximately $H_L = H_{L,0} + f_a \Delta H_{L,max}$, where f_a was selected to be in a range between 0.1 and 1.0 (10 to 100%). Generally, these target retained gas fractions were established starting from a resin-bed that is gas-free, to allow for a relatively-repeatable gas distribution in the bed. Fluidization-induced GR&R tests were conducted over a range of liquid flow rates ranging from $Q < Q_{min}$ to the flow rate needed to expand the resin bed by 40%. Some tests also included cyclic operation featuring two periods of operation repeated several times: (1) application of a fluidization flow rate for a selected period, followed by (2) a period where the flow rate was not applied and the bed was allowed to settle.

- **Continuous Gas Generation, Retention, and Fluidization-Induced Release (coGR&R)** – The purpose of these tests was to demonstrate (assess) continuous release of generated gas while maintaining the liquid flow rate of a fluidization-induced GR&R test that immediately precedes. Multiple tests were planned to separately evaluate continuous gas release at selected values of flow rate and the flow rate needed to achieve 40% bed expansion. Each coGR&R test was run for an extended period of time (e.g., multiple hours) to assess the retained gas fraction under steady-state (constant) liquid flow conditions.

An overview of the test phases described in the list above is presented in Table 6.3. An exception is the fluidization-only (fo) tests, which were performed at least once for every unique fluid condition tested, but often multiple measurements were performed and other opportunistic data was collected (upper packed bed height, settling bed height, etc.). In addition to the different simulants tested, the key parameters varied in the testing were the initial retained gas fraction at the beginning of the fiGR&R tests (~25, ~50, and ~100% of peak retention), the fluidization velocity to vary bed expansion (0-40%), and the type of test (fo, spGR&R, fiGR&R, and coGR&R). The range of initial gas fraction (~25, ~50, and ~100% (> 90%) of peak retention) was selected to span the full possible range of retained gas when fluidization was initiated. For Test 10-09 (Phase 4) shown in Table 6.3, a lower initial retained gas fraction was used that better represents what would likely be present when fluidization would be initiated following a loss of flow accident. The results of the fluidization-only testing are discussed in Section 7.0. The results of all the test types listed in Table 6.3 are presented in Section 8.0 and Section 9.0. Of particular interest are Table 9.1 and Table 9.2, which cross-reference the information in Table 6.3 with additional information regarding the chronology of the testing and the conditions of each test phase.

Table 6.3. Test Matrix of Fluidization Column Tests for Gas Retention and Release

Test Plan Test ID / Fluid	Test Phase	Test Type	Fraction of Peak Gas Retention (%)	Bed Expansion Target (%)	Notes/Comments
10-04 (alkaline water + resin)	2	spGR&R	100	N/A	Peak retained gas fraction was determined
	3	fiGR&R	> 90	40	Fluidize to release at 40% bed expansion
	4	spGR&R	100	N/A	Repeated condition to confirm peak retained gas fraction
	5	fiGR&R	> 90	40	Repeated demonstration of fluidization to release at 40% bed expansion
	6	fiGR&R	80	Range (0 – 40)	Fluidize to release gas at a range of bed expansions
10-05 (alkaline water + resin)	1A	fiGR&R	50	Range (0 – 40)	The minimum effective gas release flow rate was determined by stepping up the flow rate and then repeated at Q_{min}
	1B	fiGR&R	50	3	
	2	coGR&R	N/A	3	Immediately followed fiGR&R Phase 1B
	3A	fiGR&R	50	10	At least one flow rate > Q_{min} (from Phase 1B) and a separate test at 40% bed expansion
	3B	fiGR&R	50	40	
	4	coGR&R	N/A	40	Immediately followed fiGR&R Phase 3B
10-06 (alkaline water + resin)	1A	fiGR&R	25	3	Demonstrated fluidization to release gas at lower gas retention level
	2	coGR&R	N/A	3	Immediately followed fiGR&R Phase 1A
	3A	fiGR&R	90	3	Demonstrated fluidization to release gas at near-peak gas retention level
	4	coGR&R	N/A	3	Immediately followed fiGR&R Phase 3A
10-07 (alkaline water + resin)	1	spGR&R	100	N/A	Repeat of 10-04 Phases 2 and 4 to set conditions for 10-07 Phase 2
	2	fiGR&R	> 90	40	Follows spontaneous gas release(s) in Phase 1
	3	fiGR&R	50	3	Used the minimum achievable bed expansion determined in Tests 10-05 and 10-06 and a mid-range gas retention level
10-08 (6.1-M Na LAW simulant + resin)	2	spGR&R	100	N/A	Peak retained gas fraction was determined
	3	fiGR&R	90	40	Fluidize to release gas at 40% bed expansion near-peak gas retention level

Test Plan Test ID / Fluid	Test Phase	Test Type	Fraction of Peak Gas Retention (%)	Bed Expansion Target (%)	Notes/Comments
10-09 (6.1-M Na LAW simulant + resin)	1A	fiGR&R	50	0	Used to determine the minimum effective bed expansion, i.e. flow rate, to release gas
	1B	fiGR&R	50	3	As Phase 1A, at the minimum bed expansion level
	2	coGR&R	N/A	3	Immediately follows fiGR&R Phase 1B
	3A	fiGR&R	50	10	At least one flow rate $> Q_{min}$ (from Phase 1B) and a separate test at 40% bed expansion
	3B	fiGR&R	50	40	
	4	fiGR&R	80	N/A (cyclic)	Test cyclic fluidization at a near-peak retention level
	5	fiGR&R	10	N/A (cyclic)	Test cyclic fluidization at a low retention level
	6	fiGR&R	45	N/A (cyclic)	Test cyclic fluidization at a modest retention level
	7	fiGR&R	> 90	N/A (cyclic)	Repeat Phase 4, with retention level closer to peak

7.0 Results: Fluidization, Upper Bed Formation, and Settling

Experiments were conducted to quantify the fluidization behavior sRF resin beds, with the overall objective of determining bed expansion and upper bed formation as a function of fluidization velocity for the full range of fluid and sRF particle properties expected in the LAWPS facility. As discussed in Section 5.1, the fluid viscosity ranged from a lowest value of about 0.5 mPa·s (cP) for hot water to a highest target value of 15 mPa·s for the high-limit LAW feed. The velocity needed to fluidize a bed of particles is approximately inversely proportional to the fluid viscosity, so a velocity that just fluidizes particles in hot water will cause substantial bed expansion, and typically create a packed upper bed for LAWPS column design, with high-limit LAW. The initial results below show bed expansion for Na⁺ form sRF resin in alkaline water

7.1 Bed Expansion

Figure 7.1 shows bed expansion as a function of fluidization velocity for three separate fluidization tests with Na⁺ form sRF resin in ambient temperature alkaline water. The velocity for incipient fluidization was when motion was first visually observed in the sRF resin bed, which was typically at the bottom screen. At velocities below the incipient fluidization, there was no visual indication of sRF particle motion and no change in the resin bed height. At incipient fluidization, the particle motion within the resin bed was sufficient to allow particle re-arrangement and bed compaction to a degree that the bed height decreased, which is the slight dip in bed expansion near 2 cm/min fluidization velocity in Figure 7.1. The results in Figure 7.1 also show good repeatability for bed expansion as a function of fluidization velocity for the three different tests.

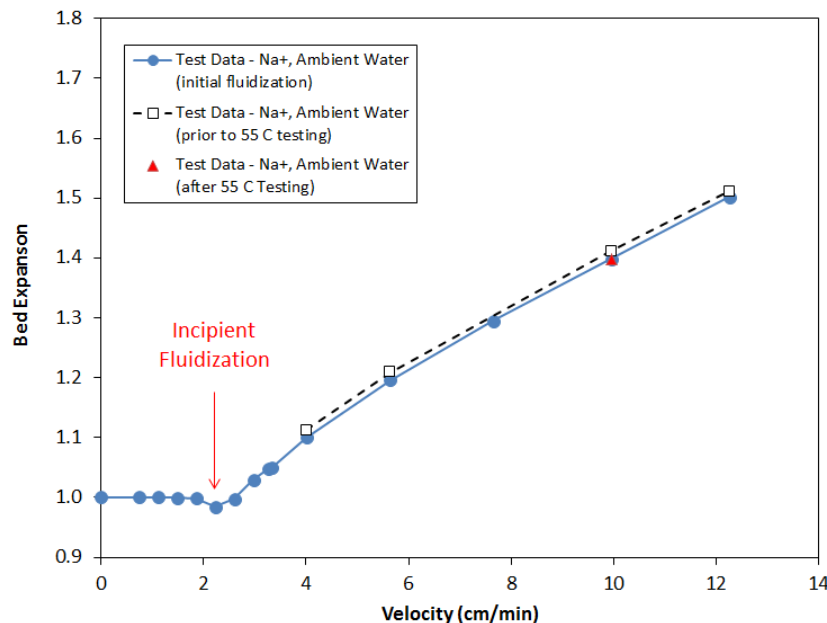


Figure 7.1. Bed expansion as a function of fluidization velocity for Na⁺ form sRF resin in ambient temperature alkaline water

Results from fluidization models are often shown with fluidization velocity on the y-axis and bed void fraction on the x-axis (Richardson 1971). Figure 7.2 compares the fluidization model results for bed expansion from Eq. (4.13) with test data for Na⁺ form sRF resin in ambient temperature alkaline water. The fluidization model used the measured liquid and particle densities and liquid viscosity shown in Table 5.1 for samples removed from the column and an initial bed porosity of 40% which is a typical value for the settled bed porosity. The agreement between the model data is quite good. Figure 7.3 shows comparisons between the fluidization model and test data for each of the sRF resin/liquid simulant pairs tested, again using measured liquid and particle densities and liquid viscosity shown in Table 5.1 and an initial bed porosity of 40%. Agreement between the model and data is good, though at low viscosity (53 °C Water) the model under predicts bed expansion and at high viscosity (High-Limit LAW) the model over predicts bed expansion. The model results in Figure 7.3 for the High-Limit LAW used the sRF resin particle density in Table 5.1 based on in-column data assuming a bed porosity of 40%. This sRF resin density was used because the resin density measurements on samples removed from the column were uncertain (see the measurement variability in the four reported measurements in Table 5.1 for 10.8 M NaOH) and the fluidization model is sensitive to the density difference between the sRF resin particle and suspending liquid. Figure 7.4 shows the effect of different bed porosity assumptions on the fluidization model predictions. Forty percent bed porosity agrees reasonably well with the bed expansion data and this porosity is typically for “loose random packing” discussed in Dullien (1992). In addition, 40% porosity was used for all the model predictions because this value provides a reasonable fit (by visual observation and not by a quantitative evaluation) of the model with all of the test data. Note that at the lowest viscosity for 53° C water the model under predicts bed expansion while the model over predicts bed expansion at the highest viscosity (high-limit LAW).

Comparing the results for Na⁺ with H⁺ resin in ambient water shows that Na⁺ resin in ambient water has less bed expansion at the same fluidization velocity and is thus more difficult to fluidize. Accordingly, elevated temperature tests used the resin/liquid pair of Na⁺ form resin in alkaline water to determine the velocity giving 3% bed expansion in the most difficult to fluidize condition. Figure 7.3 shows that 5.2 cm/min fluidization velocity is needed to achieve 3% bed expansion in this resin/liquid pair.

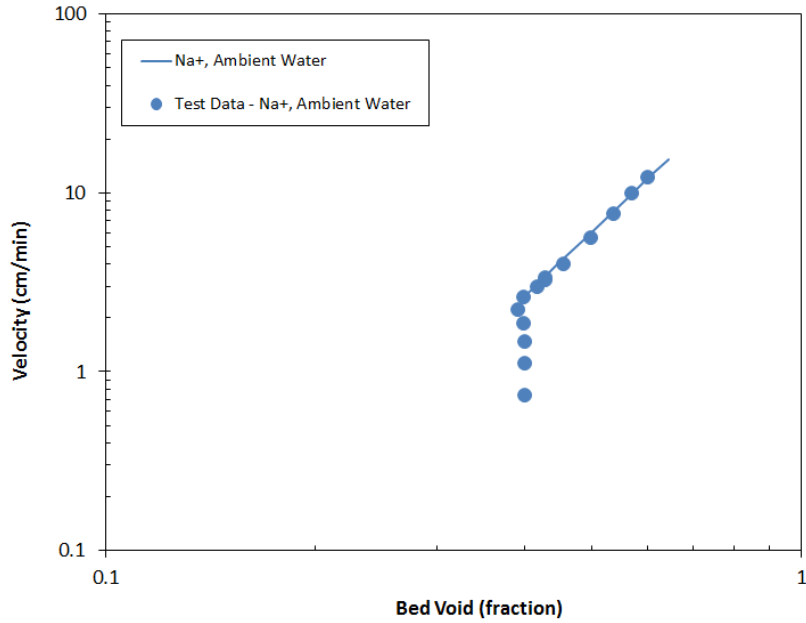


Figure 7.2. Comparison of fluidization model as given by Eq. (4.13) with test data for Na⁺ form sRF resin in ambient temperature alkaline water

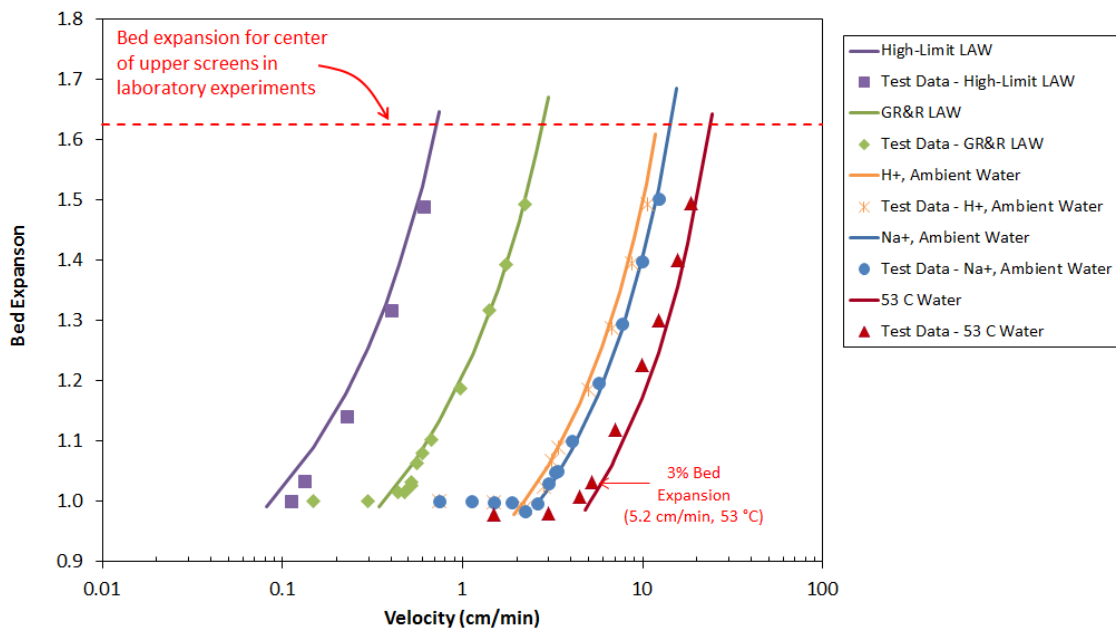


Figure 7.3. Comparison of fluidization model (solids lines) with test data (discrete points) for a range of test fluids and sRF resin properties at ambient and elevated temperature

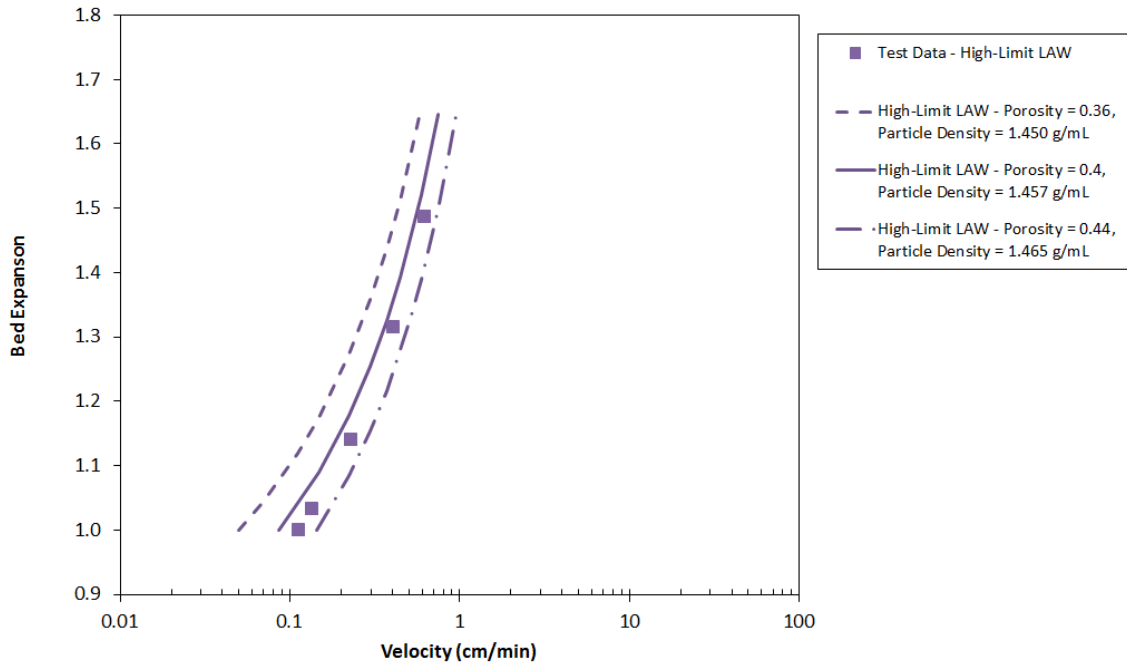


Figure 7.4. Comparison of fluidization model with three different estimates of particle density (based on different assumed bed porosities) with test data for bed expansion as a function of fluidization velocity for Na⁺ form sRF resin in the high-limit LAW simulant.

7.2 Upper Packed Bed Formation

An upper packed bed of sRF resin can occur when the fluidization velocity is sufficient to push the sRF resin to the top of the liquid in the column. Figure 7.5 shows an example of upper bed formation with the High-Limit LAW simulant and a fluidization velocity of 1.11 cm/min. The top of the fluidized bed rises over time until it reaches the top of the liquid in the column, after about 180 min of fluidization, and then an upper packed bed begins to form and expand downwards with the height at the bottom of the upper packed bed decreasing. The break in the curves for the top of the fluidized bed and the bottom of the upper packed bed occurs because it was difficult to observe the bottom of the upper bed until it moved sufficiently below the top of the liquid. As seen in Figure 7.3 for the High-Limit LAW, at a fluidization velocity of 1.1 cm/min the predicted bed expansion is above the upper screens in the fluidization column. Figure 7.6 shows upper packed bed formation for the High-Limit LAW at two higher fluidization velocities. The fluidized sRF bed reaches the top of the liquid in the column sooner and the thickness of the upper packed bed is larger at the higher velocities. Figure 7.7 shows the steady state upper packed bed height for three different liquid simulants and comparison to model predictions. These results show the size of the upper packed bed increasing (reducing height of the bottom of the upper packed bed) with increasing velocity and increasing simulant viscosity. At the velocity for two pumps running in series where a single pump would give 3% bed expansion for 55 C water, which we define as the LAWPS single-fluidization velocity, both the high-limit and nominal GR&R LAW solutions will form upper packed beds.

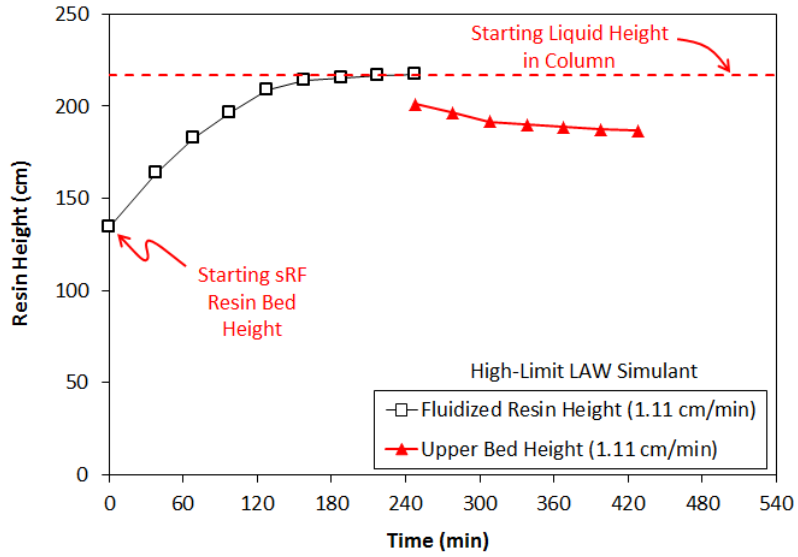


Figure 7.5. Resin height and height at the bottom of the upper bed as a function of time at fixed fluidization velocity for Na⁺ form sRF resin in high-limit LAW simulant.

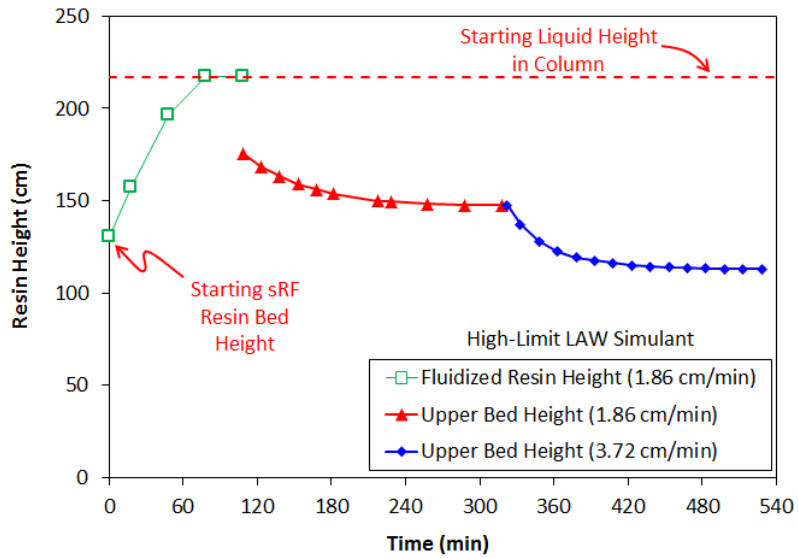


Figure 7.6. Resin height and height at the bottom of the upper bed as a function of time at two fluidization velocities for Na⁺ form sRF resin in high-limit LAW simulant.

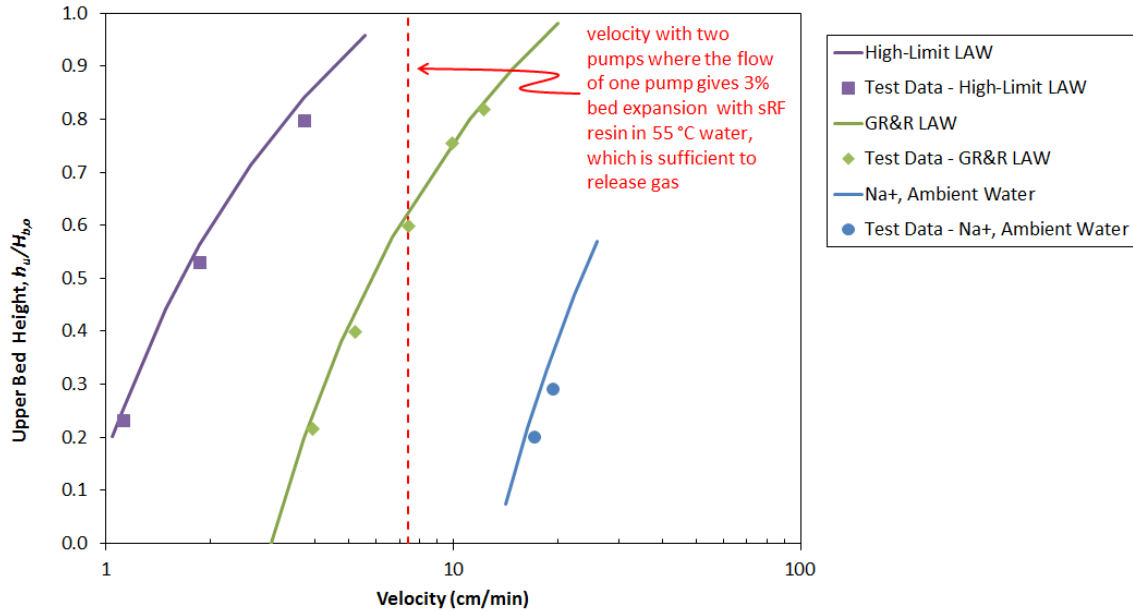


Figure 7.7. Upper bed height $h_u/H_{b,o}$ [depth from top of liquid, see Figure 4.2 and Eq. (4.18)] as a function of fluidization velocity for Na^+ form sRF resin in various simulants. Model predictions are shown by the solid lines. The vertical line shows the LAWPS single-fluidization velocity sufficient to release gas, which is discussed in Section 9.1.

Figure 7.8 shows the measured resin height as a function of time during a 5 min on:55 min off cyclical fluidization for Na^+ form sRF resin in high-limit LAW simulant. The test was run at 10 cm/min fluidization velocity, which was the estimated two-pump flow prior to collecting the bed expansion data at the 55 °C target temperature shown in Figure 7.3. The fluidized bed height never reached the top of the liquid in the column and a periodic steady state is reached at the fifth cycle. During this test, as noted in Table 5.1, the test temperature ranged from 28-30 °C and viscosity during testing was estimated to be 13 mPa·s (cP). Because the viscosity was less than the high-limit simulant target of 15 mPa·s (cP), a second cyclical test was conducted with a shorter settling period to mimic what would occur with a viscosity of 15 mPa·s (cP). This test used 5 min on:35 min off cycles¹. Figure 7.9 shows the results of this test. A periodic steady state was reached after four cycles. The resin would reach the top of the liquid in the column during fluidization and an upper packed bed would just begin to form. During the fluidization off period, the upper packed bed would fall and the resin bed would settle.

¹ If the sRF resin settling rate is inversely proportional the viscosity, then an appropriate reduced settling period would be $(13 \text{ mPa}\cdot\text{s} / 15 \text{ mPa}\cdot\text{s}) * 55 \text{ min} = 48 \text{ min}$. A settling period of 35 min is more conservative than this estimate.

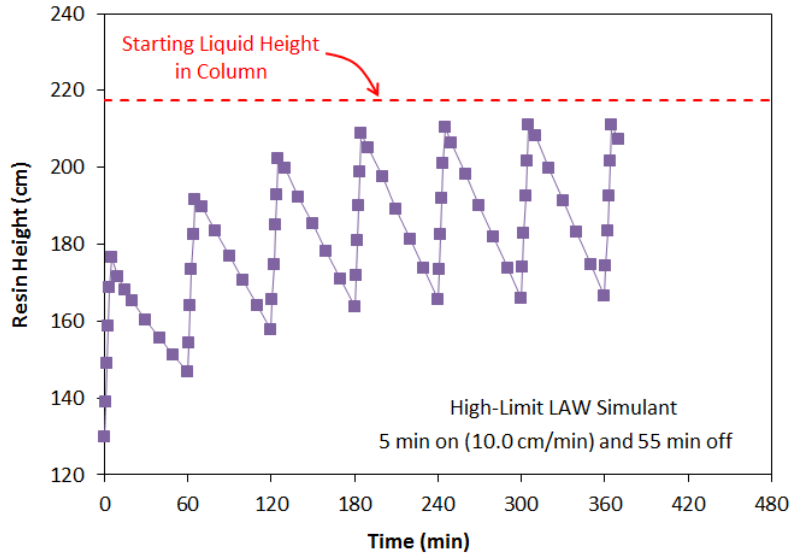


Figure 7.8. Resin height measured as a function of time during 5 min on:55 min off fluidization for Na⁺ form sRF resin in high-limit LAW simulant.

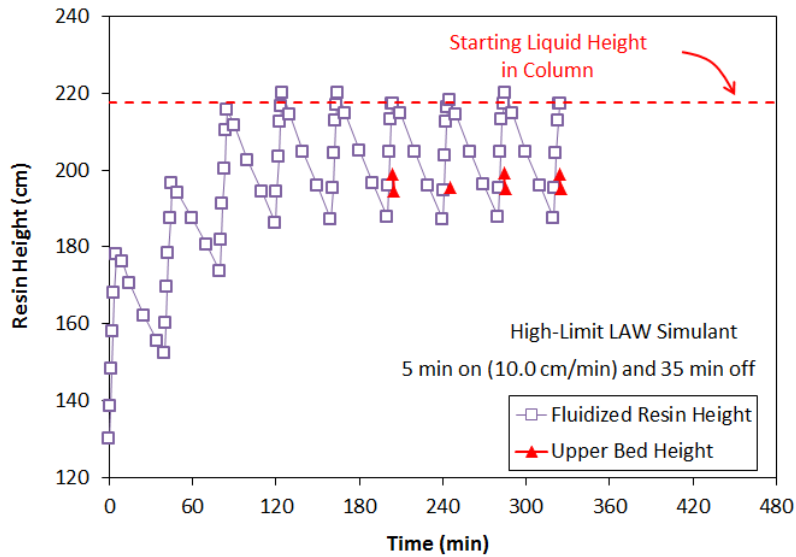


Figure 7.9. Resin height and upper bed depth measured as a function of time during 5 min on:35 min off fluidization for Na⁺ form sRF resin in high-limit LAW simulant.

7.3 Settling

During fluidization testing, there were a number of opportunities to measure the settling behavior of the sRF bed and this information was helpful for understanding the cyclical fluidization discussed above and was helpful for evaluating the fluidization model which uses the same particle settling relationships. Figure 7.10 shows a comparison of the measure sRF resin bed height as a function of time with the hindered settling model given by Eqs. (4.19) and (4.20). The comparison of model and data is equivalent to the fluidization results in Figure 7.3. Specifically, Figure 7.10 shows the model predicting slower settling than the data for the high-limit LAW (equivalent to predicting higher bed expansion than the data

in Figure 7.3) and the model predicts faster settling than the data for the 53 °C water (equivalent to predicting lower bed expansion than the data in Figure 7.3).

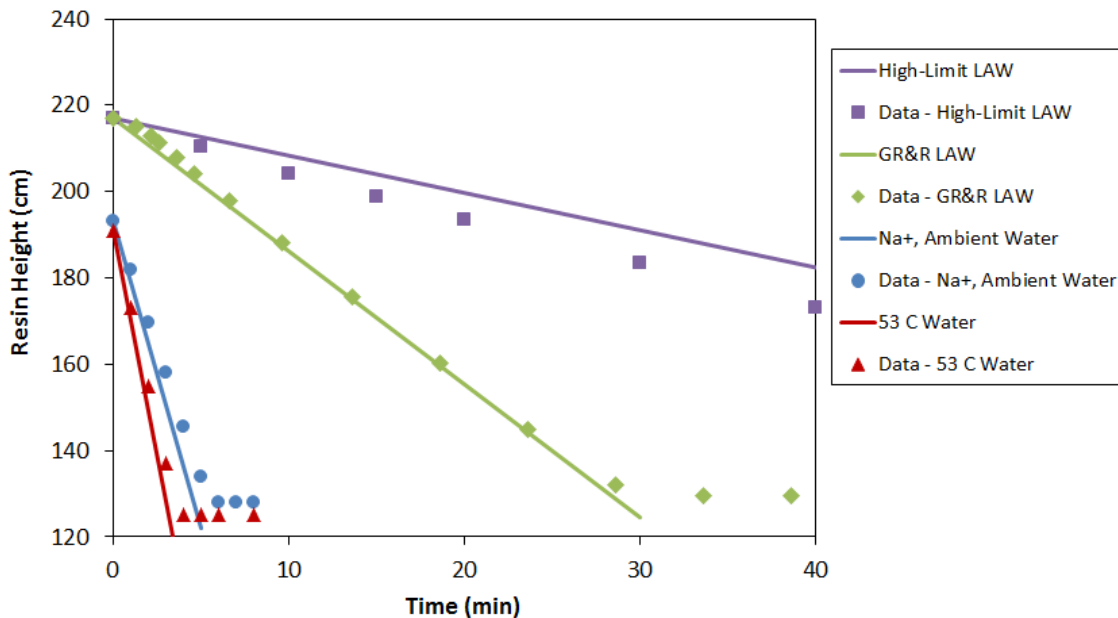


Figure 7.10. Resin height as a function of settling time for Na⁺ form sRF resin in various simulants. Model predictions are shown by the solid lines.

7.4 Fluidization and Upper Bed Formation Summary

Table 7.1 summarizes specific fluidization results for the velocity needed to achieve different bed expansion and upper bed height conditions. The table is organized left-to-right from the most difficult (highest velocity) to fluidize to the easiest based on using 3% bed expansion. Comparing the results for different liquid types for a specific fluidization and upper bed height conditions demonstrates the wide range of fluidization velocities to achieve the same fluidization conditions. As an example, achieving ~3% bed expansion requires 5.2 cm/min fluidization velocity for 53 °C water but only 0.13 cm/min for the 10.8 M NaOH. Key findings are:

- Fluidization of Na⁺ form sRF resin in alkaline water was more difficult (required a higher velocity) than H⁺ form sRF resin in acidic water for 3% bed expansion. Accordingly, we conclude that Na⁺ form sRF resin in 55 °C alkaline water is the most challenging liquid/resin pair. Test data show 5.2 cm/min. fluidization velocity is needed to reach 3% bed expansion under these conditions.
- A two pump safety system, with both pumps operating in series, and with each pump individually capable of providing 5.2 cm/min. fluidization velocity, would flow with 7.4 cm/min. This is defined as the LAWPS single-fluidization velocity.
- With a constant fluidization velocity of 7.4 cm/min., an upper packed bed of sRF resin will form in most LAW fluids. Testing results show upper bed formation would occur at this

velocity for a nominal LAW simulant (nominally 1.25 g/mL density and about 4 mPa·s viscosity) and a high-limit LAW simulant (nominally 1.35 g/mL density and 15 mPa·s viscosity). An upper packed bed is expected to retain hydrogen gas and pose a flammability hazard.

- Cyclical fluidization/settling, with cycles of 5 min on followed by 55 min. off, did not form an upper packed bed at a fluidization velocity of 10.0 cm/min (this was the predicted two-pump flow prior to conducting fluidization tests at 53 °C).
- Models were created for bed expansion and upper packed bed formation as a function of fluidization velocity and fluid and sRF resin properties. The models agree well with test data and can be used for predicting behavior of different fluid and resin pairs.

Table 7.1. Fluidization Velocity to Achieve Different Bed Expansion and Upper Bed Height Conditions

Nominal Fluidization Condition	Fluidization Measurements	Equilibrated Liquid Type and Conditions					
		Alkaline Water (53 °C)	Alkaline Water (ambient)	Acidic Water (H+ Form Resin)	6.1 M Na GR&R LAW Simulant	High-Limit LAW 10.8 M NaOH	
Incipient Fluidization	Velocity (cm/min)	4.5	2.2	2.2	0.44	0.11	
	Measured Bed Expansion (%)	0.9	-1.5	-1.1	1.5	0.1	
~3% Bed Expansion (2.5 to 3.5%)	Velocity (cm/min)	5.2	3.0	2.8	0.52	0.13	
	Measured Bed Expansion (%)	3.2	2.9	2.5	2.7 ^a 3.3 ^a	3.5	
~40% Bed Expansion	Velocity (cm/min)	16	10	8.7	1.7	0.40	0.61
	Measured Bed Expansion (%)	40.0	39.8	39.5	39.3	31.7 ^b	48.8 ^b
~20% Upper Bed Height	Velocity (cm/min)	-	17	-	3.9	1.1	
	Measured Upper Bed ($h_u/H_{b,o}$ in %)	-	20	-	22	23	

“-“ not measured

(a) repeat measurements made on different days

(b) flow giving near 40% bed expansion not specifically measured for the 10.8 M NaOH

8.0 Results: Gas Generation, Retention, and Spontaneous Release

This section addresses gas generation, retention, and spontaneous release test results that, in a sense, provide the backdrop for fluidization-induced gas release experiments that are discussed in Section 9.0. Characteristics of hydrogen gas generation from sodium borohydride at ambient temperature in various sRF resin/liquid simulant pairs are covered in Section 8.1. Quantitative aspects of gas retention in and spontaneous gas release from sRF resin beds in the same simulants are discussed in Section 8.2, while more-qualitative visual aspects of observed gas bubble retention mechanisms are presented in Section 8.3. In both of the first two sections, results are shown separately for bench-scale tests and for fluidization-column GR&R tests. Finally, the results of two bench-scale GR&R tests at elevated temperature are documented in Section 8.4.

8.1 Gas Generation (Ambient Temperature)

As noted in Section 1.2, several For-Information-Only (FIO) scoping tests were completed to evaluate various gas generation methods. After selecting SBH hydrolysis as the preferred (hydrogen) gas generation method (Section 6.4), additional preliminary FIO experiments were conducted to identify representative candidate liquid process simulants (Section 5.1) in combination with SBH concentration to provide experimentally-manageable gas generation rates as well as sufficient quantities of generated gas. Bench-scale Method Development (MD) and Vessel-Spanning Bubble (VSB) experiments were completed to finalize decisions on liquid simulant selections and to guide the choice of SBH concentration for GR&R tests in the fluidization column, as well as for other purposes discussed in this section. Gas generation rates determined in ambient temperature bench-scale tests are discussed in Section 8.1.1 before summarizing observations from the retention (growth) periods of fluidization-column experiments (Section 8.1.2). Generation rates in continuous-fluidization GR&R (coGR&R) tests are addressed separately in Section 9.2. The methods for generating hydrogen gas and quantifying it are discussed in detail in Section 6.4. This includes a number of definitions and assumptions that are applied to the results shown in this section.

8.1.1 Bench-Scale Experiments

Graduated cylinder experiments were completed with sRF resin equilibrated with alkaline water (varying pH), the 6.1-M sodium LAW simulant that was selected for fluidization-GR&R tests, and other liquid compositions to investigate VSB formation and to assess gas generation rates. In several of these experiments, the SBH concentration was varied and the effects investigated. A summary of the completed bench-scale tests including Test ID, test vessel type, sRF resin usage history, liquid composition and density, and SBH concentration (C_{SBH}) is provided in Table 5.2 in Section 5.3.2.

Figure 8.1 compares cumulative gas generation as a function of elapsed time (ET) from the start of the test for sRF resin in alkaline water at pH 12.2 (resin slurry) to 12.5 (supernatant liquid) in Test GC-01 and for sRF resin in the GR&R 6.1-M Na LAW simulant in Test MD-01, both with a nominal SBH concentration of 0.7 g SBH/L sRF resin. The quantity of generated gas is presented as molar equivalents of hydrogen (equiv. \equiv mol gas/mol SBH; Eq. (6.3) in Section 6.4). Figure 8.1 shows generated hydrogen equivalents determined in two ways for each test, from the volume of gas measured in the gas collection

cylinder and from changes in the volume of gas retained in the resin bed. The gas collection cylinder method measures gas produced both within the resin slurry (bed) and in supernatant liquid, whereas the gas retention approach only reflects gas generated within the resin bed and causing supernatant liquid level increases, as determined by correcting for any measurable gas releases and manually integrating over periods of growth. In this way, the “gas retention” metric gives a lower-bound estimate of the quantity of gas generated. By comparing the pair of curves for each test, Figure 8.1 indicates that the majority of gas was generated within the resin bed. This is especially apparent over the first day (~25 hours) in both tests, and is seen throughout the test with 6.1 M Na LAW simulant. For the alkaline water test, a minimum of 77% of the gas had been generated in the resin bed after 50 hours (0.54 equiv. gas retention / 0.69 equiv. gas collection), and for the LAW simulant test, a minimum of 94% of the gas had been generated in the resin bed after 51 hours (1.16 equiv. gas retention / 1.23 equiv. gas collection). Similar trends in the relative amounts of gas generated in resin slurry were observed in fluidization-column experiments, and these are discussed in Section 8.2.

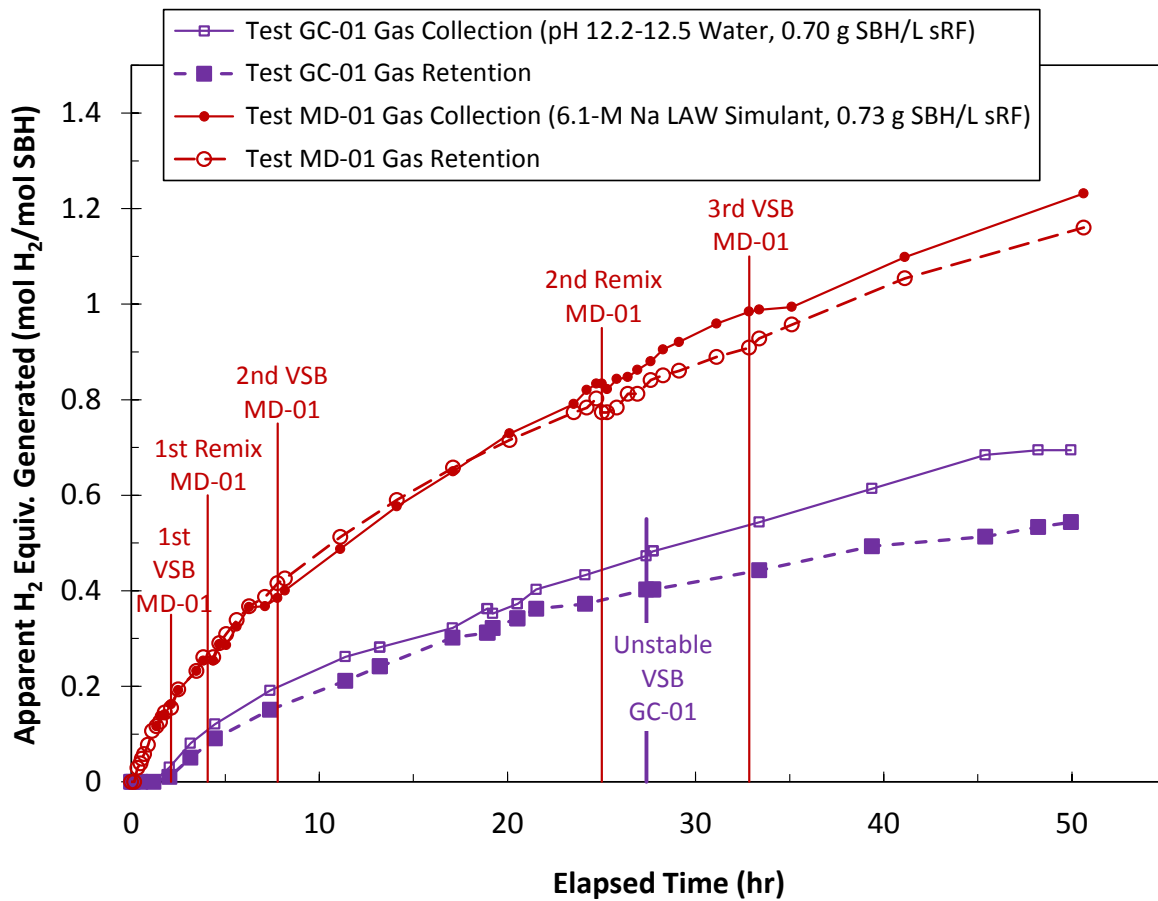


Figure 8.1. Generated Gas Volumes Represented as Molar Equivalents of Hydrogen as a Function of Elapsed Time (ET) from the Start of Tests GC-01 (sRF Resin in Alkaline Water, pH 12.2 to 12.5) and MD-01 (sRF Resin in 6.1-M Na LAW Simulant) at Constant SBH Concentration (0.7 g SBH/L sRF Resin). Equivalents from gas collection cylinder and retained gas volumes are compared, and ETs of VSB formation and remixing to release gas are shown.

Figure 8.1 shows that the gas generation rate was higher with the LAW simulant, producing about twice as much gas over about two days (~50 hours). This is consistent with FIO scoping experiments¹, which showed that the gas generation rates using various simulants comprised of sodium hydroxide (≥ 1 M, theoretical pH ≥ 14), sodium nitrate, and sodium nitrite in varying ratios and having a 1.25-g/mL liquid density target were faster than sRF resin in alkaline water at lower pH. As noted in Section 6.4, literature indicates that SBH hydrolysis reaction rates should decrease with increasing pH at constant SBH concentration. The results shown in Figure 8.1 suggest that the presence of sRF resin, possibly in combination with relatively high sodium concentration and/or other simulant components (e.g., nitrate), in some way facilitates (catalyzes) the hydrolysis reaction. Considering that relatively little gas is apparently generated in supernatant LAW simulant compared to supernatant alkaline water, as discussed in the previous paragraph, SBH in the liquid phase alone appears to follow the expected pH trend in reaction rate. Additional gas generation results for sRF resin with liquids of varying composition are presented below in this section.

Figure 8.1 also identifies key events in Tests GC-01 and MD-01. Specifically, the times at the start of formation of three stable VSBs in the LAW simulant test are shown (2 hr, 8 hr, and 33 hr ET). These VSBs may have been stable indefinitely, but were intentionally disrupted by remixing the contents of the graduated cylinder *in situ* to release essentially all retained gas followed by allowing the resin bed to resettle and reinitializing the gas collection system. The plotted hydrogen equivalents generated are cumulative across remixing events, which are also marked on the figure (4 hr and 25 hr ET). The results clearly indicate that VSB formation was repeatable for sRF resin in 6.1 M Na LAW simulant in a 250-mL graduated cylinder. In sRF resin / alkaline water Test GC-01, an “unstable” VSB started to form at ~27 hours elapsed time, which released spontaneously (without disturbance) over the course of ~20 min. See Section 8.2 and Section 8.3 for additional discussion of gas retention leading to formation of VSBs and/or spontaneous gas releases and the characteristics of VSBs.

Figure 8.2 shows normalized gas generation rates for several alkaline water and 6.1 M Na LAW simulant tests in 250-mL graduated cylinders, and the absolute (volumetric) gas generation rates for the same tests are discussed later in this section (with Figure 8.4). Variables include resin usage history, SBH concentration, and pH of the sRF resin/alkaline water batches. The results from Figure 8.1 for Tests GC-01 (pH 12.2 to 12.5, 0.7 g SBH/L fresh sRF resin) and MD-01 (GR&R LAW simulant, 0.7 g SBH/L fresh sRF resin) for the first day or so are reproduced in Figure 8.2 for comparison, but in this case, only the apparent hydrogen molar equivalents based on retained gas volumes are shown (for all tests).

In Figure 8.2, the results for Test MD-01 are most-directly comparable to Test MD-03, which was also in GR&R LAW simulant, but had a lower SBH concentration (0.5 g SBH/L resin) and a different resin source. In Test MD-01, the resin had not previously been contacted with SBH and was considered fresh, whereas the resin for Test MD-03 had been used in fluidization-GR&R tests with alkaline water and multiple SBH additions before being water-washed and equilibrated with stock 6.1 M Na LAW simulant. As noted in Section 5.3.2, Test MD-03 was completed to pre-evaluate expected gas generation performance in the planned fluidization-column experiments using the same simulant and, ultimately, the same SBH concentration. The results in Figure 8.2 showed that the previously-used sRF resin could be water-washed and contacted with the GR&R LAW simulant without complete re-conditioning of the resin

¹ The preliminary scoping studies did not follow the full requirements of the QA program outlined in Section 3.0 and should be considered For Information Only.

(i.e., conversion to H^+ form and back to Na^+ form per Section 5.2). The figure demonstrates similar gas generation rates in Tests MD-01 and MD-03 when normalized to H_2 equivalents, and differences in the resin histories do not appear to be a factor. A noticeable upturn in generation rate in Test MD-03 after the start of formation of a VSB at 12-hr ET may be the result of higher-concentration (less-reacted) SBH in the supernatant liquid contacting resin as it moved upward and liquid drained through.

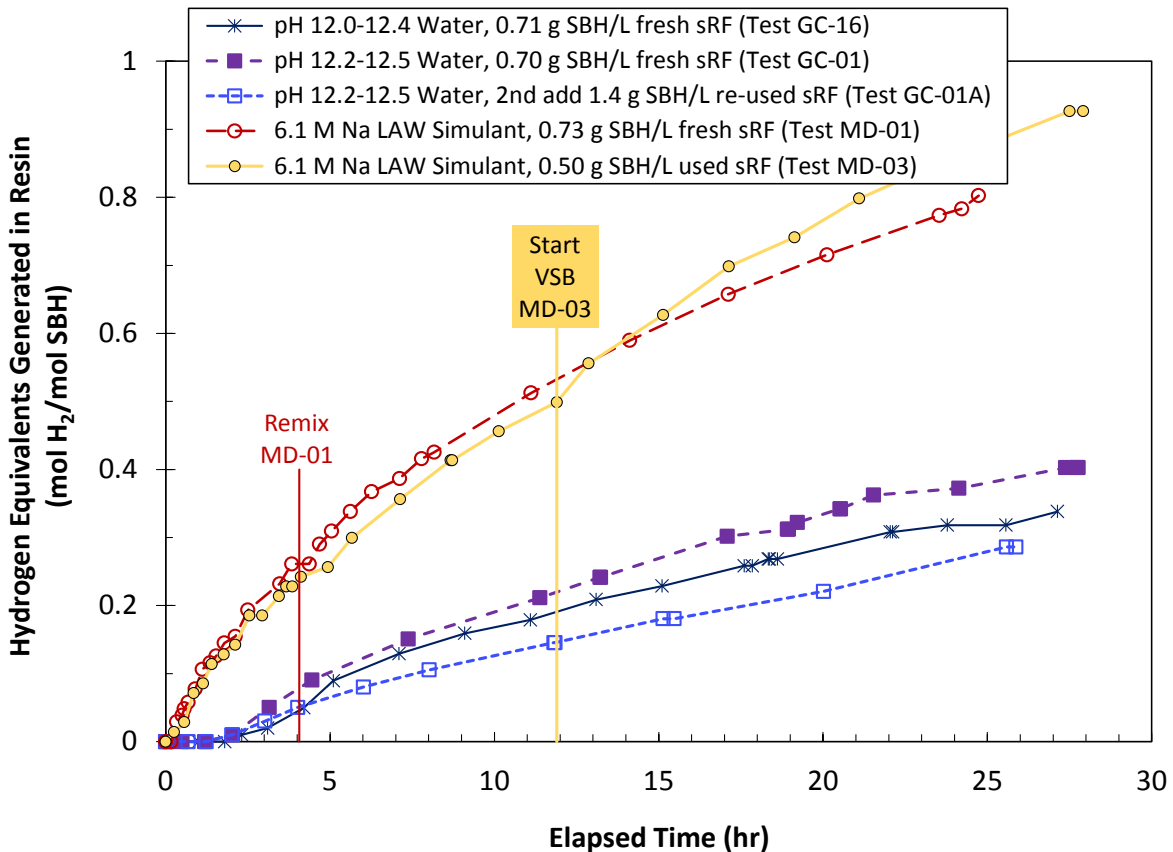


Figure 8.2. Normalized Gas Generation Rates in Graduated Cylinder Tests – Generated Gas Volumes Represented as Molar Equivalents of Hydrogen from Gas Retained in Resin as a Function of Elapsed Time (ET) from the Start of Tests GC-01, GC-01A, and GC-16 (sRF Resin in Alkaline Water, pH 12.0 to 12.5) and MD-01 and MD-03 (sRF Resin in 6.1-M Na LAW Simulant) with Varying SBH Concentration and Sources of sRF Resin (see legend). ETs of select VSB formation and remixing to release gas events are shown.

Figure 8.2 shows results for three sRF resin/alkaline water tests, all of which had lower normalized gas generation rates than the comparison GR&R LAW simulant tests. The pH values in Test GC-16 were slightly lower than in the batch for Test GC-01 (pH 12.0 vs. 12.2 resin slurry; pH 12.4 vs. 12.5 supernatant liquid). The pH difference is due to additional water washing of freshly conditioned sRF resin (Section 5.2) in the GC-16 batch, whereas the initially conditioned resin batch was used as-is in Test GC-01. The resin batch (10-04) for sRF resin/alkaline water tests in the fluidization column used the same source of conditioned resin and was diluted with water to make-up the volume needed for the experiments; the 10-04 batch pH values were the same as the GC-16 batch (pH 12.0 resin and pH 12.4 liquid). Figure 8.2 shows that at a constant SBH concentration (0.7 g SBH/L resin), the gas generation rates were similar in Tests GC-01 and GC-16, although the apparent rate was slightly lower in Test

GC-16. Based on understanding of pH effects on SBH reactivity (Section 6.4), a lower generation rate at lower pH is unexpected. However, the differences in pH in the two tests are relatively small and differences in generation rates may be within experimental uncertainty. At the start of each of the sRF resin/alkaline water tests shown in Figure 8.2, there is about a two-hour induction period (flat spot) in the gas generation curves. This may be a result of both lower reactivity and increased H₂ gas solubility¹ compared to the high-salt-content LAW simulant.

The resin slurry and supernatant liquid from Test GC-01 was re-used as-is (without washing) in Test GC-01A. After mixing to release retained gas, extra SBH at a concentration of 1.4 g SBH/L resin was added in Test GC-01A two weeks (15 days) after the first addition in Test GC-01. Figure 8.2 shows that generation rate in Test GC-01A was lower than Test GC-01, despite having twice the SBH concentration. The reduced generation rate in serial additions of SBH is a characteristic also observed in fluidization-column tests, as shown in Section 8.1.2 (and in several bench-scale FIO scoping tests²). It may be an example of Le Chatelier's Principle, in which the forward SBH hydrolysis reaction (Section 6.4) is limited by the buildup of borate reaction products as well as by the presence of dissolved H₂ at (super) saturation concentration, although this would be countered at least in part by the influx of fresh reactant (SBH). Another possibility is that potentially "reactive sites" on sRF resin are in some way consumed / deactivated during gas generation following a first addition of SBH. From a practical point of view, the results of Tests GC-01 and GC-16 indicate that an sRF resin/liquid system can be re-used in multiple fluidization-column GR&R experiments by re-dosing with SBH without reconditioning the resin in-between, although higher concentrations may be needed to achieve equivalent generation rates.

Figure 8.3 shows normalized gas generation profiles measured in bench-scale tests over multiple days (up to ~four) using sRF resin/liquid pairs of varying composition and alkalinity (concentration of sodium hydroxide [NaOH]). In order of increasing alkalinity, these are: alkaline water, 0.1 M NaOH, 0.3 M NaOH, 1.0 M NaOH, 6.1 M NaOH, 6.1 M NaOH and 2.0 M NaNO₃, and 10.8 M NaOH. As in the previous figure, the molar equivalents of hydrogen ($N_{H_2_{eq}}$) shown in Figure 8.3 are derived from retained gas volumes rather than gas collection cylinder readings. The SBH concentration was 0.5 g SBH/L resin in all tests shown in the figure except in previously-discussed alkaline-water Test GC-01 (0.7 g SBH/L resin), and all tests were run in 250-mL graduated cylinders except for VSB tests in 5-in. and 10-in. diameter vessels using 6.1 M NaOH LAW simulant (Tests MD-02 and MD-06, respectively). Including graduated-cylinder Test MD-03, the generation curves in sRF resin/GR&R LAW simulant in all vessel sizes are consistent up to ~12 hours elapsed time, which coincides with the time of formation of a stable VSB in Test MD-03. As mentioned previously, the VSB formation process may have spurred the reaction rate by contacting resin with relatively unreacted supernatant liquid. (This can also be seen in Figure 8.3 for Test MD-04 at 21-hr ET and in Test MD-08 at 40-hr ET.) Furthermore, the tests in the 5-in. and 10-in. vessels were characterized by more numerous localized (e.g., radially and vertically) and "small" (e.g., ≤ 0.1 cm ΔH_L) gas releases compared to the graduated cylinder test (Figure 8.12 in Section

¹ Lower expected H₂ solubility in salt solutions compared to (alkaline) water could be a factor in apparent initial gas generation rates. At the same molar generation rate, the salt solution simulant would become saturated with H₂ sooner and further generation of gas species would then be registered in collection cylinder measurements and by gas bubble retention, if any. After both liquids become saturated in H₂, any apparent difference in generation rates should be independent of solubility.

² The preliminary scoping studies did not follow the full requirements of the QA program outlined in Section 3.0 and should be considered For Information Only.

8.2.1), which makes accounting for gas generation from gas retention data less certain. This is the reason for the use of “Minimum” Hydrogen Equivalents in the y-axis label in Figure 8.3.

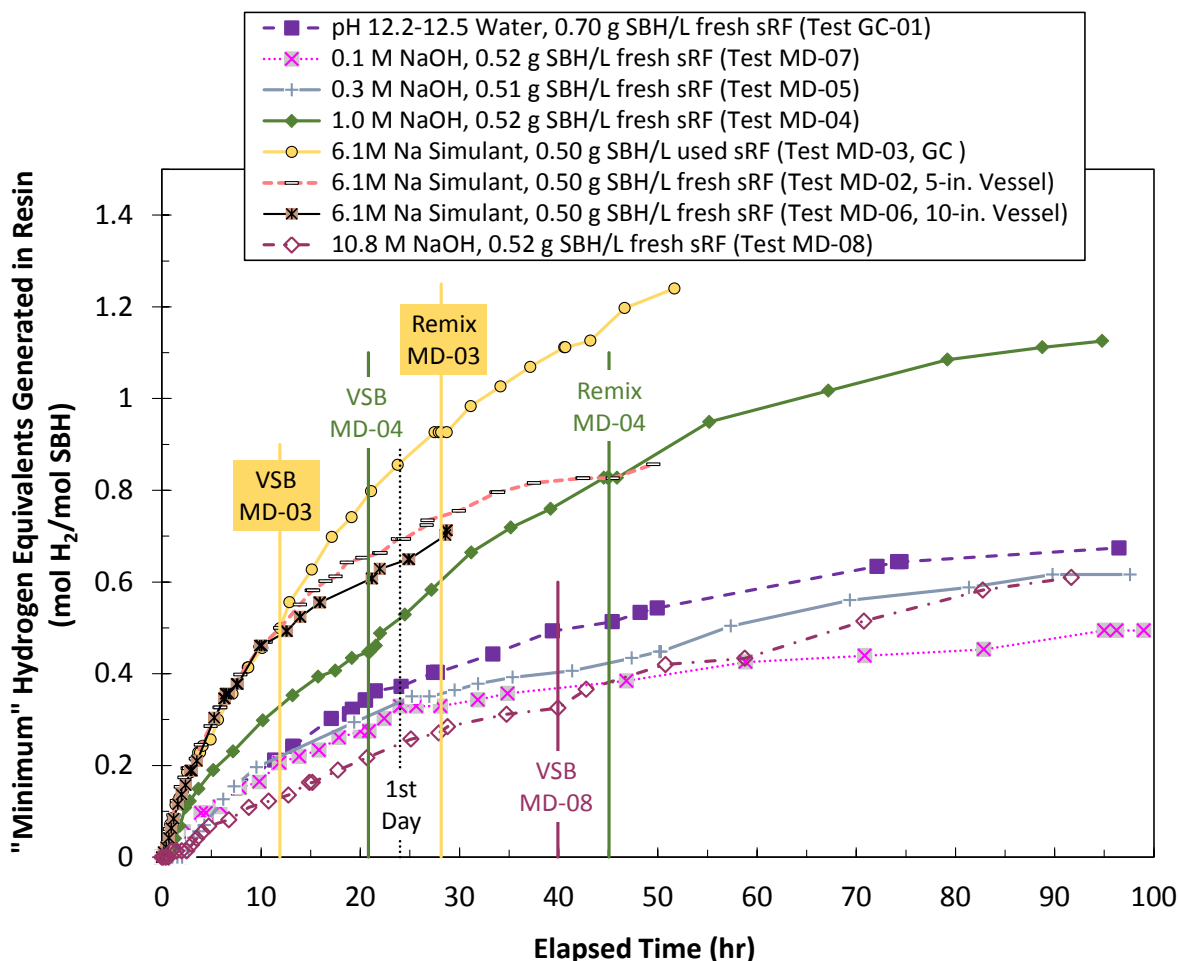


Figure 8.3. Normalized Gas Generation Rates in Bench-Scale Tests – Generated Gas Volumes Represented as Molar Equivalents of Hydrogen from Gas Retained in Resin as a Function of ET from the Start of Graduated Cylinder Tests GC-01, MD-07, MD-05, MD-04, MD-03, and MD-08, in Order of Increasing Alkalinity. For 6.1 M Na simulant, results are also shown for 5-in. (MD-02) and 10-in. (MD-06) diameter vessels. The SBH concentration is constant (0.5 g SBH/L sRF Resin) except for Test GC-01 (0.7 g SBH/L sRF Resin).

The suite of graduated cylinder tests with 0.1 M NaOH (Test MD-07), 0.3 M NaOH (Test MD-05), and 1.0 M NaOH (Test MD-04) was completed to help identify a less-reactive “water-like” (density and viscosity) simulant for use in elevated-temperature tests, in which significantly increased reaction rates were anticipated and observed (Section 8.4). 10.8 M NaOH is the composition of the selected high-limit LAW simulant with upper-bounding density and viscosity (Section 5.1) that was used in fluidization-only testing (Section 6.4). The graduated cylinder GR&R test with 10.8 M NaOH (Test MD-08) was completed to briefly investigate SBH reactivity in case initially-unplanned fluidization-GR&R tests were run, and it provided useful data for better understanding the effect of alkalinity on SBH reaction rates in the presence of sRF resin. In Figure 8.3, the “initial” gas generation rate data, e.g., taken as the measured amount of gas generated in about a day to show separation in the plot (see “1st Day” reference line), indicate increasing rate in the following order: 10.8 M NaOH < 0.1 M NaOH ≤ 0.3 M NaOH ≤ alkaline

water (pH 12.2 to 12.5) < 1.0 M NaOH < 6.1 M Na LAW simulant. This trend does not consistently follow alkalinity, and there appears to be a peak in gas generation rate at intermediate to relatively-high sodium concentration. For example, in the sodium hydroxide-only series (excluding GR&R LAW simulant), 1.0 M NaOH had the highest gas generation rate, 10.8 M NaOH had the lowest rate, as expected based on highest pH, and the rates were relatively low, but intermediate, with 0.1 and 0.3 M NaOH and alkaline water. The data for the 6.1 M Na LAW simulant is consistent in the sense that it showed the highest reaction rate(s) at an intermediate alkalinity (4.1 M NaOH). However, the significant concentration of sodium nitrate (2.0 M) in the LAW simulant may also have affected the generation rate.

Figure 8.4 shows absolute gas generation rates in 250-mL graduated cylinder tests for liquids used with sRF resin in fluidization-column GR&R tests, alkaline water and 6.1 M Na GR&R LAW simulant. Rates are shown as specific gas volume generated per Eq. (6.4) in Section 6.4, which is defined in this case in terms of the measured volume of generated gas from gas retention in the resin per unit volume of gas-free resin bed (initial volume) as a function of elapsed time from the start of the experiments. Normalized gas generation rates in apparent hydrogen molar equivalents are shown in Figure 8.2 for the same tests included in Figure 8.4: alkaline-water (pH 12.0 to 12.5) Tests GC-01 (0.7 g SBH/L resin), GC-01A (1.4 g SBH/L resin), and GC-16 (0.7 g SBH/L resin) and GR&R-LAW-simulant Tests MD-01 (0.7 g SBH/L resin) and MD-03 (0.5 g SBH/L resin). The SBH concentration and sources of sRF resin (fresh, re-used [GC-01A], and used/washed [MD-03]) varied (see additional discussion earlier in the section). The plot shows a target growth period of 6 to 12 hours for fluidization-column tests and includes a marked series of specific gas volumes corresponding to a range of possible retained gas fractions (in the form of interstitial-liquid-displacing bubbles, α_{ILD} ; Section 6.5). The gas fraction lines in Figure 8.4 are shown as α_{ILD} instead of α_{PD} , because fluidization-column test results indicate that the majority of gas was retained as (or appears to be) ILDBs instead of PDBs (Section 8.2.2). Also, conveniently, the specific volume in units of milliliters hydrogen generated per liter of resin (mL H₂ /L resin) is ten-times α_{ILD} given in volume percent.

Figure 8.4 clearly indicates that SBH concentration is a parameter that can be varied to affect absolute gas volume generation rates so that they are representative of full-scale (or not too low) and are practical for conducting experiments (see Section 6.4). For example, Figure 8.4 shows a higher absolute volumetric generation rate for 6.1-M Na LAW simulant Test MD-01 at higher SBH concentration than Test MD-03, whereas the normalized gas generation profiles for these tests are similar. These data suggest that for an initial growth period following a first addition of SBH, a concentration of 0.7 g SBH/L resin would be too high to hit the target time frame for a test in GR&R LAW simulant with an expected peak retained gas fraction at neutral buoyancy, α_{NB} , of ~6 to 8 vol% based on bench-scale tests (see Table 5.2 in Section 5.3.2 and Section 8.2.1). By comparison in Figure 8.4, a concentration of 0.5 g SBH/L resin in the GR&R LAW simulant also appears to be slightly high, but manageable, and rates decreased with time so that second and subsequent growth periods following an SBH charge would more likely fall in the target growth period.

Consistent with the normalized generation rates, the absolute generation rate shown in Figure 8.4 for Test MD-01 with GR&R LAW simulant is higher than for sRF resin / alkaline water Tests GC-01 and GC-16 at the same SBH concentration. However, at twice the SBH concentration (1.4 g SBH/L resin) in the second addition of SBH, the absolute generation rate was higher in Test GC-01A than with the first addition in Test GC-01, whereas Figure 8.2 shows that the normalized generation rate is lower in Test GC-01A. With an expected α_{NB} of ~12 to 14 vol% based on bench-scale tests for sRF resin in alkaline water (references in previous paragraph), a first SBH addition of 0.7 g SBH/L resin appears to be too low

for a 12-hour growth period to peak retention, although the expected maximum gas fraction was reasonably achieved in less than a day. A second addition of 1.4 g SBH/L resin just hits the expected gas fraction window in 12 hours. The results in Figure 8.4 were used to provide guidance for the choice of SBH concentrations in fluidization-column GR&R tests, which are discussed next.

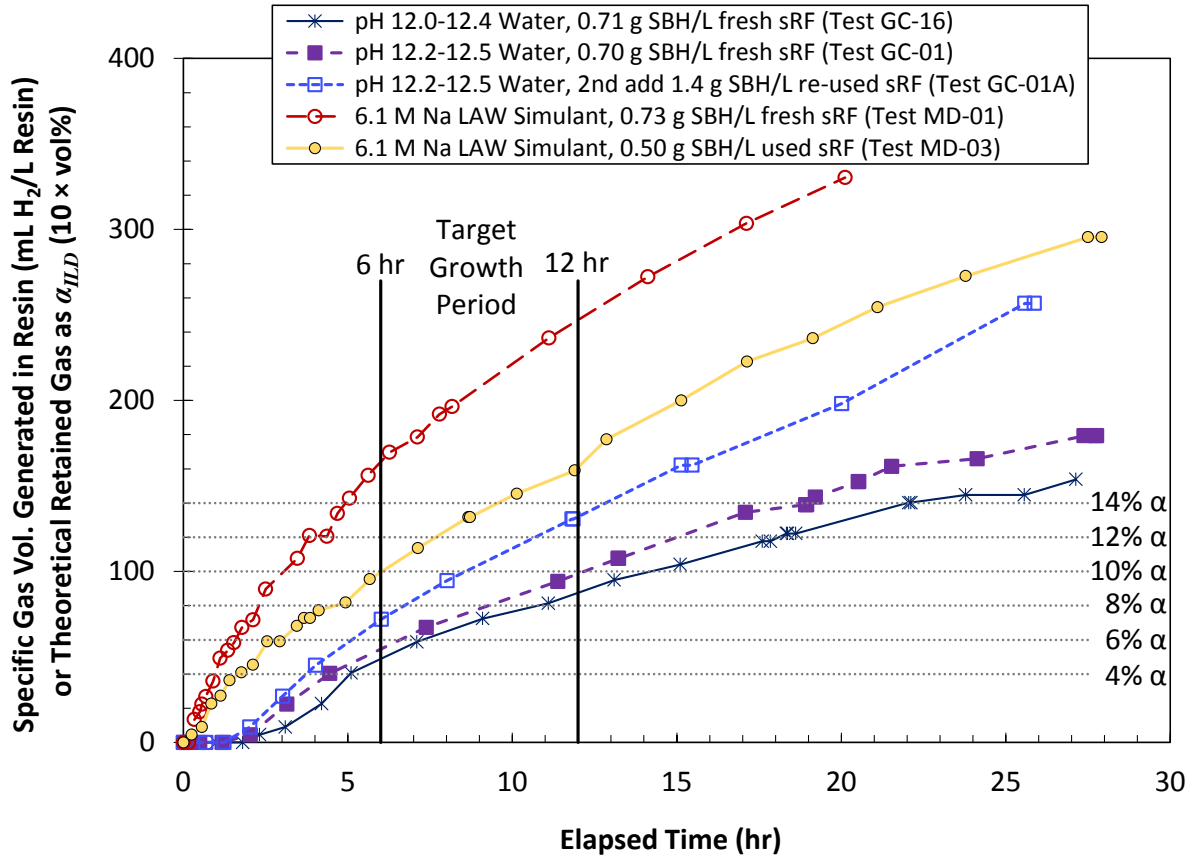


Figure 8.4. Absolute Gas Generation Rates in Graduated Cylinder Tests – Generated Gas Volumes from Gas Retention per Unit Volume of Gas-Free Resin Bed (Specific Gas Volume) as a Function of Elapsed Time from the Start of Tests GC-01, GC-01A, and GC-16 (sRF Resin in Alkaline Water) and MD-01 and MD-03 (sRF Resin in GR&R LAW Simulant) with Varying SBH Concentration and Sources of sRF Resin (see legend). A target growth period for fluidization-GR&R tests is compared to a range of possible retained gas fractions (α_{ILD}).

8.1.2 Fluidization-Column GR&R Tests

Two series of fluidization-GR&R experiments were completed using sRF resin, one set with alkaline water and the other with 6.1-M sodium GR&R LAW simulant. Multiple SBH additions were used in each series, and the SBH concentration was varied in some. Summaries of the completed tests with each liquid including Test ID and phase, test type, various operating conditions, and SBH concentration are provided in Table 9.1 (alkaline water) and Table 9.2 (GR&R LAW simulant) in Section 9.0. These test sequences are listed in order of completion, which is useful for placing the tests with respect to SBH addition. In the discussion to follow, and as noted in the tables, a post-SBH-addition gas-retention sequence identifier, “SBHx.y”, is used to indicate the number of the SBH addition, x, and the gas retention (growth) period count following the SBH addition, y. For example, “SBH3.2” means that it is

the second growth period (preceding a fluidization-induced gas release) following the third addition of SBH to the sRF resin / liquid contained in the fluidization column throughout the test series. The test matrix tables in Section 9.0 also provide the “1st Day” average gas generation rate on a test-by-test basis, which is defined in Section 6.4 and derived from data discussed below in this section.

The upper plot in Figure 8.5 compares the total volume of gas recovered in the collection cylinder and the volume of generated gas retained in the bed of sRF resin / alkaline water as a function of elapsed time from the start of growth for a representative peak retention and spontaneous gas release test in the fluidization-column (Test 10-04 Phase 2).¹ This follows immediately after the first addition of SBH to the sRF resin/alkaline water slurry (retention period SBH1.1). The plot shows that, initially, from 0 to ~6 hours elapsed time, ~100% of generated gas was retained. Gas likely continued to be generated within the resin bed, but escaped by percolation through the bed, diffusion, and/or gas release events. The plateau in retained gas volume shown in Figure 8.5 (upper) corresponds to the approach to peak gas retention, which is discussed further in Section 8.2.2 along with the gas retention characteristics of other fluidization-GR&R tests.

The lower plot of Figure 8.5 shows incremental and average gas generation rates in the same test determined from the measured gas collection cylinder volumes. The incremental-rate curve is characteristic of most gas retention periods following extended mixing to blend SBH and/or to release retained gas (e.g., during fluidization-induced gas releases) in the sense that: measurable gas generation was slow to start; a peak in generation rate (e.g., ~1.2 L/hr) was reached after, typically, a few to many hours (e.g., ~4 hr) that is somewhat to significantly higher than average (e.g., ~0.5 L/hr in the “1st Day”); and a slowly, steadily decreasing rate was observed later. The incremental rate data in Figure 8.5 (lower) are atypical in the extremity of the peak rate compared to the average, which is likely attributed to the fresh (first) addition of SBH in combination with a relatively high concentration (1.2 g SBH/L resin). One possible explanation for the generally low apparent generation rates at the start of quiescent growth periods is a net de-(super)saturation of dissolved H₂ resulting from extensive mixing and gas release in the time preceding, in which case initially generated gas must first re-(super)saturate the liquid with the gas before bubble nucleation and volumetric generation are observed. Additionally and/or alternatively, gas generation and bubble growth may be diffusion-limited during the induction period. Specifically, considering resin particles to be relatively active reaction sites compared to bulk liquid, reactants (SBH) would need to diffuse through liquid to generate H₂, and likewise, dissolved H₂ would need to diffuse to the relatively-few, but increasing population of, nucleated bubbles (also likely on resin surfaces). Once initiated, bubble growth would displace (convect) interstitial liquid to overcome diffusion limitations.

The lower plot of Figure 8.5 also shows the cumulative-average generation rate in the first day (0.49 L/hr) of testing, the overall average generation rate in the ~42-hour gas retention period (0.44 L/hr), and, for reference, the hourly generation rate (0.042 L/hr) equivalent to 1 L H₂ gas/day. This reference line scales volumetrically to ~18 L H₂/day in a full-scale IX column, which exceeds the maximum expected

¹ Test 10-04 Phases 2, 3, and 4 (up through ~44-hr elapsed time with a generated gas volume of ~12 L) were completed in the original system configuration with the gas collection cylinder and fluidization-column headspaces connected directly by tubing and both operating under the same, but time-varying, vacuum pressure. In all later tests, gas was admitted to the gas collection cylinder at ~1 in. below the water reservoir surface, and a slight, nearly-constant positive pressure was maintained in the fluidization column headspace (e.g., 1.0025 atm absolute) while the vacuum pressure in the gas collection cylinder continued to vary. As outlined in Section 6.4, corrections were applied to the early test data to make them directly comparable to later tests.

gas generation rate (see Section 6.4). Besides experimental practicality, comparison of gas generation rates to the 1-L/day reference is primarily important for continuous generation and fluidization-induced gas release test phases; these are discussed in Section 9.2.3.

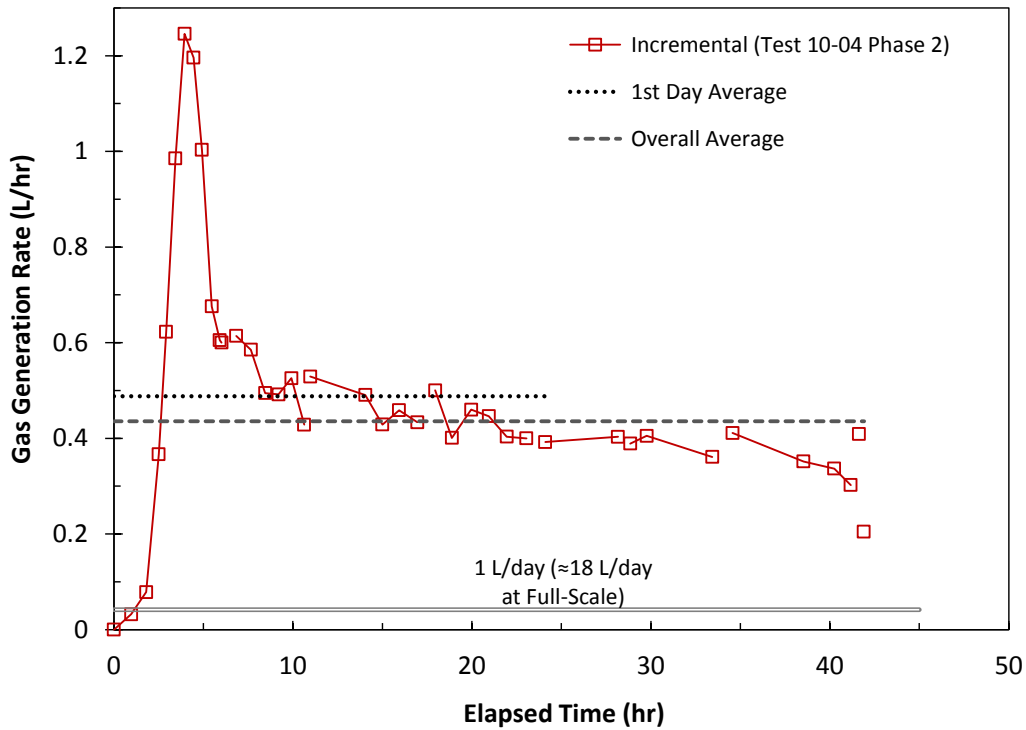
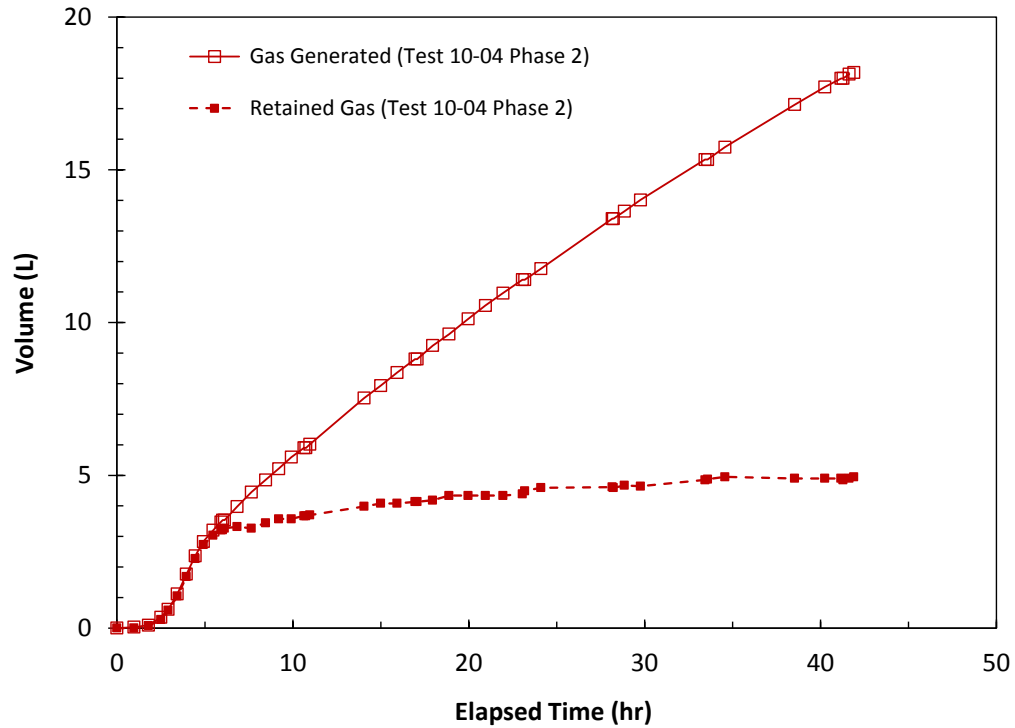


Figure 8.5. Upper: Comparison of Generated Gas (from collection cylinder) and Retained Gas (in resin bed) Volumes in sRF Resin / Water as a Function of Elapsed Time from the Start of Growth for a Representative Peak Retention / Spontaneous Gas Release Test (Test 10-04 Phase 2); Lower: Incremental Gas Generation Rates in the Same Test Compared to First Day and Overall Average Rates and the Hourly Equivalent of 1 L/day.

Figure 8.6 shows gas generation rates determined from gas collection cylinder volume measurements as a function of elapsed time from the start of quiescent growth periods of spontaneous and fluidization-induced gas release tests for sRF resin in alkaline water (Tests 10-04 to 10-07, multiple Phases). The upper plot shows the normalized amount of gas generated in terms of molar equivalents of hydrogen, and the lower plot shows absolute gas generation rates in the form of measured gas volumes. A generation rate of 1 L/day is shown for reference in the lower plot. Legend entries in Figure 8.6 include the “SBHx.y” sequence identifier (defined at the beginning of this section) for each gas retention period of spontaneous gas release (spGR&R) tests and preceding fluidization-induced gas releases (fiGR&R phases). One continuous gas generation, retention, and release (coGR&R) test is shown in the lower plot of Figure 8.6 for comparison (discussed below), and by definition, it does not have a SBHx.y identifier.

The initial concentrations of SBH in three additions to the sRF resin/alkaline water in the fluidization column were, in order, 1.2, 0.8, and 1.2 g SBH/L resin; the weighed SBH masses are included in Table 9.1 in Section 9.0. Regardless of C_{SBH} or the number count of the gas retention period following an SBH addition, the individual data curves in Figure 8.6 generally show induction periods of about two to four hours, in which the measured gas generation was minimal. This is consistent with the observed characteristics of incremental gas generation rates discussed above in conjunction with Figure 8.5. In most cases, the gas generation rate decreased in later periods of gas retention after a SBH addition, as would be expected for decreasing SBH concentration in time. Exceptions to this rule were fiGR&R Tests 10-05 Phase 3B (SBH2.1) and 10-05 Phase 1A (SBH2.2); the gas generation rate was faster in the second growth period after the second SBH addition. Possible explanations for this are the long gap (18 days) between first and second SBH additions and low residual reactive SBH after Test 10-04 Phase 6 (SBH 1.3, plus an additional four days). The minimal residual SBH in the SBH1.3 growth period is evidenced by it having the lowest generation rate of all test phases in Figure 8.6. Also likely contributing to the slow-growth (retention and generation) in SBH2.1 was the relatively low SBH concentration in the second addition in conjunction with (possibly) depleted dissolved H_2 and diffusion limitations (e.g., see discussion of Figure 8.5 above). This explanation is also supported by the data for coGR&R Test 10-05 Phase 4, which was an uninterrupted continuation of Phase 3B (SBH2.1). The lower plot of Figure 8.6 shows that the generation rate in the coGR&R test phase was higher than in SBH2.2, which followed. The lower plot also shows that first-day gas generation rates exceeded 1 L/day in all the test phases.

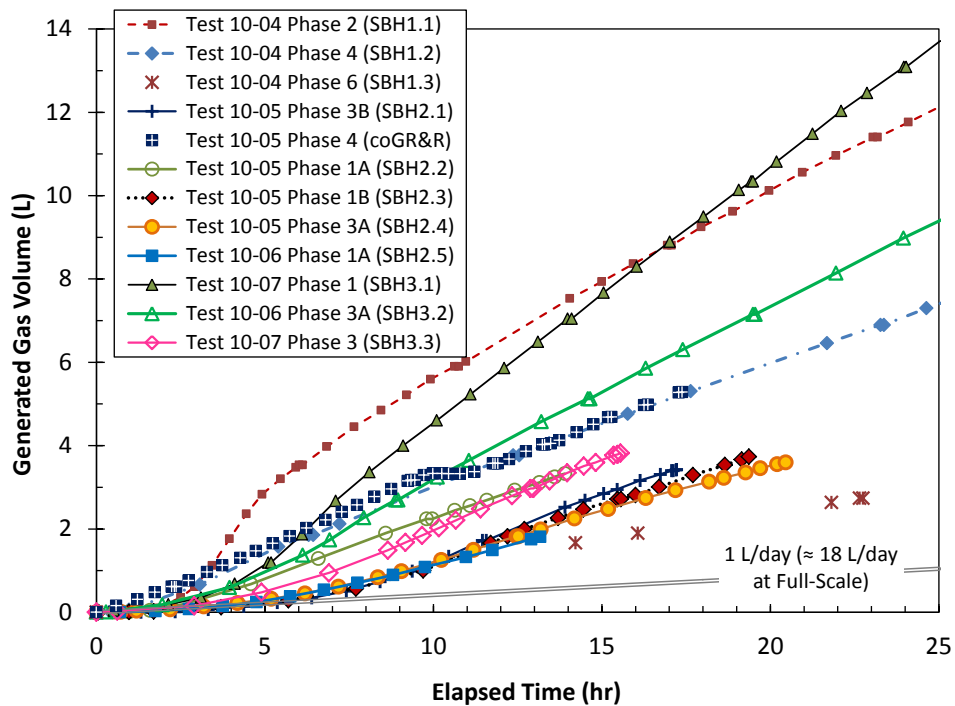
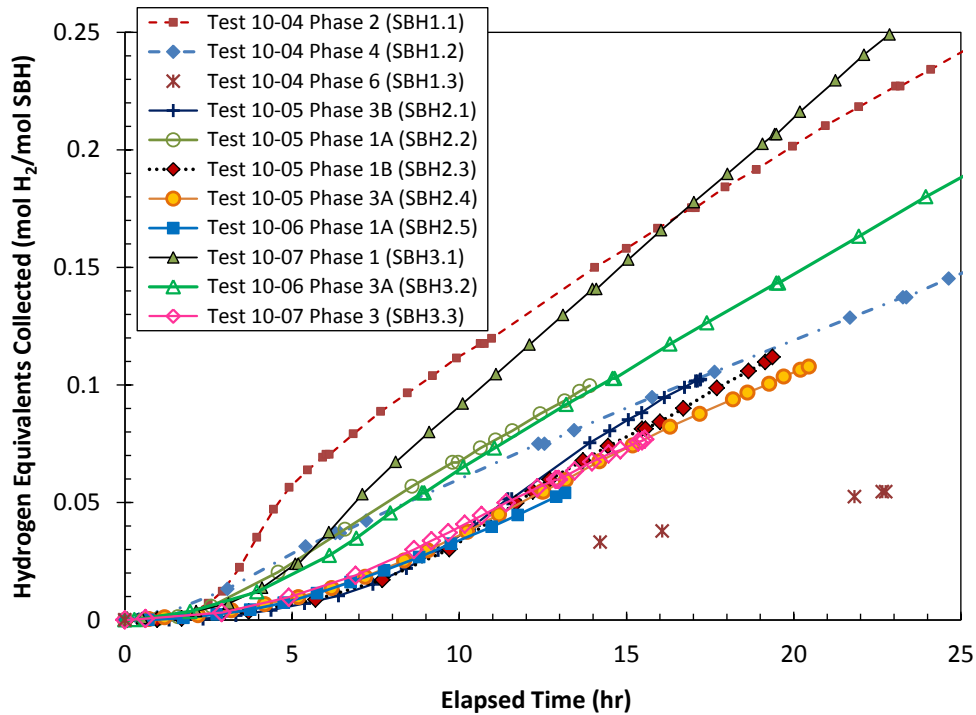


Figure 8.6. Gas Generation Determined from Gas Collection Cylinder Volume Measurements as a Function of Elapsed Time from the Start of Quiescent Growth Periods of Spontaneous and Fluidization-Induced Gas Release Tests for sRF Resin in Alkaline Water: Upper, Molar Equivalents of Hydrogen; and Lower, Measured Gas Volume. A generation rate of 1 L/day, equivalent to ~18 L/day in a full-scale IX column, is shown for reference. Legend entries include the “SBHx.y” sequence identifier. A coGR&R test phase is shown in the lower plot.

Figure 8.7 provides information similar to Figure 8.6 for fluidization-column GR&R tests with sRF Resin in 6.1-M Na GR&R LAW simulant (Tests 10-08 and 10-09, multiple Phases). The initial concentration of SBH in all three additions to the sRF resin/GR&R LAW simulant in the fluidization column was 0.5 g SBH/L resin; the weighed SBH masses are included in Table 9.2 in Section 9.0. Because the quantities of SBH in the three additions were nearly equal, the ordering and shapes of test curves in the normalized (upper) and absolute (lower) gas generation rate plots are the same, and the plots differ substantially only in the y-axis values (i.e., there is a single scaling factor that would nominally convert units for all tests from one plot to the other). More clearly than was observed for the alkaline water tests (Figure 8.6), the generation rates shown in Figure 8.7 decrease monotonically in time (with growth period) after an SBH addition. This is most obviously seen in the series following the first SBH addition, for which the “1st Day” generation rates decreased from 7.8 to 4.2 to 2.8 and to 2.2 L/day in tests SBH1.1 (Test 10-08 Phase 2), SBH 1.2 (Test 10-08 Phase 3), SBH 1.3 (Test 10-09 Phase 1A), and SBH 1.4 (Test 10-09 Phase 4), respectively. These quantitative average generation rates are tabulated in Table 9.2, not explicitly shown in Figure 8.7, although the trend is visually apparent in the plots. Again, a 1-L/day (0.042 L/hr) reference curve is included in the lower plot. Figure 8.7 also indicates that the gas generation rate decreased with subsequent additions of SBH. For example, the first-day average generation rates were 7.8 L/day for SBH1.1 (as above), 4.5 L/day for SBH2.1 (Test 10-09 Phase 1B), and 2.9 L/day for SBH3.1 (Test 10-09 Phase 6).

Both plots in Figure 8.7 show a step-like increase in generated gas volume at ~13-hours elapsed time in Test 10-08 Phase 2, which is attributed to a large gas release and gas expansion as hydrostatic pressure on the gas was reduced during release. So that results are more fairly compared, the noted “1st day” average gas generation rate for SBH1.1 excludes this gas release period. The basis for the apparent increase in gas volume generated with such a release is addressed in Section 6.4, and the specific gas release event is discussed further in Section 8.2.2 in the context of changes in retained gas fraction.

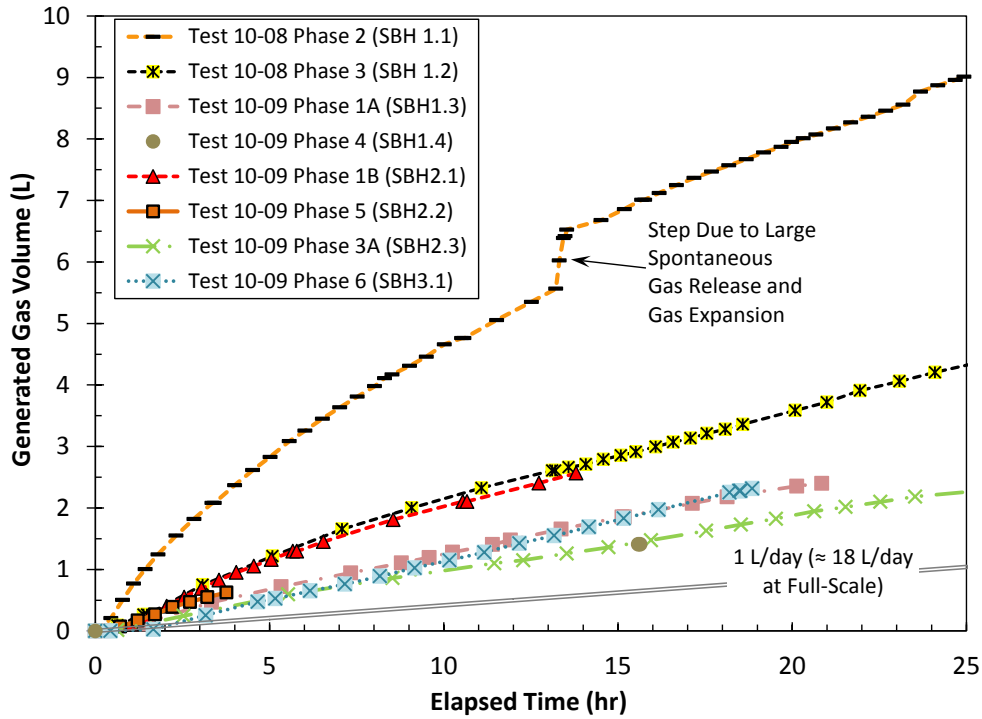
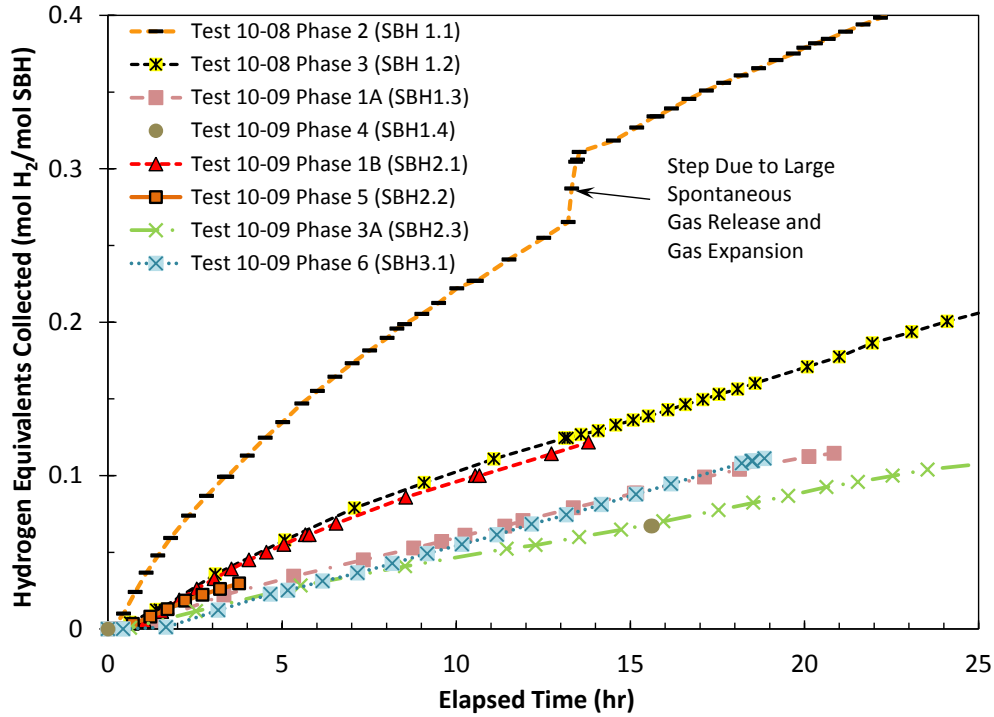


Figure 8.7. Gas Generation Determined from Gas Collection Cylinder Volume Measurements as a Function of Elapsed Time from the Start of Quiescent Growth Periods of Spontaneous and Fluidization-Induced Gas Release Tests for sRF Resin in 6.1-M Na LAW Simulant: Upper, Molar Equivalents of Hydrogen; and Lower, Measured Gas Volume. A generation rate of 1 L/day, equivalent to \sim 18 L/day in a full-scale IX column, is shown for reference. Legend entries include the “SBHx.y” sequence identifier.

8.2 Gas Retention and Spontaneous Release

This section covers retention of gas in quiescent beds of sRF resin up to the maximum retained gas fractions at the point of spontaneous gas release events (i.e. no mechanical disturbance) in both bench-scale experiments and fluidization-column tests. Peak retention evaluations in fluidization-column tests were completed, in part, in order define retained gas volume targets for fluidization-induced gas release tests that followed (Section 9.0). The gas retention characteristics in the less-than-peak retention periods preceding most fluidization-induced gas releases are also summarized in this section. In addition to providing gas generation results to inform decisions for fluidization-GR&R tests (Section 8.1), bench-scale tests were completed to help assess whether vessel-spanning bubbles formed in beds of sRF resin in vessels of increasing diameter. A key question was whether the 10-in. diameter fluidization-column was sufficiently large to avoid artificial VSBs that are considered unlikely to form in a full-scale (42-in. diameter) IX column. Below, bench-scale test results are presented first (Section 8.2.1) followed by the discussion of fluidization-GR&R tests (Section 8.2.2).

Retained gas bubble types and the methods for quantifying gas retention are described in detail in Section 6.5. This includes a number of definitions and assumptions that are applied to the results shown below. Visual examples of retained gas bubbles are given later in Section 8.3.

8.2.1 Bench-Scale Experiments

This section provides gas retention and spontaneous release results for the same bench-scale tests that were discussed in Section 8.1.1. As noted previously, a summary of the completed tests is provided in Table 5.2 in Section 5.3.2. Of particular relevance to the present discussion is the tabulation of initial resin bed densities and theoretical retained gas fractions at neutral buoyancy.

Figure 8.8 shows gas retention and release for sRF resin in alkaline water in 250-mL graduated-cylinder Test GC-01 in terms of changes in volume of the resin bed (ΔV_b), retained gas in the resin bed, determined from changes in the supernatant liquid surface level (ΔV_l), and liquid within the resin bed ($\Delta V_{L,e,gf}$) (left y-axis). As given by Eq. (6.7) in Section 6.5, the change in total volume of the resin bed is a measure of “total void” relative to the initially gas-free settled bed, and it is the sum of the retained gas volume (gas void) and the change in volume of liquid in the bed that is not affiliated with retained gas bubbles (“liquid void” or non-gas void). For gas retained as interstitial-liquid-displacing bubbles and for round bubbles filling pore bodies between resin particles (beads) without disturbing the resin, the resin bed level would not change and the volume of liquid within the porous bed would decrease equal to the volume of gas retained within the pores. For gas retained as “round” particle-displacing bubbles, the change in resin bed and retained gas volumes would be equal, and there would be no change in the volume of liquid within the porous bed. With either ILDBs or PDBs, the volume of liquid within the bed should decrease or remain constant. However, Figure 8.8 shows that the liquid volume in the resin bed increased as gas was retained. This can be explained by disturbance of the spherical-particle packing structure, likely due to PDBs, and infiltration of liquid into the bed. Associated with this additional liquid are reduced resin bed density (corrected to a gas-free state per Eq. (6.14) in Section 6.5) and increased gas-free (G-F) bed porosity, $\varepsilon_{b,gf}$ (Eq. (6.17) in Section 6.5). The variation in bed porosity from an initial estimated 0.36 void fraction is also shown in Figure 8.8 (right y-axis).

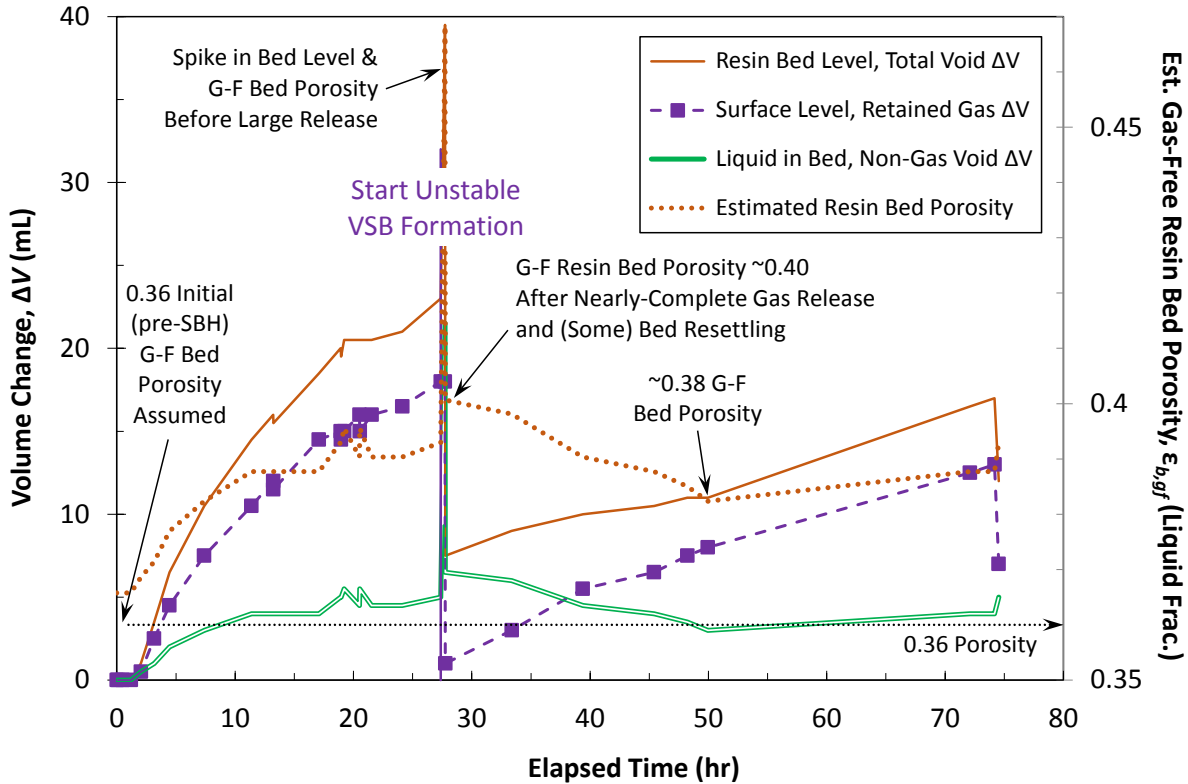


Figure 8.8. Gas Retention and Release for sRF Resin/Alkaline Water in Graduated-Cylinder Test GC-01 Depicted in Terms of: (Left y-axis) Changes in Volume of the Resin Bed, Retained Gas, and Liquid in the Resin Bed; and (Right y-axis) Estimated Gas-Free Resin Bed Porosity (0.36 initial assumed). The time of formation of an unstable VSB and an ensuing large spontaneous gas release is shown.

As indicated in Figure 8.8, an unstable VSB formed at ~27-hours elapsed time and was followed immediately by a large spontaneous release of nearly all the retained gas. The VSB migrated upward from near the bottom of the vessel, apparently gathering/coalescing gas as it progressed over ~20 minutes. It is considered “unstable” because it did not hold at a fixed elevation before releasing and was relatively short-lived. Examples of stable VSBs are given later in this section. Figure 8.8 also shows spikes in liquid volume in the resin bed and bed porosity during the transient VSB formation associated with resin bed expansion and drainage of supernatant liquid into it shortly before the gas release. Just after the gas release, with the resin bed resettled to its minimum post-release volume, a gas-free bed porosity of 0.40 is estimated; this is called out in the figure. As is also shown in the figure at an elapsed time of ~50 hours, a minimum post-gas-release $\epsilon_{b,gf}$ of ~0.38 is estimated. This indicates that the bed continued to become more compact (less porous) while gas was retained following the gas release, but that it never became as dense as it was initially ($\epsilon_{b,0}$ of 0.36 assumed before SBH addition).

Volume data from the test in Figure 8.8 are presented in Figure 8.9 as retained gas fraction as a function of elapsed time from the start of collection of level data, shortly after SBH addition. The measured retained gas volume fraction, α , is defined as the volume of retained gas divided by the total volume of the resin bed including the gas and, if present, infiltrated liquid (Eq. (6.6) in Section 6.5). Figure 8.9 also shows the estimated neutral buoyancy gas fraction calculated for gas retained as PDBs, $\alpha_{NB,PD}$, and as ILDBs, $\alpha_{NB,ILD}$. For Test GC-01, the initial gas-free settled-bed neutral-buoyancy gas

fractions were 12.3 and 14.0 vol%, respectively. Consistent with Eq. (6.15) and Eq. (6.16) in Section 6.5, the theoretical neutral buoyancy gas fractions decrease with decreasing gas-free resin bed density (given by Eq. (6.14)). Figure 8.9 shows that $\alpha_{NB,ILD}$ and $\alpha_{NB,PD}$ were both lower than the initial values after gas retention was detected, which coincides with liquid infiltration into the resin bed and the increased bed porosity noted in Figure 8.8. The initial G-F bed density and porosity (before SBH addition) were 1.138 g/mL and 0.36, respectively, and at the start of formation of the unstable VSB, they were 1.131 g/mL and 0.39 (0.393). As mentioned in Section 4.1.2, note that a relatively small change in density (-0.6%) corresponds to a relatively significant increase in porosity (9%). The retained gas fraction of 13.4 vol% at the start of the VSB event exceeded $\alpha_{NB,PD}$ (11.8 vol%) and $\alpha_{NB,ILD}$ (13.3 vol%). The “excess” retained gas may be necessary to overcome restraining forces such as wall effects in the relatively narrow graduated cylinder. Immediately before the large gas release, the estimated $\rho_{b,gf}$ decreased to 1.114 g/mL and $\alpha_{NB,PD}$ and $\alpha_{NB,ILD}$ correspondingly decreased to 10.4 and 11.7 vol%, respectively. The density-dependence is also illustrated in Figure 8.9 by the step-increase in $\alpha_{NB,ILD}$ to 13.1 vol% (and $\alpha_{NB,PD}$ to 11.6 vol%) following the large gas release, in which case $\rho_{b,gf}$ increased to 1.129 g/mL, near the value at the start of formation of the unstable VSB. Figure 8.9 also calls out a cluster of small gas releases from ~19- to ~22-hours ET (as well as one at ~13-hours ET). The majority of these occurred at gas fractions near neutral buoyancy.

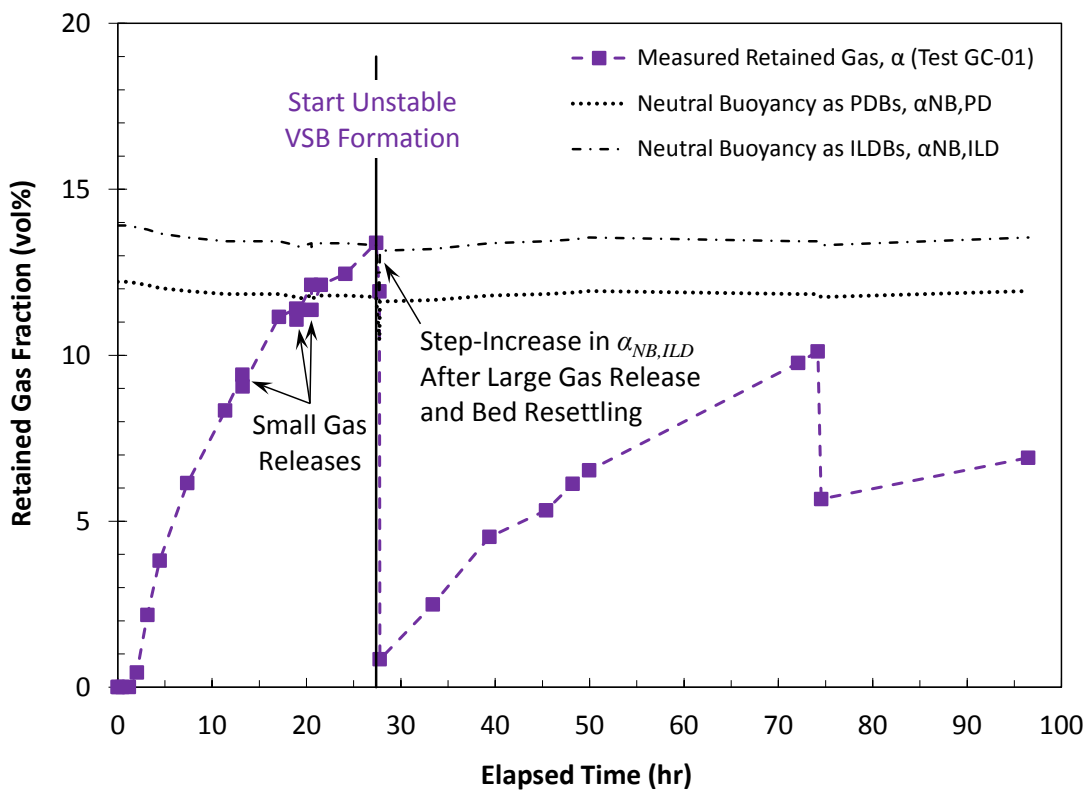


Figure 8.9. Retained Gas Volume Fraction for sRF Resin/Alkaline Water in Graduated-Cylinder Test GC-01 as a Function of Elapsed Time from the Start of Growth. The estimated time-varying PDB and ILDB neutral-buoyancy gas fractions are shown for reference, as is the time of formation of an unstable VSB and an ensuing large spontaneous gas release.

Although it is not conclusive, the change in resin bed volume exceeding (or even equaling) the retained gas volume (e.g., in Figure 8.8) suggests that gas was retained as particle-displacing bubbles

instead of interstitial-liquid-displacing bubbles. Visual observations in bench-scale tests also indicated that bubbles were typically “round” PDBs. However, although unlikely, it is possible to have ILDBs that are swamped by excess liquid infiltration from bed restructuring. See Section 6.5 for additional discussion of the metrics for estimating the fractions of gas retained as PDBs and ILDBs (e.g., Eqs. (6.8) and (6.9), respectively).

The Test GC-01 gas retention and release data from Figure 8.9 are compared to similar graduated-cylinder sRF resin/alkaline water Tests GC-01A and GC-16 in Figure 8.10. As noted in Section 8.1.1, Test GC-01A was a follow-on to Test GC-01 with a second addition of SBH, and Test GC-16 differs from Test GC-01 only in a small variation in batch pH. In Figure 8.10, neutral-buoyancy gas fractions from Test GC-16 are shown for reference: the initial gas-free value assuming gas retained as ILDBs, $\alpha_{NB,ILD}$ (13.6 vol%); the initial gas-free value assuming gas retained as PDBs, $\alpha_{NB,PD}$ (12.0 vol%); and the time-varying $\alpha_{NB,PD}$ throughout the test. As with Test GC-01, Test GC-16 exhibited a net infiltration of liquid into the resin bed during the test and a resulting decrease in $\alpha_{NB,PD}$, reaching a minimum of 11.5 vol%. The initial neutral-buoyancy gas fractions in the three tests shown in Figure 8.10 differed minimally, i.e., 0.3 to 0.4 vol%, because initial resin bed and liquid densities were also similar from test to test. The figure also shows that the tests were consistent in that small gas releases and the formation of unstable VSBs with large spontaneous gas releases occurred at retained gas fractions near or slightly above neutral buoyancy.

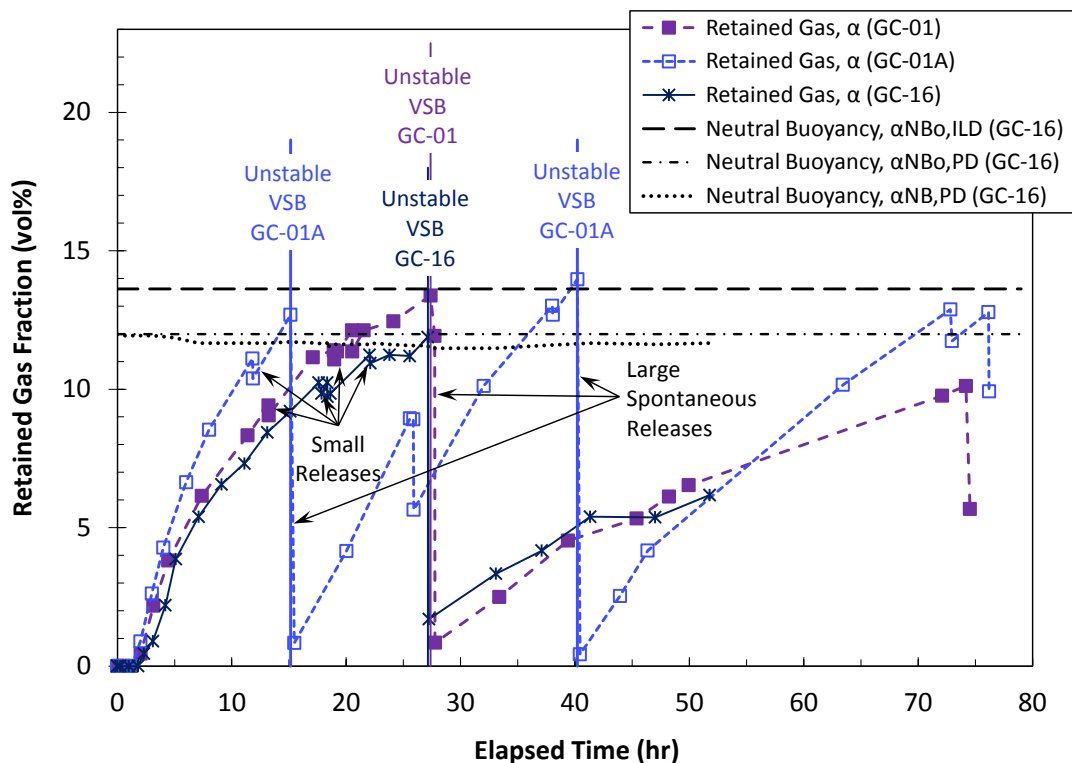


Figure 8.10. Retained Gas Volume Fractions for sRF Resin /Alkaline Water in Graduated-Cylinder Tests as a Function of Time from the Start of Level Measurements after SBH Addition. The times of formation of unstable VSBs and ensuing large spontaneous gas releases and representative neutral buoyancy gas fractions (initial as ILDBs and PDBs and measured throughout as PDBs) in Test GC-16 are shown.

Figure 8.11 shows retained gas fractions in sRF resin/6.1-M Na GR&R LAW simulant for graduated-cylinder Tests MD-01 and MD-03. As with the sRF resin/alkaline water tests discussed above, the gas generation rates for these tests are presented in Section 8.1.1; and as noted there, Test MD-01 and Test MD-03 differ in SBH concentration and the usage history of the resin prior to testing. The measured gas-free settled-bed densities in the two tests ranged from 1.327 g/mL (MD-03) to 1.335 g/mL (MD-01) with corresponding estimated $\alpha_{NB,PD}$ and $\alpha_{NB,ILD}$ ranges of 6.1 to 6.5 vol% and 6.5 to 7.0 vol%, respectively. Note that neutral buoyancy defined in terms of PDBs and ILDBs differed by only 0.5 vol% in both tests, compared to a difference of ~ 2 vol% in the alkaline water tests discussed above. The lower neutral-buoyancy gas fractions and the smaller difference in $\alpha_{NB,PD}$ and $\alpha_{NB,ILD}$ with GR&R LAW simulant are a result of the smaller difference in the resin bed and liquid densities in the simulant (0.08 to 0.09 g/mL) than in alkaline water (0.13 to 0.14 g/mL).

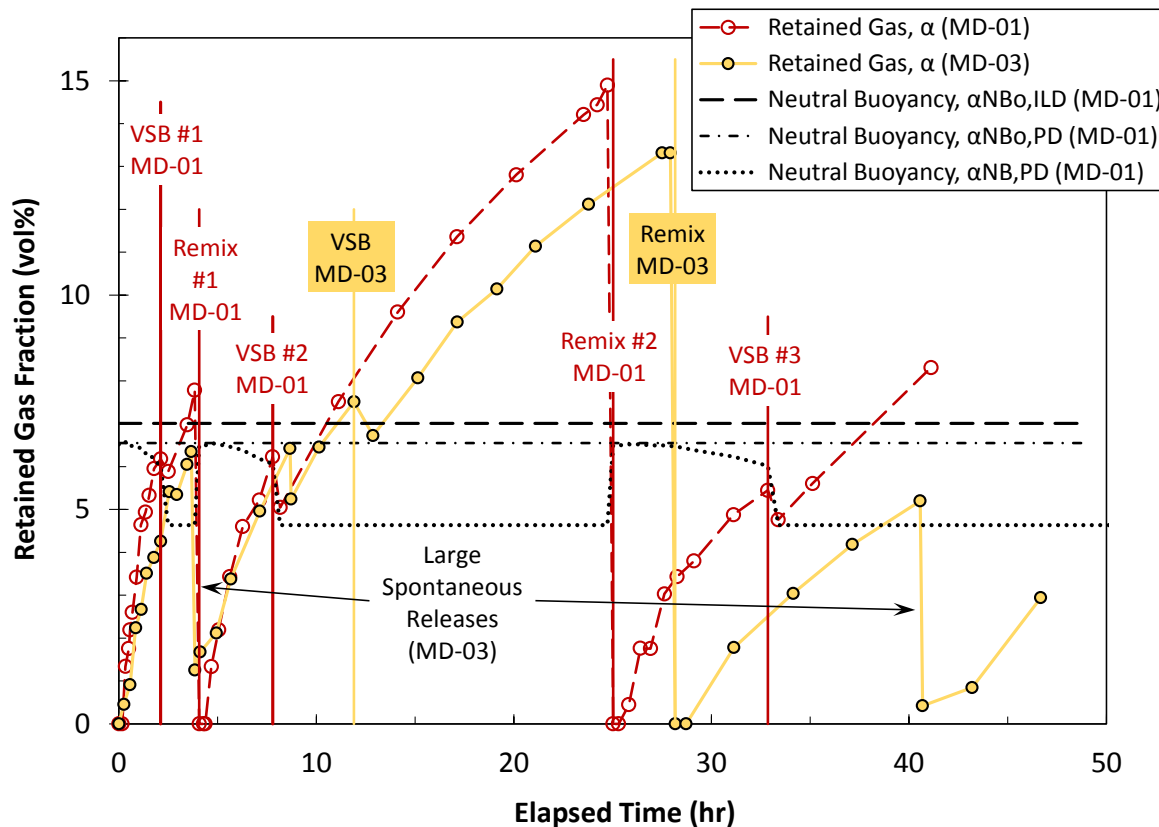


Figure 8.11. Retained Gas Volume Fractions for sRF Resin/6.1-M Na LAW Simulant as Function of Time from the Start of Level Measurements in Graduated-Cylinder Tests MD-01 and MD-03. The times of formation of stable VSBs, remixing to release gas, and large spontaneous gas releases are shown, as are representative neutral buoyancy gas fractions (initial as ILDBs and PDBs and measured throughout as PDBs) in Test MD-01.

In Figure 8.11, $\alpha_{NB,PD}$ and $\alpha_{NB,ILD}$ for Test MD-01 and the time-varying neutral-buoyancy gas fraction as PDBs are shown for reference. Like the alkaline water tests, infiltration of liquid simulant into the resin beds during the tests resulted in decreases in $\alpha_{NB,PD}$, and gas releases and VSB formation events generally occurred at near-neutral-buoyancy gas fractions. However, in the case of MD-01 and MD-03 simulant tests, indefinitely stable VSBs were observed, and these are identified in Figure 8.11. Retained gas fractions significantly exceeding neutral-buoyancy values after VSB formation are an artifact of

allowing gas to continue to generate and accumulate in and below a buoyant plug of resin up to the point that the contents were remixed to release gas, for example, at 25-hours elapsed time in Test MD-01 and 28 hours in Test MD-03. The figure further shows that VSB formation was repeatable in Test MD-01: a first VSB formed at ~2-hr ET; the batch was remixed a first time at ~4-hr ET; a second VSB formed at ~8-hr ET; and following the second remixing at ~25-hr ET, a third VSB formed (at ~33-hr ET). Also note that $\alpha_{NB,PD}$ reaches a steady-state (flat) minimum (e.g., 4.7 vol% in Figure 8.11) after VSB formation that reflects the gas-free bulk-average density of the combined resin bed and supernatant liquid (e.g., 1.309 g/mL in Test MD-01). Finally, Test MD-03 exhibited large spontaneous gas releases in addition to VSB formation that are called out in Figure 8.11. The first large release was at ~4-hr ET with a retained gas fraction of 6.3 vol%, just above the estimated $\alpha_{NB,PD}$ at that point in the test (5.7 vol%, not shown in the plot). The second large spontaneous release was at ~40-hr ET after remixing at ~28-hr ET to release the stable VSB that had formed at ~12-hr ET.

A series of tests was completed in different diameter vessels to investigate the effect of vessel size on VSB formation and stability. Graduated-cylinder Test MD-03 is compared to sRF resin/ GR&R LAW simulant tests in a 5-in. diameter vessel (Test MD-02) and in a 10-in. diameter vessel (Test MD-06) in Figure 8.12. Gas generation characteristics of these tests, all with 0.5 g SBH/L resin, are discussed in Section 8.1.1 in conjunction with Figure 8.3. Figure 8.12 shows gas retention and release behavior in terms of retained gas fractions along with the initial gas-free neutral-buoyancy gas fractions as PDBs for each test for reference. A higher bed density (1.349 g/mL) and initial neutral-buoyancy gas fraction (6.9 vol% $\alpha_{NB,PD}$) in Test MD-06 are due, at least in part, to more contacts of the resin with fresh aliquots of 6.1-M Na LAW simulant in the batch preparation process and a resulting higher equilibrated liquid (and likely particle) density. In all three tests, gas fractions ≥ 5.1 vol% were initially retained before relatively large spontaneous gas releases occurred at ~2.7, 2.9, and 3.7 hours in the 5-in. vessel, 10-in. vessel, and graduated-cylinder tests, respectively. The retained gas fractions at the point of these initial releases in the larger vessels (5.5 vol% in the 5-in. and 5.1 vol% in the 10-in.) were below neutral buoyancy. Subsequently, $\alpha_{NB,PD}$ was reached or exceeded on multiple occasions in the 5-in. vessel test, most notably at 5.8 hours ET (6.4 vol%) and 42 hours (6.5 vol%). However, the peak retained gas fraction in the 10-in. vessel test was 5.4 vol%, less than the estimated neutral-buoyancy gas fraction at the time (6.3 hours ET, 6.6 vol% $\alpha_{NB,PD}$ [not shown in the plot]). After the initial “large” release in the 10-in. vessel down to 1 vol% α , Figure 8.12 shows that the retained gas fraction tended to fluctuate between ~3 and 5 vol% with relatively frequent and small gas releases. This tendency is likely due to evolution of a non-uniform gas distribution in which, for example, large individual bubbles form and release or the retained gas fraction exceeds neutral buoyancy locally (e.g., a fraction or all of the upper resin layer) and releases, but without disturbing the entire resin bed. This process is cyclic and/or proceeds to different regions of the vessel because recently disturbed areas have lower gas fractions and become relatively stable. Although small gas releases were often observed from the upper portion of the resin bed in graduated-cylinder tests (with all liquid types), the cyclic release behavior without global buoyant events (e.g., large spontaneous releases or VSB formation) was more clearly demonstrated in the 10-in. vessel and to a lesser extent in the 5-in. vessel.

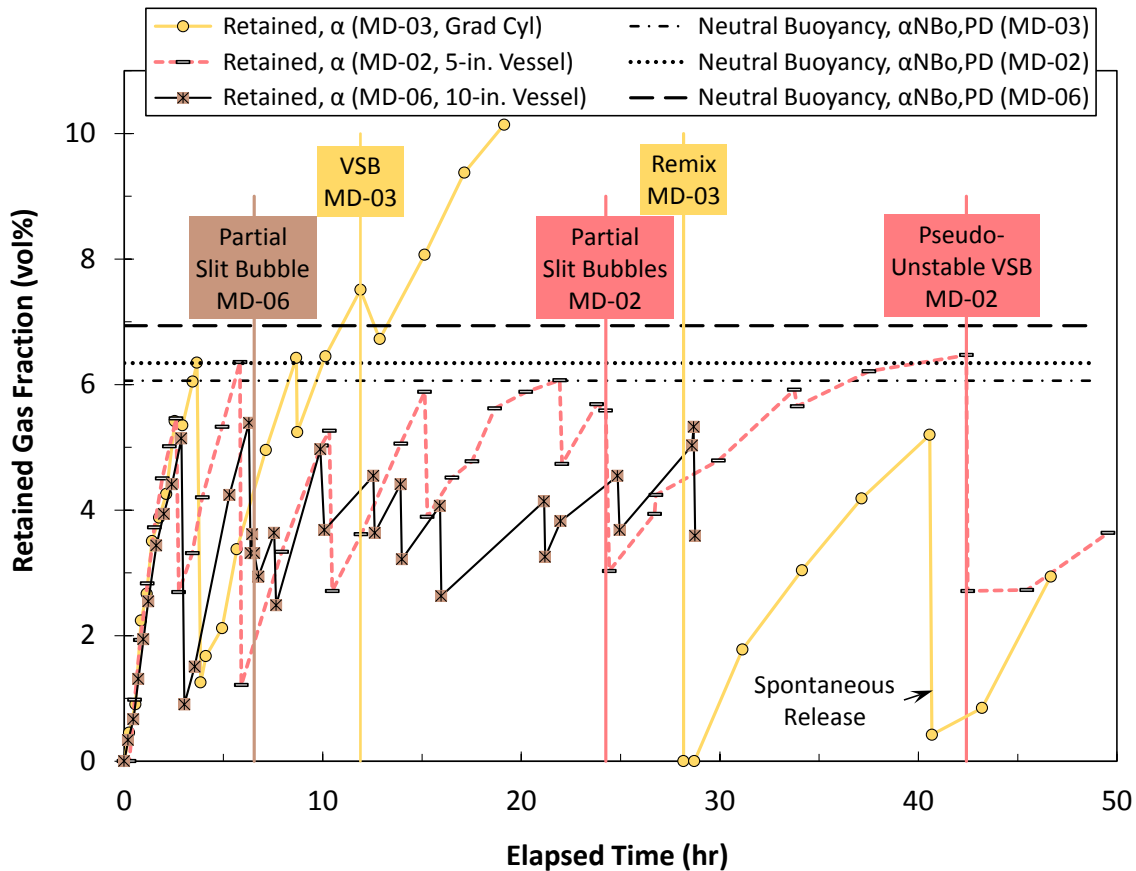


Figure 8.12. Gas Retention and Release for sRF Resin/6.1-M Na LAW Simulant Tests in Vessels of Varying Diameter (Graduated Cylinder, 5 in., and 10-in.) Presented as Retained Gas Fraction as Function of Time from the Start of Level Measurements after SBH Addition. The initial neutral buoyancy gas fractions as particle-displacing bubbles for each test are shown for reference.

Specifically, unlike Tests MD-01 and MD-03 in 1.4-in. diameter 250-mL graduated cylinders, stable VSBs were not observed in the 5-in. and 10-in. diameter vessels. The initial settled resin bed and total depths with supernatant liquid were 11 and 16 cm, respectively, in the graduated-cylinders, and 15 and 22 cm in the larger diameter vessels. The diameter dependence provided some assurance that stable VSBs were not likely to form spontaneously in the 10-in. diameter fluidization-column, although the resin bed and supernatant liquid depths were greater in the GR&R tests conducted in it (discussed in the next section). Although stable VSBs were not seen in Tests MD-02 and MD-06, some VSB-like activity was observed and is called out in Figure 8.12. In the 10-in. vessel test at an ET of 6.6 hours, a horizontal “slit” bubble formed a few centimeters from the bottom of the vessel and was seen over an estimated 20% of the vessel circumference before (apparently) releasing about 10 minutes later. Two partial-vessel slit bubbles (0.2 to 0.3 cm high and ~2 cm long) were also noted in the 5-in. vessel test at 24 hours ET and again preceded a gas release event. A more obvious, but short-lived, VSB(-like) formation and relatively large spontaneous gas release event occurred in the 5-in. vessel at an ET of 42 hours; the mostly flat bubble was observed progressing upwards and releasing over a period of 5 minutes or less.

Figure 8.13 shows retained gas fractions as a function of time for other ambient temperature graduated-cylinder tests with sRF resin in sodium hydroxide of varying concentration, as discussed in

conjunction with Figure 8.3 in Section 8.1.1. A constant SBH concentration (0.5 g SBH/L resin) was used in the four tests. The initial neutral-buoyancy gas fraction based on PDBs is plotted for each test for reference in Figure 8.13. As expected, $\alpha_{NB0,PD}$ (generally) decreases with increasing NaOH concentration and decreasing density difference between the G-F resin bed and equilibrated liquid densities, which correlate to the latter: 0.1-M NaOH (Test MD-07) – 1.000 g/mL ρ_L and 12.4-vol% $\alpha_{NB0,PD}$; 0.3-M NaOH (Test MD-05) – 1.007 g/mL ρ_L and 12.8-vol% $\alpha_{NB0,PD}$; 1.0-M NaOH (Test MD-04) – 1.036 g/mL ρ_L and 11.9-vol% $\alpha_{NB0,PD}$; and 10.8-M NaOH (Test MD-08) – 1.349 g/mL ρ_L and 4.6-vol% $\alpha_{NB0,PD}$. (Table 5.2 in Section 5.3.2 also includes $\rho_{b,0}$ and the theoretical $\alpha_{ILD0,PD}$ values.) In these, the trend of neutral buoyancy gas fraction with liquid density does not hold for the most water-like NaOH solutions, 0.1- and 0.3-M NaOH; this may be explained by slight differences in the packing efficiency of the initial gas-free settled resin bed. In later elevated-temperature graduated-cylinder tests with these same equilibrated batches of sRF resin/NaOH solution, discussed in Section 8.4, the initial ambient-temperature resin bed density (1.155 g/mL) and the theoretical neutral buoyancy gas fraction (12.8 vol%) with 0.3-M NaOH (Test MD-09) were the same as Test MD-05; but for Test MD-10 with 0.1-M NaOH, the bed density was slightly higher (1.147 versus 1.141 g/mL) as was $\alpha_{NB0,PD}$ (12.9 versus 12.4 vol%). This substantiates the hypothesis that differences in packing efficiency are the reason for sRF resin/0.3-M NaOH having a slightly higher $\alpha_{NB0,PD}$ than for 0.1-M NaOH in the first pair of tests.

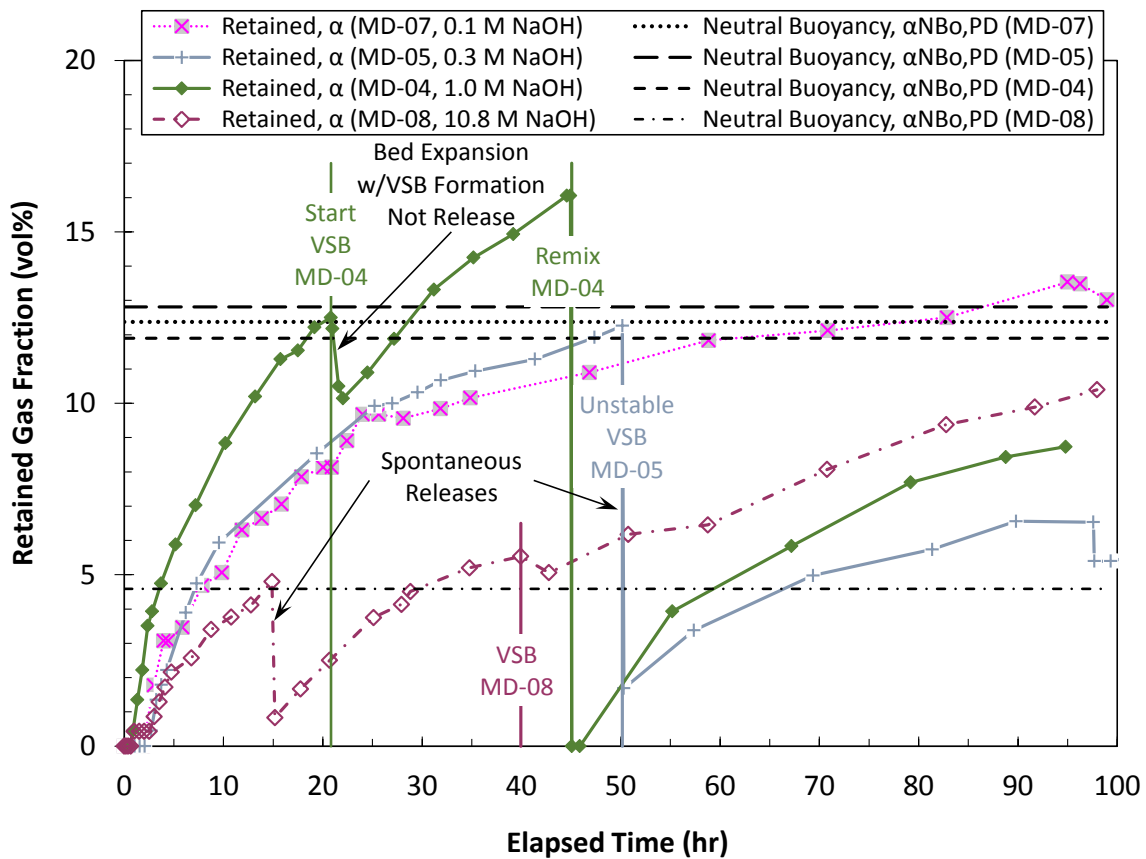


Figure 8.13. Gas Retention and Release in Graduated Cylinder Tests using sRF Resin in Varying Concentration of NaOH Presented as Retained Gas Fraction versus Elapsed Time from the Start of Level Measurements after SBH Addition. The initial neutral buoyancy gas fractions as particle-displacing bubbles for each test are shown for reference.

The gas retention and release behavior shown in Figure 8.13 is consistent with other graduated-cylinder tests discussed earlier in this section. Specifically, large spontaneous gas releases and VSB formation, if any, occurred with retained gas fractions near neutral buoyancy. For example, spontaneous gas releases were observed at 15-hours ET and 4.8-vol% retained gas fraction in 10.8-M NaOH and at 50-hours ET and 12.3-vol% α in 0.3-M NaOH. The latter was preceded by the formation of a short-lived, unstable VSB, as indicated in Figure 8.13. Additionally, stable VSBs were observed in 1.0-M NaOH (21 hr-ET and 12.5-vol% α at the start of VSB formation) and in 10.8-M NaOH (40-hr ET and 5.5-vol% α). The apparent decrease in retained gas in the ~hour-long VSB formation period in the 1.0-M NaOH test shown in Figure 8.13 is not due to gas release, but is an artifact of the definition of retained gas fraction. In this period (21- to 22-hours ET), the absolute volume of retained gas increased 1.5 mL, but the resin bed expanded over the course of VSB formation by ~46 mL as it rose to the surface; because α is the ratio of total retained gas volume to total resin bed volume, it appears to decrease with the relatively large bed expansion. In the test with 0.1-M NaOH, no large spontaneous releases or VSBs were seen, but rather the retained gas fraction plateaued at 13.5 vol% after ~4 days, 1.6 vol% above the estimated neutral buoyancy gas content for PDBs at the time (11.9 vol%). In all graduated-cylinder tests discussed in this section, note that stable VSBs were only observed in sRF resin with higher-density liquids (6.1-M Na simulant and 1.0- and 10.8-M NaOH) resulting in lower α_{NB} , whereas unstable or no VSBs were observed using less-dense, water-like liquids (alkaline water and 0.1- and 0.3-M NaOH) with higher α_{NB} .

8.2.2 Fluidization-Column GR&R Tests

This section addresses the gas retention characteristics during quiescent growth periods in the same fluidization-GR&R tests for which gas generation was discussed in Section 8.1.2. In several of these tests, gas retention was allowed to continue to, and beyond, the point of self-limiting maximum growth in conjunction with investigation of spontaneous gas releases. As noted previously, summaries of the completed tests are provided in Table 9.1 (alkaline water) and Table 9.2 (GR&R LAW simulant) in Section 9.0. Of particular relevance to this section are the tabulated nominal fractions of peak gas retention at the start of fluidization-induced gas releases that are discussed in Section 9.0.

Figure 8.14 shows a representative peak gas retention and spontaneous gas release test for sRF resin in alkaline water in the 10-in. diameter fluidization column (Test 10-04 Phase 4). A maximum supernatant liquid level growth of 10.1 cm at 111-hours elapsed time was measured in alkaline water, which corresponds to a peak retained gas fraction of 7.8 vol%. This liquid level increase is the absolute measure of gas retention that was used as a basis for determining level growth targets for fluidization-induced gas release tests starting with specific fractions of peak gas retention (e.g., f_α 25%, 50%, or \geq 90%). As shown in Figure 8.14, the measured α is \geq 4 vol% lower than the estimated initial neutral buoyancy gas fractions for PDBs (11.8 vol% $\alpha_{NB0,PD}$) and ILDBs (13.3 vol% $\alpha_{NB0,ILD}$), and this is clearly different than the behavior observed in multiple graduated-cylinder tests for resin in alkaline water discussed above (see Figure 8.10 in Section 8.2.1). Additionally, no VSBs (stable or unstable) and no large spontaneous gas releases were seen in the test shown in Figure 8.14.

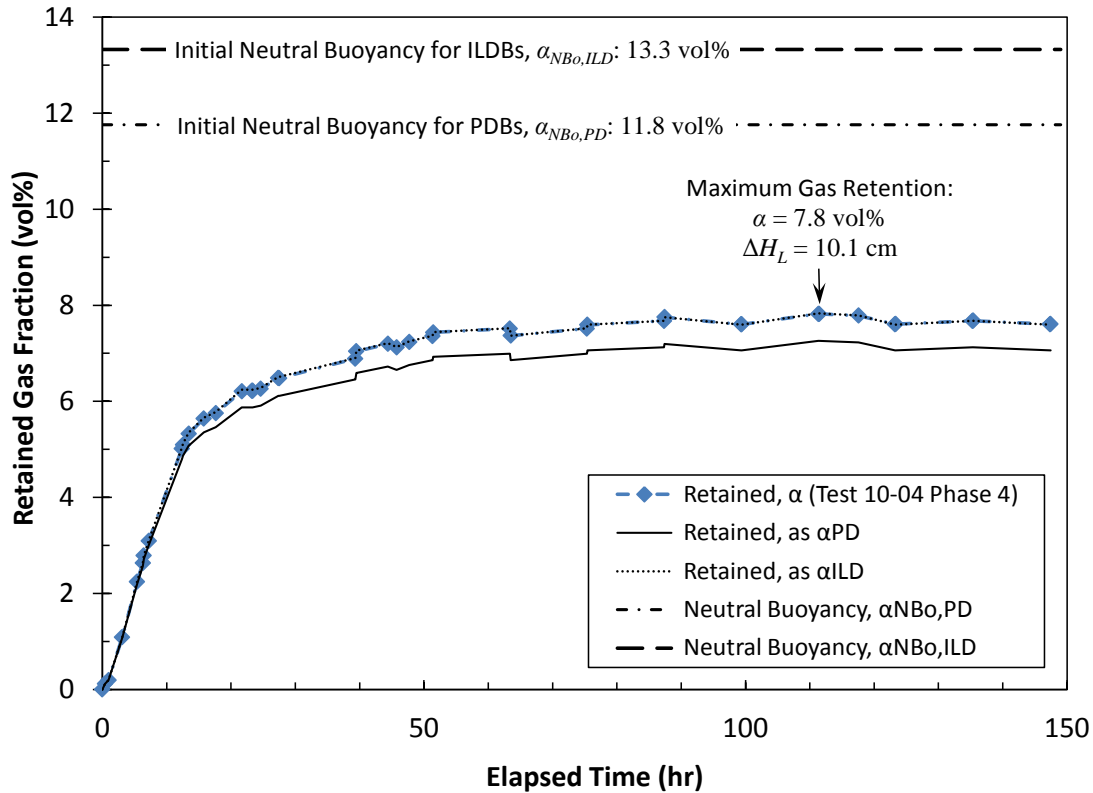


Figure 8.14. Peak Gas Retention and Spontaneous Gas Release for sRF Resin in Alkaline Water in Test 10-04 Phase 4 shown as Measured (α), Calculated Particle-Displacing (α_{PD}), and Calculated Interstitial-Liquid-Displacing (α_{ILD}) Retained Gas Fraction vs. Elapsed Time from the Start of Growth. The estimated neutral buoyancy gas fractions for ILDBs and PDBs based on initial gas-free conditions are shown for reference.

Also different than the bench-scale tests, resin bed level data in the fluidization-column experiment do not indicate a net liquid infiltration to the resin bed (i.e., the bed did not expand greater than would be expected for gas retained as particle-displacing bubbles). On the contrary, Figure 8.14 shows that the retained gas is best represented as interstitial-liquid-displacing bubbles. As given by Eqs. (6.10) and (6.11) in Section 6.5, the retained gas fraction based on the initial gas-free resin bed volume ($V_{b,0}$) can be defined for PDBs, $\alpha_{PD} = V_g / (V_g + V_{b,0})$, and for ILDBs, $\alpha_{ILD} = V_g / V_{b,0}$, where V_g is the volume of gas retained. Retained gas fractions calculated in these ways are compared to the measured α in Figure 8.14. The α_{ILD} curve is essentially indistinguishable from the test data, which supports a conclusion of gas retained primarily as ILDBs. As noted previously, however, would-be round particle-displacing bubbles (expected in the upper portion of the resin bed) could form in the pore bodies between resin beads up to a certain size (and gas fraction) without displacing resin and, thereby, behave as ILDBs. Also, with the fluidization-column isolated from the recirculation system in periods of quiescent gas retention, bubbles formed and/or collected under the bottom Johnson screen would either push liquid into the resin bed causing it to expand and register as liquid infiltration (not observed) or push through the resin bed, again appearing to be ILDBs. (The tables in Section 9.0 summarize observations of gas collected below and by the bottom screen.) It is postulated that in the relatively deep sRF resin bed used in these column tests that connected gas channels were formed through the lower region of the resin bed at gas fractions below neutral buoyancy, and this allowed gas to be transported (e.g., percolate) to the upper region of the resin

bed where it released into the supernatant liquid directly as small bubbles or combined with larger “round” PDBs which released intermittently.

In fluidization-induced gas release tests, it is necessary to define the retained gas fraction with reference to the initial gas-free resin bed volume instead of the time-varying measured gas-containing resin bed volume, as is typically done during quiescent gas retention and spontaneous release tests (e.g., in this section). This is so when the resin bed is expanded due to fluidization, in addition to gas retention, which gives the appearance of a reduction in the retained gas fraction α even without gas release. Considering the data shown in Figure 8.14, α_{ILD} rather than α_{PD} was selected for this purpose.

The measured gas retention data for Test 10-04 Phase 4 shown in Figure 8.14 are compared to two other peak gas retention and spontaneous gas release tests in sRF resin/alkaline water in Figure 8.15 (Tests 10-04 Phase 2 and 10-07 Phase 1). Figure 8.15 shows that the results are repeatable both in terms of peak retention and in the lack of large spontaneous gas releases. The peak retained gas fractions in the three tests ranged from 7.5 to 7.8 vol% or, in terms of supernatant liquid level growth, from 9.7 cm to 10.1 cm. The maximum values from Test 10-04 Phase 4 are again shown in Figure 8.15. Additionally, by coincidence, the retention curves for Tests 10-04 Phase 4 and 10-07 Phase 1 essentially overlap. This is inconsistent with the gas generation rates for the tests in Figure 8.6 in Section 8.1.2, which shows that the rate is faster in Test 10-07 Phase 1 except for the first ~ 6 hours. The differences in generation rate are countered by a larger fraction of the generated gas being retained in Test 10-04 Phase 4; this is demonstrated in Figure 8.18 later in this section.

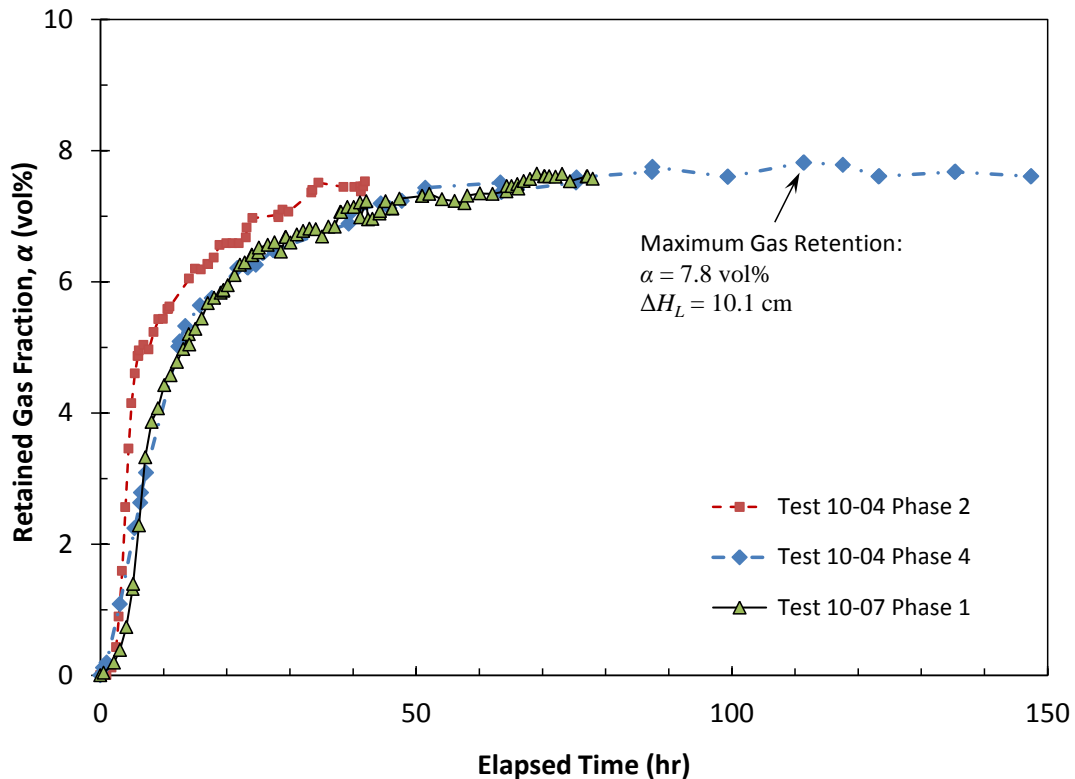


Figure 8.15. Reproducible Peak Gas Retention in Spontaneous Gas Release Tests for sRF Resin in Alkaline Water shown as Retained Gas Fraction as a Function of Elapsed Time from the Start of Growth (Tests 10-04 Phase 2, 10-04 Phase 4, and 10-07 Phase 1).

Figure 8.16 shows the peak gas retention and spontaneous gas release test for sRF resin in 6.1-M Na GR&R LAW simulant in the fluidization column (Test 10-08 Phase 2). A maximum supernatant liquid level growth of 9.75 cm equivalent to a peak retained gas fraction of 7.2 vol% was measured at 13-hours elapsed time. This ΔH_L was used as a basis for determining level growth targets to specific f_a values (e.g., 50% or $\geq 90\%$) for fluidization-induced gas release tests in the simulant. Test 10-08 Phase 2 was the only dedicated peak gas retention test conducted in the fluidization column with the GR&R LAW simulant. However, a comparable maximum gas fraction of 7.2 vol% (9.65-cm ΔH_L) was observed preceding opportunistic fluidization-induced gas release Test 10-09 Phase “7” at 470 hours (20 days) after the start of the untracked retention / spontaneous release period. This result is shown in Figure 8.16 at 15-hr ET for comparison. Note that no VSBs (stable or unstable) were seen in the tests shown in Figure 8.16.

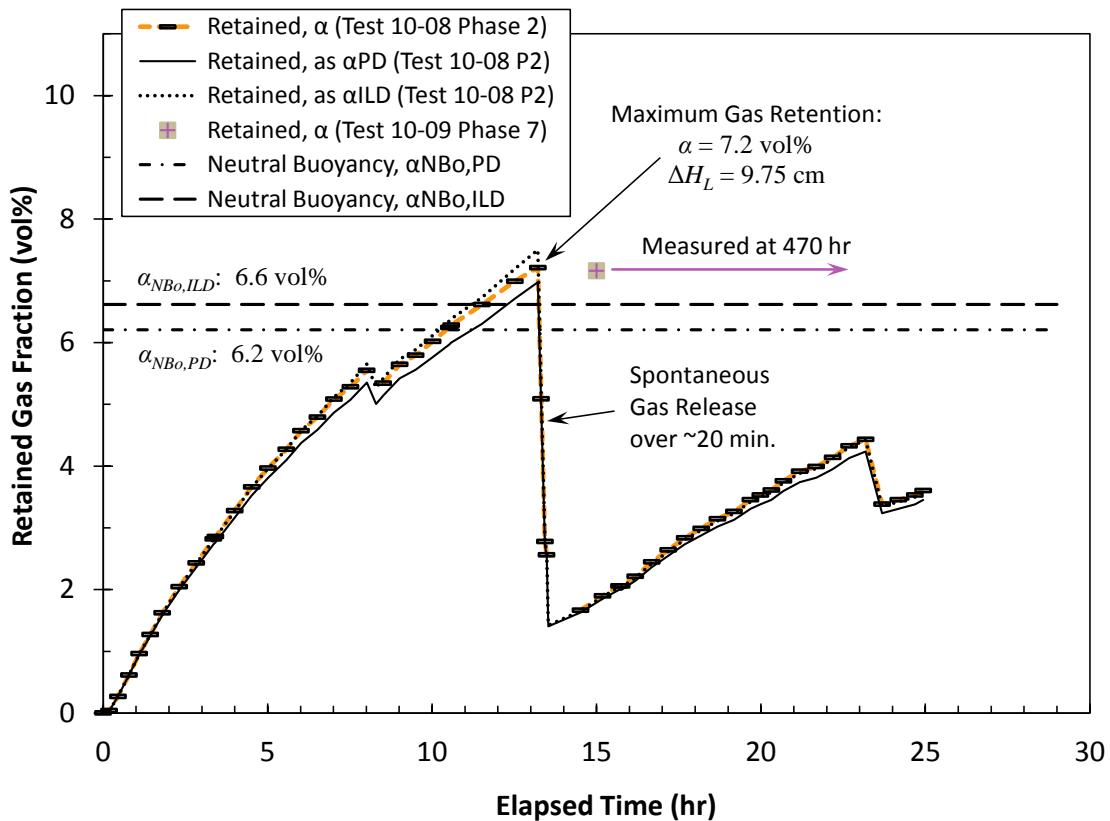


Figure 8.16. Peak Gas Retention and Spontaneous Gas Release for sRF Resin in 6.1-M Na LAW Simulant in Test 10-08 Phase 2 shown as Measured (α), Calculated Particle-Displacing (α_{PD}), and Calculated Interstitial-Liquid-Displacing (α_{ILD}) Retained Gas Fraction vs. Elapsed Time from the Start of Growth. α measured at 470 hours in opportunistic Test 10-09 Phase 7 is shown at 15-hr ET for comparison. The estimated neutral buoyancy gas fractions for ILDBs and PDBs based on initial gas-free conditions are shown for reference.

Figure 8.16 also shows that the measured (average) peak α preceding a large spontaneous gas release in Test 10-08 Phase 2 was 1 vol% higher than the estimated initial neutral buoyancy gas fraction for PDBs (6.2 vol% $\alpha_{NB0,PD}$) and 0.6 vol% higher than the estimate for ILDBs (6.6 vol% $\alpha_{NB0,ILD}$). This is nominally consistent with the behavior observed in bench-scale tests for resin in the 6.1-M Na simulant discussed above (see Figure 8.11 and Figure 8.12 in Section 8.2.1), in which a number of spontaneous gas

releases occurred with α at or slightly exceeding $\alpha_{NB0,PD}$, and in graduated-cylinder Test MD-03, the retained gas fraction at the start of formation of a stable VSB (7.5 vol% at 12-hr ET) exceeded estimated neutral buoyancy gas fractions by at least 1 vol% (6.1 vol% $\alpha_{NB0,PD}$ and 6.5 vol% $\alpha_{NB0,ILD}$). Possible restraining forces such as resin bed strength (e.g., yield stress) (Meyer et al. 1997; Gauglitz et al. 2018) and column wall-effects could be reasons for the retained gas exceeding that for neutrally buoyancy at the start of the gas release event. Additionally, gas bubbles below the bottom Johnson screen would register as retained gas, which is treated as being in the resin bed, without imparting upward buoyant force (see Section 6.5); but, no pancake bubble and minimal total gas was found collected under the screen at the end of Test 10-08 Phase 2 (see Comments in Table 9.2 in Section 9.0).

Gas distribution and retained bubble types have roles in the characteristics of gas retention and spontaneous release, but there is insufficient experimental information to determine these quantitatively with a high degree of certainty in the GR&R tests discussed in the report. However, expansion of gas from varying depths in the resin bed during the large spontaneous release shown at 13-hr ET in Figure 8.16 is the reason for the apparent step-increase in gas generation rate in Test 10-08 Phase 2 shown in Figure 8.7 (Section 8.1.2), and for this scenario, an analysis in Section 6.4 gave an estimated volume expansion of 19% upon release for gas retained at mid-depth in sRF resin/GR&R LAW simulant in the fluidization column. Like Figure 8.14 for the alkaline-water test case, Figure 8.16 shows α_{PD} and α_{ILD} determined from the initial gas-free bed volume and the time-varying retained gas volume for comparison to α values measured throughout Test 10-08 Phase 2. For the majority of the LAW simulant test, the α_{ILD} curve tracks the directly-measured retained gas fraction data. But, in the few hours leading up to the peak retention and spontaneous release, α data fall between the α_{PD} and α_{ILD} curves, suggesting that gas is retained both as particle-displacing and interstitial-liquid-displacing bubbles. At peak retention, nearly an even split in the two is calculated (53% f_{PD} and 47% f_{ILD} , where the fractions are defined by Eqs. (6.8) and (6.9) in Section 6.5). However, as noted in the discussion of bench-scale test results above, liquid infiltration to the resin bed associated with changes in particle packing structure (porosity) could cause the resin bed to expand and present as PDBs. Consistent with the data in Figure 8.16, such expansion seems most likely to occur as (portions of) the resin bed approaches/exceeds neutral buoyancy and slowly begin to move. Unlike the bench-scale tests, liquid infiltration, if any, does not swamp expulsion of liquid by ILDBs (and/or due to bed compaction, porosity reduction). It is concluded that ILDBs were present to a significant extent throughout the sRF resin/6.1-M Na LAW simulant test shown in Figure 8.16, and once again, α_{ILD} is used to represent the retained gas fraction during fluidization-induced gas release tests with this liquid (Section 9.0).

In most of the fluidization-induced gas release tests, fluidization was initiated when the retained gas reached a pre-determined target fraction of the peak gas retention, f_α , for the particular sRF resin/liquid combination being used. Given the significant variability in gas generation (and retention) rates (see Section 8.1.2), hitting a target f_α (per Eq. (6.12) in Section 6.5) was accomplished by monitoring supernatant liquid level changes over time and being prepared to run fluidization-induced release tests at any time of day. Figure 8.17 summarizes the quiescent retention/growth periods of both spontaneous and fluidization-induced gas release tests using sRF resin in alkaline water (upper plot) and in 6.1-M Na LAW simulant (lower plot) in the fluidization column. As with the gas generation rate plots in Section 8.1.2 for these same tests, legend entries in Figure 8.17 include the “SBHx.y” identifier. Gas retention in these plots is presented as fraction of maximum retention. Therefore, data from peak gas retention and spontaneous release experiments that were shown in terms of retained gas fraction in Figure 8.15 and Figure 8.16 have maximum values at or near 100% in Figure 8.17. (Note that the peak gas retention in

Test 10-04 Phase 4 was reached at 111-hr ET, and this is not shown in the upper plot of Figure 8.17, because the x-axis is truncated at 80 hours to expand the scale; see Figure 8.14 for complete Test 10-04 Phase 4 data.) The endpoints in most of the retention curves depicted in Figure 8.17 were the start of corresponding fluidization-induced gas release tests, which are picked up in Section 9.0. As shown in the figure, a majority of the tests in both alkaline water and 6.1-M Na simulant were run with f_a of ~50% or \geq ~90%. A few others were run with f_a of ~10% (Test 10-09 Phase 5, lower plot), ~25% (Test 10-06 Phase 1A, upper plot), or not-defined (as-is) in some opportunistic tests (e.g., Tests 10-04 Phase 6, upper, and 10-09 Phase 4, lower), all of which will be discussed in more detail in Section 9.0.

The amount of gas retained in fluidization-column GR&R tests (see immediately above) is compared in Figure 8.18 to the volume of gas generated, as determined by gas collection cylinder measurements (Section 8.1.2). Results are shown for sRF resin in alkaline water in the upper plot and in GR&R LAW simulant in the lower plot. Gas retention is shown in terms of supernatant liquid level change in centimeters from the initial gas-free state, which is readily converted to volume of gas retained through the geometric scaling factor 0.51 L/cm, i.e., the slope in the 10-in. diameter fluidization-column level-volume correlations (at each ruler): $V_g = \Delta H_L \times 0.51$ L/cm. Liquid level change is shown in Figure 8.18 instead of retained gas volume to demonstrate the use of levels as the directly-observed experimental metric of gas retention for evaluation of the approach to f_a targets, per the discussion following Eq. (6.12) in Section 6.5.

The concept of comparing retained and generated gas volumes was introduced in Section 8.1.2 in discussion of the upper plot of Figure 8.5, which shows separate curves for gas generation rate (collected gas volume versus time) and gas volume retained in the resin bed over time for fluidization-column Test 10-04 Phase 2 with alkaline water. The cross-plots of retained gas (as ΔH_L) versus the total volume of generated (collected) gas in Figure 8.18 provide a more-direct indication of how much of the generated gas was retained. To further facilitate this comparison, 100% gas retention reference lines are shown in the plots, indicating the expected liquid level change if all generated gas was retained. With a few notable exceptions in the upper plot of Figure 8.18, the gas retention versus generation curves for sRF resin/alkaline water tend to collapse to trend lines with similar characteristics: they are nominally linear in ΔH_L vs. cumulative generated gas volume, ΔV_c , up to approximately 3 to 4 liters collected and have slopes approaching, but generally less than the 100% retention line; and above this transition region (volume generated), the retention curves flatten with a further reduced slope compared to the 100% retention line. In both regions, less than 100% retention indicates that gas is being generated in the supernatant liquid and/or within the bed and releasing continuously. Test 10-04 Phases 2, 4, and 6, all following the first addition of SBH and shown in the upper plot of Figure 8.18, tend to follow a single trend line throughout the generation/retention process and closely follow the 100% retention curve up to the transition point. In all later tests, after the second and third SBH additions, the retained vs. generated gas volume curves tended to collapse to a single trend in which more gas was generated than retained, even early in the growth periods (i.e., falling below the 100% retention curve). The shift away from the 100% curve may be associated with, in some way, the chemistry and/or system condition changes that give rise to continuing decreases in gas generation rates (molar equivalents basis) with multiple additions of SBH (Section 8.1). Additionally, the knee in an alkaline water test curve might be due to reaching a “critical” gas fraction above which gas percolation through the resin bed starts and new ILDB retention sites must be formed (nucleated) in order to reach f_a targets or maximum retention.

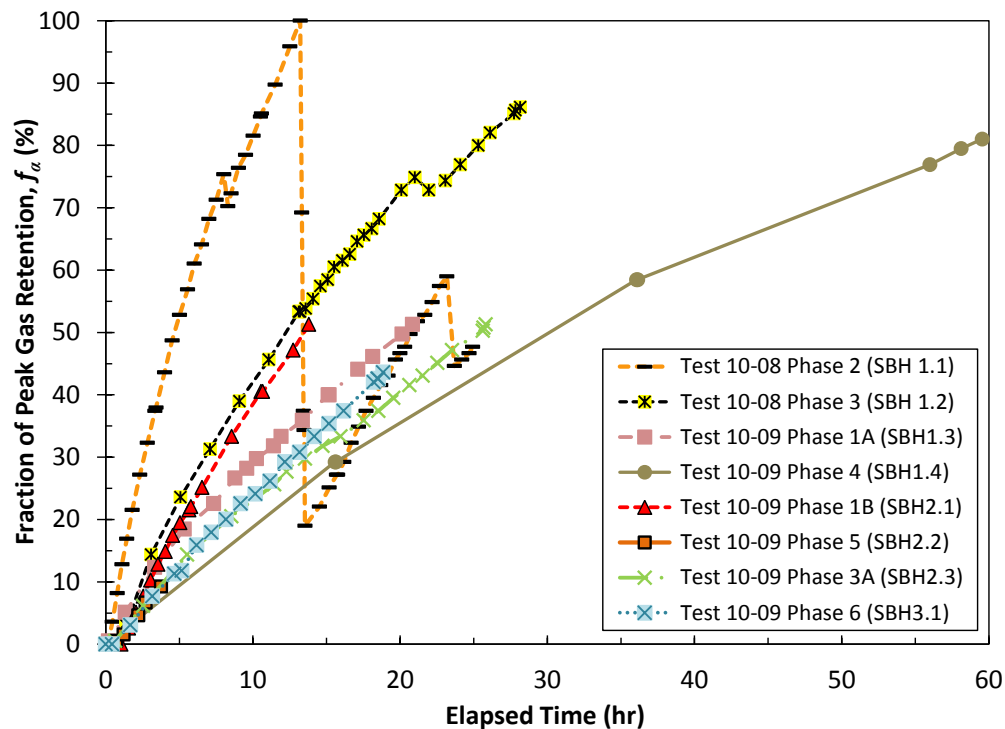
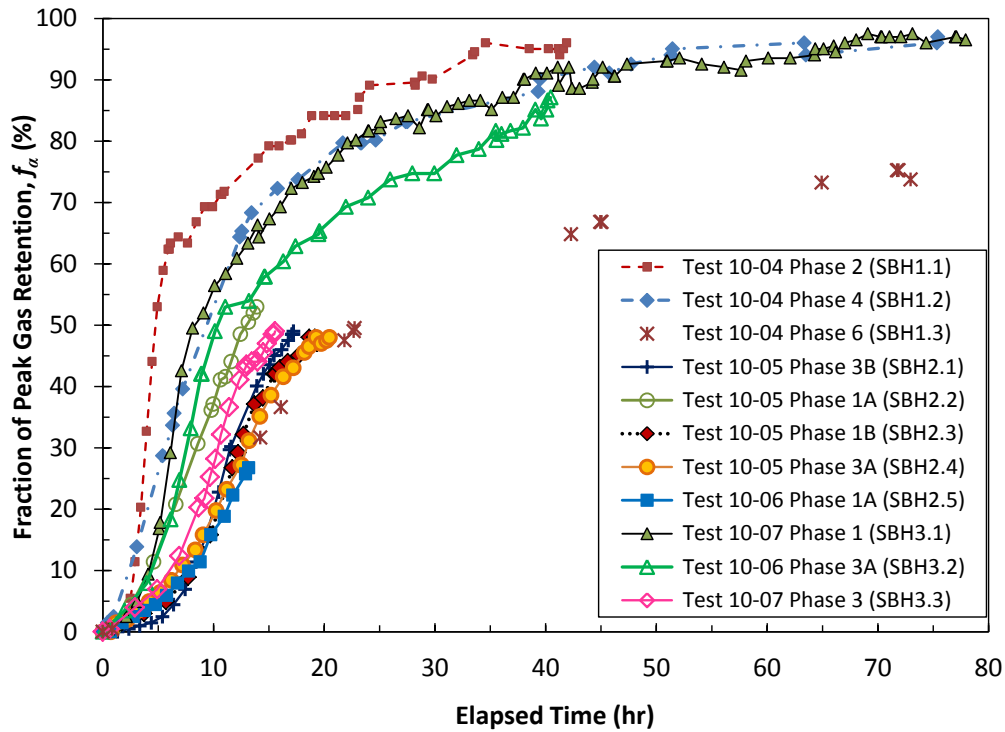


Figure 8.17. Gas Retention in Quiescent Growth Periods of Spontaneous and Fluidization-Induced Gas Release Tests for sRF Resin in Alkaline Water (upper) and in 6.1-M Na Simulant (lower), shown as the Fraction of Peak Gas Retention versus Elapsed Time from the Start of Growth. Legend entries include the “SBHx.y” sequence identifier.

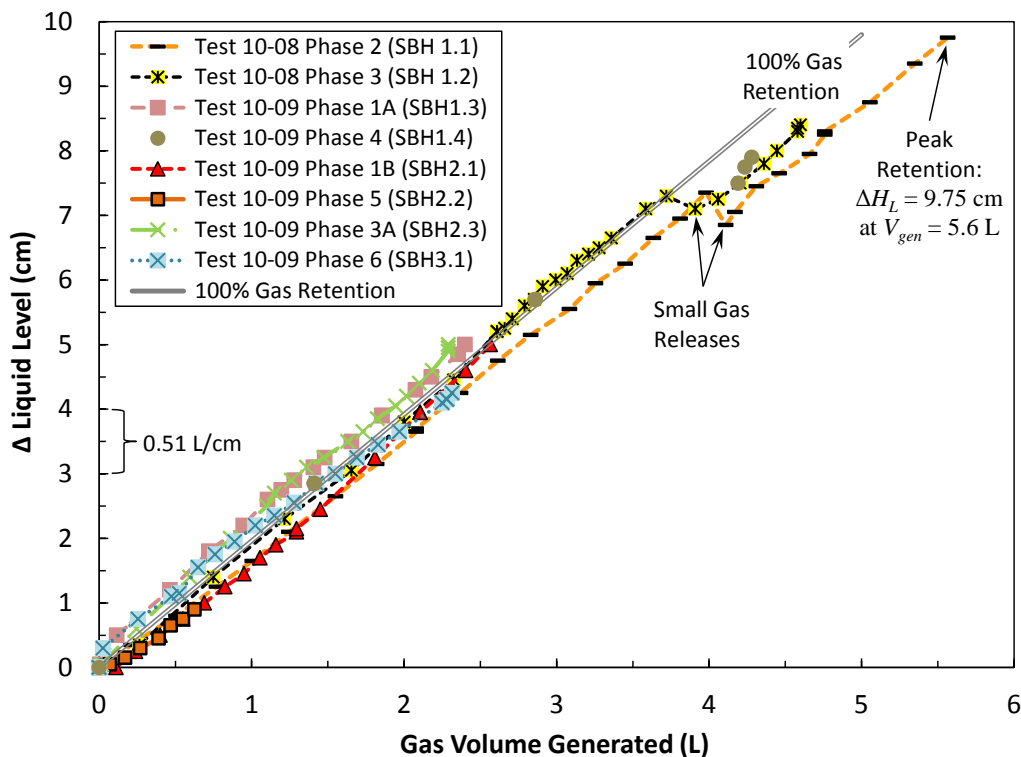
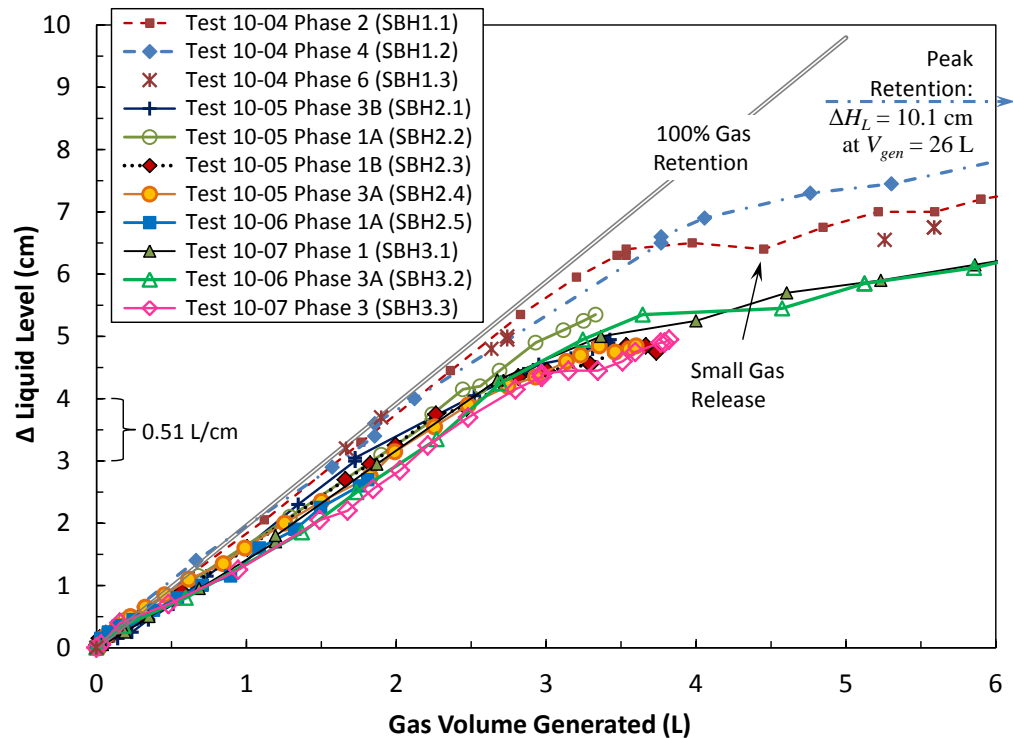


Figure 8.18. Retained Gas in Fluidization-Column Tests, Represented by Supernatant Liquid Level Change, as a Function of Gas Volume Generated (Collected) in sRF Resin in Alkaline Water (upper plot) and in 6.1-M Na Simulant (lower plot). 100% gas retention reference lines are shown, indicating liquid level change if all generated gas is retained.

In contrast, the lower plot of Figure 8.18 shows that the 100% retention curve was generally followed closely in all GR&R-LAW-simulant tests, which also included three additions of SBH. Differences from the alkaline water curves may be due to a more fundamental dependence on resin (sites) for SBH reactivity in the simulant (e.g., little generation in supernatant liquid alone). Additionally, the relatively-higher apparent fraction of PDBs in resin/simulant compared to 100% ILDBs in resin/water (see Figure 8.14 and Figure 8.16 earlier in this section) may play a role in curve shape, as is suggested at the end of previous paragraph. Finally, deviations from the 100% retention line in the lower plot of Figure 8.18 at \geq ~4-L generated gas are due, at least in part, to observed gas releases in Test 10-08 Phases 2 and 3 (and suspected, but not documented, in Test 10-09 Phase 4).

8.3 Observed Mechanisms of Gas Retention and Bubble Types

Five different types of bubbles were observed during testing. These were 1) particle-displacing bubbles (PDBs) in the settled sRF resin bed; 2) interstitial-liquid displacing bubbles (ILDBs) in the settled sRF resin bed; 3) a pancake-shaped bubble that could span the column cross section below the screen supporting the sRF resin; 4) a vessel-spanning bubble (VSB) that formed within the settled sRF bed during fluidization for gas release; and 5) hitchhiker bubbles where sRF particles attached to individual bubbles and moved as aggregates. PDBs, ILDBs, and VSBs were generally expected and these types of bubbles were described in Section 1.1. The relative proportion of PDBs and ILDBs in the column is important for gas retention and release because the gas volume fractions to reach neutral buoyancy of the bed with the supernatant liquid are different for these bubble types so peak gas retention may also be different. VSBs are expected to be an artifact of conducting tests in a column that is smaller in diameter than the planned full-scale column (see discussion in Section 1.1). Bubbles beneath the bottom screen that could grow, coalesce, and form a large pancake bubble spanning the column cross section had been considered possible based on earlier work, but they were observed during gas retention and release testing for the first time in the current study. Previous evaluations of pancake bubbles are discussed in Section 1.1. Pancake bubbles are important for gas retention and release because the gas retention below the bottom screen increases the total retained hydrogen, thus increasing the hydrogen flammability hazard, and they cause flow maldistribution that interferes with the ability of bed fluidization to release gas. Finally, hitchhiker bubbles with sRF resin particles attached to individual bubbles that would move as agglomerates were not anticipated prior to testing, but were observed in a few tests. Examples of these different bubble types are given in the section below. Hitchhiker bubbles were observed to collect on the upper Johnson screen and are an additional mechanism of gas retention that needs to be considered when evaluating the potential total quantity of retained hydrogen. These bubbles types were observed in a number of tests, but the images shown below in this section were all recorded during the first fluidization column test sequence of gas retention to near peak retention followed by fluidization to release the gas.

Figure 8.19 shows images of bubbles from the top to the bottom of the column that were taken after about 15 hrs of bubble growth with a retained gas fraction of about 6%. Towards the top of the column the retained bubbles displace the individual sRF resin particles, because the weight of the bed above the bubbles is small enough that it is easier for a bubble to displace resin particles than overcome the force from surface tension that resist the gas bubble fingering between the resin particles (Gauglitz et al. 1995). Deeper in the sRF resin bed at a height of about 70 cm above the bottom screen, the retained bubbles have fingered between the sRF resin beads and are interstitial-liquid-displacing bubbles. At this depth, the weight of the sRF resin bed above the bubbles is sufficiently high that expanding bubbles will overcome resistance of surface tension and finger between the sRF resin particles rather than lift and

displace bed upwards. Figure 8.20 shows a close up image of interstitial-liquid-displacing bubbles at a height of 50 cm above the bottom screen at about 22 hrs after the start of bubble growth. The reflection of light from particles located behind gas bubbles helps to visually distinguish gas bubbles from liquid-filled pores in the bed of sRF resin particles with interstitial-liquid-displacing bubbles. These two types of retained gas bubbles change the bulk density of an sRF resin bed differently as they grow, thus changing the retained gas fraction for when the sRF resin bed is neutrally buoyant in the supernatant liquid above the bed. While this is important for evaluating the gas release behavior, no attempt was made to quantify the transition between particle-displacing (upper region) and interstitial-liquid-displacing (lower region) bubbles.

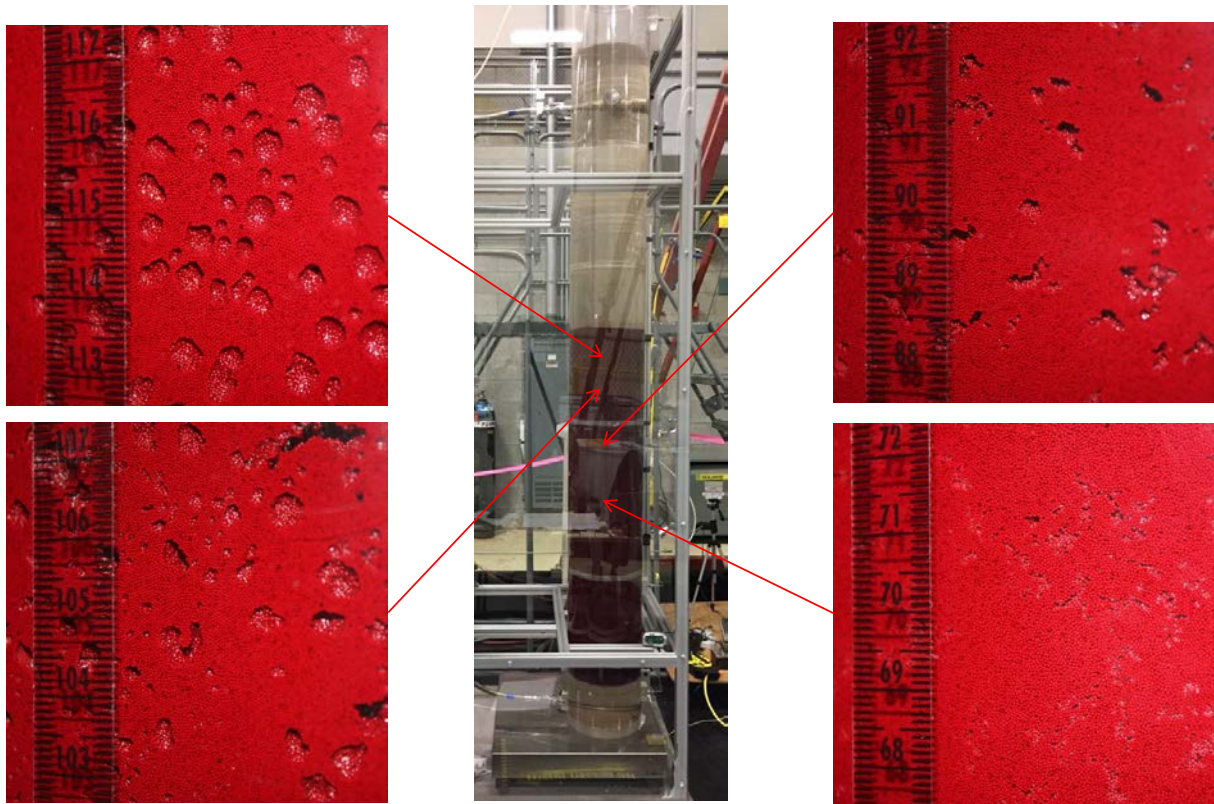


Figure 8.19. Images of particle-displacing bubbles in the upper portion of the column (left two images), interstitial-liquid displacing bubbles (bottom right-hand image), and bubbles in the transition between these two bubble types (upper right hand image). Ruler shows height in cm above the bottom screen. Image taken about 15 hrs after start of bubble growth with about 6.2% retained gas fraction (see Figure 8.15 Test 10-04 Phase 2).

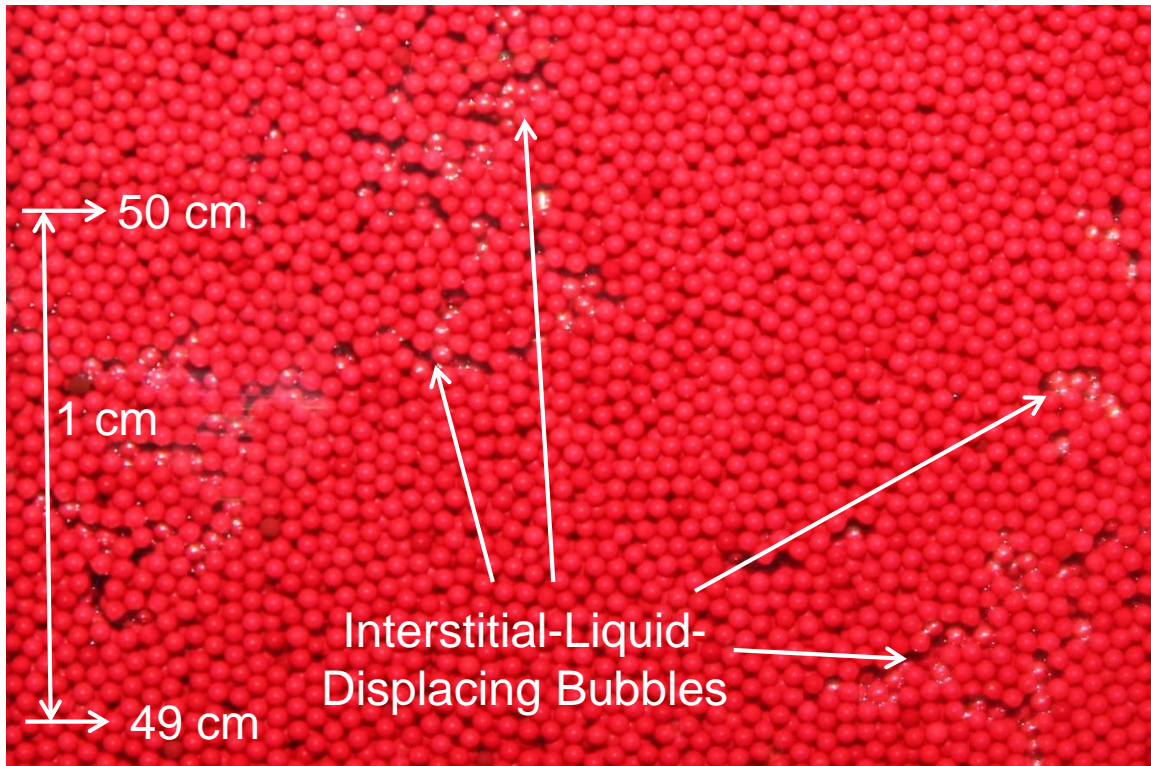


Figure 8.20. Close-up image of interstitial-liquid-displacing bubbles at a height of ~ 50 cm above the bottom screen. Image taken about 22 hrs after start of bubble growth with about 6.6% retained gas fraction (see Figure 8.15 Test 10-04 Phase 2).

Figure 8.21 shows a vessel-spanning bubble that was observed after an initial short period of fluidization for the test with retain bubbles shown in Figure 8.19 and Figure 8.20. Fluidization was initiated when the retained gas fraction was about 7.5%. For this test, the fluidization pump did not run continuously due to cavitation from gas in the liquid recirculation line (the gas/liquid separator upstream of the pump inlet was used in later tests to avoid this problem). Approximately 10 minutes after formation and without the fluidization pump running, the VSB released spontaneously. In a full-scale IX column with a diameter of 42 in., rather than 10 in. diameter column used in these laboratory tests, the VSB would have been more unstable and may never have formed. This observed VSB is thought to be an experimental artifact of testing in a smaller diameter column and also partly a result of intermittent fluidization. At the start of fluidization, the gas fraction was also very near peak retention and there was a complete pancake bubble below the bottom screen. This relatively large quantity of gas probably also contributed to forming the VSB. In a repeat of this test with better pump operation a VSB was not observed.

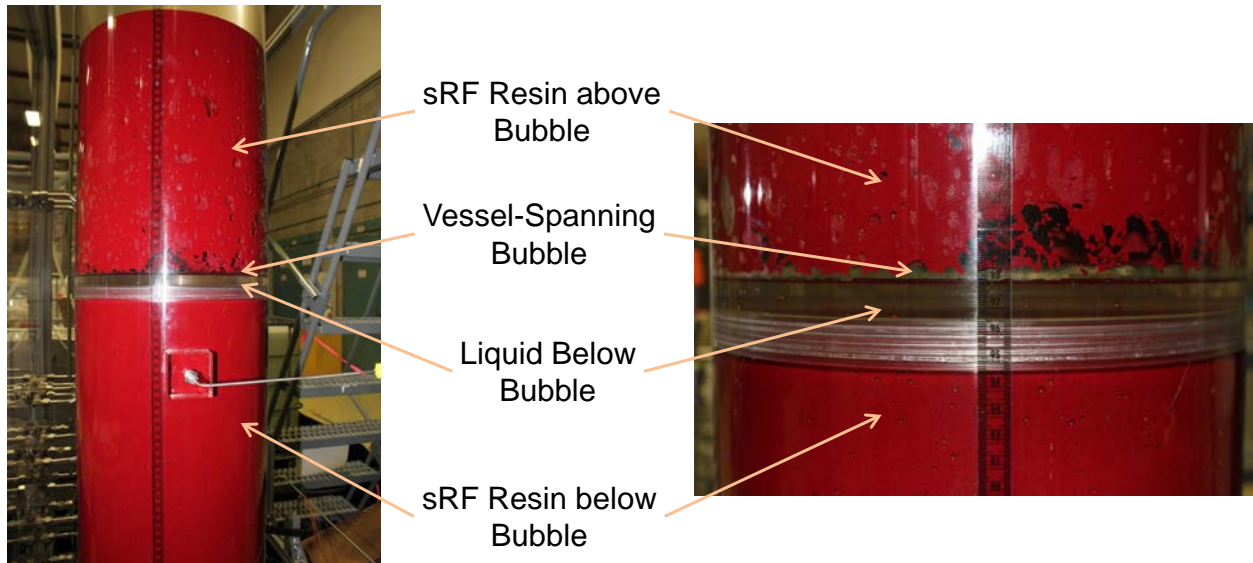


Figure 8.21. Vessel-spanning bubble observed after an initial short period of fluidization where the fluidization pump did not run continuously. Approximately 10 minutes after formation, the VSB released spontaneously (fluidization pump was not running).

Figure 8.22 shows bubbles on the underside of the bottom Johnson screen during the growth period of a gas retention test. The image taken about 22 hrs after start of bubble growth with about 6.6% retained gas fraction in the column (see Figure 8.15 Test 10-04 Phase 2). There are small individual bubbles that would grow and coalesce into larger bubbles that would reside within the channels formed by the rods supporting the Vee-Wire® (see Figure 1.3). As the channel bubbles grew they would combine to form a partial pancake bubble. Eventually, the pancake bubble would span the entire cross section of the column below the bottom screen. When fluidization flow was started, the pancake bubble completely spanned the column. As liquid was injected below the bottom screen, a portion of the pancake bubble was displaced upwards and openings formed in the pancake bubble for the up-flowing liquid to pass through. Figure 8.23 shows an image of the pancake bubble during fluidization. During fluidization, the openings would expand and contract slightly but stayed in one place. As a result of the pancake bubble, much of the bottom of the column was blocked and liquid only entered in a fraction of the column cross section and resulted in significant maldistribution of liquid fluidizing the sRF.

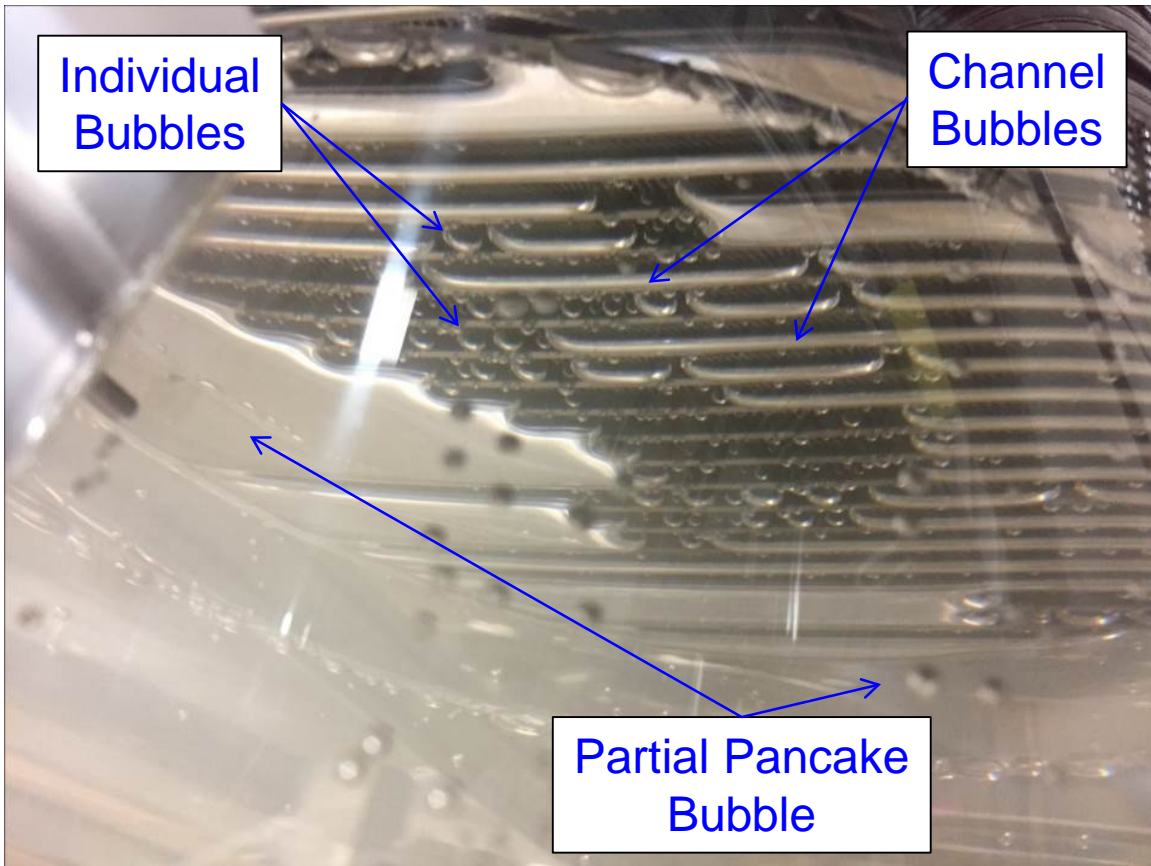


Figure 8.22. Small bubbles, bubbles in channels, and a partial pancake bubble beneath the lower Johnson screen. Image taken about 22 hrs after start of bubble growth with about 6.6% retained gas fraction (see Figure 8.15 Test 10-04 Phase 2).

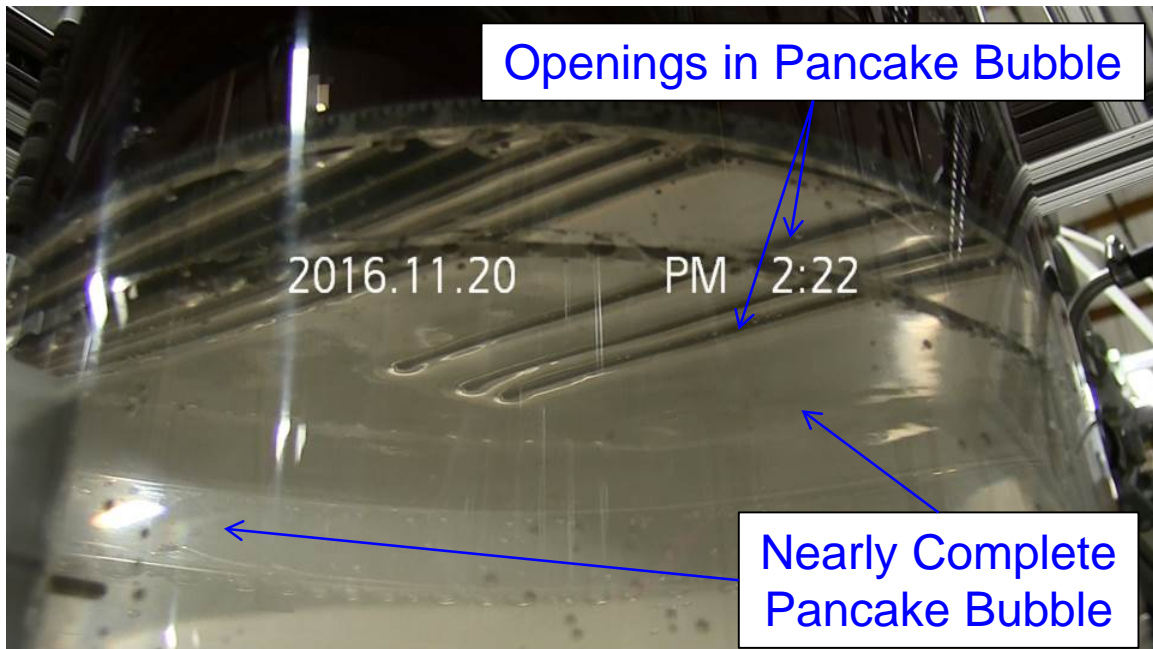


Figure 8.23. Pancake bubble spanning nearly the entire cross section of the column beneath lower Johnson screen. Image taken during fluidization and the openings in the pancake bubble were created by the up flow through the screen.

During fluidization to release retained gas, hitchhiker bubbles when present were observed above the fluidized resin bed. Figure 8.24 shows images of these agglomerates of sRF resin particles attached to gas bubbles. The agglomerates, being a combination of sRF resin particles that are more dense than the liquid and a buoyant gas bubble, can be nearly neutrally buoyant and rise or fall slowly compared to individual bubbles or sRF resin particles. Typically, a hitchhiker bubble would rise slowly, reach the upper gas/liquid surface where the gas bubble would coalesce and release the gas to the headspace, and then the individual sRF resin particles would fall. The hitchhiker bubbles were also pulled towards the upper Johnson screen where liquid was being removed (and re-injected at the bottom of the column). Figure 8.25 shows the collection of hitchhiker bubbles around the upper screen.

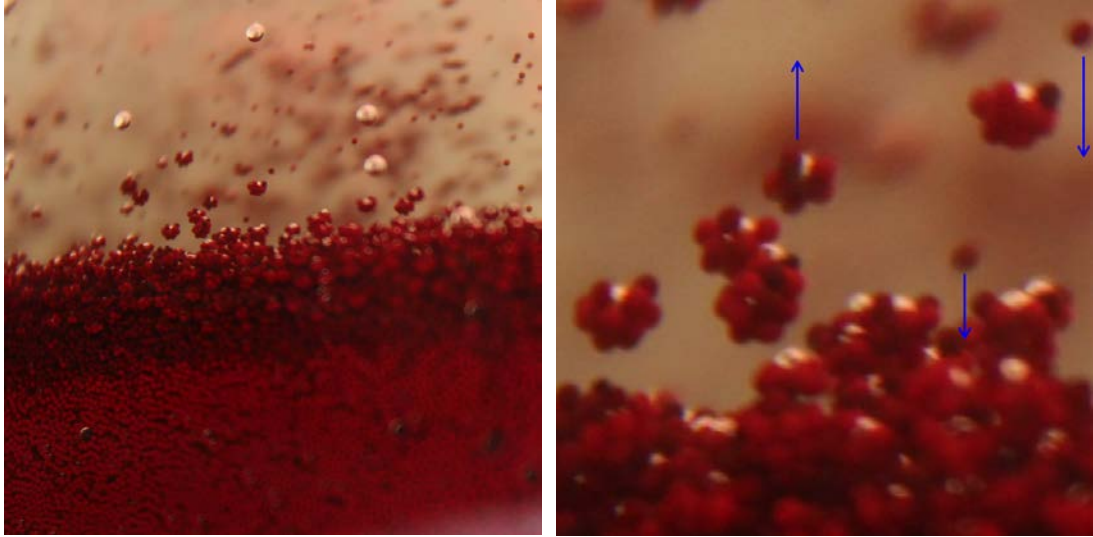


Figure 8.24. Hitchhiker bubbles at the top of the fluidized resin bed (right hand image is expanded view of left hand image). sRF resin particles attached to a bubble would typically rise (upward arrow is an example), reach the upper gas/liquid surface where the gas bubble would coalesce and release the gas to the headspace, then the individual sRF resin particles would fall (downward arrows highlight examples).

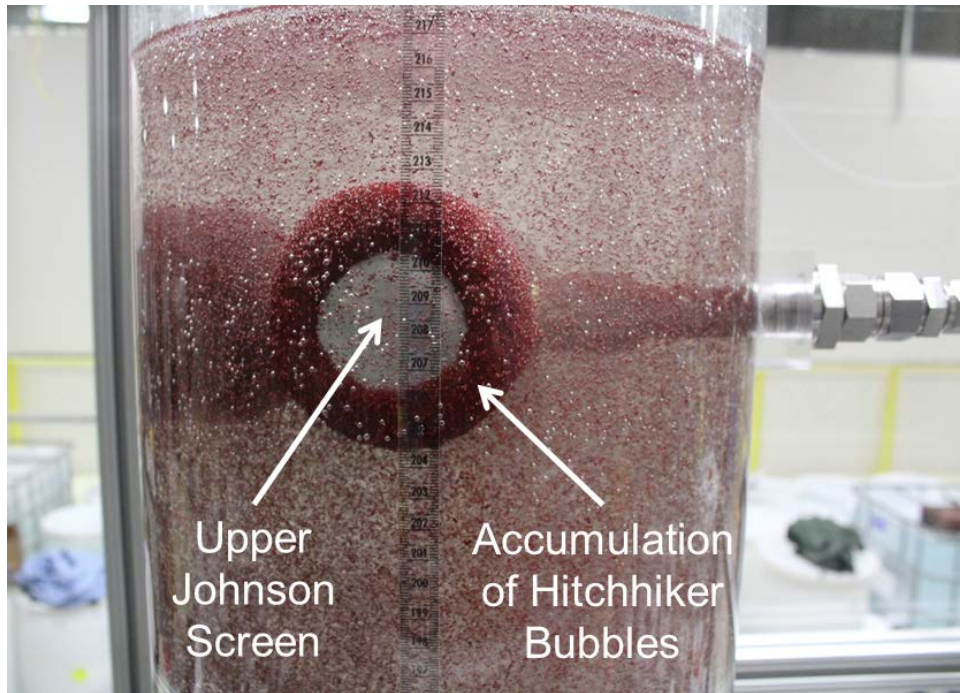


Figure 8.25. Hitchhiker bubbles collecting on the upper Johnson screens during fluidization with withdrawal of liquid through the upper screens.

8.4 Elevated-Temperature Gas Retention

In initially planned elevated-temperature gas retention and fluidization-induced gas release tests,¹ target test conditions included attaining ~50% of the peak retention measured at ambient temperature while holding the resin bed for 12 hours or more at 55 °C before initiating fluidization to release gas. The intent was to investigate the efficacy of fluidization to release gas from a potentially thermally-modified resin bed in an off-normal event scenario. (See Section 5.4 for a discussion of the thermal effects on sRF resin properties determined in bench-scale experiments.) The gas retention target was less than peak retention so that spontaneous releases would not disturb any bed “structure” (e.g., increased particle cohesion and/or shear strength) that might impede fluidization from releasing gas. To this end, a limited number of elevated-temperature bench-scale method development tests were completed to identify liquid simulants and SBH concentration with suitable gas generation kinetics for anticipated fluidization-column tests.

To limit gas generation and SBH consumption while heating from ambient temperature, the fluidization-column heating system was designed with a goal of reaching the 55 °C target in about an hour. Therefore, a first step in preparation for bench-scale GR&R tests was to develop a heating scheme that would be representative of the larger-scale test. The bench-scale system was comprised of a 200-mL jacketed graduated cylinder (the test vessel), a thermostatically-controlled water bath with a built-in pump, and connecting tubing. Preliminary baseline heating experiments were completed using the same volume of settled resin bed (110 mL) and supernatant liquid (50 mL), 160-mL total, as planned GR&R tests. The sRF resin/alkaline water used in pre-testing was a portion of Resin Batch 10-04 that had been prepared for fluidization-column testing (Section 5.2) and no SBH was added so that the system was nominally “gas-free” after stirring and tapping (settling) to release entrained gas. For evaluating heating profiles in the preliminary tests, calibrated type-K thermocouples were placed in the water bath and near the vertical (~55 mL level) and radial center of the resin bed. The following simple procedure gave the desired approximately one-hour heat up of the resin bed to 55 °C: at the start of heating (elapsed time zero), the water bath set-point controller was adjusted to 56 °C (non-calibrated, FIO indicator) and flow was started. Water bath and resin bed temperatures were recorded every half minute initially and every one to two minutes later in the pre-test. Figure 8.26 shows both the water bath and resin bed heating profiles in a preliminary, baseline (non-GR&R) evaluation of the heating method. The figure shows that water bath reached 55.0 °C at ~34 min., whereas the “coldest” region (presumably) of the resin bed got to the target temperature in ~62 min.; both temperatures leveled out a fraction of a degree higher. Figure 8.26 also shows measured water-bath temperatures in elevated-temperature GR&R Tests MD-09 (sRF

¹ The project test plan (TP-LPIST-015 Rev. 1) included scope for elevated-temperature fluidization-only (Section 6.4) and a fluidization-GR&R test (plus a repeat). The objective of the GR&R test was to: determine the quantity and rate of gas release induced by bed fluidization that had been held at 55 °C for at least 12 hours using a Na⁺ form sRF bed in the simulant identified in bench-scale method-development tests. The target retained gas volume prior to fluidization was to be 50% of the peak retention determined at ambient temperature. The fluidization velocity was to start at the minimum velocity that effectively released gas (e.g., >90% release) in ambient temperature testing, after further correcting for temperature effects on fluid properties (e.g., liquid viscosity), and the velocity was to be stepped up, as needed, to effectively release gas at elevated temperature. Additionally, planned scope included demonstrating continual gas release (with continuous gas generation) during fluidization at the selected gas release velocity. Later project decisions resulted in discontinuing the elevated-temperature fluidization-GR&R testing. However, a limited amount of supporting bench-scale method-development testing was completed, as discussed in this section.

resin in 0.3-M NaOH) and MD-10 (with 0.1-M NaOH). The same heating protocol was used in all the tests shown in the figure and, expectedly, the temperature data from the GR&R test are highly consistent with the established baseline water-bath heating profile. For testing simplicity and to minimize potential disturbance of the resin bed, no thermocouple was used in the resin bed in the GR&R tests. Rather, it is presumed that the GR&R test bed temperatures also followed the baseline resin bed heating profile. This assumes that the thermal properties of the 0.1- and 0.3-M NaOH used in the GR&R tests were sufficiently water-like to have minimal impact on the heating characteristics.

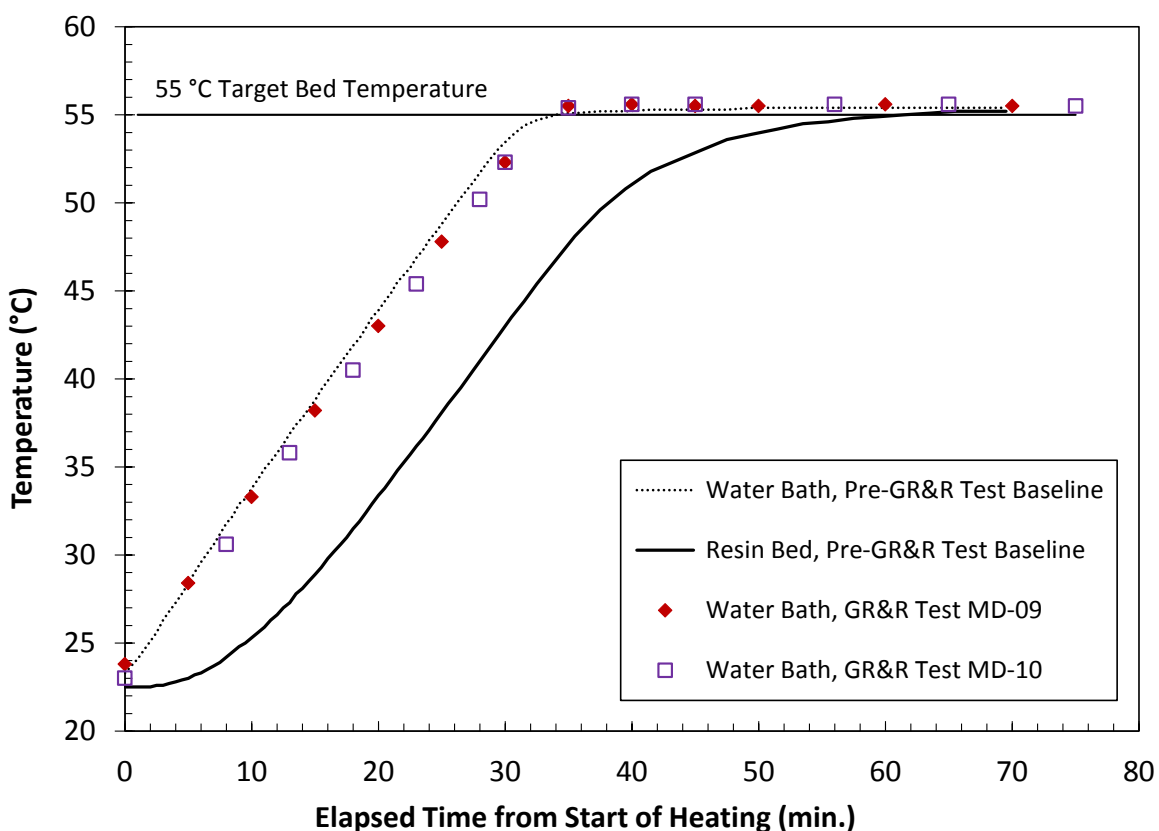


Figure 8.26. Water Bath and *In Situ* Resin Bed Heating Profiles in Jacketed Graduated Cylinder Tests from a Baseline Pre-GR&R Evaluation Compared to the Consistent Measured Water Bath Temperatures in GR&R Tests MD-09 (0.3-M NaOH) and MD-10 (0.1-M NaOH) Using the Same Amounts of Resin and Liquid and Following the Same Heating Protocol.

Resin bed and supernatant liquid (total) volumes were also tracked during the baseline heating profile evaluation test. No change in resin bed level was observed, indicating that the beads did not measurably swell (increase in diameter) at 55 °C (although it cannot be determined whether the sRF resin [polymer] expanded within particles). However, the supernatant liquid level increased to as much as 162 mL, a 2.0 mL change. Figure 8.27 shows the baseline heating profiles (left y-axis; same as Figure 8.26) and the change in total volume (supernatant liquid level) as function of time and temperature (right y-axis). The supernatant liquid volume change, ΔV_L , appears to follow the resin bed temperature profile in the early stages of heating, up to 20 minutes or so, and then transitions to more closely track the water bath temperature profile at about 28 minutes. The correlation of ΔV_L with water bath temperature is especially noticeable in Figure 8.27 starting at ~34 minutes, when the water bath reaches 55 °C (resin bed at 47 °C) and ΔV_L

reaches and levels out at its maximum, 2.0 mL. This is likely explained by the bulk of the liquid and resin bed being closer to the water bath temperature than the “minimum” resin bed temperature at the center of the vessel: natural convection in the supernatant liquid would enhance heat transfer to it and in the upper resin bed, and resin slurry along the cylinder walls would be (nearly) at the wall temperature established by water flowing through the jacket.

Minimally, an approximately 1.2% increase in the volume of liquid in the test vessel is expected because of the decrease in water density from 0.9971 g/mL at an initial temperature of ~22 °C to 0.9857 g/mL at 55 °C ($0.9971/0.9857 = 1.0116$) (CRC 66th ed.). Figure 8.27 shows, for reference, the minimum (~1.0 mL) and maximum (~1.6 mL) estimated liquid volume increase resulting from the change in liquid density, $\Delta\rho_L$ (assuming no change in volume of the sRF resin structure). These values differ in conjunction with the assumption of how much liquid in the resin bed undergoes expansion. In both cases, the 50 mL of supernatant liquid is affected. In the “minimum” case, the interstitial (inter-particle) liquid in the resin bed, at an assumed minimum bed porosity (ϵ_b) of 0.36, also expands (40 mL pore liquid = 0.36×110 mL resin bed). In the “maximum” case, the liquid volume in the complete bed pore structure, including both interstitial and intrastitial void (within resin beads), is considered. As noted in Section 4.1.1, the total porosity within the resin bed can be defined in terms of the dry resin bed and resin bead skeletal densities, $\epsilon_t = 1 - \rho_{db}/\rho_s$, and using nominal density values for Na⁺-form sRF resin from literature (0.37-g/mL ρ_{db} [Na-form mass and volume bases] and 1.62-g/mL ρ_s ; see Section 4.1.1), a total liquid fraction in the resin bed of 0.77 is estimated. This gives a total liquid volume in the bed of 85 mL (= 0.77×110 mL resin bed), which is assumed to expand along with the supernatant liquid and gives the ~1.6-mL maximum estimated ΔV_L . Several other factors may, and likely did, contribute to the observed volume change shown in Figure 8.27 exceeding the maximum expected ΔV_L resulting from $\Delta\rho_L$ alone: 1) existing gas bubbles, if any, would undergo ~11% thermal expansion equivalent to the ratio of final-to-initial absolute temperatures ($328.15\text{ K}/295.15\text{ K} = 1.112$), in accordance with the ideal gas law; 2) assuming that existing or newly-formed gas bubbles are saturated with water vapor, the bubbles will also grow due to increasing water vapor pressure (P_v , equals saturation partial pressure) with increasing temperature; a bubble existing at nominally 1 atm (760 mm Hg) total pressure and 22 °C ($P_v = 19.8$ mm Hg) would increase in volume by 15% at 55 °C ($P_v = 118$ mm Hg) due to water vapor contributions alone (neglecting the direct thermal expansion discussed in factor 1) (CRC 66th ed.);¹ and 3) decreased solubility of non-condensable gas species (e.g., air) in the liquid with increasing temperature could nucleate new bubbles or cause existing bubbles to grow as dissolved gas species come out of solution. Evaporation (and condensation on cooler surfaces elsewhere in the test system) would contribute to decreased liquid levels, but this is not likely a significant factor in the relatively-short duration of heating shown in Figure 8.27.

¹ At each temperature, the mole fraction of non-condensable species (e.g., air) in a bubble, x_{air} , is the ratio of the partial pressure of air, P_{air} , to the total pressure, P_t (assume 1 atm or 760 mm Hg): $x_{air} = n_{air}/n_t = P_{air}/P_t = (P_t - P_v)/P_t$, where P_v is the water vapor partial pressure and n_{air} and n_t are the moles of air and total moles in the bubble, respectively. Rearranging gives the total moles as a function of the moles of air, total pressure, and water vapor pressure, $n_t = n_{air}P_t/(P_t - P_v)$. For constant n_{air} and P_t , the ratio of total moles at two temperatures, T_1 and T_2 , is $n_t(T_2)/n_t(T_1) = [P_t - P_v(T_1)]/[P_t - P_v(T_2)]$. With P_v of 19.8 mm Hg at 22 °C and 118 mm Hg at 55 °C, the ratio of total moles is $n_t(55\text{ °C})/n_t(22\text{ °C}) = 1.153 = (760 - 19.8)\text{ mm Hg}/(760 - 118)\text{ mm Hg}$, indicating 15% more moles in the bubble at the higher temperature. The volume of the bubble would also increase by this 15% due to the higher vapor pressure of water alone, i.e., neglecting direct thermal expansion effects. Thermal expansion equivalent to the ratio of final-to-initial absolute temperatures ($328.15\text{ K}/295.15\text{ K} = 1.112$) would have a compounding effect, giving a total bubble volume increase of 28% (= $[1.153 \times 1.112 - 1]100$).

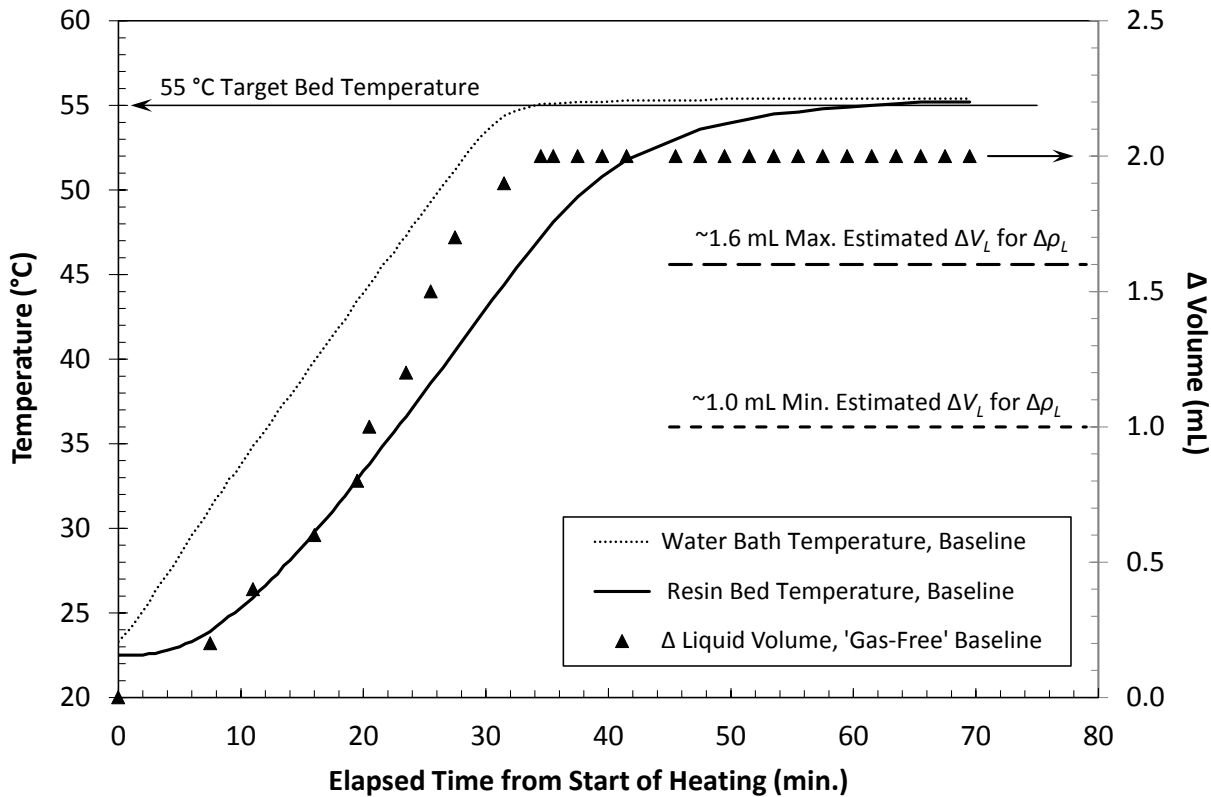


Figure 8.27. Comparison of (Left y-axis) Water Bath and *In Situ* Resin Bed Heating Profiles to (Right y-axis) Change in Total Volume (Supernatant Liquid Level) in a Nominally “Gas-Free” Baseline Pre-GR&R Jacketed Cylinder Test with sRF Resin in Alkaline Water (Initial Volumes: 110 mL Resin Bed and 160 mL Total). The estimated minimum and maximum volume expansion due to decrease in water density at 55 °C are shown for reference.

All the temperature-dependent factors noted in the previous paragraph that (potentially) affect liquid and resin levels in the jacketed graduated cylinder were (presumably) at play in the two elevated-temperature GR&R tests. Because of these not-fully-quantified temperature effects, and others impacting the volume of gas transferred to the collection cylinder, the as-measured volumes give *apparent* “retained gas” and *apparent* “gas generated” quantities. Figure 8.28 and Figure 8.29 show the measured apparent “retained gas” volumes, as determined from the change in the supernatant liquid surface level (total volume), and the apparent “gas generated” volumes for Tests MD-09 (0.3-M NaOH) and MD-10 (0.1-M NaOH), respectively. These are shown as a function of elapsed time from the start of heating. In both tests, the initial gas-free resin bed and total volumes were nominally 110 mL and 160 mL, respectively, and 0.21 g SBH/L resin was added at room temperature. To mimic the anticipated SBH addition and initial (continuous) pre-mixing process in fluidization-column tests (not executed), approximately an hour lag period¹ at room temperature after SBH addition was built-in to the graduated cylinder tests; in this period, the resin/liquid in the cylinder was remixed every 10 minutes for the first 50 minutes to release retained gas, if any. No gas retention was detected in either test in the 10 to 15 minutes between the initial readings of settled bed and supernatant liquid levels and the start of heating.

¹ In Test MD-09, some challenges in starting the heating protocol resulted in an overall ambient-temperature lag period of 76 minutes. This lag duration was then applied intentionally in Test MD-10 for consistency.

Figure 8.28 and Figure 8.29 show that maximum gas retention occurred at 2.2 to 2.5 hours in both Tests MD-09 and MD-10, and the same “peak” measured apparent “retained gas” volumes were present at ~three hours. These results and the measured apparent volumes of “generated gas” are shown as data labels in the plots: 12.5 mL “retained” and 31.0 mL “generated” at 3.0 hours in Test MD-09, and 11 mL “retained” and 30.3 mL “generated” at 3.3 hours in Test MD-10. Without corrections/adjustments for temperature effects, the data suggest that the gas generation rates and retention behavior were similar in the two tests, as they were in their ambient temperature counterparts (0.3-M NaOH in Test MD-05 and 0.1-M NaOH in Test MD-07). See, for example, Figure 8.3 in Section 8.1.1 and Figure 8.13 in Section 8.2.1. In both elevated-temperature tests, the apparent “retained gas” volumes leveled out and held within 0.5 mL of their observed maxima while held at 55 °C; minor fluctuations were due to intermittent small gas releases of individual bubbles (e.g., 0.1 to 0.3 cm) and as a result of (presumed) evaporation and condensate drainage back into the supernatant liquid. The lack of large spontaneous gas releases and/or VSBs suggests that true peak retention (i.e., the most the resin could hold) was not reached before gas production within the resin predominantly stopped, which was a goal in selecting the relatively-low SBH concentration. In ambient temperature tests with the same initial volumes of resin and supernatant liquid, the maximum gas retention in 0.1-M NaOH was 18 mL (without gas release, but slightly above the neutral buoyancy gas fraction; Test MD-07) and in 0.3-M NaOH it was 16 mL at the start of unstable-VSB formation and a large gas release event (Test MD-05). These volumes are greater than the elevated-temperature tests despite thermal effects which tend to enhance the apparent volume of gas generated (and retained) within the resin bed. However, it should be noted that temperature-dependent thermal expansion of retained bubbles and additional bubble growth due to increases in water vapor (partial) pressure legitimately count toward retained gas volume. On the other hand, measured retained gas volumes at elevated temperature are confounded by liquid density changes and losses due to evaporation with external condensation.

As determined from gas collection cylinder measurements and shown in Figure 8.28 and Figure 8.29, gas continued to be generated (apparently) after maximum gas retention was attained, but at a significantly reduced rate. It is probable that some gas was still being generated in the interstitial and/or supernatant liquid and not retained. Apparent gas generation may also be due in part to establishing thermal equilibrium in the headspace of the jacketed graduated cylinder¹ and to ambient temperature fluctuations affecting it and the gas in the collection cylinder. The increasing water vapor (partial) pressure in the headspace of the GR&R test vessel with increasing (average) temperature in it displaced non-condensable gas (e.g., hydrogen) into the gas collection cylinder headspace. The latter was assumed to be at or near room temperature, because the gas/vapor passed through an air-cooled “condenser” (see last footnote) and no condensate was observed in (or plugged) the connecting 0.125-in. O.D. tubing. In other words, even though the gas in both vessels was saturated with water vapor at their respective temperatures, changes in the water vapor content of the headspaces of the vessels could have the appearance of gas generation. A specific example of temperature effects is called out in Figure 8.28. A surprising upturn in apparent “gas generation” at 43 to 46 hours coincides with atypically high measured

¹ The jacketed graduated cylinder plus ball socket joint and glass fittings had a measured total volume of 280 mL up to a ~12-cm long section of 0.25-in. O.D. stainless steel tubing that served as an ambient air-cooled condenser and was connected with a stainless steel fitting to 0.125-in. O.D. plastic tubing that carried gas to the collection cylinder. The measured volume to the top seam of the water jacket was 242 mL, 200 mL of which was graduated, leaving 38 mL (=280 mL - 242 mL) of uninsulated headspace above the “heated zone”. The configuration was prone to thermal gradients, natural convection, and evaporation of water from the heated resin/liquid and condensation on relatively cooler surfaces above.

room temperatures of 27 to 30 °C; outside this isolated period (43 to 47 hours), measured room temperatures were 21 to 25 °C.

Temperature effects on measured volumes are more clearly and definitively demonstrated upon cooling the GR&R test vessels back to (near) room temperature. In Test MD-09 (Figure 8.28), this was done by adjusting the water bath set point to 23.5 °C (FIO) at 46-hours ET. As shown in the figure at ~50-hours, after cooling was complete, the apparent “generated gas” volume had decreased by 24 mL (41.6 mL at 55 °C down to 17.5 mL) and the apparent “retained gas” volume had decreased by 5 mL, from 12 mL to 7 mL. Post-test analyses gave estimated volumes of liquid lost by evaporation and held up by condensation on system glassware above the supernatant liquid and/or and transfer to the gas collection cylinder of 1.0 to 1.5 mL in both elevated-temperature experiments.¹ Using the higher estimate with the 7 mL apparent “retained gas” measured at ambient temperature gives a total corrected estimated volume of retained hydrogen of ~8.5 mL in Test MD-09, which provides a more direct comparison to the maximum retained gas volume in ambient-temperature Test MD-05 (16 mL), as discussed above. Water bath heating was stopped at 20-hours ET in Test MD-10 and the system was allowed to cool naturally to room temperature. Measurements made at ambient temperature at an ET of 117 hours are shown in Figure 8.29 at 25 hours (for convenience). The figure shows similar decreases in the apparent “generated gas” volume (-21 mL, from 38.1 mL at 55 °C down to 16.8 mL) and in the apparent “retained gas” volume (-4 mL, from 10.5 mL at 55 °C down to 6.5 mL) upon cooling.

Regarding corrections to apparent “retained gas” volumes at 55 °C, note that the volume of liquid lost from the resin slurry due to evaporation and external condensation (1 to 1.5 mL) is similar in magnitude to the theoretical volume increase due to decrease in liquid density (1 to 1.6 mL). For the case of sRF resin in alkaline water, the latter is discussed in conjunction with Figure 8.27 above. Similar relative liquid density and volume changes with temperature are expected for the low-concentration NaOH solutions used in the elevated-temperature tests. Assuming that the evaporation and density expansion effects nominally offset one another, the as-measured “retained gas” volumes can more-correctly be considered representative of “retained gas and water vapor” volumes at temperature.

Figure 8.28 and Figure 8.29 also show that the maximum increases in resin bed volumes (e.g., 16 mL shown at 21 hours for Test MD-09, and 13.5 mL shown at 3.3 hours for Test MD-10) exceeded the maximum apparent “retained gas” volumes. This is again consistent with the comparative room-temperature experiments (Tests MD-05 and MD-07) and other graduated cylinder tests in general. As discussed in Section 8.2.1, a resin level increase exceeding the volume of (apparent) retained gas is

¹ Following completion of the two elevated-temperature tests, the amount of condensate held up on the room-temperature glassware and fittings of the GR&R test vessel and/or water vapor lost to the gas collection system was measured and/or estimated. In Test MD-09, by weighing wet and subsequently drying to get a tare weight, 0.76 g of water was found in the glassware and fittings above the jacketed graduated cylinder, and another 0.25 to 0.5 mL was estimated visually to be hung up in the neck of the graduated cylinder. On the low end, this gives a total estimated 1.0 mL of condensate. In Test MD-10, the total volume of liquid lost from the resin/liquid was determined by: carefully disassembling the test vessel to avoid reintroducing condensate and drying the walls of the graduated cylinder above the supernatant liquid with a paper towel; and then, stirring *in situ* to release retained gas and comparing the final supernatant liquid level to the initial room-temperature volume. By this method, 1.5 mL was estimated to have been lost by evaporation and associated condensation during the test, 7.5 mL of residual retained gas was measured, and the resin bed volume decreased by 11 mL to a final settled bed volume that was only 0.5 mL higher than the initial gas-free value. These data support the model that increases in resin bed volume exceeding the retained gas volume were due to changes in the bed pore structure rather than swelling of resin particles.

explained by a change in the pore structure of and net infiltration of liquid into the resin bed. Swelling of the resin particles in the elevated-temperature tests is another possibility, but resin bed expansion was not observed in non-GR&R baseline heating tests (discussed above in this section). Figure 8.28 and Figure 8.29 indicate that while there were 3-mL (Test MD-09) and 1-mL (Test MD-10) decreases in the resin bed levels upon cooling, the change was less than the apparent “retained gas” volume, even considering corrections for evaporation/condensation. Therefore, the relatively-expanded resin bed persisted after cooling.

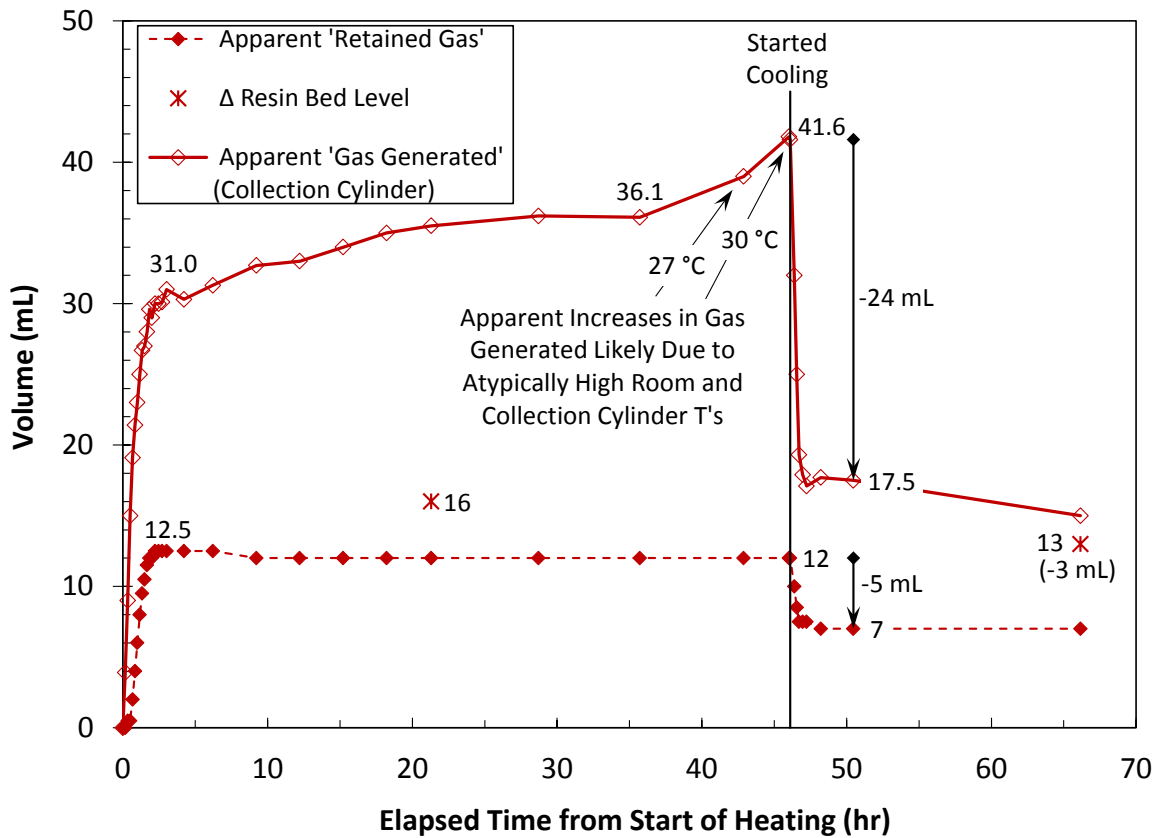


Figure 8.28. Apparent “Retained Gas”, Apparent “Generated Gas”, and Change in Resin Bed Volumes as a Function of Elapsed Time from the Start of Heating to 55 °C for sRF Resin in 0.3-M NaOH (Test MD-09). Cooling was started at 46-hours ET. Volumes are shown adjacent to select key or representative data points. Downward vertical arrows and negative values at ~50-hours and 66-hours ET indicate changes in volume upon cooling.

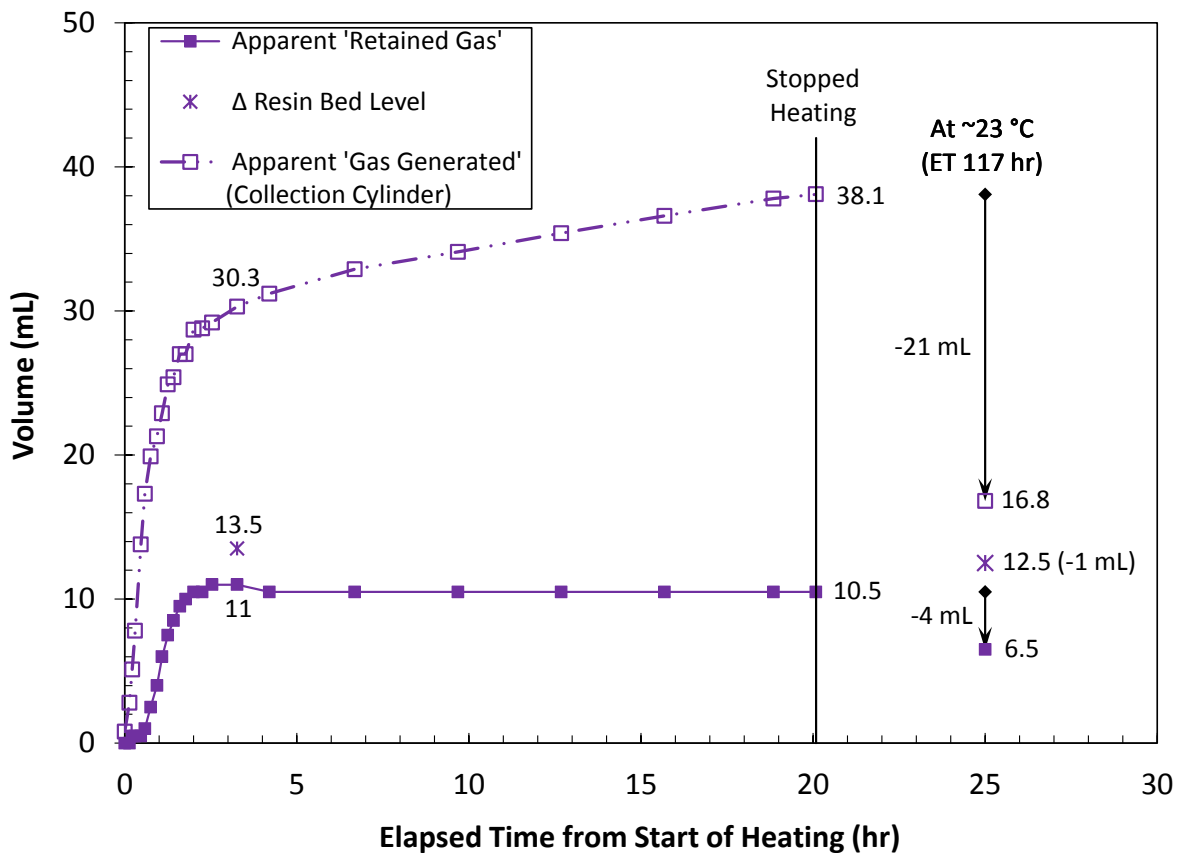


Figure 8.29. Apparent “Retained Gas”, Apparent “Generated Gas”, and Change in Resin Bed Volumes as a Function of Elapsed Time from the Start of Heating to 55 °C for sRF Resin in 0.1-M NaOH (Test MD-10). Water bath heating was stopped at 20-hours ET and the system was allowed to cool naturally to room temperature. Measurements made at ambient temperature at an ET of 117 hours are shown on the plot at 25 hours (for convenience). Volumes are shown adjacent to select key or representative data points. Downward vertical arrows and negative values at 25-hours ET indicate changes in volume upon cooling.

Figure 8.30 provides a comparison of (apparent) retained gas fractions as a function of elapsed time from the start of level measurements for ambient and elevated-temperature tests in 0.1-M NaOH (Tests MD-07 and MD-10) and 0.3-M NaOH (Tests MD-05 and MD-09). From the perspective of planning to conduct a fluidization-column experiment at 55 °C (not completed), the figure provides relevant information on in-bed “gas generation rates” (or, more correctly, “gas retention rates”). Data for room-temperature Tests MD-05 and MD-07 are repeated from Figure 8.13 in Section 8.2.1, which shows available results out to 100-hours ET. Figure 8.30 shows relatively little difference in the (apparent) gas generation and retention behavior for the two NaOH solution simulants at common test temperatures. Rate increases are obviously driven by temperature, as is indicated in the figure using an apparent retained gas fraction of 8 vol% for comparison: in the 55 °C tests, 8 vol% α was reached in 2 hours (between 1.6 and 1.9 hours), which included 10 to 15 minutes at room temperature after initial levels were read and before the start of heating; and in the ambient-temperature tests, the 8 vol% benchmark was reached in 18 to 20 hours. This alone suggests a 10-fold increase in the reaction rate at 55 °C. Also considering that the SBH concentration was 2.5-times higher in the ambient temperature tests (0.5 vs. 0.2 g SBH/L resin), and assuming reaction rates are nominally linear with SBH concentration (Section 8.1.1),

the rate increase at elevated temperature was 25-fold higher overall. As noted above, however, apparent H₂ gas generation rates determined from retention data (assuming 100% retention) in the elevated-temperature tests are likely to be overestimated because of thermal effects, most significantly bubble expansion due directly to temperature changes and increases in water vapor fractions. Finally, the apparent reaction termination after ~3 hours in the 55 °C tests is thought to be due to (near) complete consumption of SBH within the resin bed, as discussed above in this section.

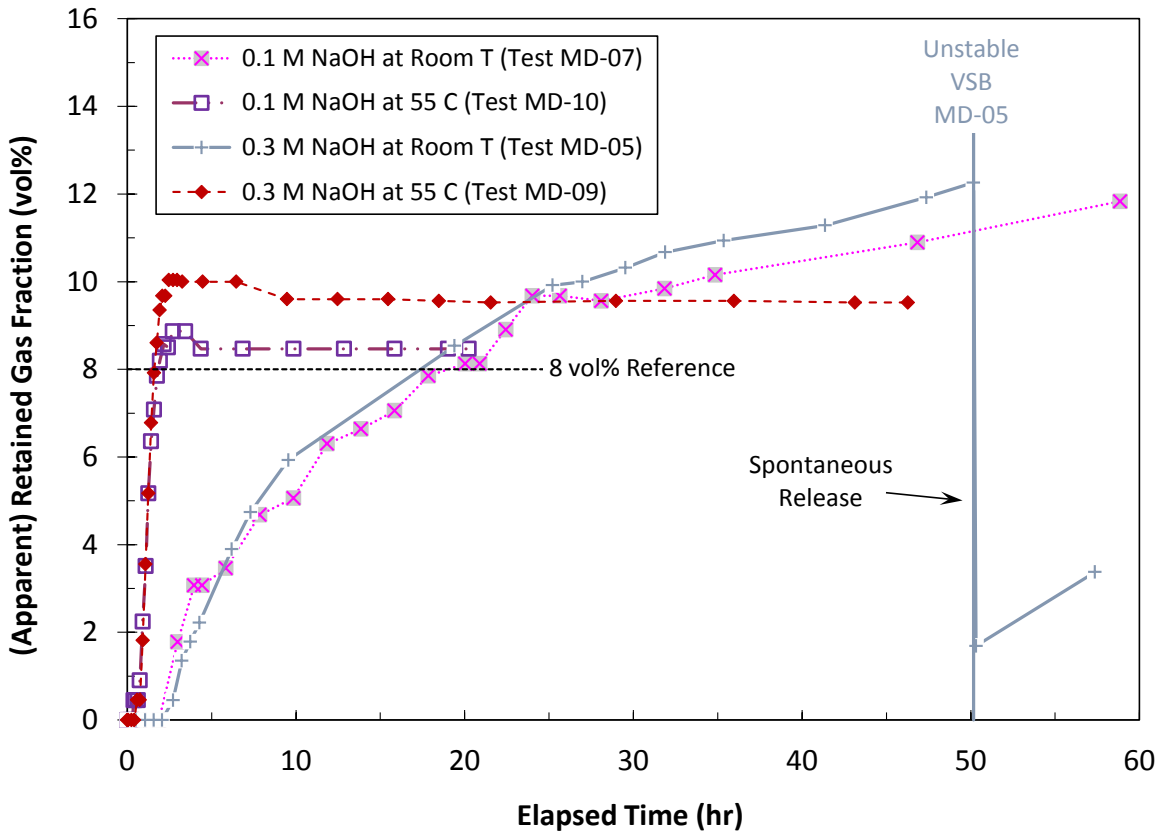


Figure 8.30. Comparison of “Gas Generation Rates” in Tests at Room Temperature and 55 °C Presented in Terms of (Apparent) Retained Gas Fractions as a Function of Elapsed Time from the Start of Level Measurements

8.5 Gas Retention and Spontaneous Release Summary

Peak retention for sRF resin/alkaline water in fluidization-column GR&R tests was 7.8 vol% retained gas, which was well below the theoretical α_{NB} and no large spontaneous gas release was observed. The less-than neutral buoyance peak retention values for alkaline water is likely due to a significant fraction of gas retained in interstitial-liquid-displacing bubbles in the relatively deep resin bed in the fluidization-column (compared to bench-scale tests) and formation of connected gas channels below α_{NB} . With the nominal GR&R LAW simulant in fluidization-column GR&R tests, the peak retention at the point of spontaneous gas release was 7.2 vol%, consistent with the theoretical neutral buoyancy values for the gaseous resin bed to become neutrally buoyant in the supernatant liquid. A large spontaneous release (i.e., not induced by fluidization) to <2 vol% retained gas was observed after reaching the peak.

Five different types of bubbles were observed during testing. These were 1) particle-displacing bubbles (PDBs) in the settled sRF resin bed; 2) interstitial-liquid displacing bubbles (ILDBs) in the settled sRF resin bed; 3) a pancake-shaped bubble that could span the column cross section below the screen supporting the sRF resin; 4) a vessel-spanning bubble (VSB) that formed within the settled sRF bed during fluidization for gas release; and 5) hitchhiker bubbles where sRF particles attached to individual bubbles and moved as aggregates. These bubble types affect gas retention and release in different ways.

9.0 Results: Fluidization-Induced Gas Release

The purpose of fluidization-induced gas release tests was to assess the efficacy of fluidization to release gas as a function of fluidization velocity (flow rate) and the amount of gas retained in the resin bed. As described in this section, this was done with sRF resin/alkaline water and sRF resin/6.1-M Na (GR&R) LAW simulant systems. Section 9.1 summarizes experiments that were conducted to determine the minimum liquid flow rate for effective gas release. The defined minimum effective fluidization velocity and other pre-defined flow rates were applied in multiple tests to release gas from resin beds initially containing a specified fraction of the peak retained gas volume (e.g., ~0.25, ~0.5, or ~0.9). These fractions of peak retention were selected to span the possible range of initial gas, though they are higher than the likely initial retained gas when fluidization would be started for the LAWPS system in a loss of flow accident. In several of these tests, the liquid flow rate used in the initial fluidization-induced gas release was maintained for an extended period of time to demonstrate (assess) continuous release of generated gas while fluidizing. These initial fluidization-induced and continuous gas release tests are discussed in Section 9.2. During the course of testing, an off-normal-event operating strategy option was proposed in which the fluidization pump(s) would operate intermittently (cyclically) rather than continuously. To help evaluate this scenario, a number of on/off cycle tests with gas retention and release were conducted using sRF resin/LAW simulant, and these are addressed in Section 9.3.

Before proceeding, the sequence of fluidization-column GR&R tests and an overview of test conditions are summarized in Table 9.1 for sRF resin/water and in Table 9.2 for sRF resin/LAW simulant. Within each table, the matrix of tests is listed in order of completion, which is often, but not always in order by test “number”. This unique identifier consists of the abbreviated Test ID, 10-0# (short for GRR-10-0#), and the Test Phase under the given Test ID number. Phase numbers increase sequentially in the order they were originally planned, starting from 1. Phase numbers in quotations, e.g., Test 10-04 Phase “5” in Table 9.1, are for opportunistic or otherwise extra phases that were not originally scheduled. Some fluidization-induced gas release phases include #A and #B sub-phases; the pair had the same retained gas fraction target at the start of fluidization, but different flow rate and bed expansion goals. Test Descriptors in the tables also include the test type: gas retention and spontaneous release (spGR&R); fluidization-induced gas release following a retention period (fiGR&R), including on/off cycle tests with LAW simulant; or continuous GR&R (coGR&R), which followed as an extension of fiGR&R phases in some cases. Note that Tests 10-04 Phase 1 and 10-08 Phase 1 were fluidization-only experiments without gas generation, retention, and release and are discussed in Section 7.0. Results for spGR&R test phases are presented in Section 8.2.2.

Table 9.1 and Table 9.2 summarize Fluidization /GR&R (test) Parameters including: a) the nominal (e.g., nearest 5%) growth-period retained gas target (or actual) represented as a fraction of the peak retention measured in a spGR&R test phase, f_a ; b) the resin bed expansion target as a percentage increase from the initial gas-free bed height; and c) the column up-flow liquid flow rate in Lpm and gpm and the corresponding superficial velocity in cm/min. Gas Generation related information from Section 8.1.2 is also summarized in the tables: a) the concentration (kg SBH/L of resin) and mass of freshly added SBH in the three phases per sequence (table) in which it was added (and mixed prior to the gas retention period of the phase); b) the “SBHx.y” post-SBH-addition gas retention period sequence identifiers, where x is the addition number and y is the growth period count following the addition; and c) the “1st day” average volumetric gas generation rate in L/day, determined from cumulative gas collection cylinder

measurements. Finally, Comments in the table provide additional test-specific information such as observations of pancake bubbles below the bottom Johnson screen.

Table 9.1. Sequence and Conditions for Fluidization-Column GR&R Tests Using sRF Resin / Alkaline Water (in Order of Completion)

Test Descriptors ^(a)			Fluidization/GR&R Parameters				Gas Generation			Comments
			Fraction of Peak Gas, f_a (%) ^(b)	Bed Expansion Target(s) (%)	Liquid Flow		SBH Addition		Generation Rate, "1 st Day" ^(e) (L/day)	
ID ^(a)	Phase ^(a)	Type ^(a)			Rate (Lpm) ((gpm))	Velocity (cm/min.)	Conc. (kg/L bed) / Mass (g) ^(c)	Post-Add Retention Sequence ^(d)		
10-04	2	spGR&R	100	N/A	0 (0)	0	1.2 / 79.2	SBH1.1	11.7	Before gas collection system/column headspace configuration change. ^(f) Bottom screen ^(g) near end of phase: 100% P, ~0.5-cm thick.
10-04	3	fiGR&R	> 90	40	5.07 (1.34)	10.0	–	–	–	Before gas collection system/column headspace configuration change. ^(f) Bottom screen ^(g) before fluidization – 100% P (from Test 10-04 Phase 2); and later in phase – 10% O; 90% P (C). VSB observed for ~13 min. (see Section A.1).
10-04	4	spGR&R	100	N/A	0 (0)	0	–	SBH1.2	7.1	Gas collection system/column headspace configuration changed ^(f) .
10-04	"5"	fiGR&R	> 90	40	5.07 (1.34)	10.0	–	–	–	Bottom screen ^(g) ~1 hr after start of fluidization: 20% O; 80% C (likely P)
10-04	"6"	fiGR&R	80	0 to 40	0.4 to 5.07 (0.1 to 1.34)	0.7 to 10.0	–	SBH1.3	2.9	Test purpose included evaluating a new gas/liquid separator added to the flow system. Bottom screen ^(g) before fluidization & after gas release: <5% O; >95% C (likely P).
10-05	3B	fiGR&R	50	40	5.07 (1.34)	10.0	0.8 / 52.8	SBH2.1	4.8	Bottom screen ^(g) before fluidization – 80% O; 20% C w/0% P; and after gas release – 50% O; 50% C (as P).
10-05	4	coGR&R	N/A	40	5.07 (1.34)	10.0	–	–	7.3	Bottom screen ^(g) ~0.5 hr into phase: 10% O; 90% C w/40% P
10-05	1A	fiGR&R	50	0 to 40	0.4 to 5.07 (0.1 to 1.34)	0.7 to 10.0	–	SBH2.2	5.7	Bottom screen ^(g) before initial/restart of fluidization: 85/80% O; 15/20% C w/ 0% P
10-05	1B	fiGR&R	50	3	1.5 (0.4)	3.0	–	SBH2.3	4.6	Bottom screen ^(g) before fluidization: 50% O; 50% C w/0% P
10-05	2	coGR&R	N/A	3	1.5 (0.4)	3.0	–	–	5.2	Bottom screen ^(g) during phase: 10 to 5% O; 90 to 95% C w/ 70 to 80% P. Bottom gas removed later in test to assess effect on fluidization and retention.
10-05	3A	fiGR&R	50	10	2.0 (0.54)	4.0	–	SBH2.4	4.2	Bottom screen ^(g) before fluidization: 40% O; 60% C w/10% P
10-06	1A	fiGR&R	25	3	1.5 (0.4)	3.0	–	SBH2.5	3.3	Bottom screen ^(g) before fluidization: 70% O; 30% C w/0% P
10-06	2	coGR&R	N/A	3	1.5 (0.4)	3.0	–	–	3.9	Bottom screen ^(g) at start of phase – 20% O; 80% C w/40% P; and near end of phase – 5% O; 95% C w/75% P
10-07	1	spGR&R	100	N/A	0 (0)	0	1.2 / 79.2	SBH3.1	13.1 ^(h)	Bottom screen ^(g) at end of phase: 100% P, ≥0.8-cm thick.

Test Descriptors ^(a)			Fluidization/GR&R Parameters				Gas Generation			Comments
			Fraction of Peak Gas, f_a (%) ^(b)	Bed Expansion Target(s) (%)	Liquid Flow		SBH Addition		Generation Rate, "1 st Day" ^(e) (L/day)	
ID ^(a)	Phase ^(a)	Type ^(a)			Rate (Lpm) ((gpm))	Velocity (cm/min.)	Conc. (kg/L bed) / Mass (g) ^(c)	Post-Add Retention Sequence ^(d)		
10-07	2	fiGR&R	> 90	40	5.07 (1.34)	10.0	–	–	–	Bottom screen ^(g) before fluidization – 100% P (from Test 10-07 Phase 1); 2 min. after start of fluidization – 95% O; 5% C w/0% P; and later in phase after gas release – 20% O; 80% C w/60% P
10-06	3A	fiGR&R	90	3	1.5 (0.4)	3.0	–	SBH3.2	9.0	Bottom screen ^(g) before fluidization – 100% P, ~0.7-cm thick; and with the start of fluidization – 15% O; 85% C w/70% P
10-06	4	coGR&R	N/A	3	1.5 (0.4)	3.0	–	–	8.6	Bottom screen ^(h) during phase: <5 to 10% O; >95 to 90% C w/ 90 to 50 % P
10-07	3	fiGR&R	50	3	1.5 (0.4)	3.0	–	SBH3.3	5.9	Bottom screen ^(g) at start of fluidization – 20% O; 80% C w/25% P; and later in phase – 5% O; 95% C w/85% P

“–” – Not measured, not applied, or not applicable; N/A – Not Applicable

(a) – Test Descriptors include test plan and test instruction derived information: i) abbreviated Test ID, 10-0# (full ID GRR-10-0#); ii) the Test Phase number under the Test ID; Phase numbers in quotations, e.g., Test 10-04 Phase “5”, are for opportunistic or otherwise extra phases that were not originally scheduled; and iii) Test Type – i) spGR&R for peak retention and spontaneous gas release; fiGR&R for fluidization-induced gas release, typically including the preceding gas retention (growth) period; and iii) coGR&R for continuous fluidization phases following some fiGR&R phases. It was originally planned to run tests in order by Test ID and Test Phase; the table shows the actual order of test completion, which proved to be more practical / efficient experimentally.

(b) – Nominal (e.g., nearest 5%) retained gas as a fraction of maximum retention measured in spGR&R phases or at the start of fluidization in fiGR&R phases

(c) – Concentration in kg SBH/L of settled resin bed and mass in grams of newly added SBH, neglecting previous additions and possible unreacted residual

(d) – The post-SBH-addition gas retention sequence identifier, “SBHx.y”, indicates the number of the SBH addition, x, and the gas retention (growth) period count following SBH addition, y. For example, “SBH3.2” for fiGR&R Test 10-06 Phase 3A means that it is the second growth period (preceding a fluidization-induced gas release) following the third addition of SBH to the sRF resin / alkaline water contained in the fluidization column throughout the series of tests.

(e) – The apparent gas generation rate determined directly from collection cylinder measurements without correction to a reference pressure (e.g., 1 atm) for the first day (~24 hr) of a longer retention period, for the overall retention period, if less than a day, or for the entire duration of a coGR&R test phase:
 $z.z \text{ L/day} = \text{total collected (L)} / \text{collection period (hr)} \times 24 \text{ hr/day}$.

(f) – In the initial gas collection system configuration, the collection cylinder and fluidization-column headspaces were both under varying vacuum pressure throughout the test (> 0.955 atm absolute). After the configuration change (~25% into Test 10-04 Phase 4), the column headspace was maintained at a slight and nearly constant positive pressure (~1-in. water column or 1.0025 atm) while the collection cylinder continued to operate under varying vacuum. The pre-configuration change data were normalized to the positive pressure to make them directly comparable to later tests and resulted in corrections to the collected gas volumes. See Section 8.1.2 for additional discussion of the configuration change and corrections.

(g) – Visual observations of bubbles below the bottom Johnson screen were made intermittently. Estimates were made of the “open” (O) screen area fraction (%) that was nominally free of bubbles that might impede liquid flow or, alternatively, of the total area fraction blocked or “covered” (C) by all bubble types. The fraction of the screen area that was covered by contiguous “pancake” (P) bubble(s) crossing more than one screen channel was also often estimated. P is a subset of C.

(h) – Gas generation rate data include an interpolated estimate (based on before and after incremental generation rates) for an overnight period in which the 4-L capacity of the collection cylinder was exceeded.

Table 9.2. Sequence and Conditions for Fluidization-Column GR&R Tests Using sRF Resin / 6.1-M Na LAW Simulant (in Order of Completion)

Test Descriptors ^(a)			Fluidization/GR&R Parameters				Gas Generation			Comments
			Fraction of Peak Gas, f_a (%) ^(b)	Bed Expansion Target(s) (%)	Liquid Flow		SBH Addition		Generation Rate, "1 st Day" ^(e) (L/day)	
ID ^(a)	Phase ^(a)	Type ^(a)			Rate (Lpm) ((gpm))	Velocity (cm/min.)	Conc. (kg/L bed) / Mass (g) ^(c)	Post-Add Retention Sequence ^(d)		
10-08	2	spGR&R	100	N/A	0 (0)	0	0.5 / 32.8	SBH1.1	7.8	Bottom screen ^(f) at end of phase: 80% O; 20% C w/0% P
10-09	3B	fiGR&R	50	40	0.24 (0.91)	1.8	–	–	--	Bottom screen ^(f) before fluidization & after gas release: 80% O; 20% C w/0% P
10-08	3	fiGR&R	90	40	0.24 (0.91)	1.8	–	SBH1.2	4.2	Bottom screen ^(f) before fluidization & during and after gas release: 80% O; 20% C w/ 0% P
10-09	1A	fiGR&R	50	0	0.02 & 0.04 (0.08 & 0.15)	0.15 (0.2) & 0.3	–	SBH1.3	2.8	Bottom screen ^(f) before and during fluidization & after gas release: 75% O; 25% C w/ 0% P
10-09	"4"	fiGR&R (cyclic)	80	N/A	1.34 (5.07)	10.0	–	SBH1.4	2.2	Bottom screen ^(f) before fluidization and during & after gas release: 70 to 80% O; 30 to 20% C w/ 0% P
10-09	1B	fiGR&R	50	3	0.070	0.5	0.5 / 32.9	SBH2.1	4.5	Bottom screen ^(f) before fluidization & after gas release: 90% O; 10% C w/0% P
10-09	2	coGR&R	N/A	3	0.070	0.5	–	–	3.5	Bottom screen ^(f) throughout test phase: ~90% O; ~10% C w/0% P
10-09	"5"	fiGR&R (cyclic)	10	N/A	1.34 (5.07)	10.0	–	SBH2.2	4.0	Bottom screen ^(f) before fluidization / after gas release: 90/80% O; 10/20% C w/ 0% P
10-09	3A	fiGR&R	50	10	0.090	0.7	–	SBH2.3	2.2	Bottom screen ^(f) at start of fluidization & after gas release: 80% O; 20% C w/0% P
10-09	"6"	fiGR&R (cyclic)	45	N/A	1.34 (5.07)	10.0	0.5 / 32.7	SBH3.1	2.9	Bottom screen ^(f) before fluidization & after gas release: 80% O; 20% C w/0% P
10-09	"7"	fiGR&R (cyclic)	> 90	N/A	1.34 (5.07)	10.0	–	SBH3.2	--	Bottom screen ^(f) before fluidization, after gas release & later in test: 60 to 75% O; 40 to 25% C all w/ 5% P

“–” – Not measured, not applied, or not applicable; N/A – Not Applicable

(a) – Test Descriptors include test plan and test instruction derived information: i) abbreviated Test ID, 10-0# (full ID GRR-10-0#); ii) the Test Phase number under the Test ID; Phase numbers in quotations, e.g., Test 10-09 Phase “4”, are for opportunistic or otherwise extra phases that were not originally scheduled; and iii) Test Type – i) spGR&R for peak retention and spontaneous gas release; (cyclic) fiGR&R for fluidization-induced gas release, typically including the preceding gas retention (growth) period; and iii) coGR&R for continuous fluidization phases following some fiGR&R phases. It was originally planned to run tests in order by Test ID and Test Phase; the table shows the actual order of test completion, which proved to be more practical / efficient experimentally.

(b) – Nominal (e.g., nearest 5%) retained gas as a fraction of maximum retention measured in spGR&R phases or at the start of fluidization in fiGR&R phases

(c) – Concentration in kg SBH/L of settled resin bed and mass in grams of newly added SBH, neglecting previous additions and possible unreacted residual

(d) – The post-SBH-addition gas retention sequence identifier, “SBHx.y”, indicates the number of the SBH addition, x, and the gas retention (growth) period count following SBH addition, y. For example, “SBH2.3” for fiGR&R Test 10-09 Phase 3A means that it is the third growth period (preceding a fluidization-induced gas release) following the second addition of SBH to the sRF resin / alkaline water contained in the fluidization column throughout the series of tests.

(e) – The apparent gas generation rate determined directly from collection cylinder measurements without correction to a reference pressure for the first day (~24 hr) of a longer retention period, for the overall retention period, if less than a day, or for the entire duration of a coGR&R test phase: $z.z \text{ L/day} = \text{total volume (L)}/\text{collection period (hr)} \times 24 \text{ hr/day}$.

(f) – Visual observations of bubbles below the bottom Johnson screen were made intermittently. Estimates were made of the “open” (O) screen area fraction (%) that was nominally free of bubbles that might impede liquid flow or, alternatively, of the total area fraction blocked or “covered” (C) by all bubble types. The fraction of the screen area that was covered by contiguous “pancake” (P) bubble(s) crossing more than one screen channel was also often estimated. P is a subset of C.

9.1 Determining Minimum Effective Fluidization Velocity

Experiments were conducted to determine the minimum liquid flow rate (Q_{min}) and superficial velocity (v_{min}) for effective fluidization-induced gas release in both the sRF resin/water and sRF resin/GR&R LAW simulant systems. “Effective” was defined as release of gas to less than ten percent of the peak retention, which was 10.1-cm level growth due to gas retention in water and a 9.75 cm in G&RR LAW simulant (Section 8.2.2). Therefore, in both cases, fluidization was considered effective if < 1.0-cm retained gas remained, regardless of the initial retained gas content at the start of fluidization (e.g., 50% or 90% of maximum retention).

To determine Q_{min} with each equilibrated-liquid type, up-flow in the fluidization column was initiated at a flow rate below the incipient (minimum) superficial velocity for fluidization (v_f) identified in fluidization-only experiments (Section 7.1), and resin and liquid levels were monitored for gas release while the flow rate was maintained ~constant for a period of typically 20 min. or more. As needed to effectively release gas, the flow rate was increased in steps, and in some cases, observation of fluidization and gas retention/release behavior was continued to still-higher flow rates. Figure 9.1 shows the results for such an experiment using sRF resin in water and starting with ~50% of peak retained gas (Test 10-05 Phase 1A). The upper plot in the figure shows the retained gas fraction in the form of interstitial-liquid-displacing bubbles (α_{ILD}) for the first ~2.8 hours after the start of fluidization (as discussed in Section 8.2.2, α_{ILD} gives retained gas fraction based on an initial gas-free bed volume and does not change with bed expansion by fluidization unless there a release or change in retained gas volume. In this period, four flow rates were used (0.7, 1.1, 1.5, and 2.2 cm/min. [0.1, 0.15, 0.2, and 0.3 gpm]),¹ the highest of which was previously identified as the incipient fluidization velocity. Both the upper and lower plots of Figure 9.1 show a large and relatively quick gas release starting at 1.8-hours elapsed time and coinciding with the transition from 1.1 to 1.5 cm/min. (0.15 to 0.2 gpm)². The release is characterized by a decrease in α_{ILD} from 4.7 to 0.4 vol% (upper plot) and in fraction of peak retention (f_a) from 60%³ to 5% (lower plot), below the 10%-threshold for effective release. Despite acceptable gas release at a lower velocity, the flow rate that gave ~3% bed expansion in fluidization-only testing (0.4 gpm [3.0 cm/min.]) was selected to ensure a more robust v_{min} for off-normal-event operations.⁴

¹ The pump was stopped and restarted a number of times at the two lowest flow rates because of issues with pump stability (e.g., due to entrained gas and cavitation). The “off” periods are not shown in Figure 9.1. Stoppages were not needed at flow rates of 0.2 gpm and higher, possibly due to increased awareness of signs indicating that removal of gas from the gas/liquid separator was needed.

² Test notes indicate that the flow rate had drifted up briefly from the 0.15 gpm target to 0.2 gpm ~four minutes before the official switch to 0.2 gpm shown in Figure 9.1. It is accurate to state that the gas release occurred during the transition in flow rates, but claiming release while at 0.15 gpm (1.1 cm/min.) is not.

³ The retained gas had increased from an initial f_a of 52% (50% target) to 60% at the time of the release. This does not invalidate the finding that gas release occurred at $v < v_f$. Additionally, other experiments, shown later in this section (9.0), were conducted using v_{min} and other flow rates with initial retained gas closer to 50% f_a .

⁴ WRPS staff including a Nuclear Safety representative (J. M. Grigsby) was consulted on the decision to use the flow rate for ~3% bed expansion as the absolute minimum for fluidization-induced gas release in off-normal-events. Still-higher flow rates would have been selected for Q_{min} if later testing under various initial conditions (e.g., retained gas fractions) had shown one was needed to effectively release gas.

The lower plot of Figure 9.1 includes higher flow rates later in the test than the upper plot and also indicates measured resin bed expansion throughout the test. Negative bed expansion, suggesting settling to a more compact packing structure, was observed immediately after the gas release and while flowing at 1.5 cm/min. This may be related to the gas release, but it is also consistent with observations in fluidization-only testing for some flow rates below and near v_f . Figure 9.1 also shows a reference line at 3% resin bed expansion for the expected steady-state response at the v_{min} flow rate. In the test shown, a maximum 2.2% BE at 3.0 cm/min. was found at 3.0-hours ET. Attainment of bed expansion targets in GR&R tests and factors affecting it are discussed further in Section 9.2 below.

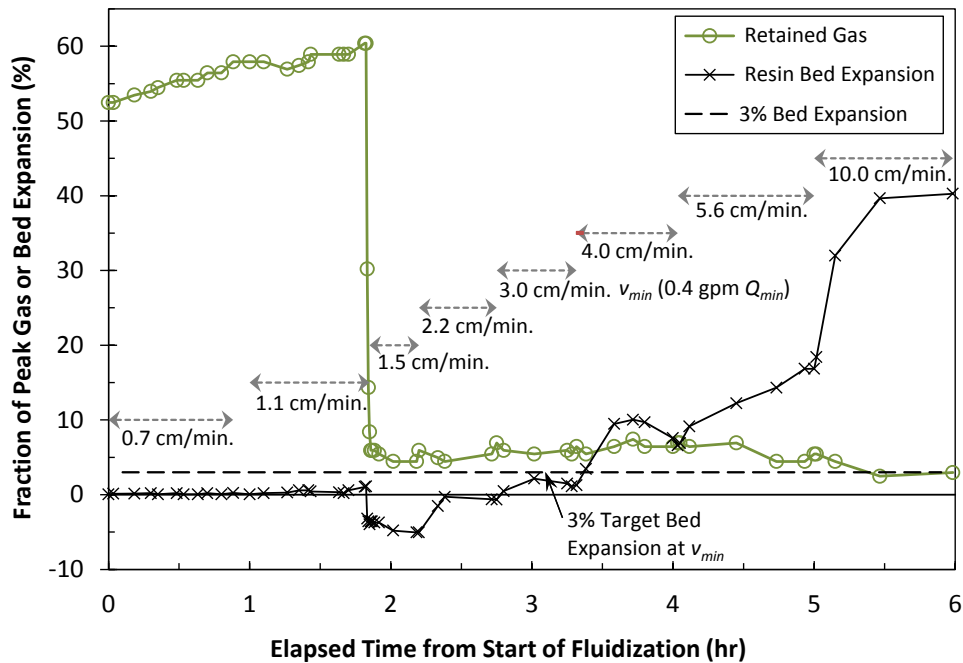
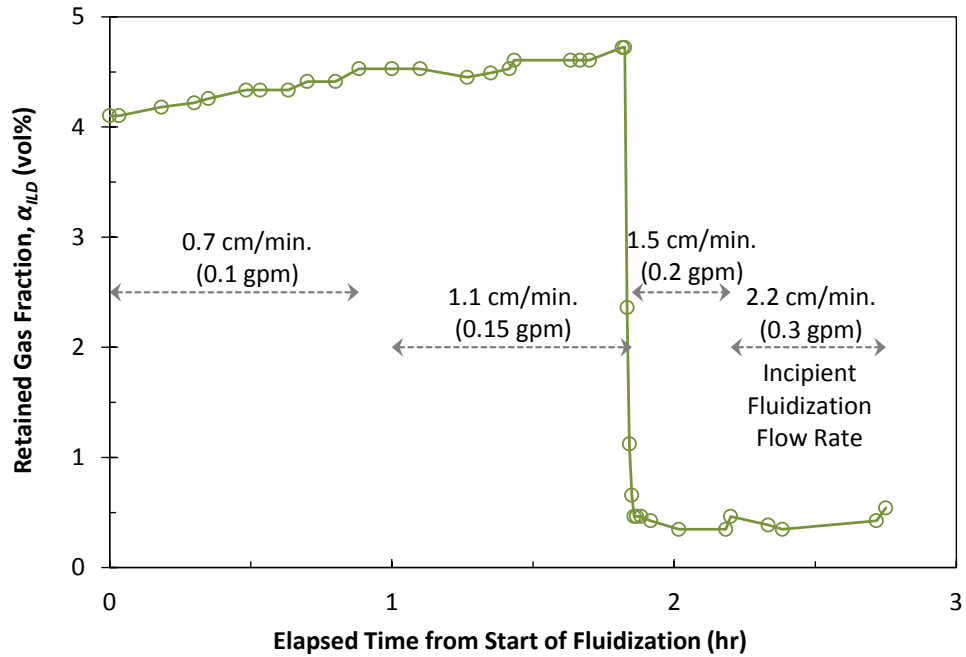


Figure 9.1. Effective Fluidization-Induced Gas Release from sRF Resin in Water with ~50% of Peak (Initial) Retained Gas at Flow Rates Starting Below that for Incipient Fluidization determined in fluidization only tests (2.2 cm/min. at 0.3 gpm, see Table 7.1) shown by: Upper – Retained Gas Fraction as a Function of Time and Fluid Velocity (flow rate); and Lower – Retained Gas as a Fraction of Peak and Resin Bed Expansion vs. Time and Fluid Velocity in Test 10-05 Phase 1A. The defined minimum effective fluidization velocity for gas release (3.0 cm/min. at 0.4 gpm for 3% bed expansion, see Table 7.1 and footnote 4 in Section 9.1 above) and target 3% bed expansion at that flow rate are identified in the lower plot.

Figure 9.2 shows an evaluation of the minimum flow rate for effective gas release from sRF resin in GR&R LAW simulant with initial retained gas of ~50% of maximum retention. As with the previous figure, y-values in the upper plot are retained gas fraction as α_{ILD} , and in the lower plot they are fraction of peak retention and bed expansion, both as percentages. Also similar to the sRF resin/water system discussed above, Figure 9.2 shows that gas release from sRF resin/LAW simulant occurred at a flow rate (0.04 gpm [0.3 cm/min.]) below that for incipient fluidization determined in fluidization-only testing (0.44 cm/min. [0.059 gpm] , see Table 7.1). Essentially all the gas was released over a period of ~25 minutes starting at ~34-min. ET with 4.0-vol% α_{ILD} and 53% f_a at that time. Note that the gas release from sRF resin in LAW simulant was somewhat slower than that it was from resin in water, which occurred over 12 minutes or so (~0.2 hours, Figure 9.1). It is also worth noting that up to 2.7% resin bed expansion was observed with flow rates below v_f , as shown in the lower plot of Figure 9.2. Resin bed expansion appeared to increase steadily after flow was initiated at 0.02 gpm (0.15 cm/min.), reach a maximum shortly before the gas release started, and decrease to the near-zero initial value after most of the gas was released and the bed resettled. This phenomenon is likely due to a combination of upward movement of gas within the bed before release with bubble expansion under reduced hydrostatic load and associated disturbance of the bed packing structure. Because the bed expansion returned to zero after the release, it is not thought to be a direct-fluidization effect in the sense of gas-free fluidization-only testing. Similar to fluidization release in alkaline waster shown in Figure 9.1, acceptable gas release occurred at a velocity below incipient fluidization, and a selecting a flow rate that gives ~3% bed expansion is a robust v_{min} for off-normal-event operations.

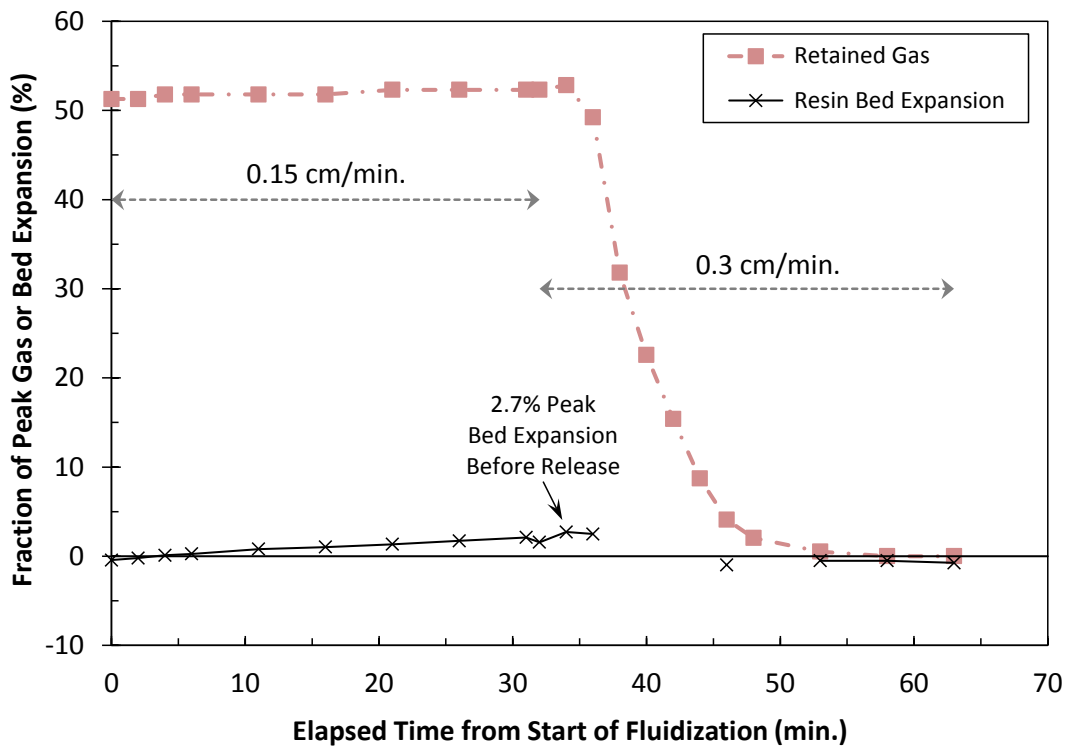
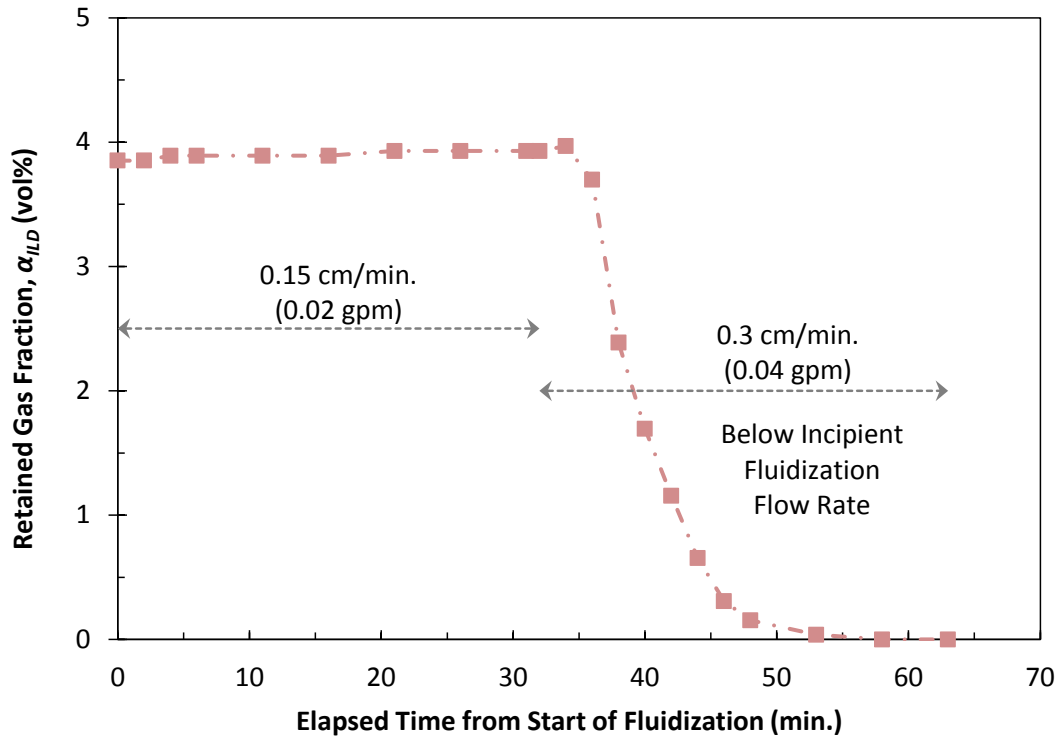


Figure 9.2. Effective Fluidization-Induced Gas Release from sRF Resin in 6.1-M Na Simulant with ~50% of Peak (Initial) Retained Gas at Velocities (0.15 cm/min. and 0.3 cm/min.) Below that for Incipient Fluidization, shown by: Upper – Retained Gas Fraction as a Function of Time and Fluid Velocity (flow rate); and Lower – Retained Gas as a Fraction of Peak and Resin Bed Expansion vs. Time and Fluid Velocity in Test 10-09 Phase 1A.

9.2 Gas Release with Varying Initial Gas Fraction and Fluidization Velocity

The defined minimum effective fluidization velocity and other pre-defined flow rates were applied in multiple fluidization-induced gas release tests with sRF resin in both alkaline water and GR&R LAW simulants. The retained gas content at the start of fluidization was also varied, giving a matrix of fiGR&R tests with v (Q) and f_a being the adjustable parameters. These initial fluidization-induced gas releases are discussed in Section 9.2.2. Several of these fiGR&R test phases were continued at the same flow rate for multiple hours to evaluate continuous release of generated gas while fluidizing. These coGR&R test phases are discussed in Section 9.2.3. First, a brief overview of the characteristics of a representative test is given in Section 9.2.1.

9.2.1 Characteristics of a Typical Test

Figure 9.3 provides representative results for a coupled fiGR&R and coGR&R test series in sRF resin / alkaline water (Test 10-05 Phases 1B and 2). The upper plot shows the measured retained gas fractions in the form of interstitial-liquid-displacing bubbles throughout the experiment. It includes the third quiescent gas retention period following the second SBH addition (0.8 g SBH/L resin) to the resin/water in the fluidization-column, i.e., identifier SBH2.3. The gas generation and gas retention characteristics of this growth period were previously compared to other tests in Sections 8.1.2 and 8.2.2, respectively. In the case shown in Figure 9.3, the growth period was, as typical, part of the fiGR&R test phase (Test 10-05 Phase 1B). Alternatively, in test sequences in which a fluidization-induced gas release followed a peak gas retention experiment, the growth period was generally part of the spGR&R test phase, provided it satisfied the retained gas fraction target of the succeeding fiGR&R phase.

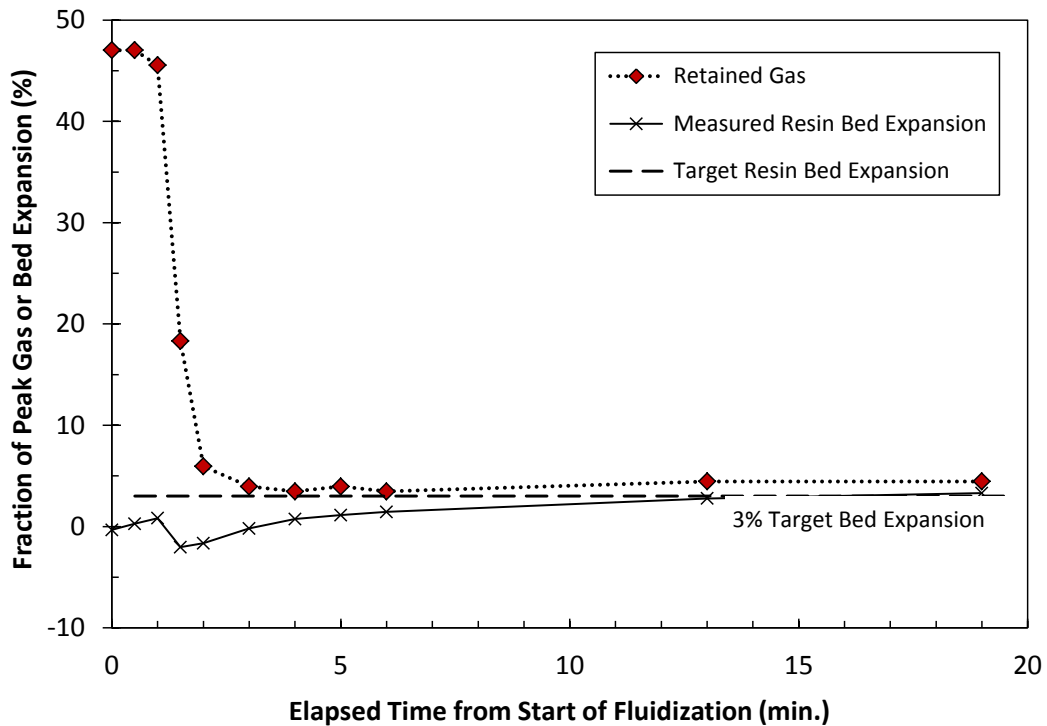
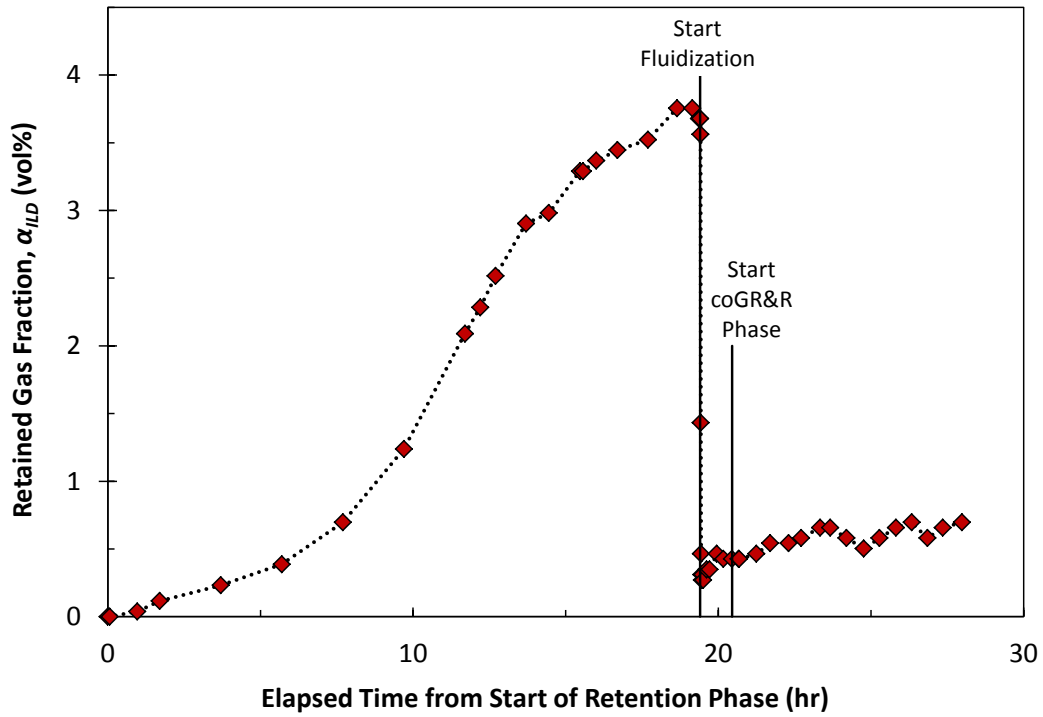


Figure 9.3. Quiescent Growth to ~50% of Peak Retained Gas in sRF Resin / Water and Fluidization-Induced Gas Release at the Established Minimum Effective Flow Rate for Gas Release (3.0 cm/min. [0.4 gpm], 3% Bed Expansion Target): Upper – Retained Gas Fraction in the Growth and the Initial and Continuous Fluidization-Induced Gas Release Phases; and Lower – Early Stages of the fiGR&R Period Shown in Terms of Fraction of Peak Retention and Resin Bed Expansion (Test 10-05 Phases 1B and 2).

In the experiment shown in Figure 9.3, the target retained gas fraction of ~50% of maximum (f_a) was reached at 19.4-hours elapsed time from the start of gas retention, and fluidization to release gas was initiated at that point, as indicated in the upper plot. Unlike the Q_{min} evaluation tests in Section 9.1, a single target fluidization velocity was used in the fiGR&R and coGR&R tests discussed in this section (9.2). The defined minimum-effective fluidization velocity of 3.0 cm/min. (0.4 gpm) was used as the single flow rate in the test discussed here. The target flow was typically established in less than a minute, and often within ~20 seconds.¹ Provided gas was appreciably released, a typical fiGR&R phase was run for about one hour. However, in many of the tests discussed in Section 9.2.2, only results for the more limited active release period are plotted. This is true in the lower plot in Figure 9.3, which shows details during the first ~20 minutes of the initial fluidization-induced gas release. Retained gas is plotted in terms of f_a along with bed expansion as a percentage increase from the initial gas-free bed depth. The plot includes a reference line for the expected 3% bed expansion for the flow rate used. Gas was released from 47 to 4% of the peak retained gas volume over about four minutes and held nearly constant in the period shown, and the bed had expanded to the expected (target) by 13-min. ET. An extension of the lower plot in Figure 9.3 including the coGR&R phase is presented in Section 9.2.3. The data in the lower plot and other fiGR&R test results are alternatively shown in terms of retained gas fraction (α_{ILD}) in Section 9.2.2 without bed expansion information.

Figure 9.3 (upper plot) indicates that a transition from the fiGR&R phase to the coGR&R phase (Test 10-05 Phase 2) occurred without a break at 20.4-hours ET. The continuous gas generation, retention, and release phase was run for 7.5-hour in this test. Typical of other coGR&R tests discussed in Section 9.2.3, the test shown in Figure 9.3 was terminated based on criteria for the lack of evidence of continually increasing gas retention and generation of sufficient gas that level growth in the fluidization-column would have been appreciable (e.g., 3 cm) if all generated gas had been retained.

9.2.2 Initial Fluidization-Induced Gas Release

Results for the matrices of initial fluidization-induced gas release tests in alkaline water and GR&R LAW simulant are discussed in this section in three groups. First, the retained gas fraction target is constant and the fluidization velocity is varied. In the second, the flow rate is fixed at that for 40% bed expansion and the initial retained gas fraction is adjusted. Finally, use of the minimum effective fluidization flow rate with varying initial retained gas content is shown for sRF resin in alkaline water (only). Many of the data sets fit in more than one of these categories and are repeated.

The peak gas retention values measured in spontaneous gas release tests and discussed in Section 8.2.2 are particularly relevant to this section: in alkaline water, 100% f_a corresponds to a supernatant liquid level increase of 10.1 cm, a retained gas fraction α based on measured bed depth of 7.8 vol%, and a retained gas fraction α_{ILD} assuming interstitial-liquid-displacing bubbles and constant resin bed depth (also) of 7.8 vol%; for sRF resin in GR&R LAW simulant, these are 9.75 cm, 7.2 vol%, and 7.5 vol%,

¹ This was true except for a few early tests with sRF resin in alkaline water. In this learning period, pump cavitation issues often prevented reaching the target flow rate quickly and reliably. Remedies included addition of a gas-liquid separator near the pump(s) and changing the gas collection system configuration so that the fluidization column headspace was under slight positive pressure instead of partial vacuum (Section 6.4).

respectively. The use of α_{ILD} to represent retained gas fraction in fluidization-GR&R tests instead of α or α_{PD} is addressed in Section 6.5 and Section 8.2.2. While α_{ILD} is used to characterize changes in retained gas fraction in this section, initial retained gas content at the start of fluidization is based on a target f_α value (not α), which is linearly related to liquid level growth (Eq. (6.12)): ΔH_L at the target, relative to the initial gas-free liquid level, is the product of f_α and $\Delta H_{L,max}$.

Released gas in the fluidization-GR&R tests discussed below was typically observed as a combination of small individual round bubbles ranging upward from <0.1 cm, such as seen in pictures of hitchhiker bubbles in Section 8.3, and larger coalesced entities that appeared as mushroom-cap bubbles of 10-cm or greater diameter when rising through the supernatant liquid layer. The larger bubbles tended to occur intermittently in burps whereas smaller bubbles were more often seen in steady streams. Many larger-appearing bubble releases were more visually impressive than they were volumetrically significant, although others were large in both regards.

Figure 9.4 shows fluidization-induced gas releases from sRF Resin in alkaline water at flow rates for 3%, 10%, and 40% resin bed expansion targets, which were $v_3 = v_{min} = 3.0$ cm/min. (Test 10-05 Phase 1B and repeat Test 10-07 Phase 3), $v_{10} = 4.0$ cm/min. (Test 10-05 Phase 3A), and $v_{40} = 10.0$ cm/min. (Test 10-05 Phase 3B), respectively. In each test, the initial retained gas was ~50% of peak retention with α_{ILD} ranging from 3.6 to 3.9 vol%. In all the tests, the plot shows that, gas released to < 1 vol% within 2 minutes from the start of fluidization and a minimum 0.2 to 0.4 vol% α_{ILD} was attained by 5 minutes elapsed time and held steady to the end of the 15-min. ET depicted. The repeatability demonstrated at the lowest (minimum-effective) flow rate of 3.0 cm/min. for 3% bed expansion solidified its selection. Except for a dip in α_{ILD} at 2- to 4-min. ET with the highest flow rate, the curves in Figure 9.4 are almost indistinguishable. The cause of the “overshoot” in Test 10-05 Phase 3B is not well understood, although it might simply be experimental uncertainty in part due to surface motion during the gas release – the dip is equivalent to 0.2-cm difference in liquid level. As summarized in Table 9.1 in Section 9.0, gas bubbles beneath the bottom Johnson screen were observed to cover an estimated 50 to 80 % of the area at the start of fluidization in three of the four tests, but was somewhat more open (80%, 20% covered) in Test 10-05 3B. Apparently, however, this amount of gas beneath the screen, and variability in it, did not have an overly-significant impact on the ability to release retained gas from the resin bed.

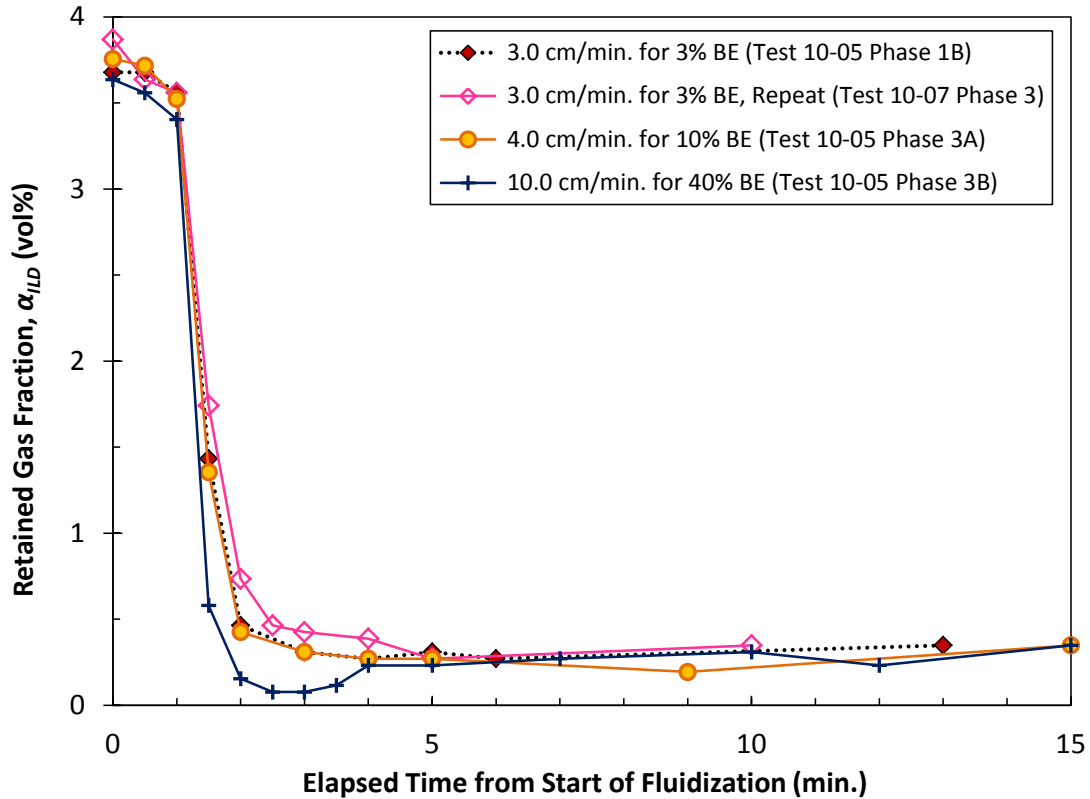


Figure 9.4. Retained Gas Fractions During Fluidization-Induced Gas Releases from sRF Resin in Alkaline Water at Flow Rates for 3%, 10%, and 40% Resin Bed Expansion Targets ($v_3 = v_{min} = 3.0$ cm/min., $v_{10} = 4.0$ cm/min., and $v_{40} = 10.0$ cm/min., respectively) with an Initial Gas Fraction of $\sim 50\%$ of Peak Retention (Test 10-05 Phases 1B, 3A, and 3B and Test 10-07 Phase 3). Repeatability is demonstrated at the lowest (minimum effective) flow rate.

Figure 9.5 shows comparable information to Figure 9.4, but for tests with sRF resin in GR&R LAW simulant. The primary suite of tests again used flow rates for 3%, 10%, and 40% resin bed expansion targets, which in this simulant were $v_3 = v_{min} = 0.5$ cm/min. (Test 10-09 Phase 1B), $v_{10} = 0.7$ cm/min. (Test 10-09 Phase 3A), and $v_{40} = 1.8$ cm/min. (Test 10-09 Phase 3B), respectively. In these three tests, the initial retained gas was $f_a \sim 50\%$ of peak retention and α_{ILD} was 3.8 vol%. Figure 9.5 shows that each the three core flow rates was effective at releasing essentially all gas in 20 to 25 minutes, although differences are seen in the time to the start of gas release. At a velocity of 1.8 cm/min., some gas release was evident between 2- and 4-min. ET, but initial gas release was delayed by 6 to 8 minutes at 0.5 and 0.7 cm/min., respectively. The general trend of more rapid initial gas release with significantly higher flow rate is not surprising. The flow-rate dependence may be more of a factor with the GR&R LAW simulant than for alkaline water, because the transient for bed expansion (and resin settling, Section 7.3) is considerably longer for the relatively-high viscosity and smaller resin particle-liquid density difference in the GR&R LAW simulant. Despite a long transient time, the resin bed would reach an absolute bed expansion sooner at higher flow rate and might facilitate earlier in-bed release and upward migration of gas bubbles. The overall tendency for near-total gas release in alkaline water being 4- to 5-times faster than in GR&R LAW simulant (e.g., ~ 5 min. vs. 20 to 25 min.) is most likely related to the differences in transient time constants. More directly, the measured viscosity of the GR&R LAW simulant being $\sim 4\times$

greater than alkaline water (3.9 cP vs. 1.04 cP at 20 °C; Table 5.1 in Section 5.3.1) would slow the rise of equally-sized gas bubbles even without hindrance by resin particles..

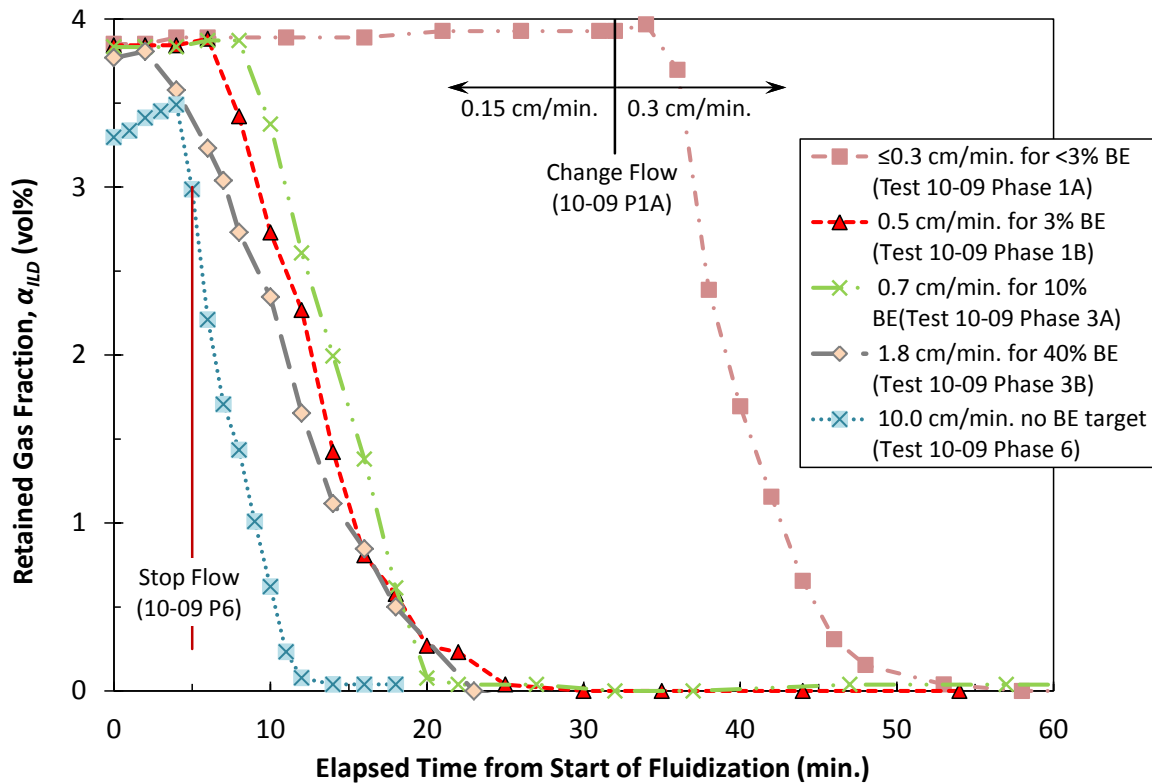


Figure 9.5. Retained Gas Fractions During Fluidization-Induced Gas Releases from sRF Resin in GR&R LAW Simulant at Flow Rates for <3%, 3%, 10%, 40%, and >40% Resin Bed Expansion Targets ($v \leq 0.3$ cm/min., $v_3 = v_{min} = 0.5$ cm/min., $v_{10} = 0.7$ cm/min., $v_{40} = 1.8$ cm/min., and $v = 10.0$ cm/min. [1.34 gpm], respectively) with an Initial Gas Fraction of ~50% of Peak Retention (Test 10-09 Phases 1A, 1B, 3A, 3B, and 6). Times of flow stoppage in on:off cycle Test 10-09 Phase 6 and a step-change in flow rate for Test 10-09 Phase 1A are shown.

Figure 9.5 also compares results of a test at lower flow rates (0.15 and 0.3 cm/min. in Test 10-09 Phase 1A) and another at much higher velocity (10.0 cm/min. in Test 10-09 Phase 6). The low-velocity test data are reproduced from Figure 9.2 in Section 9.1, in which the minimum effective fluidization flow rate was determined. As noted in the earlier discussion, 0.3 cm/min. was below the incipient fluidization velocity. Perhaps coincidentally, the ~20 to 25-min. duration from the time that the flow rate was changed from 0.15 to 0.3 cm/min. (ET 32 min.) to complete gas release at between 53- and 58-min. ET is consistent with the results for flow rates between 0.5 and 1.8 cm/min. The higher flow rate data in Figure 9.5 come from the start of a cyclic fluidization-GR&R test that is discussed further in Section 9.3. It is comparable here because the initial amount of retained gas (44% f_a and 3.3 vol% α_{ILD}) was similar to, although slightly lower than, the others shown in the figure. The cycle test was conducted with the pump on for 5 min. at 10.0 cm/min. (1.34 gpm) followed by an off period of 55 min. Figure 9.5 gives the appearance that the retained gas fraction steadily increased to 3.5 vol% in the first four minutes of the on period, but this is almost certainly attributable to gas expansion associated with rapid bed expansion, upward bulk motion of the “still-retained” gas, and reduced hydrostatic load. Evidence of gas release was measured at 5-min. ET, coinciding with stopping the pump. Gas release continued with the pump off and

while resin settled, and all gas was released in about 15 minutes, 5 or more minutes sooner than with the other flow rates.

Gas release from sRF resin in alkaline water with different fluidization velocities was also investigated with constant initial retained gas content of $\sim 90\% f_a$. Figure 9.6 shows the results for flow rates of 3.0 cm/min. ($v_3 = v_{min}$; Test 10-06 Phase 3A) and 10.0 cm/min. (v_{40} ; Test 10-07 Phase 2), and initial retained gas fractions (α_{ILD}) of 6.6⁽¹⁾ and 7.5 vol%, respectively. In both cases, the gas release was nominally linear over about 4 minutes and nearly complete, reaching minimum retained gas fractions of 0.2 to 0.4 vol%. The end states of the gas releases are very similar to those shown in Figure 9.4 for $\sim 50\% f_a$ initial, as is the overall time frame for release, e.g. $\leq \sim 5$ minutes. However, the releases with the lower initial gas fractions were somewhat more precipitous at around 2-min. elapsed time. The effect of initial gas content on gas release at constant fluidization velocity is compared directly in the figures that follow in this section.

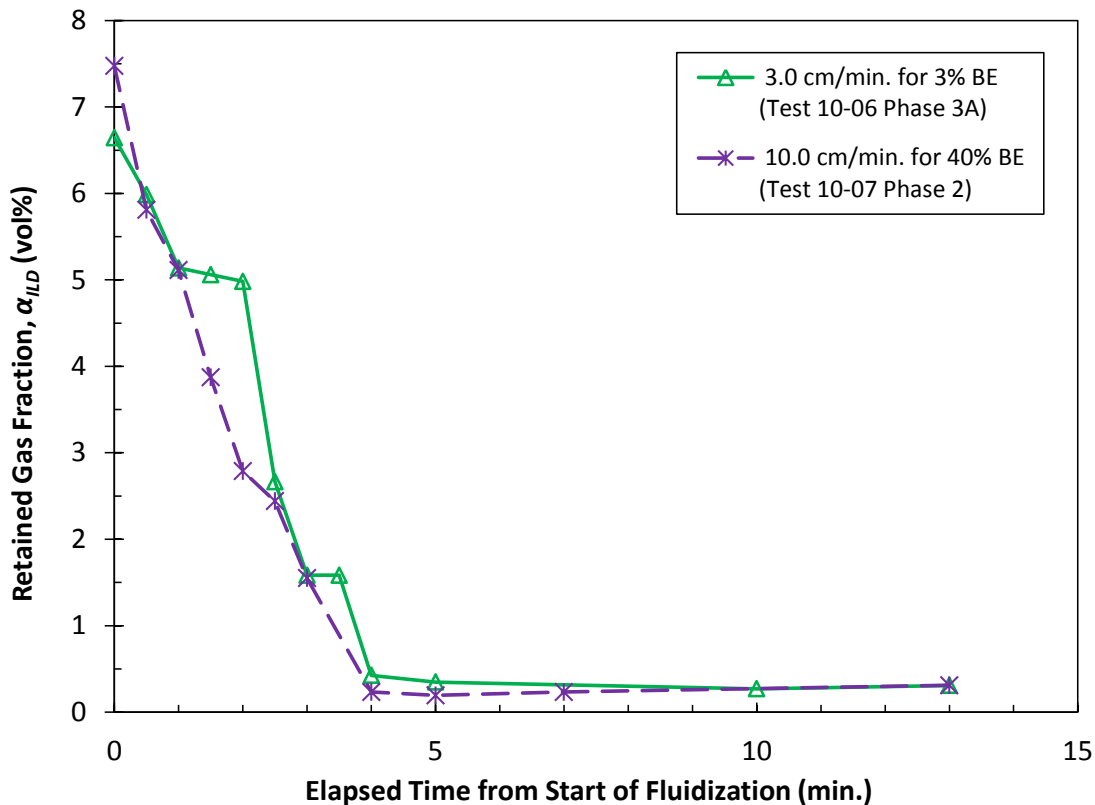


Figure 9.6. Retained Gas Fractions During Fluidization-Induced Gas Releases from sRF Resin in Alkaline Water at Flow Rates for 3% and 40% Resin Bed Expansion Targets ($v_3 = v_{min} = 3.0$ cm/min. and $v_{40} = 10.0$ cm/min.) with an Initial Gas Fraction of $\sim 90\%$ of Peak Retention (Tests 10-06 Phase 3A and 10-07 Phase 2).

¹ After a ~ 40 -hr gas retention period and a decision was made to proceed with the induced release test, a small spontaneous gas release about 10 minutes before the start of fluidization reduced f_a from 87% to 85% and α_{ILD} from 6.8 to 6.6 vol%. Despite the reduction, this is considered to qualify in the grouping of tests having approximately 90% f_a .

Figure 9.7 provides a first head-to-head example of the impact of retained gas fraction on fluidization-induced gas release at a set velocity. For the sRF resin/alkaline water system shown in the upper plot, the velocity was 10.0 cm/min. for a target 40% bed expansion, and the initial retained gas volumes were ~50% and ~90% of peak retention in Tests 10-05 Phase 3B and 10-07 Phase 2, respectively. These data sets are reproduced from Figure 9.4 and Figure 9.6, in order. As noted in the previous paragraph, gas release in the test with higher initial retained gas fraction is approximately linear in time for ~four minutes starting from time zero. While there was a one-minute lag to the start of appreciable gas release in the test with a lower initial gas fraction, the release was essentially complete in the second minute. The apparent trend of somewhat faster near-total release with decreasing initial retained gas fraction in sRF resin/alkaline water is discussed further with Figure 9.8 below.

The lower plot of Figure 9.7 shows fluidization-induced gas releases using v_{40} for sRF resin in GR&R LAW simulant (1.8 cm/min), again with initial f_a values of ~50% and ~90%. Results in the plot for an initial retained gas volume of 50% of peak retention (Test 10-09 Phase 3B) are reproduced from Figure 9.5. New data are shown in Figure 9.7 (lower) for a test with an initial retained gas fraction (α_{ILD}) of 6.5 vol% and a ~90% of peak retention target (Test 10-08 Phase 3). The release data with the higher initial gas content indicate a 6-min. period with no apparent gas release, and in fact, there is a slight increase in α_{ILD} to 6.6 vol%, which may be due to gas expansion with a net upward movement. This behavior is more consistent with the results for velocities of 0.5 cm/min. (v_{min}) and 0.7 cm/min. (v_{10}) with ~50% f_a shown in Figure 9.5 than it is for v_{40} and ~90% f_a plotted in both Figure 9.7 and the earlier figure. It showed only a 2-min. delay before providing evidence of release at 4 minutes and was followed by a smooth, steady decay in α_{ILD} to complete release at 23-min. ET. Although there was a delay in the 1.8-cm/min., ~90% f_a test, it released its gas at higher rate and reached < 0.1-vol% α_{ILD} by 18 min. The steeper release trajectory might be explained by gathering / coalescing of gas in the delay period followed by release of relatively-larger bubbles with higher rise velocity.

Figure 9.8 shows a another example of initial retained gas fraction effects on gas release, this time using the defined minimum fluidization velocity for effective gas release, 3.0 cm/min. Two of the three sets of alkaline water test data in the figure are again reproduced from Figure 9.4 (Test 10-05 Phase 1B, ~50% f_a) and Figure 9.6 (Test 10-06 Phase 3A, ~90% f_a). New data are shown in Figure 9.8 for a test with an initial retained gas fraction (α_{ILD}) of 2.2 vol% corresponding to a nominal 25% of peak retention target (28% actual, Test 10-06 Phase 1A). Like the 50% f_a comparison test, appreciable gas release was delayed by about a minute for the lower initial retained gas fraction; however, in the latter test, the bulk of the gas was released in the half-minute ending at 1.5-min. ET. Overall, Figure 9.8 indicates a trend of increasing release period (to near-complete release) with increasing initial retained gas fraction: ~1.5 to 2 minutes with ~25% f_a initial; 2 to 3 minutes with ~50% f_a ; and 4 to 5 minutes with ~90% f_a . Neglecting the slightly delayed (non-linear) start with initial f_a of ~50% or less, the observed trend is consistent (not inconsistent) with a simple model of constant volumetric release rate, in which a longer time is required to release a larger retained gas volume. In any case, the 3.0-cm/min. v_{min} selected for use with sRF resin in alkaline water appears to be effective at releasing gas regardless of the initial retained gas fraction at the start of fluidization-induced gas release. Nonetheless, the release duration was about 4 to 5 times longer in GR&R LAW simulant than in alkaline water at comparable f_a and v_{40} , which is similar to the characteristics in the different liquids with f_a of ~50% and varying fluidization velocity shown in Figure 9.4 and Figure 9.5. Again, this is likely due primarily to differences in fluid properties (e.g., viscosity) and associated transient response.

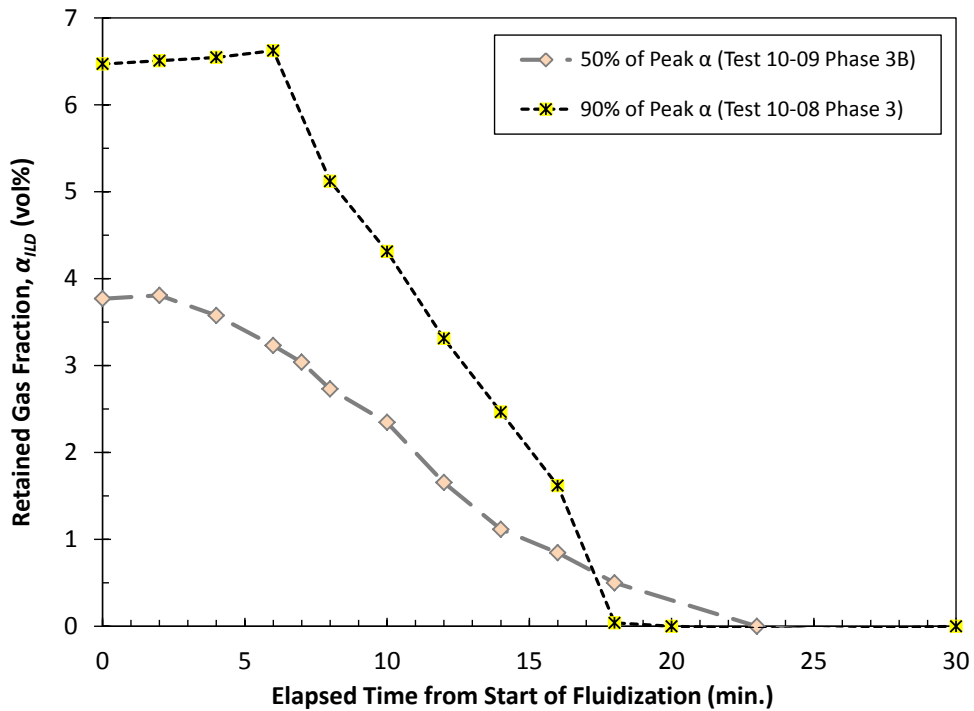
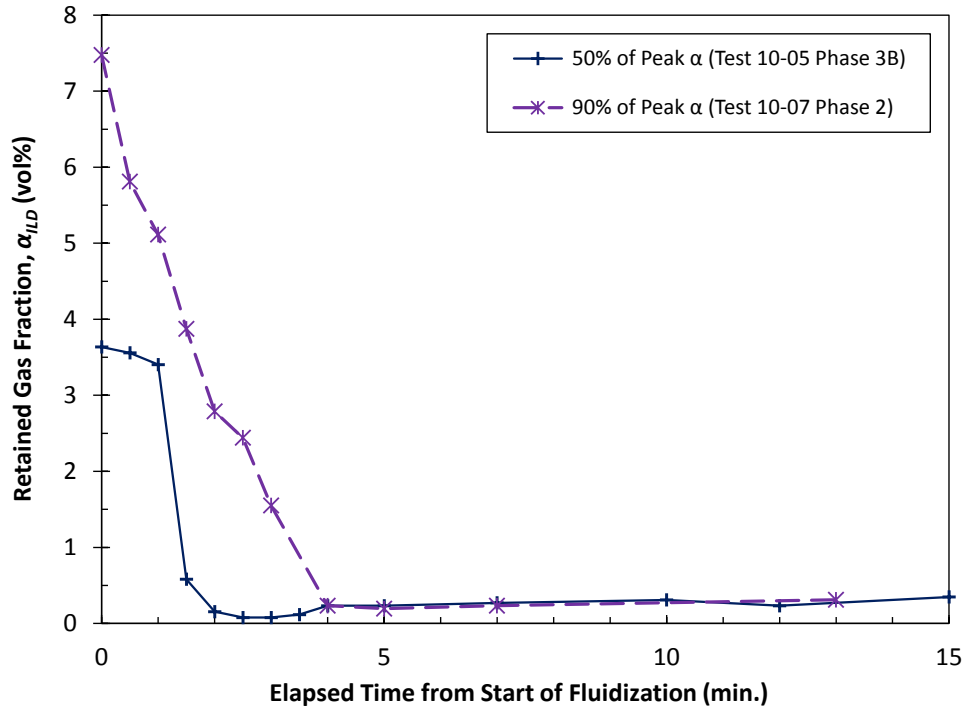


Figure 9.7. Retained Gas Fractions During Fluidization-Induced Gas Releases from sRF Resin in Alkaline Water (upper plot) in GR&R LAW Simulant (lower plot) with Initial Gas Fractions of ~50% and ~90% of Peak Retention at the Flow Rate for 40% Resin Bed Expansion ($v_{40} = 10.0$ cm/min. in water [Tests 10-05 Phase 3B and 10-07 Phase 2] and 1.8 cm/min. in simulant [Tests 10-08 Phase 3 and 10-09 Phase 3B]).

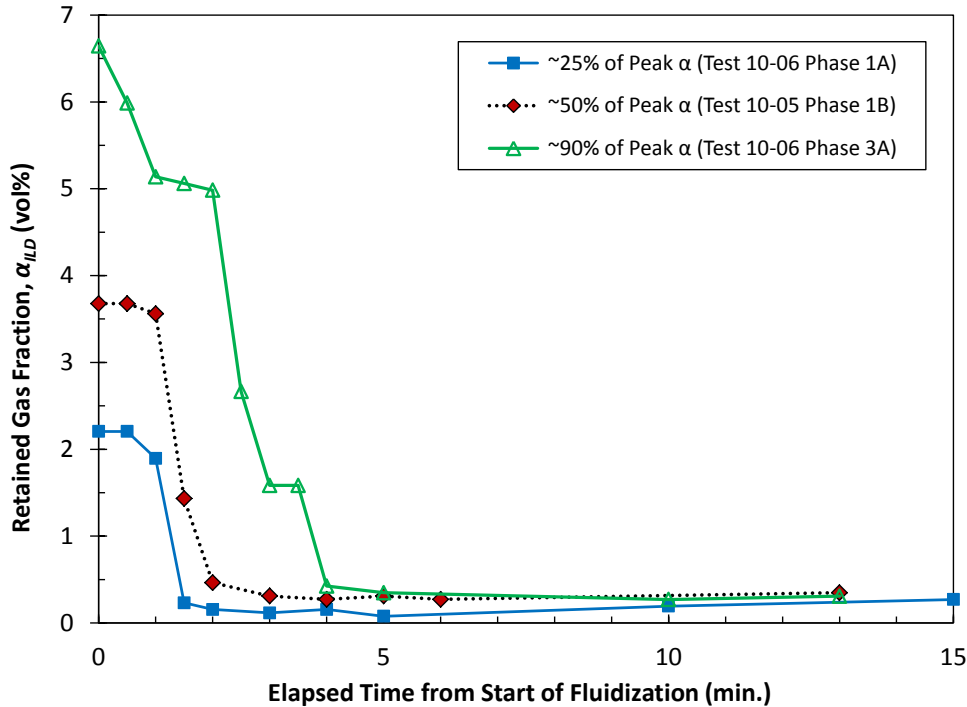


Figure 9.8. Retained Gas Fractions During Fluidization-Induced Gas Releases from sRF Resin in Alkaline Water with Varying Initial Gas Fractions (f_a of ~25%, ~50%, and ~90%) at the Identified Minimum Effective Flow Rate for Gas Release and 3% Resin Bed Expansion ($v_3 = v_{min} = 3.0$ cm/min. [Tests 10-05 Phase 1B and 10-06 Phases 1A and 3A]).

9.2.3 Continuous Fluidization and Gas Release

Four of the fiGR&R tests in alkaline water and one in GR&R (6.1 M Na) LAW simulant discussed in the previous section were extended as continuous gas generation, retention, and release (coGR&R) test phases that are presented in this section. Because of the coupling of fiGR&R and coGR&R tests, Test IDs in this section often include the test phase numbers for both parts. In the alkaline water tests, the initial retained gas fraction (in the preceding fiGR&R test phase) and the fluidization velocity were varied. In addition to continuous gas release, resin bed expansion during coGR&R test phases is shown for representative cases. Gas generation rate data for all the coGR&R tests are compared to a 1-L/day reference, which, when scaled volumetrically, represents a generation rate greater than the bounding limit expected in a full-scale ion exchange column (see Section 6.4).

Each coGR&R test was run for an extended period of time (e.g., multiple hours) to assess the retained gas fraction under steady-state (constant) liquid flow conditions, α_{ss} . Minimally, the tests were continued until the volume of gas generated (collected) was sufficient that the supernatant liquid level growth (ΔH_L) would have been 3 cm if all the generated gas was retained in the resin bed. Considering that maximum retention in both alkaline water and GR&R simulant was ~10 cm, 3-cm increase in level would correspond to a fraction of peak retention (f_a) of ~30%. This is a factor of three higher than the criterion for effective gas release, which was defined as release of $\geq 90\%$ of the peak retained gas or $f_a \leq 10\%$. With maximum measured retained gas fractions of less than 8 vol% in both liquids, effective release was also characterized by post-release α_{ILD} (and α) of < 1 vol%.

Figure 9.9 shows the coGR&R test results for alkaline water at the minimum velocity for effective gas release ($v_{min} = 3.0$ cm/min.) and an initial retained gas volume of ~50% of peak (Test 10-05 Phases 1B and 2). The lower plot includes and is a continuation of the fiGR&R test data shown in Figure 9.3 (lower) and discussed in Section 9.2.1. Figure 9.9 (lower) shows fraction of peak retention (on a compressed scale to highlight the results in the coGR&R test phase) and resin bed expansion (percent increase) throughout the test period; elapsed time is from the start of fluidization in the fiGR&R phase. After reaching a minimum retained gas volume of ~4% f_a during the initial gas release, f_a climbed to as high as 9% in the ~7.5-hr coGR&R phase. The plot also shows that resin bed expansion reached the expected 3% increase shortly after the initial gas release, and may have been aided by it, but then dropped and held relatively steady at below zero BE. A bed expansion < 0 means that the bed was more compact than the initial gas-free state; this was also observed in fluidization-only tests (without GR&R) at some flow rates less than the incipient fluidization velocity (Section 7.1). The low bed expansion and increased gas retention after initial gas release are both indicators of significant maldistribution of flow in the resin bed, which is attributed here to the presence of gas bubbles retained below the bottom Johnson screen. As noted in Table 9.1 at the beginning of Section 9.0, the bottom screen was 50% open with no pancake bubble at the start of fluidization, but was 90 to 95% blocked with 70 to 80% being pancake bubble during the coGR&R phase. The impact of the screen coverage is shown in Figure 9.9 at an elapsed time of 9.3 hours. At the end of the coGR&R test phase, a majority of the pancake bubble and other blocking gas was removed by applying vacuum through a 1/8-in. tube that was snaked below and moved around the bottom screen while liquid flow was maintained at 3.0 cm/min. in the column. After returning liquid that was incidentally removed in the process, retained gas and bed expansion were re-evaluated: the lower plot shows that bed expansion returned to the expected 3% and retained gas dropped to zero. The latter is likely due to a combination of the volume of pancake bubble / bottom gas removed and release of additional gas from the resin bed in regions that had been relatively stagnant with the flow maldistribution.

The upper plot of Figure 9.9 shows retained gas in terms of supernatant liquid level growth (ΔH_L) relative to the initial gas-free state. The plot includes data for the expected ΔH_L if all generated gas, as determined by gas collection cylinder measurements, was retained. This represents a potential level increase of 3.2 cm during the coGR&R test phase and a maximum ΔH_L of 3.7 cm relative to a gas-free condition, considering the initial 0.5-cm equivalent gas volume retained at the start of the phase. The plot clearly indicates that only a small fraction of the generated gas was retained, despite the poor flow distribution noted in the previous paragraph.

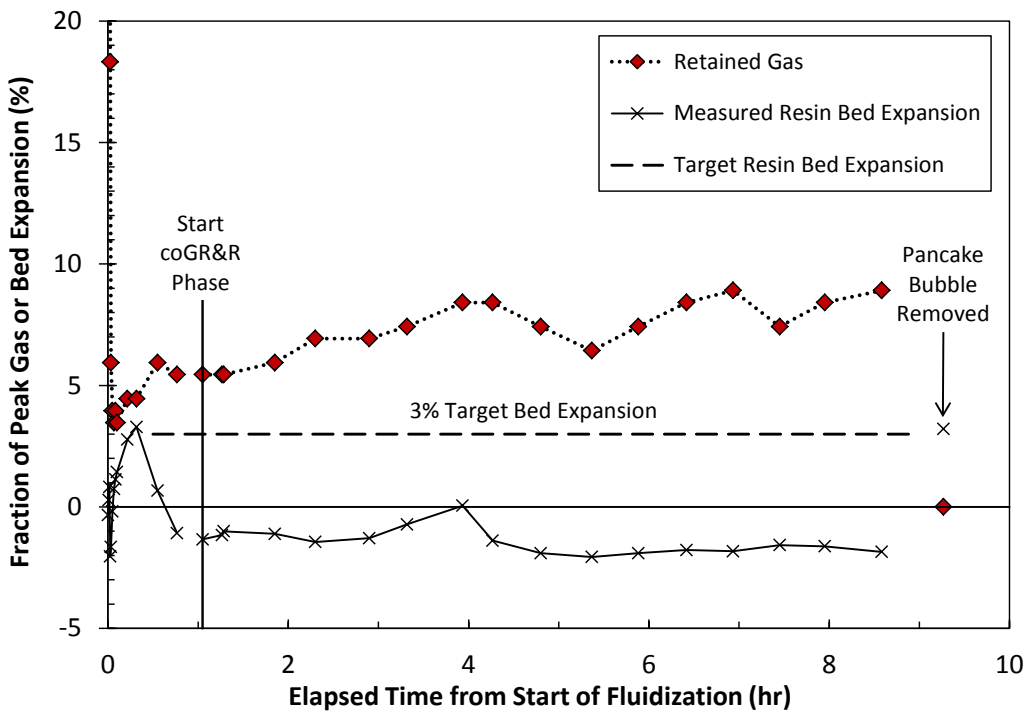
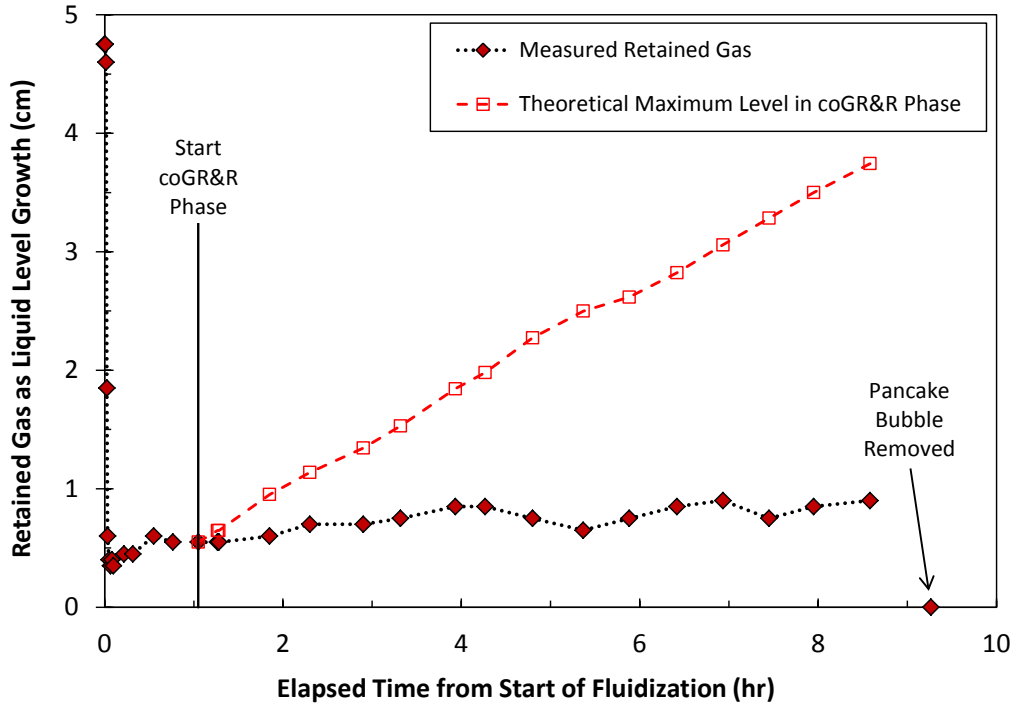


Figure 9.9. Continuous Gas Release Following an Initial Fluidization-Induced Release Phase at v_{min} (3.0 cm/min.) for sRF Resin in Alkaline Water: Upper – Measured Retained Gas Fraction and Theoretical Gas Fraction if All Generated Gas was Retained, Shown as Liquid Level Increase from Gas-Free; Lower – Fraction of Peak Retention and Resin Bed Expansion Throughout the fiGR&R and coGR&R Phases (y-axis compressed to show detail). Plots show the effects of removing the pancake bubble at the end of the experiment (Test 10-05 Phases 1B and 2).

Using the same metrics as the previous figure, Figure 9.10 gives results of the combined fiGR&R and coGR&R test phases for sRF resin in alkaline water with an initial f_a of ~50% and the fluidization flow rate for 40% bed expansion, $v_{40} = 10.0$ cm/min. (Test 10-05 Phases 3B and 4). The lower plot shows that bed expansion ranged from ~35 to 39% in the coGR&R phase, with some fluctuations correlated to observed changes in the extent of the pancake bubble below the bottom screen, as indicated with text on the plot. Compared to the test with v_{min} , bed expansion at v_{40} was close to target even though gas covered, for example, about 90% of the bottom screen at ~0.5 hours into the coGR&R phase (Table 9.1). However, even with greater fluidization, gas retention steadily increased after the initial gas release to ~14% f_a at an elapsed time of 10.5 hours, in which case continuous fluidization to release gas did not appear to be effective. But, it was determined that a significant volume of gas had collected in the gas-liquid separator (GLS) near the pump inlet; this displaced liquid through the recirculation system and registered as a supernatant liquid level increase. Figure 9.10 (lower) highlights a period of extensive clearing of gas from the GLS starting at 10.5-hr ET. The process involved opening a small valve connected to the GLS headspace and applying vacuum with a hand-operated plastic syringe through 0.5-in. plastic tubing (connected by stainless steel fittings); any liquid drawn into the tubing was returned either by pump suction or by pushing it in with the syringe. “Extensive” denotes that the evacuation process was repeated multiple times until mainly liquid was drawn into the tube when operating the syringe. Following this action, f_a immediately dropped to 4% and held at that level or lower for the duration of the test. This success was due in part to more-routine clearing of gas from the GLS; these events are called out in the lower plot of Figure 9.10. Generally, more maintenance of the GLS was needed with higher flow rates, which is thought to be a result of greater suction at the pump inlet and increased exsolution of (super-saturated) dissolved hydrogen.

Driven by the observation of f_a steadily increasing and exceeding 10%, the test was run longer the minimum 3-cm-potential-growth period. This is demonstrated in the upper plot of Figure 9.10. After the major GLS clearing process noted above, the test was continued for more than 7 hours, which could have resulted in another ~4-cm level growth if all gas was retained. Both upper and lower plots indicate that gas was continuously and effectively released once the GLS was cleared and maintained, approaching a retained gas fraction near zero ($f_a \leq 1\%$) at the end of the test. Also note that the theoretical level increase curve has a flat spot just after the large volume of gas was removed from the GLS. This is attributed to a temporary reduction of the column headspace pressure associated with the GLS clearing process and a need to rebuild pressure to that sufficient to push gas into the gas collection cylinder (e.g., 1.0025 atm; see Section 6.4).

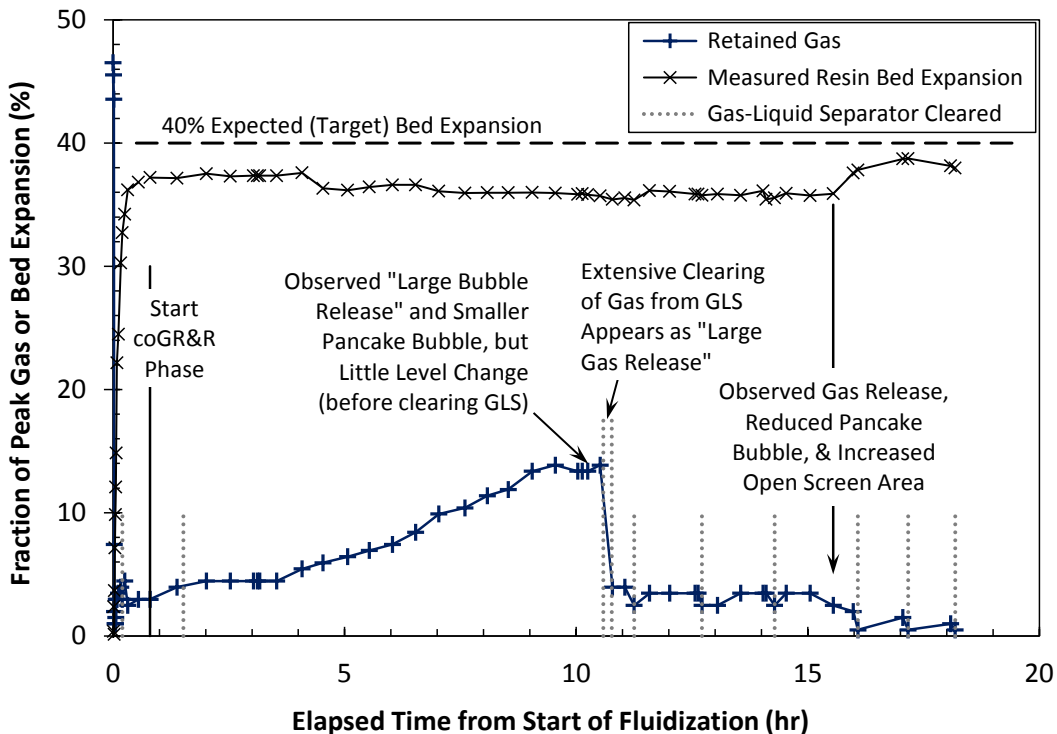
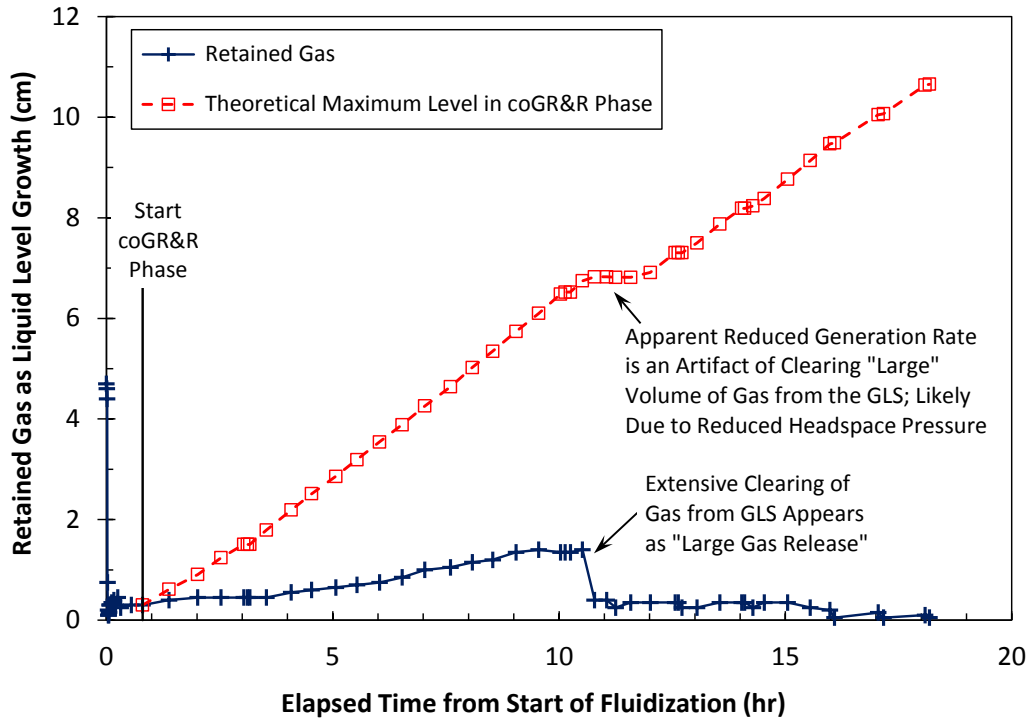


Figure 9.10. Continuous Gas Release Following an Initial Fluidization-Induced Release Phase at v_{40} (10.0 cm/min.) for sRF Resin in Alkaline Water: Upper – Measured Retained Gas Fraction and Theoretical Gas Fraction if All Generated Gas was Retained, Shown as Liquid Level Increase from Gas-Free; Lower – Fraction of Peak Retention and Resin Bed Expansion Throughout the fiGR&R and coGR&R Phases. Plots show the effects of clearing the gas/liquid separator and gas release events (Test 10-05 Phases 3B and 4).

Figure 9.11 shows equivalent plots for the fiGR&R/coGR&R test in GR&R LAW simulant using the minimum fluidization velocity ($v_{min} = 0.5$ cm/min.) and an initial retained gas volume of ~50% of peak (Test 10-09 Phases 1B and 2). As was demonstrated in Figure 9.5 in the previous section, complete gas release was achieved within 25 to 30 minutes of the start of fluidization. This held constant throughout the coGR&R test phase, except for an inconsequential increase in liquid level of 0.1 cm and a blip to f_a of 1% at the very end of the test, which coincided with a clearing of gas from the GLS. In this test, and in all the fluidization-GR&R experiments in the GR&R LAW simulant, relatively little gas was found beneath the bottom Johnson screen, as noted in Table 9.2 in Section 9.0; the screen was at least 60% open, and more typically $\geq 80\%$ open, with most blockage resulting from distributed bubbles and at most 5% coverage by pancake bubbles. A lower gas content below the screen compared to alkaline water is likely due to a combination of lower flow rates, reduced gas generation within free liquid, and possible reduced hydrogen solubility in the high-salt simulant. In the test shown in Figure 9.11 (lower), the relatively-little gas beneath the screen was apparently not a factor in bed expansion. In fact, the observed bed expansion exceeded the expected 3% by 2 to 3%, i.e., 5 to 6% total bed expansion. The reason for this is unclear. Measured resin bed temperatures in the GR&R test shown were 22 to 23 °C, which is essentially the same as the fluidization-only experiment in which the bed expansion-flow rate correlation was developed; therefore, differences in liquid viscosity should not have been a significant factor. The upper plot in Figure 9.11 shows that the test was continued to a potential ΔH_L of ≥ 3 cm if all generated gas was retained, and as noted above, essentially no change in liquid level was observed.

Retained gas fraction results in the four coupled fiGR&R-coGR&R tests conducted in alkaline water are summarized in Figure 9.12. The tests with ~50% initial f_a and fluidization velocities of 3.0 cm/min ($v_3 = v_{min}$; Test 10-05 Phases 1B and 2) and 10.0 cm/min. (v_{40} ; Test 10-05 Phases 3B and 4) are discussed above with Figure 9.9 and Figure 9.10, respectively. Two additional coGR&R tests were run using v_{min} and initial retained gas volumes of ~25% and ~90% of peak retention; in order, these are Test 10-06 Phases 1A and 2 and Test 10-06 Phases 3A and 4. Retained gas data in Figure 9.12 are presented in terms of α_{ILD} rather than f_a and ΔH_L that were used in plots earlier in this section. After the initial gas release in the test with ~90% initial f_a , α_{ILD} reached a maximum 0.9 vol% at an elapsed time of 3.4 hours from the start of fluidization, but it decreased to 0.5 vol% by test end. With ~25% initial f_a , α_{ILD} also leveled out at 0.5 vol% late in the test. Also including the third test at v_{min} (~50% initial f_a), gas holdup at steady-state fluidization of 3.0 cm/min. was approximately 0.5 to 0.7 vol% (α_{ss} in terms of α_{ILD}). However, as demonstrated in the lower plot of Figure 9.9 these results could, and likely would, have been improved (lower average retained gas fraction) in the absence of gas retained below the Johnson screen. In all three v_{min} tests, bubbles below the screen blocked ~80 to >95% of the screen area, including pancake bubbles that covered up to 90% (Table 9.1 in Section 9.0), and in each of these coGR&R test phases, fractional bed expansion fell below 1.0 (e.g., to 0.98) instead of the expected 3% increase (1.03 fraction) (only shown in Figure 9.9). In the v_{40} test discussed previously, maintenance of the gas-liquid separator proved to be as much or more of a factor than pancake bubbles in terms of the (apparent) amount of gas retained in the resin bed. Figure 9.9 shows that α_{ss} (as α_{ILD}) was between 0 and 0.3 vol% after extensive clearing of the GLS.

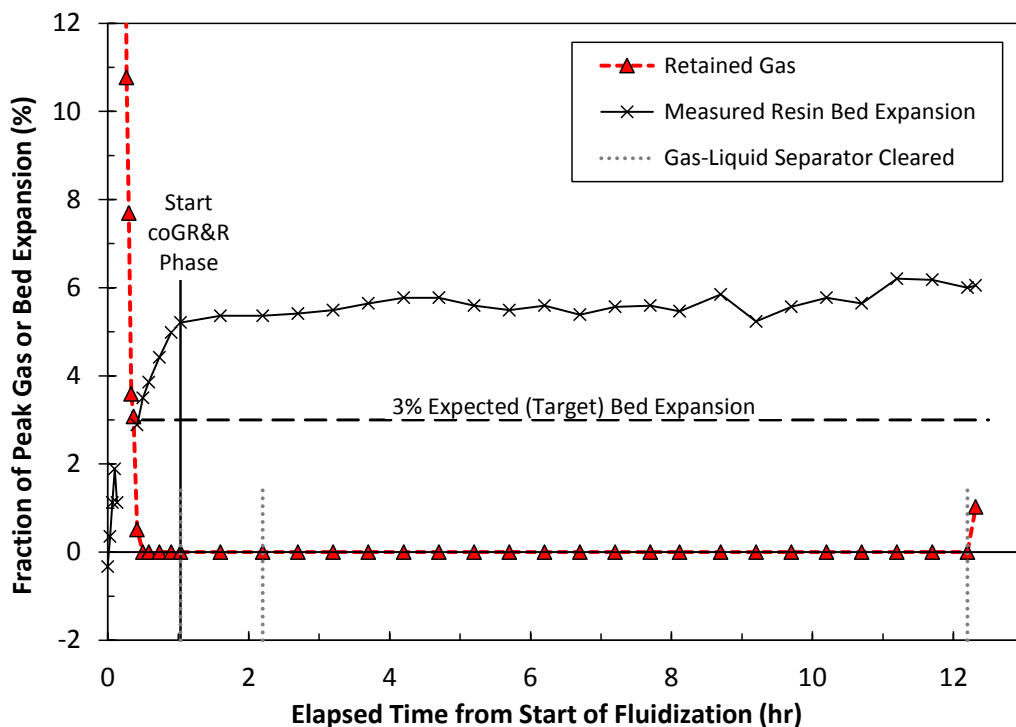
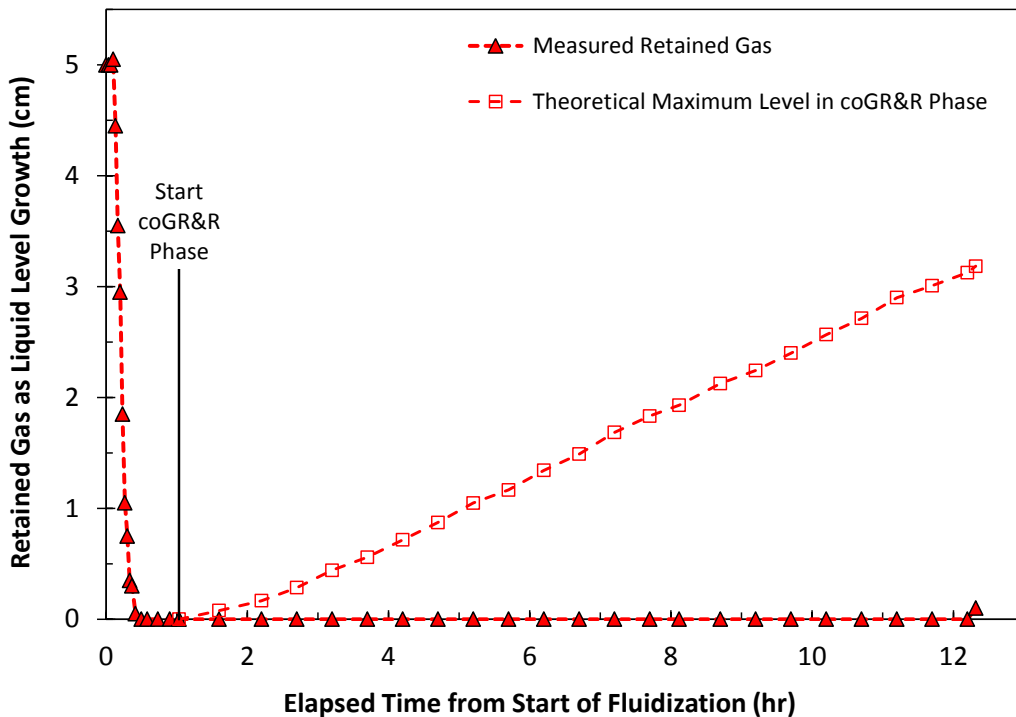


Figure 9.11. Continuous Gas Release Following an Initial Fluidization-Induced Release Phase at v_{min} (0.5 cm/min.) for sRF Resin in 6.1-M Na Simulant: Upper – Measured Retained Gas Fraction and Theoretical Gas Fraction if All Generated Gas was Retained, Shown as Liquid Level Increase from Gas-Free; Lower – Fraction of Peak Retention and Resin Bed Expansion Throughout the fiGR&R and coGR&R Phases (y-axis compressed to show detail). Plot shows the times of clearing the gas/liquid separator (Test 10-09 Phases 1B and 2).

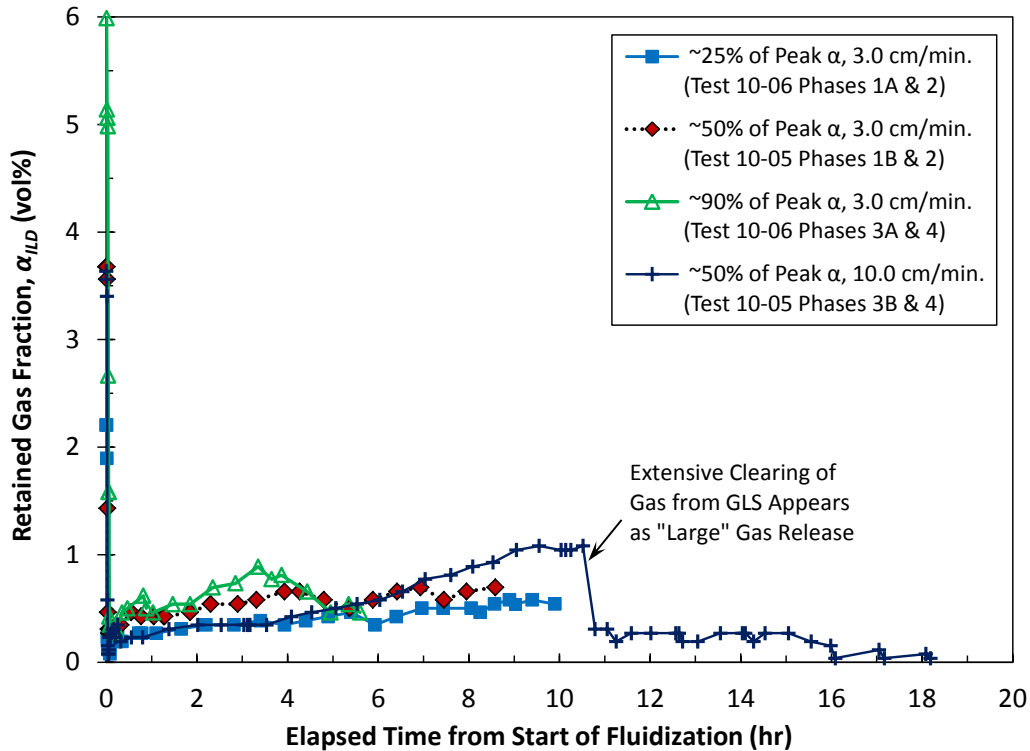


Figure 9.12. Retained Gas Fractions During Continuous Fluidization-Induced Gas Releases from sRF Resin in Alkaline Water at the Established Minimum Effective Flow Rate for Gas Release ($v_{min} = 3.0$ cm/min.) with Initial Gas Fractions of ~25%, ~50%, and ~90% of Peak Retention and at v_{40} (10.0 cm/min.) with Initial $f_{\alpha} \sim 50\%$ (Tests 10-06 Phases 1A and 2, 10-05 Phases 1B and 2, 10-06 Phases 3A and 4, and 10-05 Phases 3B and 4, respectively).

Gas generation rate could also be a factor in steady-state gas holdup, with α_{ss} expected to increase along with gas generation rate. Figure 9.13 shows gas generation rates in terms of cumulative volume of gas collected as a function of elapsed time in the coGR&R test phase. The upper plot includes the results for the four tests in alkaline water, and the lower plot shows the results for the lone coGR&R test conducted with GR&R LAW simulant. Each plot includes a horizontal reference line at 1.53 L, which is equivalent to a ΔH_L of 3.0 cm in the fluidization column if all gas was retained, and that was used as a criterion for test completion. The plots also show 1-L/day gas generation rate reference lines. This generation rate is equivalent to 18 L/day in a full-scale ion exchange column, and it is considered to be a conservatively-high bounding estimate (Section 6.4). Figure 9.13 indicates that gas generation rates easily exceeded the 1-L/day benchmark in all the reported coGR&R tests; by inspection, the measured generation rates were at least a factor of 2- and upwards of 8-times higher. Differences in gas generation rates amongst the tests are due to a combination of SBH concentration and the amount of testing completed after SBH addition up to the point of testing. Although SBH sequence identifiers were not defined for coGR&R test phases, those for the preceding fiGR&R phases can help place them with respect to each other. In order of increasing generation rate for the alkaline water tests shown in the upper plot of Figure 9.13, the sequence identifiers are: SBH2.5, SBH2.3, SBH2.1, and SBH3.2. In the series of tests following the second addition of SBH, the generation rate order is consistent with the number of tests (gas retention periods) completed after the addition. Comparison of the generation rate data in Figure 8.6 (Section 8.1.2) for the SBH2.1 and SBH3.2 gas retention periods is also consistent with the

rate-ordering in the coGR&R test phases. Early portions of the retained gas fraction curves for the v_{min} tests in Figure 9.12 (e.g., up to 4 hours from the start of fluidization) show a trend of increasing retained gas fraction with increasing generation rate (in Figure 9.13), but at later times, the trend fails. Additionally, because of other noted factors, such as the impact of pancake bubbles below the bottom screen on retained gas, no correlation between α_{ss} and gas generation rate can be drawn conclusively in these tests. The overall conclusion of the coGR&R tests is that continuous fluidization at or above the minimum velocity for gas release (giving 3% bed expansion) effectively maintains retained gas at a low level.

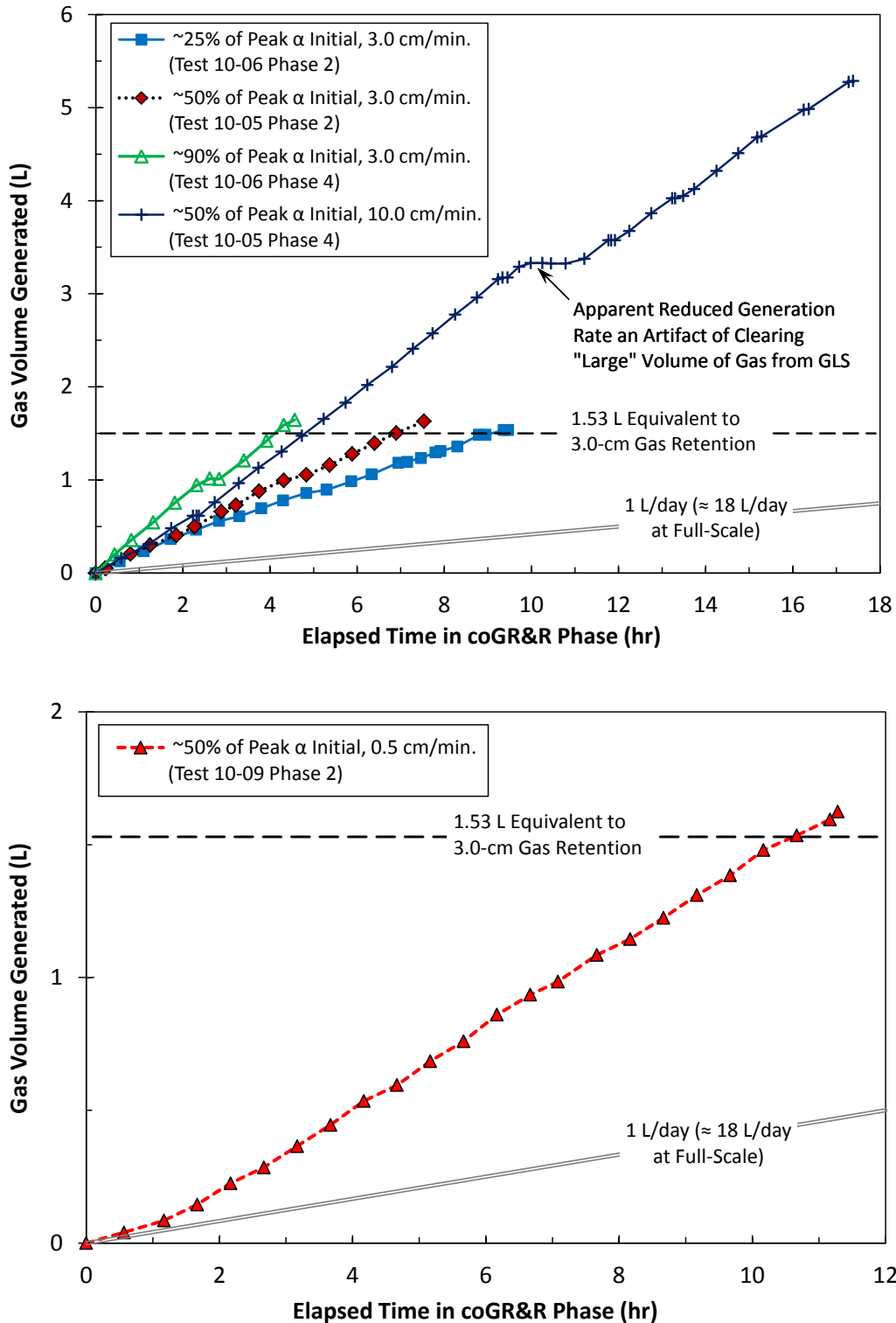


Figure 9.13. Gas Volumes Generated During Continuous Fluidization-Induced Gas Release Tests with sRF Resin in Alkaline Water (Upper) and in 6.1-M Na Simulant (Lower) Compared to a 1 L/day Gas Generation Rate (equivalent to \sim 18 L/day in a full-scale IX column) and to the Gas Volume Equivalent of 3.0-cm Gas Retention. Initial retained gas fractions (f_α), fluidization velocities, and Test IDs are shown in the plot legends.

9.3 Gas Release with Cyclic Fluidization

In an off-normal event, a likely strategy would be to turn on a pump, and its backup, to fluidize the ion exchange resin bed to release hydrogen gas and continuously maintain acceptable levels of hydrogen in the column. If only a single flow rate is used for this purpose, regardless of the contents in the ion exchange, it would be necessary to effectively release gas under the most challenging conditions. Based on modeling predictions this was predicted to be sRF resin in alkaline water at the upper-bound temperature (55 °C), primarily because the liquid viscosity would be lowest and higher velocity would be required to fluidize the bed. Assuming that 3% bed expansion would be effective at releasing gas at elevated temperature like it was under ambient conditions (Section 9.1), and that the primary pump plus the backup would automatically start in series, a preliminary (FIO) estimate indicated that a fluidization velocity would be 10.0 cm/min. After later testing with alkaline water at 55 °C that is discussed in Section 7.0, the velocity estimate for a two pump safety system was revised to 7.4 cm/min. It was anticipated (again before fluidization-only testing), and confirmed in direct testing (see Figure 7.7), that continuous operation at such high flow rates would create upper packed resin beds (UPBs; Section 7.2) in high-limit LAW having upper bounding viscosity and density and that these upper beds would hinder gas release. With this in mind, on/off cyclic fluidization was proposed in which the pumps would operate for a period of time to fluidize and release gas and be turned off to allow the resin bed to (at least partially) settle so that UPBs would not be present continuously.

Four opportunistic cyclic fluidization gas release tests were completed to help assess this safety system approach, and the results are presented in this section. These were all run with sRF resin in the 6.1-M sodium GR&R LAW simulant that was used in other fluidization-induced gas release testing discussed earlier in this section. The fluidization velocity was 10.0 cm/min. in all pump-on periods, based on the preliminary estimate noted above. Test objectives and strategy evolved over the course of the limited suite of tests, and therefore, initial retained gas fractions and on/off cycle times were varied.

The first test (Test 10-09 Phase 4) was completed with an overly-conservative-high (compared to the likely initial gas when fluidization would be initiated following a loss of flow accident) initial retained gas fraction (81% f_a and 6.0 vol% α) and a relatively-long 15-min. “on” period and 45-min. “off” period (15:45 cycles). The on time was expected to be sufficient to form a UPB with the GR&R LAW simulant, in the way that a shorter on time would likely produce a UPB with high-limit LAW. Collapse of the UPB and a partial bed settling in the 45-min. off-period was also expected, but it was unclear if multiple on:off cycles would lead to a continuous UPB. Figure 9.14 shows the test results during the first two cycles in terms of retained gas as a fraction of peak retention (f_a), resin bed expansion as percentage increase from the initial gas-free settled resin bed height, and the fraction (percentage) of the resin bed that was in the upper packed bed. After a few-minute delay, gas released to 30% f_a at ~8 minutes into the first on-period, at which point gas release abruptly stopped and f_a held steady. This essentially coincided with the resin bed expanding to the supernatant liquid surface (69% BE) by 10-min. elapsed time, after which a UPB formed. At 15-minutes ET, when the pump was stopped, ~50% of the resin was in the upper bed. The UPB only partially collapsed after stopping the pump, and it remained nominally stationary and contained ~30% of the resin from ~20-min. ET to after the start of the second cycle. Note in Figure 9.14 that the f_a and UPB curves coincidentally overlap at 30% for an extended period of time making it more difficult to see the UPB data.

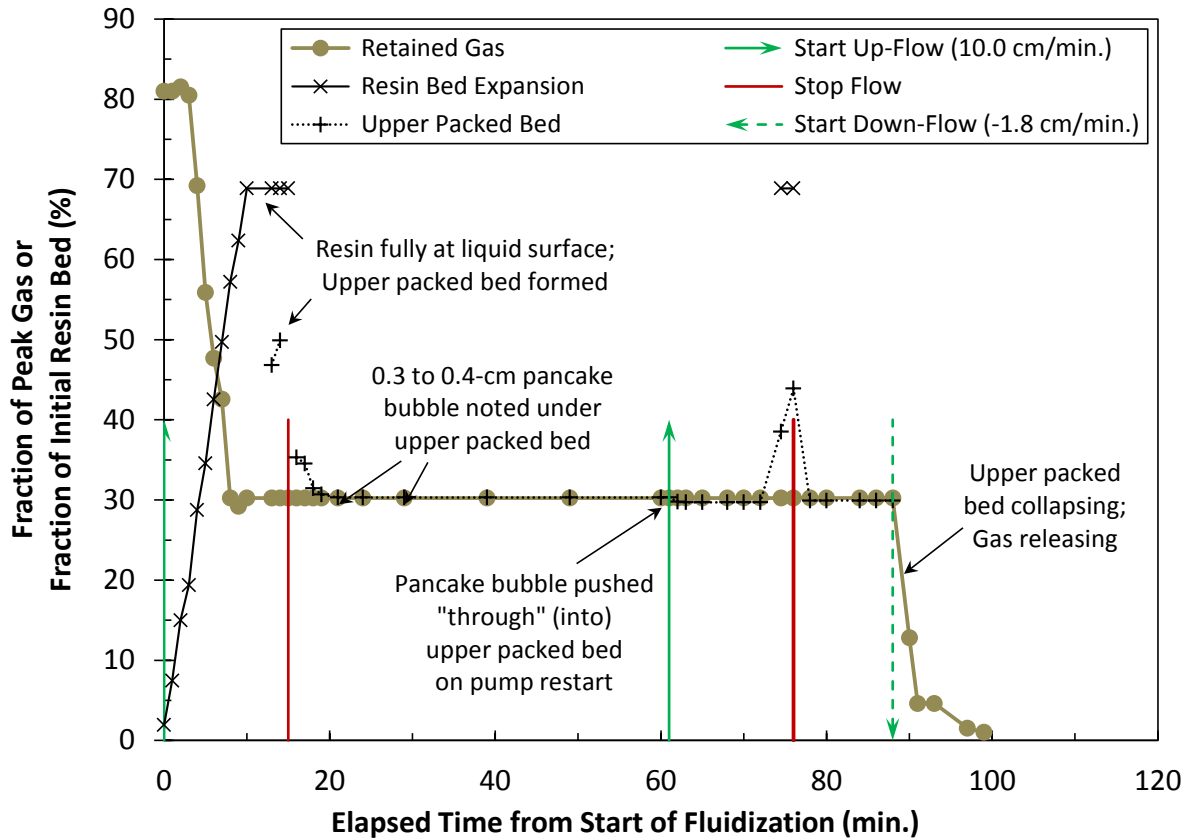


Figure 9.14. Gas Release and Resin Bed Expansion During 15 min./45 min. On/Off Fluidization Cycles with sRF Resin in 6.1-M Na Simulant at an Initial Gas Fraction of ~80% of Peak Retention and at the Predicted Off-Normal Event Flow Rate, $v = 10.0$ cm/min. (Test 10-09 Phase 4).

Importantly, the stable upper bed prevented complete gas release and likely contained a portion of it. As noted in the plot, a 0.3- to 0.4-cm thick pancake bubble was observed (and documented in test notes) between ~20- and 30-min. ET. It is thought to have formed by release of gas from the lower resin bed that was trapped by the UPB. The pancake bubble appeared to push into the UPB when the pump was restarted at 61-min. ET (instead of 60 min., inadvertently). In the second on-period, no additional gas released, and the UPB grew in the last few minutes of it. The UPB fraction and f_a remained constant at 30% after the pump was stopped in the second cycle, and it appeared that this condition would persist indefinitely. For this reason, the cyclic fluidization was terminated, and the recirculation system was operated in column down-flow at -1.8 cm/min starting at 88-min. ET. Figure 9.14 shows that the upper bed readily collapsed and essentially all remaining gas was released.

The initial retained gas fraction in the first cyclic fluidization-GR&R test was very challenging, and much higher than the initial gas when fluidization would be initiated following a loss of flow accident, because the safety system would have been turned on long before reaching 6 vol% retained gas. Therefore, a more-realistic initial α of 0.7 vol% (~10% f_a and 1-cm ΔH_L) was used in the second test (Test 10-09 Phase 5) with the same 15-min.:45-min. on/off fluidization cycle of the first test. The results for the first two cycles are shown in Figure 9.15 using similar metrics to those in the previous figure. Gas was released completely by about 8 minutes after the start of fluidization in the first cycle, a few minutes before the resin bed expanded to the supernatant liquid surface (69% BE). In both cycles shown in Figure

9.15, resin remained at the surface in the last few minutes of the on-periods, but no distinct formation of an upper packed bed was observed. The bed expansion behavior in the two cycles was nominally repeatable, and the retained gas remained near zero after the initial release (although gas generation data were not evaluated for the extent of possible growth in this test). By comparison to Figure 9.14, the formation and persistence of the UPB in the earlier test was apparently due to the initially-high retained gas fraction, in conjunction with the relatively-long on-period.

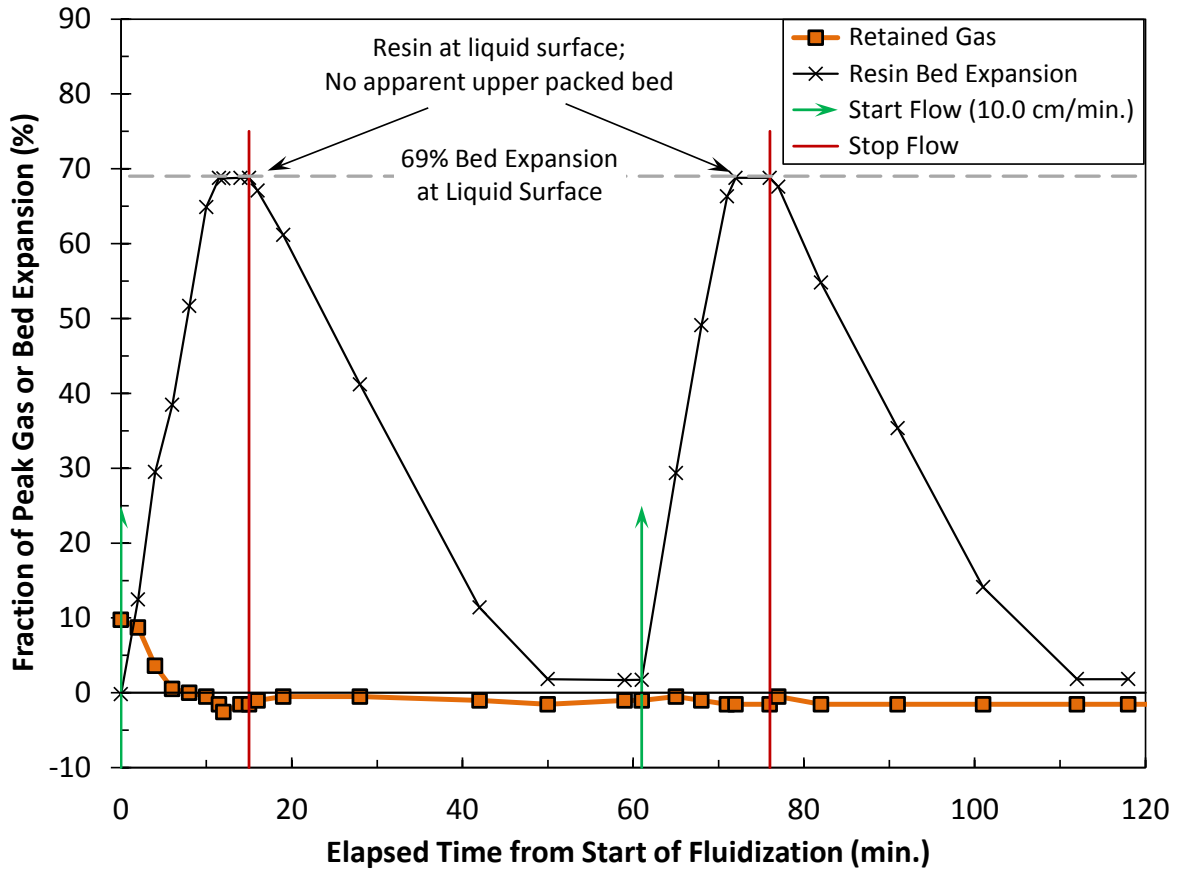


Figure 9.15. Gas Release and Resin Bed Expansion During 15 min./45 min. On/Off Fluidization Cycles with sRF Resin in 6.1-M Na Simulant at an Initial Gas Fraction of ~10% of Peak Retention and at the Predicted Off-Normal Event Flow Rate, $v = 10.0$ cm/min. (Test 10-09 Phase 5).

Based on the results of the first two tests, a “more-challenging”, but intermediate, initial retained gas fraction (44% f_a , 3.3 vol% α) was used in the third cyclic-GR&R test (Test 10-09 Phase 6). To compensate for the more-likely formation of a UPB with increased retained gas, the fluidization on-period was reduced to 5 minutes¹ and used with a 55-minute off period (5:55 cycles). The fraction of peak gas retention and bed expansion results are shown in Figure 9.16 for the first two cycles. The initial gas release behavior was previously presented in Figure 9.5 (Section 9.2.2) in terms of α_{ILD} and compared to other tests using a range of fluidization velocities, but with similar initial gas fractions. As noted earlier, gas release started in the last minute of the first on cycle, and the majority of the gas was released in ~9

¹ In consultation with WRPS, 5 minutes was the minimum duration of any on or off-period, based on the functionality of candidate safety system cycle controllers.

minutes after the pump was stopped. Retained gas stayed near zero after the initial release, peaking at 1% f_a . Comparison of the bed expansion data in the two cycles plotted in Figure 9.16 shows that the gas release impacted resin bed settling in the first off period. For example, as indicated in the plot, bed settling was delayed due to (re)suspension of resin with gas release. A maximum 36% bed expansion was measured in the second cycle and was well short of forming an upper packed bed.

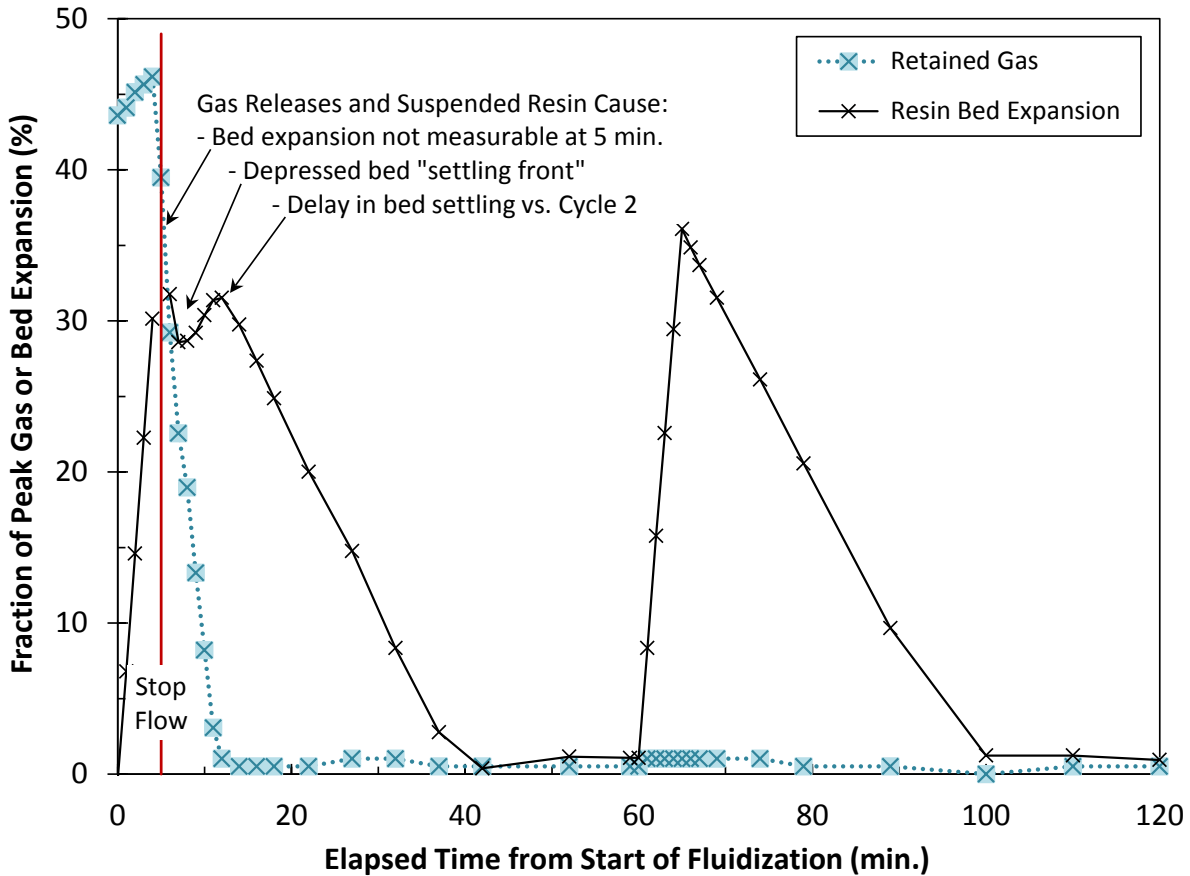


Figure 9.16. Gas Release and Resin Bed Expansion During 5 min./55 min. On/Off Fluidization Cycles with sRF Resin in 6.1-M Na Simulant at an Initial Gas Fraction of ~50% of Peak Retention and at the Predicted Off-Normal Event Flow Rate, $v = 10.0$ cm/min. (Test 10-09 Phase 6).

The final cyclic fluidization-GR&R test (Test 10-09 Phase 7) was the most opportunistic of any. It was conducted a few weeks after all other planned GR&R tests were completed, and the retained gas was at 99% of maximum (7.2 vol% α). This was used as-is with 5-min. on/10-min. off fluidization cycles, and the results for six cycles are shown in Figure 9.17. Gas release started in the second minute of fluidization and decreased to 64% f_a when the pump was stopped at 5-minutes elapsed time. Gas release continued with the pump off and was completely released by 14-min. ET, one minute before the pump was restarted for the second cycle. Only 36% bed expansion was attained by the end of the first on-period, so no upper packed bed formed in the way it did in the other high-initial-gas test (Figure 9.14). Because the 10-min. off period was relatively short in the test shown in Figure 9.17, the bed did not settle completely in off periods and bed expansion increased (to a point) in on-periods. The expanded resin bed reached the liquid surface (66% BE) at the end of the third on-period, which also became the steady-state

maximum in the fourth and higher cycles. No upper packed bed formed. At steady state, the resin bed settled to a minimum bed expansion of 45% in each cycle.

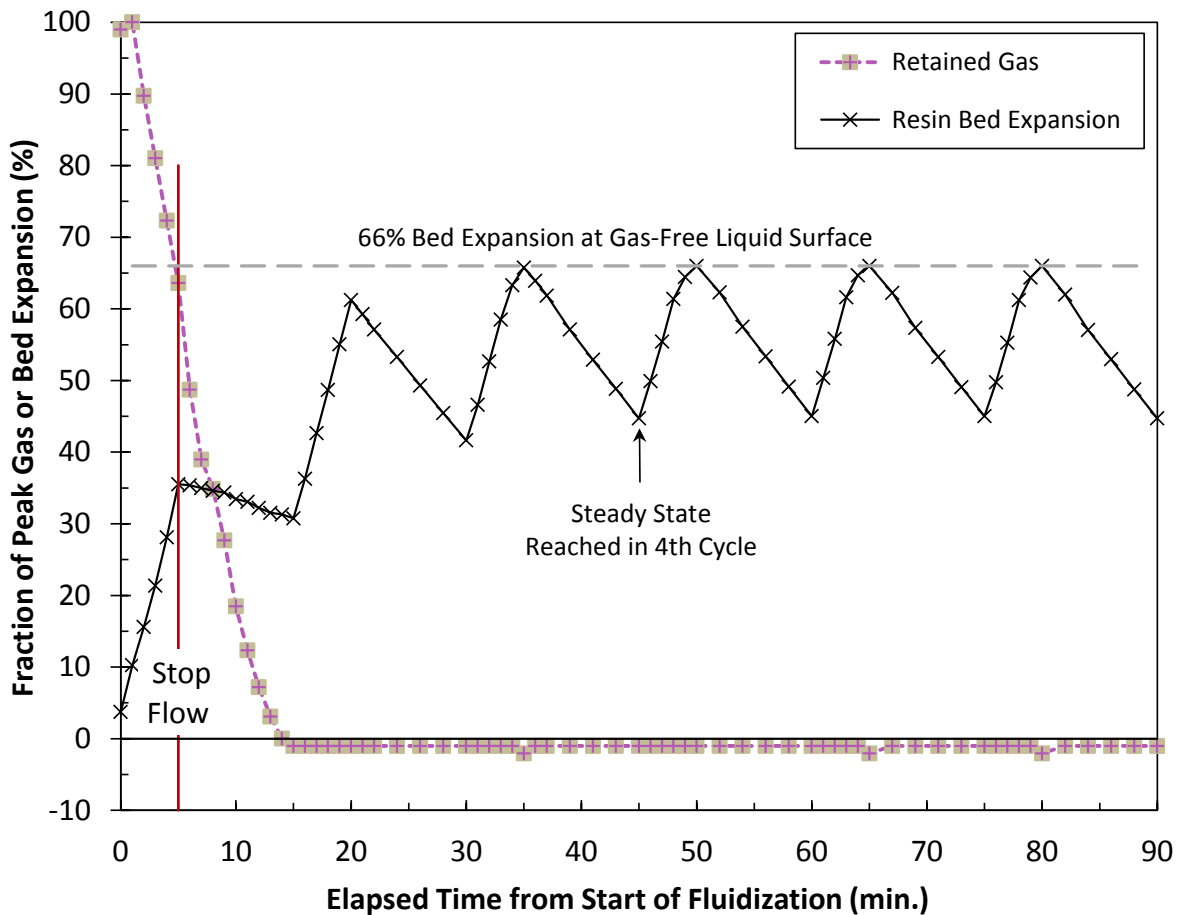


Figure 9.17. Gas Release and Resin Bed Expansion During 5 min./10 min. On/Off Fluidization Cycles with sRF Resin in 6.1-M Na Simulant at an Initial Gas Fraction of ~100% of Peak Retention and at the Predicted Off-Normal Event Flow Rate, $v = 10.0$ cm/min. (Test 10-09 Phase 7).

Fluidization was continued without interruption in two 8-min. on/10-min. off cycles. The intent was to (perhaps) better represent the resin bed expansion and settling behavior that would be observed with high-limit LAW in, for example, 5:55 cycles. (The test with GR&R LAW simulant discussed here was conducted before the [no GR&R] upper packed bed tests with high-limit LAW simulant that are covered in Section 7.2.) Figure 9.18 shows the resin bed expansion and upper packed bed results for the seventh and eighth (total) cycles; because gas was released in the earlier cycles, additional f_a data are not shown. The timeline in Figure 9.18 is for each cycle so that cycle-to-cycle behavior can be more-easily compared. Starting at 45% bed expansion from cycle 6 and with a longer on-period (8 min. vs. 5 min.), an upper packed bed readily formed. When flow was stopped in both cycles 7 and 8, 32% of the initial resin bed (depth) was in the upper packed bed (42 cm). Somewhat surprisingly, the resin bed resettled to 46% BE even with UPB formation, only 1% higher than steady state in the preceding 5:10 cycles without upper beds. Only two 8:10 cycles were run, because expansion behavior appeared to be repeatable. GR&R performance with these cycle times cannot be predicted conclusively, but the data in Figure 9.14 and Figure 9.17 provide an indication that gas would be substantially released in the first cycle. Specifically,

gas release stopped in the earlier (15:45) test after ~8 min., because continued fluidization caused a stable upper packed bed to form; if flow was stopped at 8 min., gas release would likely continue while resin settled, similar to that observed in the later (5:10) test.

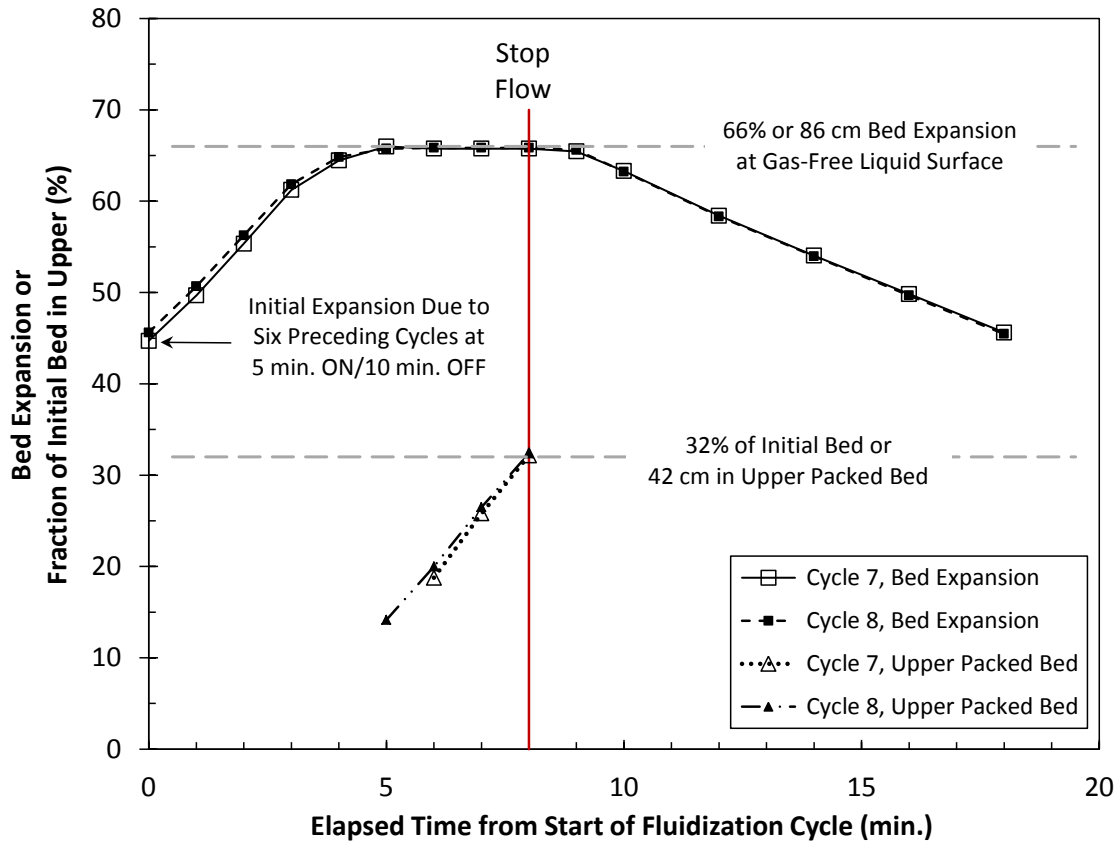


Figure 9.18. Resin Bed Expansion and Upper Packed Bed Formation During 8 min./10 min. On/Off Fluidization Cycles with sRF Resin in 6.1-M Na Simulant at the Predicted Off-Normal Event Flow Rate, $v = 10.0$ cm/min. (Test 10-09 Phase 7; immediately following six 5 min./10 min. on/off cycles in which gas was released).

First-cycle gas releases in the four cyclic fluidization-GR&R tests are summarized in Figure 9.19. Gas retention / release data are shown in terms of retained gas fraction (α_{LD}) rather than fraction of peak (f_a) that is used in earlier plots of individual test data. As discussed above and shown in Figure 9.19, gas was effectively released in fluidization cycle tests except in the 15-min. on/45-min. off test which formed an indefinitely-stable upper packed bed. This initial retained gas fraction is higher than what would likely be present when fluidization would be initiated following a loss of flow accident. However, with a low initial retained gas fraction, gas was completely released during the first on-period of a 15:45 cycle. In the two tests with 5-min. on-periods and moderate to very high initial α , gas release continued after the pump was stopped, and all gas was released in about 15 minutes.

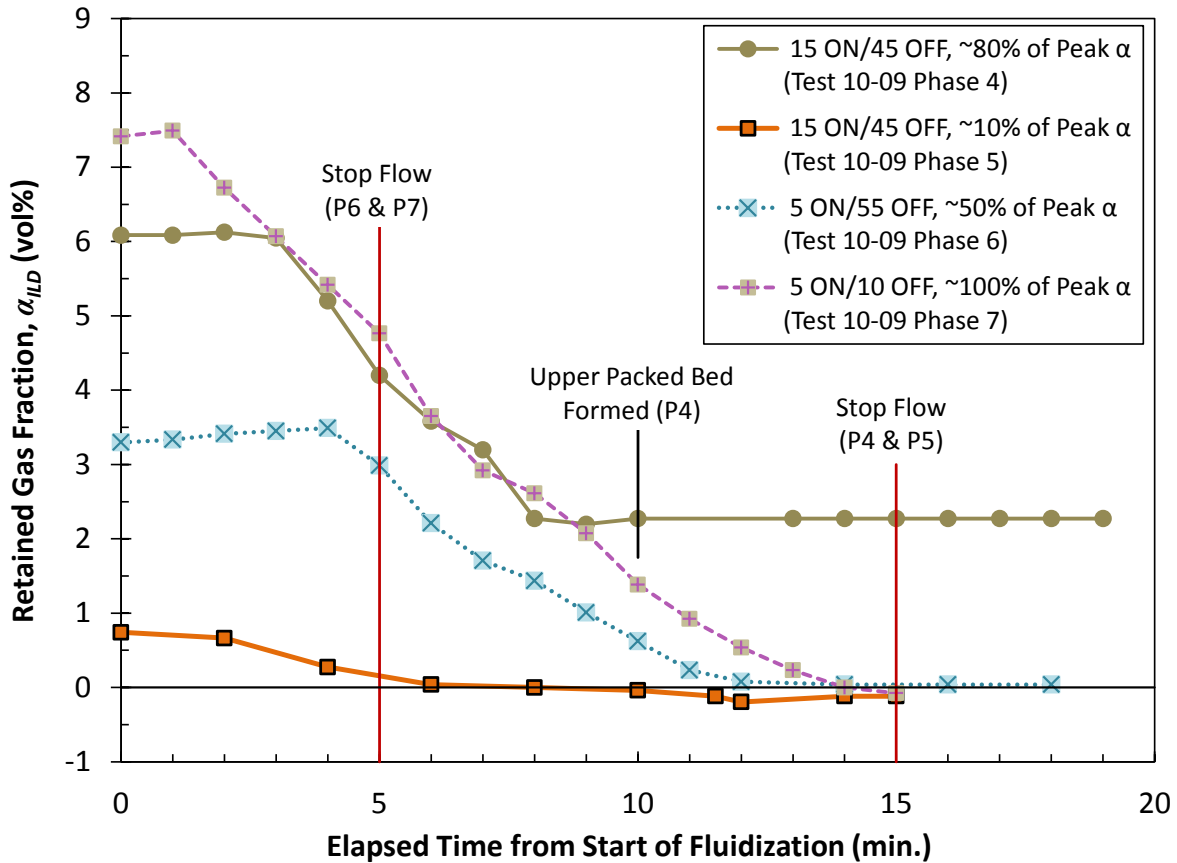


Figure 9.19. Retained Gas Fractions During First Cycles of Cyclic Fluidization-Induced Gas Releases from sRF Resin in 6.1-M Na Simulant with Varying Initial Gas Fractions and On/Off Cycle Durations, All at the Predicted Off-Normal Event Flow Rate, $v = 10.0$ cm/min. (Test 10-09 Phases 4, 5, 6, and 7; see plot legend for on/off cycle periods in minutes and initial gas content as a fraction of peak retention).

9.4 Fluidization Gas Release Summary

Based on these fluidization studies, the results demonstrate that a fluidization velocity giving 3% bed expansion was adequate to release both gas retained in an initially settled sRF resin bed and gas continuously generated in a fluidized sRF resin bed. Although initially retained gas was also released at lower velocities, thus the minimum velocity for gas release by fluidization was less than the velocity needed to achieve 3% bed expansion, a velocity giving 3% bed expansion is recommended as a robust fluidization velocity for effective gas release. A two pump safety system, with both pumps operating in series, and with each pump individually capable of providing 5.2 cm/min. fluidization velocity, would flow with 7.4 cm/min. With a constant fluidization velocity of 7.4 cm/min., an upper packed bed of sRF resin will form in most LAW fluids. Testing results show upper bed formation would occur at this velocity for a nominal LAW simulant (nominally 1.25 g/mL density and about 4 mPa·s viscosity) and a high-limit LAW simulant (nominally 1.35 g/mL density and 15 mPa·s viscosity). An upper packed bed is expected to retain hydrogen gas and pose a flammability hazard and in one test a stable upper packed bed with retained gas was observed. Cyclic on/off fluidization appears promising for avoiding upper bed formation and providing robust release of retained gas. The test results suggest that on/off fluidization

could be developed as an approach for using a single fluidization velocity to release hydrogen gas for all fluid and sRF resin pairs. There are three known limitations for this approach that have not been fully quantified: 1) the “on” period of fluidization needs to be sufficiently short to avoid forming an upper bed, 2) the initial retained gas when the first cycle begins must be relatively low, and 3) although not specifically studied, it is expected that the duration of the settling period needs to be sufficiently long to allow a reasonable degree of settling

10.0 Conclusions

Experiments and analysis were conducted to evaluate the effectiveness of fluidization to release initially retained hydrogen gas from an sRF resin bed, to maintain hydrogen gas retention at low levels, and, thereby, to avoid conditions where hydrogen gas poses a flammability hazard. Testing included determining if effective hydrogen gas release would occur using a single constant fluidization velocity for all sRF resin/liquid conditions expected in the column. The key conclusions of the study are the following:

- A fluidization velocity giving 3% bed expansion was adequate to release both gas retained in an initially settled sRF resin bed and gas continuously generated in a fluidized sRF resin bed. Although initially retained gas was also released at lower velocities, thus the minimum velocity for gas release by fluidization was less than the velocity needed to achieve 3% bed expansion, a velocity giving 3% bed expansion is recommended as a robust fluidization velocity for effective gas release.
- Gas release was effective for flow rates from 3% to 40% bed expansion with initial retained gas fractions from ~25% to ~100% (> 90%) of the peak gas retention measured in spontaneous release tests. Near-complete gas releases occurred in 5 minutes or less in alkaline water and closer to 20 to 25 minutes in 6.1 M sodium GR&R simulant. The longer release time with the simulant is attributed to higher viscosity and other factors that also contribute to longer settling times in fluidization-only experiments.
- Retained gas fractions (holdup) in multiple continuous gas release tests at steady-state fluidization at velocities from v_{min} for 3% bed expansion to that for 40% bed expansion was at most 0.7 vol% (average) and was near zero in some cases. If pancake bubbles were eliminated by an appropriate column re-design, gas holdup would likely be reduced closer to zero. Gas generation rates in continuous gas release tests were more than two-times higher than the maximum expected at full-scale, when scaled on a resin volume basis. Higher experimental generation rates are expected to conservatively bound gas holdup. However, the expected dependence of holdup on gas generation rates could not be determined because of other factors affecting gas retention (e.g., pancake bubbles).
- In addition to the gas volume retained in the gas below the screen, it was demonstrated that the pancake bubble caused flow maldistribution resulting in lower than expected bed expansion. The gas retention below the bottom screen increases the total retained hydrogen, thus increasing the hydrogen flammability hazard, and flow maldistribution interferes with the ability of bed fluidization to release gas.
- Fluidization of Na⁺ form sRF resin in alkaline water was more difficult (required a higher velocity) than H⁺ form sRF resin in acidic water. Accordingly, Na⁺ form sRF resin in 55 °C water was thus considered to be the most challenging liquid/resin pair, and test data show 5.2 cm/min. fluidization velocity is needed to reach 3% bed expansion under these conditions.

- A two pump safety system, with both pumps operating in series, and with each pump individually capable of providing 5.2 cm/min. fluidization velocity, would flow with 7.4 cm/min. This is the fluidization velocity for evaluating the full range of fluid and sRF resin properties.
- With a constant fluidization velocity of 7.4 cm/min., an upper packed bed of sRF resin will form in most LAW fluids. Testing results show upper bed formation would occur at this velocity for a nominal LAW simulant (nominally 1.25 g/mL density and about 4 mPa·s viscosity) and a high-limit LAW simulant (nominally 1.35 g/mL density and 15 mPa·s viscosity). An upper packed bed is expected to retain hydrogen gas and pose a flammability hazard and in one test a stable upper packed bed with retained gas was observed.
- Cyclical fluidization/settling, with cycles of 5 min on followed by 55 min. off, did not form an upper packed bed at a fluidization velocity of 10.0 cm/min (this was the predicted two-pump flow prior to conducting fluidization tests at 55 °C) even for the high-limit LAW and was effective at releasing gas from sRF resin in a GR&R LAW simulant with nominal properties. This suggests that on:off fluidization could be developed as an approach for using a single fluidization velocity to release hydrogen gas for all fluid and sRF resin pairs. There are three known limitations for this approach that have not been fully quantified: 1) the “on” period of fluidization needs to be sufficiently short to avoid forming an upper bed, 2) the initial retained gas when the first cycle begins must be relatively low, and 3) although not specifically studied, it is expected that the duration of the settling period needs to be sufficiently long to allow a reasonable degree of settling. For example, in a 15:45 cycle test with a considerably-higher retained gas fraction than would be expected in the plant, a stable upper packed bed formed on the first cycle before all gas was released, and the upper did not collapse when flow was stopped. This led to the use of shorter on-cycles and/or the use of more realistic and bounding retained gas fractions in other noted cyclic GR&R tests.
- Models were created for bed expansion and upper packed bed formation as a function of fluidization velocity and fluid and sRF resin properties. The models agree well with test data, based on a comparison model and test results for a range of fluidization velocities with five liquid/resin pairs for bed expansion and three liquid/resin pairs for the upper bed heights. Accordingly, these models can be used for estimating the behavior of different fluid and resin pairs that were not specifically tested.
- With the nominal GR&R LAW simulant in fluidization-column GR&R tests, the peak retention at the point of spontaneous gas release was 7.2 vol%, consistent with the theoretical neutral buoyancy values for the gaseous resin bed to become neutrally buoyant in the supernatant liquid. A large spontaneous release (i.e., not induced by fluidization) to <2 vol% retained gas was observed after reaching the peak.
- Peak retention for sRF resin/alkaline water in fluidization-column GR&R tests was 7.8 vol% retained gas, which was well below the theoretical α_{NB} and no large spontaneous gas release was observed. Two repeat tests gave similar results – in terms of supernatant liquid level growth due to retained gas, the maxima ranged from 9.7 to 10.1 cm. The less-than neutral buoyance peak retention values for alkaline water is likely due to a significant fraction of gas retained in interstitial-liquid-displacing bubbles in the relatively deep resin bed in the

fluidization-column (compared to bench-scale tests) and formation of connected gas channels below α_{NB} .

11.0 References

- Aguilar F. 2016. *Test Specification for the Low-Activity Waste Pretreatment System Full-Scale Ion Exchange Column Test and Engineering-Scale Integrated Test (Project T5L01)*. RPP-RPT-58683, Rev. 3, Washington River Protection Solutions LLC, Richland, WA.
- Ansolabehere AA. 2016. *Project T5L01 Low Activity Waste Pretreatment System Specification*. RPP-SPEC-56967, Rev. 6, Washington River Protection Solutions LLC, Richland, WA.
- Camenen, B. 2007. "Simple and General Formula for the Settling Velocity of Particles." *Journal of Hydraulic Engineering* - ASCE 133(2):229–233.
- Chhabra RP. 1993. *Bubbles, Drops, and Particles in Non-Newtonian Fluids*, CRC Press, Inc., Boca Raton, FL.
- Colburn HA, SA Bryan, DM Camaioni, and LA Mahoney. 2018. *Gas Generation Testing of Spherical Resorcinol-Formaldehyde (sRF) Resin*. PNNL-26869 (RPT-LPIST-002), Rev. 0, Pacific Northwest National Laboratory, Richland, WA.
- CRC. 2005. *Handbook of Chemistry and Physics*, 86th edition, DR Lide (ed.). CRC Press, Taylor & Francis Group, Boca Raton, FL.
- Daniel RC, CA Burns, RL Russell, PP Schonewill, SD Hoyle, and EJ Antonio. 2018. *Crossflow Filtration of LAWPS Simulants*. PNNL-27251 (RPT-LPIST-003), Rev. 0, Pacific Northwest National Laboratory, Richland, WA.
- Dullien FAL. 1992. *Porous Media: Fluid Transport and Pore Structure*, 2nd edition. Academic Press, Inc., San Diego, CA.
- Epstein, M, and PA Gauglitz. 2010. An Experimental Study of the Stability of Vessel-Spanning Bubbles in Cylindrical, Annular, Obround, and Conical Containers. FAI/09-272, Rev. 2, Fauske and Associates, LLC, Burr Ridge, Illinois.
- Flint AL and LE Flint. 2002. *Particle Density*. *Methods of Soil Analysis, Part 4: Physical Methods*, JH Dane, GC Topp, and GS Campbell (eds.), SSSA Book Series No. 5, pp. 229-240. SSSA, Madison, WI.
- Gauglitz PA, BE Wells, CLH Bottenus, and PP Schonewill. 2018. *Maximum Potential Hydrogen Gas Retention in the sRF Resion Ion Exchnage Column for the LAWPS Process*, PNNL-26995, Rev 0 (RPT-LPIST-004), Pacific Northwest National Laboratory, Richland, Washington.
- Gauglitz PA, JR Bontha, RC Daniel, LA Mahoney, SD Rassat, BE Wells, J Bao, GK Boeringa, WC Buchmiller, CA Burns, J Chun, NK Karri, H Li, and DN Tran. 2015. *Hydrogen Gas Retention and Release from WTP Vessels: Summary of Preliminary Studies*, PNNL-24255 (WTP-RPT-238), Rev 0, Pacific Northwest National Laboratory, Richland, Washington.

Gauglitz PA, WC Buchmiller, SG Probert, AT Owen, and FJ Brockman. 2012. *Strong-Sludge Gas Retention and Release Mechanisms in Clay Simulants*. PNNL-21167 (EMSP-RPT-013), Rev. 0, Pacific Northwest National Laboratory, Richland, WA.

Gauglitz, PA, B Buchmiller, JJ Jenks, J Chun, RL Russell; AJ Schmidt, and MM Mastor. 2010. *The Disruption of Vessel-Spanning Bubbles with Sloped Fins in Flat-Bottom and 2:1 Elliptical-Bottom Vessels*. PNNL-19345 Rev 0, Pacific Northwest National Laboratory, Richland, Washington.

Gauglitz, PA, BE Wells, JA Fort, and PA Meyer. 2009. *An Approach to Understanding Cohesive Slurry Settling, Mobilization, and Hydrogen Gas Retention in Pulsed Jet Mixed Vessels*. PNNL-17707 Rev. 0, Pacific Northwest National Laboratory, Richland, Washington.

Gauglitz, PA, SD Rassat, PR Bredt, JH Konynenbelt, SM Tingey, and DP Mendoza. 1996. *Mechanisms of Gas Bubble Retention and Release: Results for Hanford Waste Tanks 241-S-102 and 241-SY-103 and Single-Shell Tank Simulants*. PNNL-11298, Pacific Northwest National Laboratory, Richland, Washington.

Gauglitz, P.A., S.D. Rassat, M.R. Powell, R.R. Shah, and L.A. Mahoney. 1995. *Gas Bubble Retention and Its Effect on Waste Properties: Retention Mechanisms, Viscosity, and Tensile and Shear Strengths*. PNL-10740, Pacific Northwest Laboratory, Richland, Washington.

Gauglitz, P.A., L.A. Mahoney, D.P. Mendoza, and M.C. Miller. 1994. *Mechanisms of Gas Bubble Retention*. PNL-10120, Pacific Northwest Laboratory, Richland, Washington.

Meyer PA, ME Brewster, SA Bryan, G Chen, LR Pederson, CW Stewart, and G Terrones. 1997. *Gas Retention and Release Behavior in Hanford Double-Shell Waste Tanks*. PNNL-11536, Rev. 1, Pacific Northwest National Laboratory, Richland, WA.

NQA-1-2000, *Quality Assurance Requirements for Nuclear Facility Applications*. American Society of Mechanical Engineers, New York, NY.

NQA-1-2008, *Quality Assurance Requirements for Nuclear Facility Applications*. American Society of Mechanical Engineers, New York, NY.

NQA-1a-2009, *Addenda to ASME NQA-1-2008*. American Society of Mechanical Engineers, New York, NY.

Peurrung, L.M., L.A. Mahoney, C.W. Stewart, P.A. Gauglitz, L.R. Pederson, S.A. Bryan, and C.L. Shepard. 1998. *Flammable Gas Issues in Double-Contained Receiver Tanks*. PNNL-11836, Rev. 2, Pacific Northwest National Laboratory, Richland, Washington.

Rassat, S.D., and P.A. Gauglitz. 1995. *Bubble Retention in Synthetic Sludge: Testing of Alternative Gas Retention Apparatus*. PNL-10661, Pacific Northwest Laboratory, Richland, Washington.

Richardson, JF. 1971. "Incipient Fluidization and Particulate Systems." Chapter 2 in *Fluidization*, JF Davidson and D Harrison Editors, Academic Press, New York.

Russel RL, PP Schonewill, and CA Burns. 2017. *Simulant Development for LAWPS Testing*. PNNL-26165 (RPT-LPIST-001), Rev. 0, Pacific Northwest National Laboratory, Richland, WA.

Schonewill PP, PA Gauglitz, RW Shimskey, KM Denslow, MR Powell, GK Boeringa, JR Bontha, NK Karri, LS Fifield, DN Tran, SA Sande, DJ Heldebrant, JE Meacham, DB Smet, WE Bryan, and RB Calmus. 2014. *Evaluation of Gas Retention in Waste Simulants: Tall Column Experiments*. PNNL-23340 (DSGREP-RPT-005), Rev. 0, Pacific Northwest National Laboratory, Richland, WA.

Stewart, CW, ME Brewster, PA Gauglitz, LA Mahoney, PA Meyer, KP Recknagle, HC Reed. 1996. *Gas Retention and Release Behavior in Hanford Single-Shell Tanks*. PNNL-11391, Pacific Northwest National Laboratory, Richland, Washington.

Wells BE, JM Cuta, SA Hartley, LA Mahoney, PA Meyer, and CW Stewart. 2002. *Analysis of Induced Gas Releases During Retrieval of Hanford Double-Shell Tank Waste*. PNNL-13782 Rev. 1, Pacific Northwest National Laboratory, Richland, WA.

Wells, BE, PA Gauglitz, and DR Rector. 2012. *Comparison of Waste Feed Delivery Small Scale Mixing Demonstration Simulant to Hanford Waste*. PNNL-20637 Rev. 2, Pacific Northwest National Laboratory, Richland, Washington.

Wilson RA, and MR Landon. 2017. *Low-Activity Waste Pretreatment System Full-Scale Ion Exchange (IX) Column Test Report (T5L01)*, RPP-RPT-60314, Rev 0, Washington River Protection Solutions LLC, Richland, WA.

Appendix A Additional Test Data

This appendix presents results for tests that were not addressed in Section 8.0 or Section 9.0.

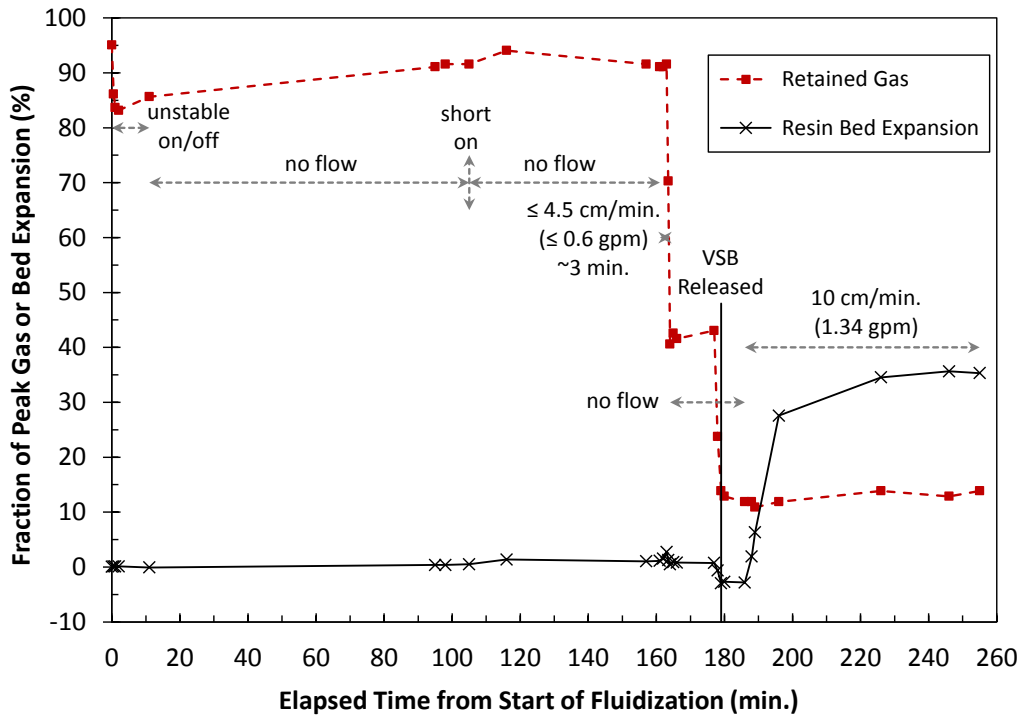
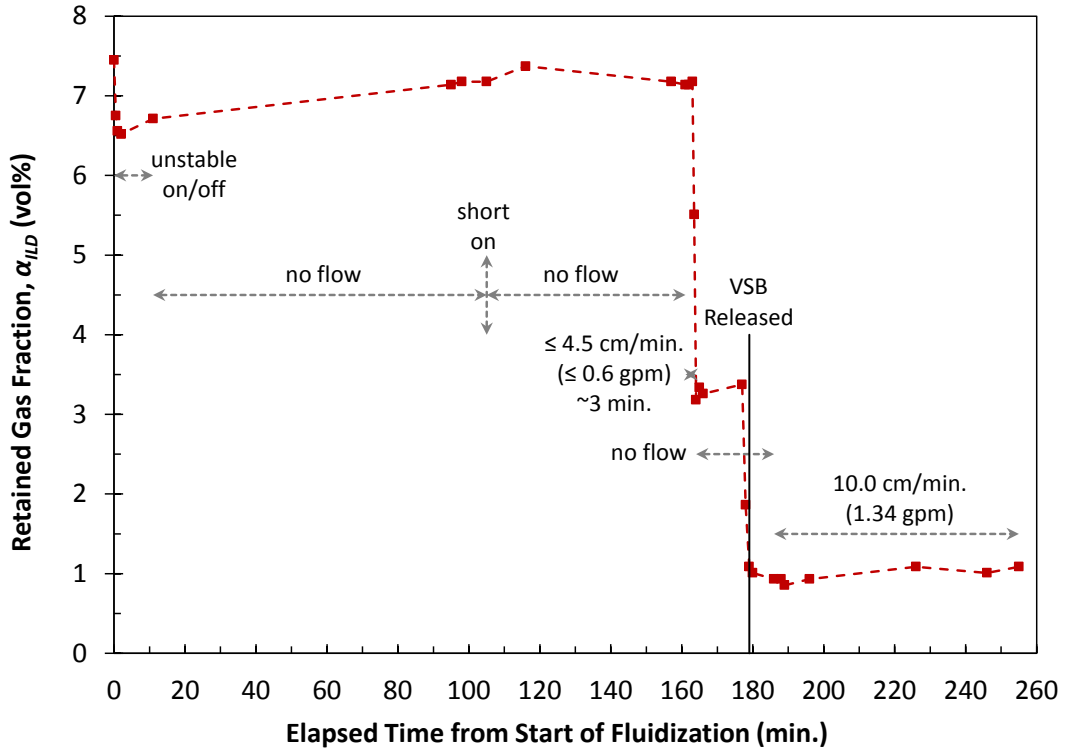


Figure A.1. Initial Fluidization-Induced Gas Release Test (10-04 Phase 3) for sRF Resin in Water Starting with >90% of Peak Retained Gas and with the Flow Rate Target for 40% Bed Expansion (10.0 cm/min., 1.34 gpm) shown by: Upper – Retained Gas Fraction as a Function of Time and Fluid Velocity (flow rate); and Lower – Retained Gas as a Fraction of Peak and Resin Bed Expansion vs. Time and Fluid Velocity.

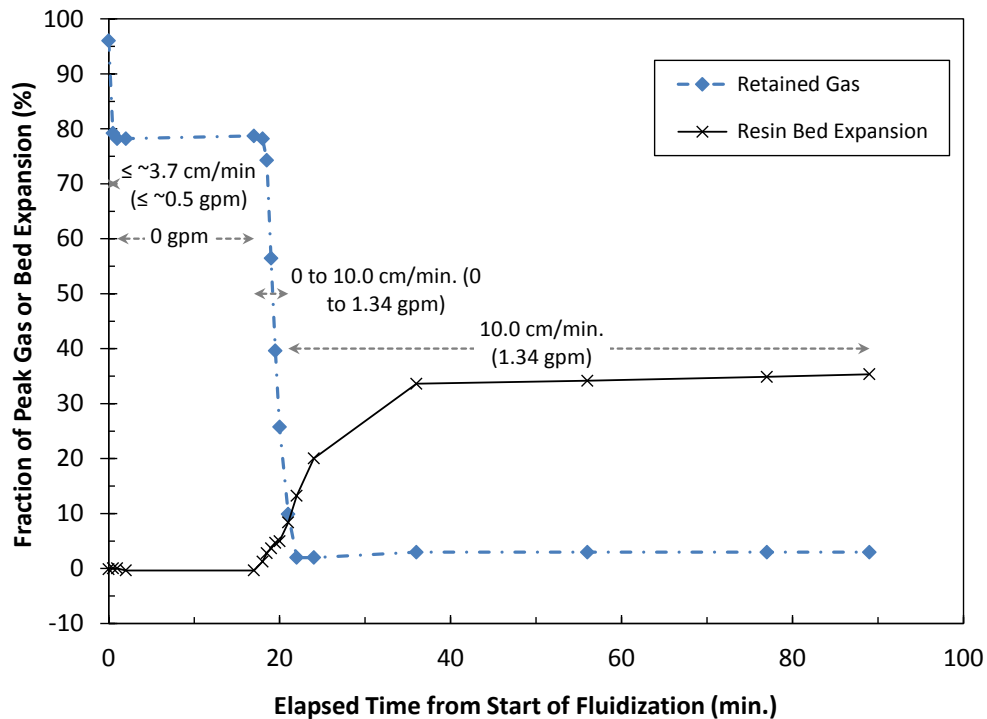
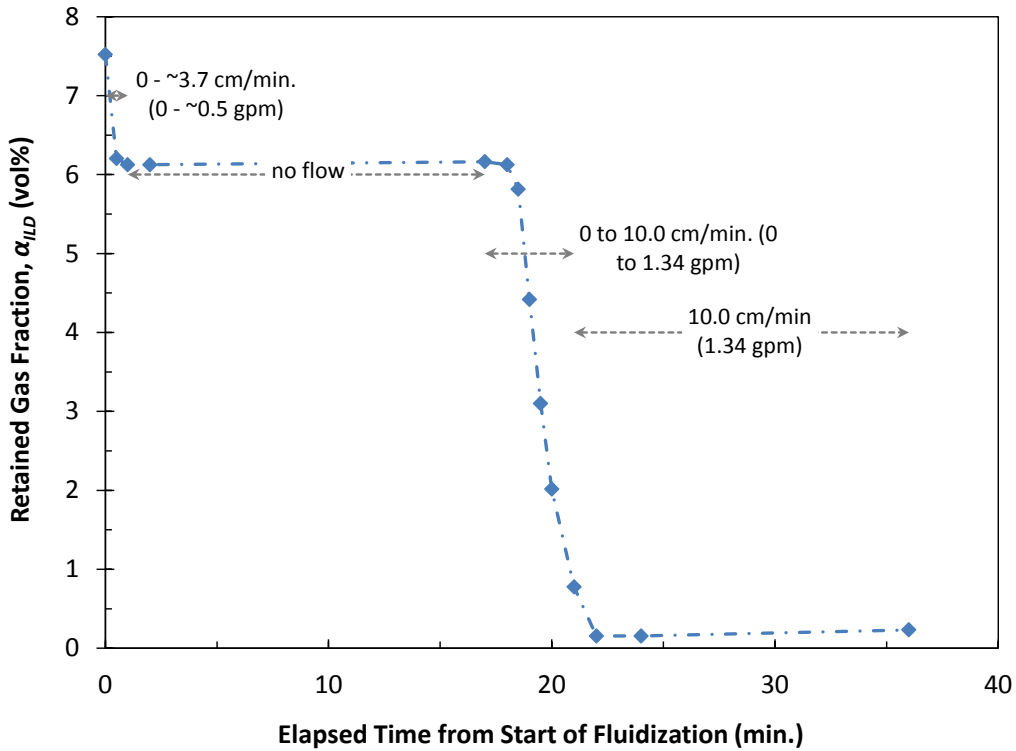


Figure A.2. Second Fluidization-Induced Gas Release Test (10-04 Phase 5) for sRF Resin in Water Starting with >90% of Peak Retained Gas and with the Flow Rate Target for 40% Bed Expansion (10.0 cm/min., 1.34 gpm) shown by: Upper – Retained Gas Fraction as a Function of Time and Fluid Velocity (flow rate); and Lower – Retained Gas as a Fraction of Peak and Resin Bed Expansion vs. Time and Fluid Velocity.

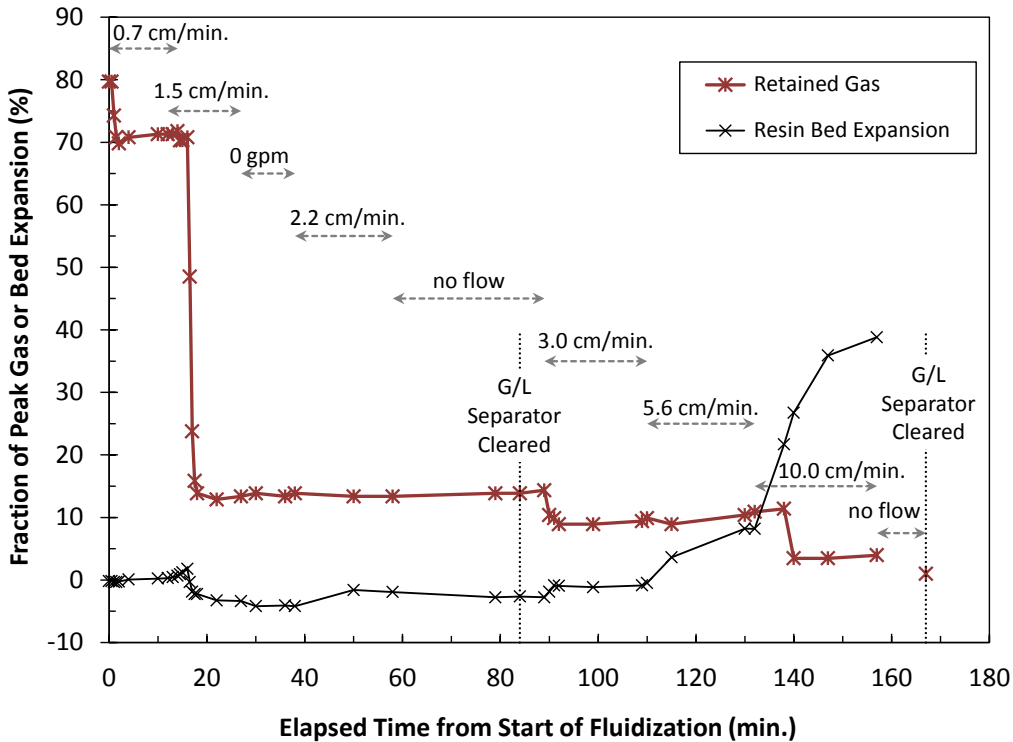
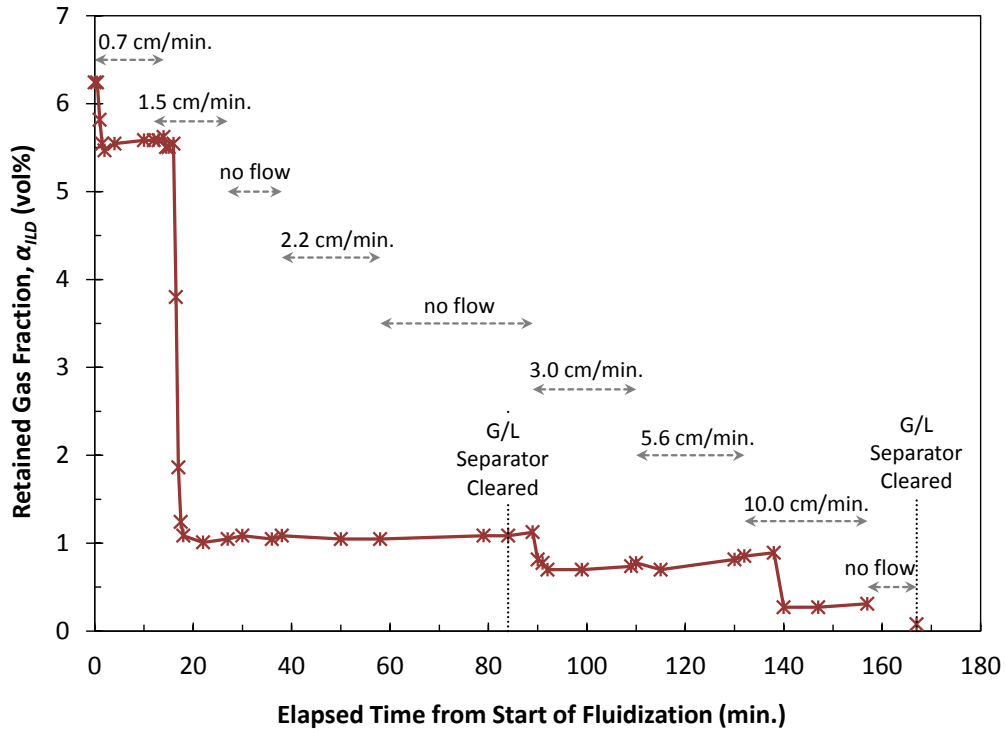


Figure A.3. Opportunistic Fluidization-Induced Gas Release Test (10-04 Phase 6) for sRF Resin in Water Starting with ~80% of Peak Retained Gas at Flow Rates Starting Below that for Incipient Fluidization (2.2 cm/min. at 0.3 gpm) shown by: Upper – Retained Gas Fraction as a Function of Time and Fluid Velocity (flow rate); and Lower – Retained Gas as a Fraction of Peak and Resin Bed Expansion vs. Time and Fluid Velocity.

Distribution*

Washington River Protection Solutions

KE Ard

MR Landon

JE Meacham

RM Russell

TE Sackett

WRPS Documents – TOCVND@rl.gov

LAWPS Document – LAWPSVENDOR@rl.gov

DOE – Office of River Protection

SC Smith

Pacific Northwest National Laboratory

GK Boeringa

CLH Bottenus

RC Daniel

PA Gauglitz

DT Linn

LA Mahoney

SD Rassat

BJ Riley

PP Schonewill

CM Stewart

BE Wells

Project File

Information Release (pdf)

*All distribution will be made electronically.



Pacific Northwest
NATIONAL LABORATORY

*Proudly Operated by **Battelle** Since 1965*

902 Battelle Boulevard
P.O. Box 999
Richland, WA 99352
1-888-375-PNNL (7665)

U.S. DEPARTMENT OF
ENERGY

www.pnnl.gov